NUMERICAL INVESTIGATION OF FLOOD INDUCED SEEPAGE UNDER LEVEES

A Thesis Submitted to
the Graduate School of Engineering and Sciences of
İzmir Institute of Technology
in Partial Fulfillment of the Requirements for the Degree of

MASTER OF SCIENCE

in Civil Engineering

by
Aykut SEMERCİ

DECEMBER 2018
İZMİR

We approve the thesis of **Aykut SEMERCİ**

Examining Committee Members:

_____

Prof. Dr. Gökmen TAYFUR
Department of Civil Engineering, İzmir Institute of Technology

_____

Prof. Dr. Alper BABA
Department of Civil Engineering, İzmir Institute of Technology

_____

Prof. Dr. Yeliz YÜKSELEN AKSOY
Department of Civil Engineering, Dokuz Eylül University

24 December 2018

_____

Prof. Dr. Gökmen TAYFUR
Supervisor, Department of Civil Engineering
İzmir Institute of Technology

_____

Assist. Prof. Dr. H.Fırat PULAT
Co-supervisor, Department of Civil Engineering, Katip Çelebi University

_____

Prof. Dr. Şebnem ŞEKER ELÇİ
Head of the Department of Civil Engineering

_____

Prof. Dr. Aysun SOFUOĞLU
Dean of the Graduate School of Engineering and Science

ACKNOWLEDGMENT

I would like to thank my thesis advisor Prof. Dr. Gökmen TAYFUR of the Department of Civil Engineering at Izmir Institute of Technology. The door to Prof. Dr. Gökmen TAYFUR office was always open when I ran into a trouble spot or had a question about my thesis or writing.

I would like to thank my thesis co-advisor Assist. Prof. Dr. H. Fırat PULAT and jury members as Prof. Dr. Yeliz YÜKSELEN AKSOY and Prof. Dr. Alper BABA.

I would also like to thank my parents. They always supported me and encouraging me with their best wishes.

ABSTRACT

NUMERICAL INVESTIGATION OF FLOOD INDUCED SEEPAGE UNDER LEVEES

Flood creates the most complex problems of engineering hydrology and extreme flood contains the crucial risk for urban areas, infrastructure, industry and agriculture.

The aim of this paper is to study the transient flow caused by flood for levee of Filyos River. Numerical modeling based on finite element method was performed in the analyses. Plaxflow is an add-on module to Plaxis 2-D, is used for the time variation of seepage in several points of interest within the levee. Transient exit velocity at several points of interest within the levee and degree of saturation of levee and hydraulic gradient were investigated based on whether the levee contained covered materials (riprap, filter and geocomposite materials) along upstream face of levee or not. In addition, under seepage of water through different soil types underneath Filyos levee was examined. Moreover, the results of transient flow analyses when piping occurred and sand boil formed were presented for different soil types.

Key Words: Seepage, Transient flow, Levee, Flood, Finite Element Method

ÖZET

SEDDELER ALTINDAKİ TAŞKIN SEBEPLİ SIZMANIN SAYISAL ARAŞTIRILMASI

Taşkın, mühendislik hidrolojisinin en karmaşık problemlerini meydana getirir ve aşırı taşkın kentsel alanlar, altyapı, endüstri ve tarım için hayati risk taşır.

Bu çalışmanın amacı Filyos nehrinin seddeleri için taşkından kaynaklanan geçici(süreksiz) akışı incelemektir. Analizlerde sonlu elemanlar yöntemine dayalı sayısal modelleme yapılmıştır. Plaxis 2-D'nin eklenti modülü olan PlaxFlow yazılımı seddenin birçok noktasında sızmanın zamana bağlı değişimi için kullanılmıştır. Seddenin ilgili birçok noktasındaki geçici (süreksiz) çıkış hızı, doygunluk derecesi, hidrolik eğimleri ve seddenin nehir akış yüzeyi boyunca kaplama materyali veya materyalsiz (riprap, filtre, geokompozit materyaller) incelenmiştir. Buna ek olarak, sedde altındaki sızma da incelenmiştir. Ayrıca borulanma ve kaynama oluşumu geçici (süreksiz) akış analiz sonuçlarına göre farklı zemin tipleri için gözlemlenmiştir.

Anahtar Kelimeler: Sızma, Geçici (süreksiz) akış, Sedde, Taşkın, Sonlu Elemanlar Metodu

TABLE OF CONTENTS

LIST OF FIGURES

LIST OF TABLES

CHAPTER 1

INTRODUCTION

1.1. General

Floods is one of the most complex and important problems of engineering hydrology. It is a widespread problem in many countries, including Turkey. They form the risk for urban areas, infrastructure, industrial structures and agriculture. There are several reasons, causing the floods, such as extreme rainfall, snowmelt, storm surge, and collapse of dams. Due to the climate change, this event is frequently observed in places where the rainfall amount is quite low throughout a year. For example; the rainfall amount is less than 100 mm/year in Wadi Dayqah river basin in Oman, yet the peak flow rates can reach up to 10,000 m^3/s (Kutoglu 2005). Limpopo river in Mozambique reaches peak flow rates up to 10,000 m^3/s where the annual rainfall amount is higher than 100 mm/year (Kutoğlu 2002).

In order to mitigate the effects of floods due to the overflow of rivers, the levees are constructed along a river sides all over the world, including Turkey. Seepage is the main problem that can cause the failure of a levee and therefore the control of this event is quite important.

1.2. Problem Statement and Scope of the Study

The aim of this thesis was to study the transient seepage flow caused during floods for the levees of Filyos River, located in Zonguldak. Numerical modeling based on finite element method performed the analyses. In particular, Plaxflow is an add-on module to Plaxis 2-D and it was used for the transient variation of flow in several points of interest within these structures. Transient exit velocities at the levee toe, seepage forces, and hydraulic gradients were investigated according to whether levee contains geomembrane. In addition, the underseepage of water through different soil types below Filyos levees were studied and the results of the transient flow were analyzed when piping occurs and sand boil forms.

1.3. Organization of the Thesis

This thesis is composed of eight chapters. The contents of each chapter are summarized as follows:

Chapter 1 consists of three subtitles. The first subtitle is general of the thesis, which includes definition of a flood, natural disasters induced flood and aim of this study.

Chapter 2 starts with the background information study about the flood events globally and levee applications all over the world.

Chapter 3 gives brief description about the hydraulogic accounts and Darcy Law, including seepage affecting factors. Further, differences between steady or unsteady model for anlaysis. Additionally, deformation induced seepage from soil to upward subjects are studied.

Chapter 4 presents levee design and further, seepage problems and including geosynthetic materials for protecting seepage surface.

Chapter 5 contains levee design and cross sections of Filyos Levee.

Chapter 6 presents the details of the soil properties and unit hydrograph of Filyos basin.

Chapter 7 gives finite element analysis methods in Plaxflow software program.

Chapter 8 gives discussion of results and it presents aprooaches about piping, sand boils and heaving from different autors.

Chapter 9 provides conclusions and the scope for further research; this chapter is followed by references and then Appendix A and B.

CHAPTER 2

BACKGROUND

2.1. Introduction

Flood disasters are natural events that have caused the death of many people, environmental destruction and economic loses. Figure 2.1 shows the distribution of disasters where flood related one forms 14% of all the disasters.

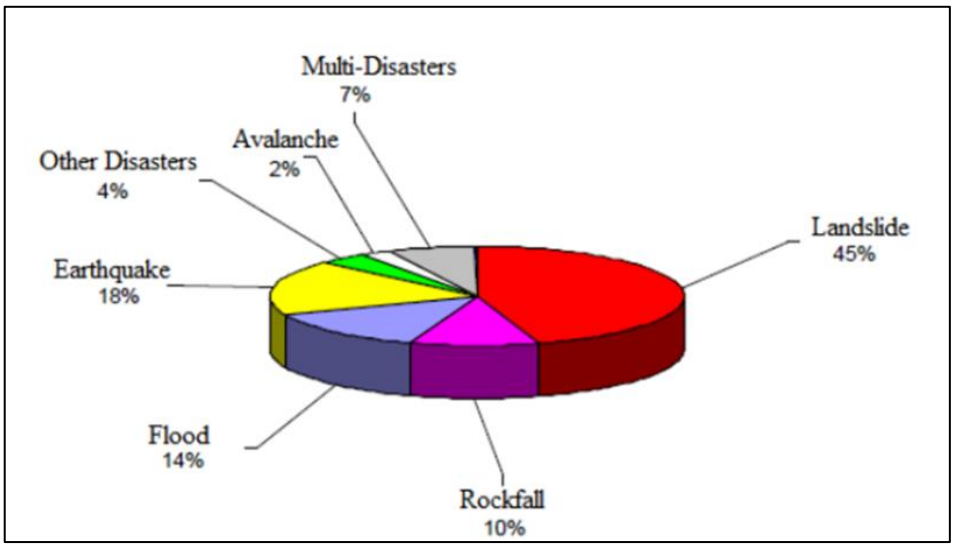

Figure 2.1 Distribution of type of disaster (Source: Gulbahar 2016)

A flood is defined as the unusually high state of a river. For protection, reliable hydraulic structures must be constructed according to the magnitude and characteristics of the projected floods. Also, the soil properties of flood region must be known aprior. Levees are constructed along rivers to protect the surrounding areas. Figure 2.2 shows some examples of levee applications in the world.

A sudden increase in flow rate can destroy the protective barries a long the rivers (Rinaldi and Casagli 1999). Overtopping, internal erosion of banks due to seepage and settling of the structure are the most frequent causes of failures. The most dangerous phenomenon is the seepage under and within levees.

Levee Applications in The World	
(1)-San Joaquin River Levee California USA	
(2)-Mississippi River Levee USA	
(3)-Queensland River Levee Australia	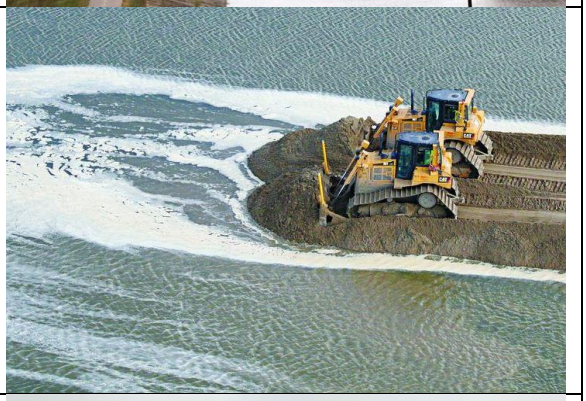
(4)- Filyos river levee Zonguldak/Turkey	

Figure 2.2 Levee applications in the world

Seepage analysis is a very important part of geotechnical and hydrological engineering. It involves basic geotechnical problems which are seepage failures, contamination of ground water, slope stability issues, foundations and design of earthfill structures. Figure 2.3 shows some examples of failed on levees such as erosion and sand boil formation.

Figure 2.3 Erosin and Sand Boil formations Mississipi and Louisiana river levee (Source: Sherman 2008)

These seepage failures are generally protected with levees of clay material, rock fill, concrete bags, breakwaters, sheet pile walls etc.

CHAPTER 3

CALCULATION METHODS AND LITERATURE REVIEW

3.1. Flood Prediction Methods

One of the purpose of hydrological studies is the determination of flooding extend that may occur in a river basin. The peak discharge of flood hydrograph should be calculated for the maximum flood that any structure can safely pass. The hydrologic and meteorologic data are the most important parts of any flood hydrological analysis during and after severe flood events. They are deterministic and statictical methods for calculating flood/peak discharge.

3.2. Deterministic Methods for Flood Hydrograph Predictions

In the design of storage structures on rivers, not only the flood peaks but also the hydrograph of recurrence must be determined. The shape of the hydrograph varies based on the characteristics of the drainage area and rainfall that produces the flood.

3.2.1. Unit Hydrograph Method

Sherman (1932) was the first person who proposed the unit hydrograph concept. The unit hydrograph is described as the direct runoff hydrograph resulting from a unit volume of excess rainfall of constant intensity and uniformly distributed over the drainage area. Unit hydrograph is obtained from either the observed values or synthetically. Figure 3.1 and Figure 3.2 show general unit hydrograph diagrams during a flood.

The variables of unit hydrograph diagrams stand for time of rise (T_R): the time from the start of rainfall excess to the peak of the hydrograph, (t_p): the time from the center of mass of rainfall excess to the peak of the hydrograph. The time it takes for water to propagate from the most distant point in the watershed to the outlet is called the time of concentration (t_c).Time base (T_b): the total duration of the DRO hydrograph.

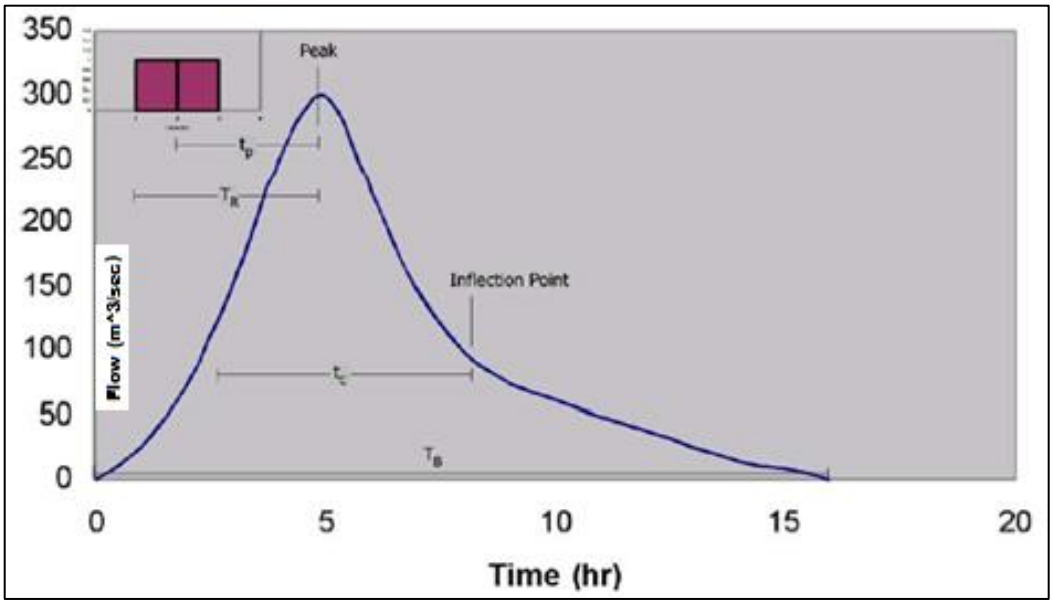

Figure 3.1 Unit Hydrograph members (Source: Nptel 2008)

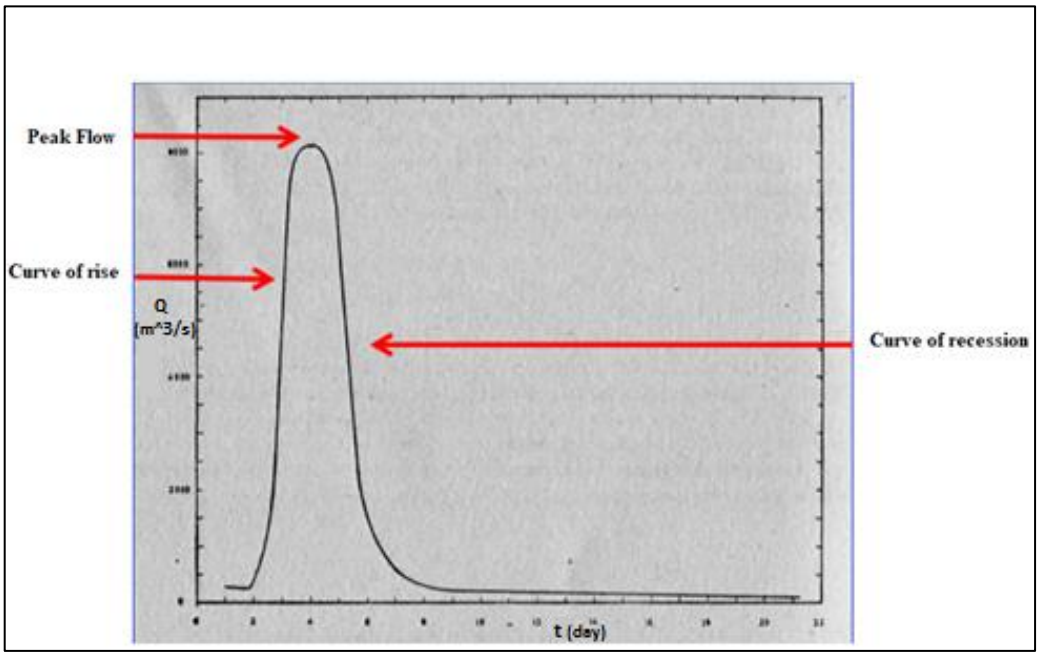

Figure 3.2 Change of flow in a river section according to time (Source: Aki 2018)

3.2.1.1. Synthetic Method

Synthetic unit hydrographs allow the calculation of flood values that may occur from river basins without long-term reliable flow observations. The Synthetic Method is used when time to peak t_p > 2 hour and the drainage area < 1000 km². Figure 3.3. shows relation between the yield for 1mm flow and drainage area. Equation 3.1 and 3.2 uses to obtain yield for 1mm flow.

$$S = \left(\frac{10}{\sum \frac{1}{\sqrt{s_i}}} \right)^2 \tag{3.1}$$

S = Harmonic slope of the longest river reach

L = Length of levee *(km)*

L_c = Length of between the centry of gravity of basin and exit point of basin *(km)*

$$Curve\ Number = \left(\frac{L \times L_c}{\sqrt{S}} \right) \tag{3.2}$$

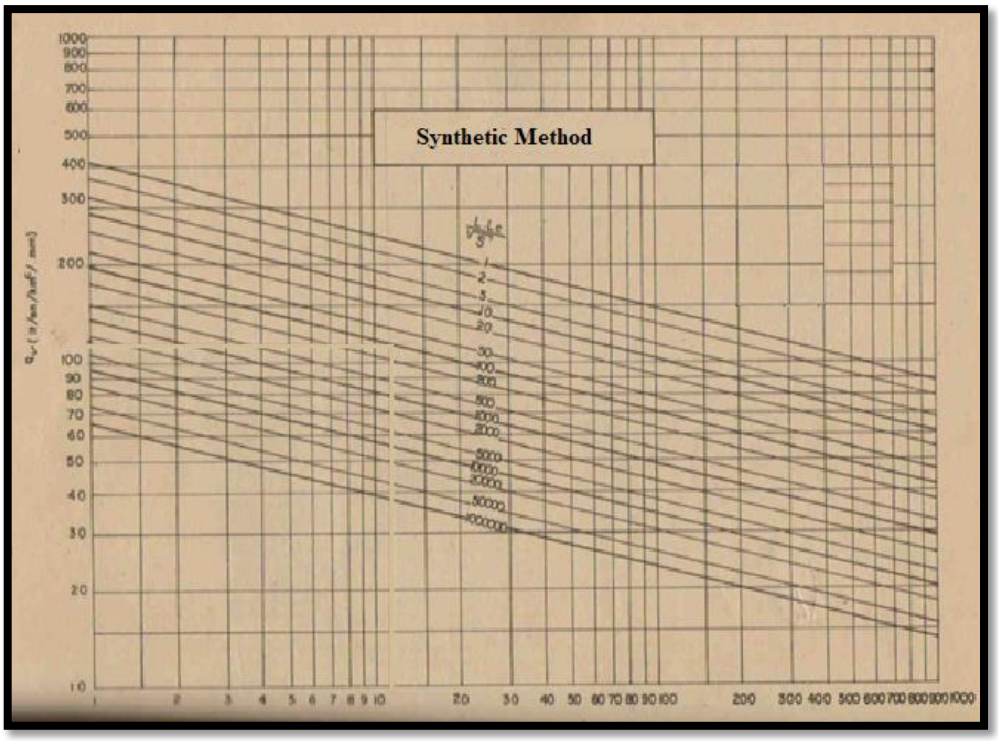

Figure 3.3 Synthetic Method (Source: Aki 2018)

$Q_P = A.1.q_v.10^{-3}$ (m^3/sec) (Peak discharge of unit hydrograph) (3.3)

$$T_p = \frac{A \cdot 0.001 \cdot 10^6}{a \cdot Q_p} \text{ (Time of rise of unit hydrograph)} \quad (3.4)$$

A = Drainage area (km^2)

q_v = The yield for 1mm flow *(lt/sec/km^2/mm)*

3.2.1.2. Mockus Method

Victor Mockus developed Mockus Method (Gulbahar 1949). It is easy to apply and to draw triangular hydrograph. Triangular hydrographs generally are sensitive like other normal hydrographs. This method is applied when the concentration time less than or equal 30 minutes in the basin (Usul 2008).

The formulas are as follows;

$$T_c = 0.00032.\left(\frac{L_h}{S^{0,385}} \right)^{0,77} \quad (3.5)$$

$$D = 2.T_c^{1/2} \quad (3.6)$$

$$\Delta D = \frac{T_c}{S} \quad (3.7)$$

$$T_p = 0.5 \cdot \Delta D + 0.6 \cdot T_c \quad (3.8)$$

$$q_p = \frac{K.A}{T_p} \quad (3.9)$$

$$Q_p = q_p.h_a \quad (3.10)$$

Where;

T_c = time of concentration (h)

L_h = the length of drainage area (m)

S = average slope of drainage area (%)

D = time of duration of precipitation (h)

ΔD = time of heavy rainfall (h)

T_p = the time of duration for peak discharge (h)

h_a = annual rainfall depth of 100 years (cm)

k = coefficient of basin (0.21-1.60)

q_p = discharge generated by 1 mm rainfall

Q_p = discharge generated by 100 years rainfall (m^3/s)

3.2.1.3. Snyder Method

Snyder Method was developed by Snyder in USA in 1938 and it is one of the synthetic methods to generate unit hydrograph. This method considers the basin characteristics which are area, shape, topography, channel slope, and stream density. As basin coefficients are not determined in all basins in Turkey, this method may not be used in Turkey (Ozbek *et al.* 1987).

The formulas are given as follows;

$$T_r = \frac{T_p}{5.5} \tag{3.11}$$

$$T_p = 0.75 \cdot C_t \cdot (L \cdot L_c) \cdot 0.3 \tag{3.12}$$

$$q_p = \frac{2.75 \cdot C_p}{T_p} \tag{3.13}$$

$$T_p = T_{PR} + 0.25\left(T_r - T_R\right) \tag{3.14}$$

Where;

T_r : effective precipitation

T_p : basin delay (h)

q_p : peak discharge per unit area ($m^3/sec/km^2$)

C_p : basin coefficient

C_t : basin coefficient

Basin coefficients of Table 3.1 use to create unit hydrograph of Snyder method. C_t and C_p values are used to calculate equation 3.12 and 3.13.

Table 3.1 Basin coefficients (Source: Celik 2012)

Soil Types	C_t	C_p
Sandy	1.65	0.56
Peat	1.50	0.63
Clayey and Gravelly	1.35	0.69

Figure 3.4. is used to find width of hydrograph. $0.75\,q_p$ and $0.50\,q_p$ is equal to Tw75 and Tw50 to obtain unit hydrograph like a Fig. 3.5. via found q_p (peak discharge).

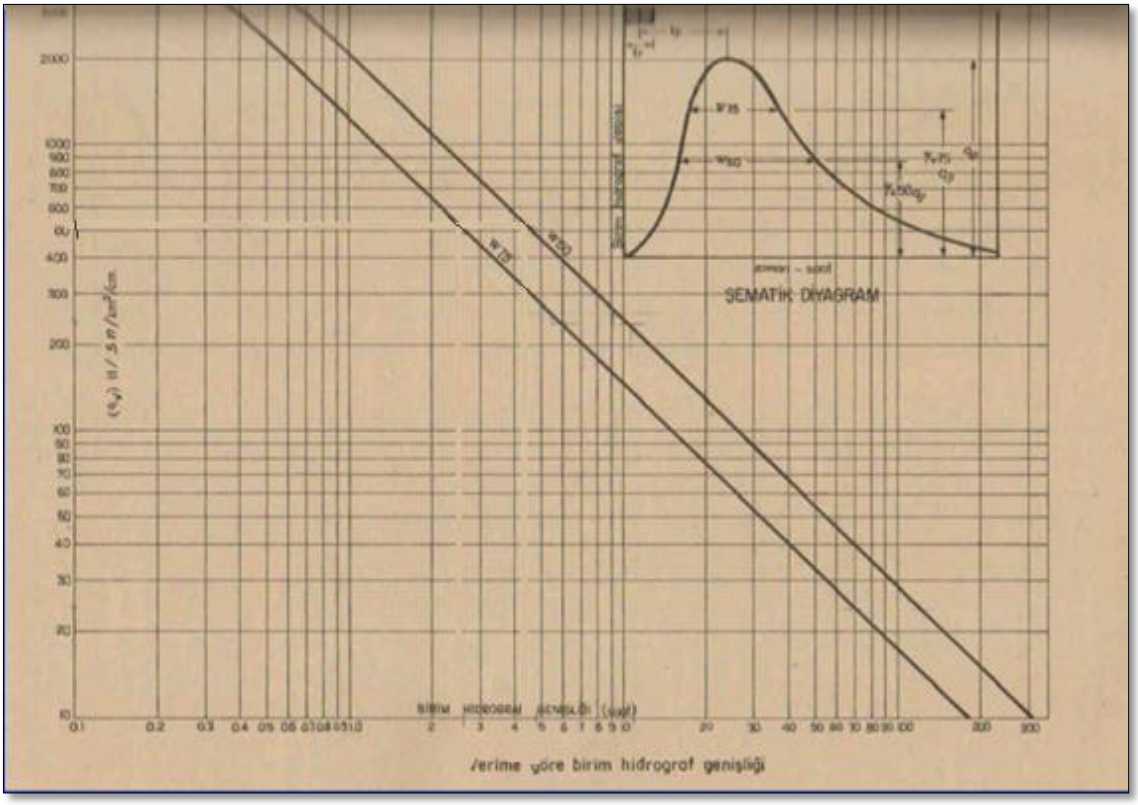

Figure 3.4 Relation of between width of hydropraph and flow field (Source: Celik 2012)

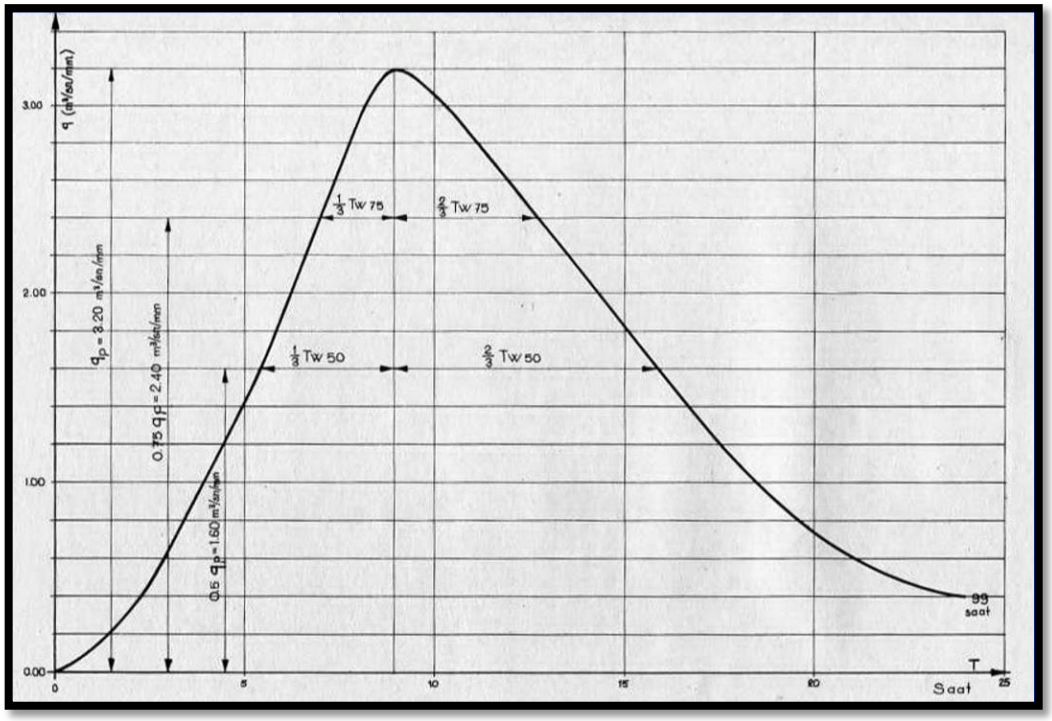

Figure 3.5 Unit Hydrograph of Snyder Method (Source: Celik 2012)

This formula has also some limitations. If $T_{PR} = 5.5.T_r$ then, $T_R = T_r$ and $q_{PR} = q_p$ can be taken, C_t and C_p can be obtained above Table 3.1 C_t and C_p are functions of basin characteristics and slope. If t_{PR} is different from $5.5.T_r$; then basin lag calculated with the following formula;

$$T_p = T_{PR} + 0.25\left(T_r - T_R\right) \tag{3.15}$$

Where;

T_r : effective precipitation

T_p : basin delay (h)

T_R : time of rise

T_{PR} = determining basin delay

3.3. Calculation of Flood Peak

Flood peaks must be known to project levee design. Each river has a flood peak. Besides, different rainfalls form different flood peaks.

3.3.1. Empirical Formulas

There are several methods to determine flood hydrograph and these are empirical formulas and statistical methods. Rational method is used as empirical formulas.

3.3.1.1. Rational Method

The formula 3.16 are used to determine the largest flood that the river brings. (Ozal 1972). The method usually gives good results for areas smaller than 5 km². Runoff coefficient changes depending on vegetation, a permeability of soils and slope of the basin. Table 3.2 shows c values in the rational form.

$$Q = c.I.A \tag{3.16}$$

Q : Flood peak (m^3/s)

I : Rainfall intensity (m/s)

c : The coefficient

A : Precipitation area (m^2)

Table 3.2 c values in the rational form (Source: Ozal 1972)

Topography and Vegetation		Soil Type		
		Pervious Sandy	Clayey and Moist	Impervious and Clayey
Forestlike	Plain (%0-5 slope)	0.10	0.30	0.40
	Wavy (%5-10 slope)	0.25	0.35	0.50
	Defective (%10-30 slope)	0.30	0.58	0.60

(cont. on next page)

Table 3.2 (cont.)

Topography and Vegetation		Soil Type		
		Pervious Sandy	Clayey and Moist	Impervious and Clayey
Pasture	Plain	0.10	0.30	0.40
	Wavy	0.16	0.36	0.55
	Defective	0.22	0.42	0.60
Agricultural Field	Plain	0.30	0.50	0.60
	Wavy	0.40	0.60	0.70
	Defective	0.52	0.72	0.82
Urbanized Area		%30 impervious	%50 impervious	%70 impervious
	Plain	0.40	0.55	0.75
	Wavy	0.50	0.65	0.80

The concentration time in the rational method is calculated by the following equation;

$$T_c = 0.02\left(\frac{L^{3/2}}{H^{1/2}}\right)^{0.77} \tag{3.17}$$

T_c = Concentration Time (hr)

H = Harmonic slope (m)

L = The main waterway of the canal basin to the vertical projection of the center of gravity point of the distance between the point where the basin exits (m)

3.3.2. Statistical Methods for Flood Hydrograph

One of the methods used to create the flood hydrograph is statistical methods and one of the these methods is frequency analysis. They are Normal Distrubutions, Log-Normal Distributions and Gumbel Distributions.

3.3.2.1. Frequency Analysis

Flood frequency analysis may be investigated on the past record data of annual flood peak discharges estimated by a suitable method. Otherwise, freguency analysis relies on the available record of annual rainfall events of the region.

Estimating the future probabilities of occurance and predicting the magnitude of an event corresponding to a specific return period are investigated by flood frequency analysis studies. Predicition of flood flow of large return periods may be found and this is in retun can be used to extrapolate the magnitude outside the observed of range of data.

There are a number of probability distributions f(x), which are used by many statisticians. The more common are (Lindeboom 2011) :

1. Normal distribitions
2. Log-Normal (II ve III parameter)
3. Gumbel distributions

3.3.2.1.1. Normal Distributions

One of the most important distributions is the Normal Distribution in statistical hydrology. It is used to provide empirical distributions with skewness coefficient close to zero. The probability density function (PDF) of the distribution is given by (Lindeboom 2011):

$$f(x) = \frac{1}{\sigma\sqrt{2\pi}} \exp\left[-\frac{1}{2}\left(\frac{x-\mu}{\sigma} \right)^2 \right]; \qquad -\infty < x < \infty \tag{3.19}$$

Where, μ is the location parameter (mean value) and σ is the scale parameter (standard deviation). The cumulative distribution function (CDF) of the normal distribution is given by (Lindeboom 2011):

$$F(x) = \frac{1}{\sigma\sqrt{2\pi}} \int_{-\infty}^{x} \exp\left[-\frac{1}{2}\left(\frac{x-\mu}{\sigma} \right)^2 \right] \tag{3.20}$$

3.3.2.1.2. Log – Normal Distributions

If the logarithms, lnx, of a variable x are normally distributed, the variable x is log normally distributed so that (Lindeboom 2011):

$$f(x) = \frac{1}{x\sigma_y\sqrt{2\pi}} \exp\left[-\frac{1}{2}\left(\frac{x-\mu}{\sigma_y}\right)^2\right] \tag{3.21}$$

Where, μ_y and σ_y are the mean and standard deviation of the natural logarithm of x. The variable x has a lower boundary x_0, different from zero, and the variable $z = x - x_0$, follows a lognormal distribution, then x is log normally distributed with three parameters. The probability distribution function of the lognormal distribution with parameters is (Lindeboom 2011):

$$f(x) = \frac{1}{(x-x_0)\sigma_y\sqrt{2\pi}} \exp\left[-\frac{1}{2}\left(\frac{In(x-x_0)-\mu_y}{\sigma_y}\right)^2\right] \tag{3.22}$$

Where, μ_y (mean value), σ_y (standard deviation) and x_0 are named the scale, the shape and the location parameters respectively. Parameter x_0 is generally estimated by trial and error.

3.3.2.1.3. Gumbel Distributions

Gumbel distribution is a member of family of Extreme Value distributions with the value of parameter k = 0. It has a two parameter distribution and is often used in hydrology.

The PDF is given as (Lindeboom 2011):

$$f(x) = \frac{1}{a} \exp\left[-\frac{x-\mu}{a} - \exp\left\{-\frac{x-\mu}{a}\right\}\right] \tag{3.23}$$

And CDF is given as (Lindeboom 2011);

$$F(x) = \exp\left[-\exp\left\{-\frac{x-\mu}{a}\right\}\right] \tag{3.24}$$

3.4. Methods for Determining Parameters

Knowledge of soil properties is important for seepage analysis. These soil properties are permeability of soils, hydraulic gradients, specific gravity and void ratio.

3.4.1. Permeability of Soils

Soil permeability is a property of the soil transmitting water and it is one of the most important qualities to consider for seepage analyses. Permeable materials generally contain continous voids. The more permeable the soil is the greater the seepage. Some soils are so permeable hence it is not possible to build hydraulic structures without techniques. The permeability of soils is really important to determine the effect on stability of foundations, seepage loss through embankments of reservoirs, drainage of subgrades, excavation of open cuts in water bearing sand, rate of flow of water into wells and many others. Soil permeability is influenced by many factors such as pore size, particle shape, particle density, fluid density and number of pores. Finer soil texture shows slow permeability. Darcy developed an empirical formula for the behavior of flow through saturated soils in 1856. Figure 3.6 presents relation between the flow velocity and hydraulic gradients based on Darcy's Law.

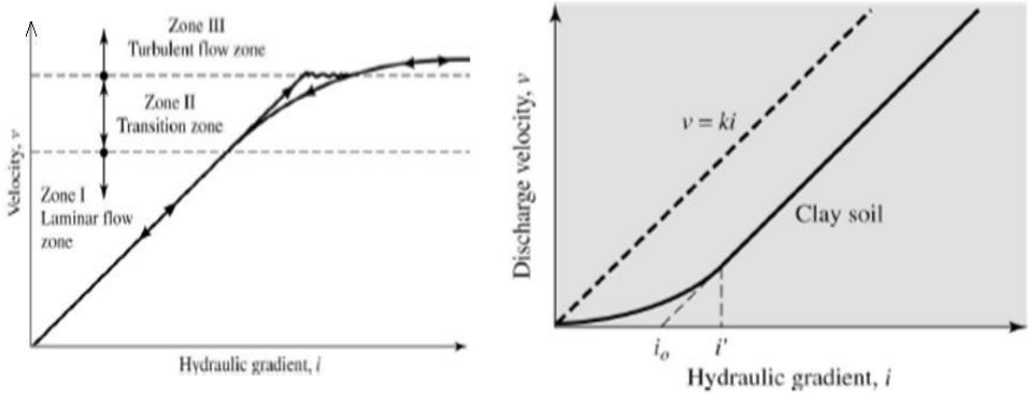

Figure 3.6 Between the flow velocity and hydraulic gradients (Source: Das 2010)

3.4.2. Darcy's Law

According to Bernoulli's energy theorem, the total head for the current from any section of the ground, is given as fallows;

$$H = z + \frac{p}{\gamma_w} + \frac{v^2}{2g} \tag{3.27}$$

Where ;

H =Total head;

z =Gravity head;

p / γ_w = Pressure head

$v^2 / 2g$ =Velocity head

p =pressure (pa)

v =seepage velocity (m/s)

γ_w =unit weight of water (kN/m^3)

g =gravity acceleration (m/s^2)

z =elevation head in (m)

First term and second term of this equation include influences of hydrostatic and artesian. Velocity head can be neglected due to the very slow water movement.

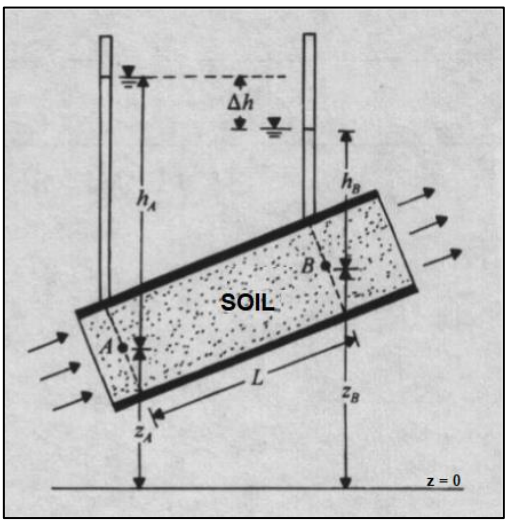

Figure 3.7 Darcy Law (Source: Das 1997)

Accordingly Fig. 3.7, Total heads in sections A and B;

Total Head $A = z_A + h_A$ (3.28)

Total Head $B = z_B + h_B$ (3.29)

where;

z_A =elevation head from $z = 0$

z_B =elevation head from $z = 0$

h_A=difference between the total head A and elevation head from $z = A$

h_B=difference between the total head B and elevation head from $z = B$

Loss of head between cross section A and B (Δh);

$$\Delta h = \left(z_A + h_A\right) - \left(z_B + h_B\right) \quad (3.30)$$

Hydraulic gradient (i); $i = \Delta h / L$ (3.31)

where;

L =Length of soil piece

In 1856, Darcy found a linear relationship between the seepage velocity and hydraulic gradient.

$$v = k.i \quad (3.32)$$

where;

v=seepage velocity (m/s)

k =soil permeability (m/s)

i = Hydraulic gradient

Accordingly, Seepage quantity (q)

$$q = k.i.A \quad (3.33)$$

where;

k =soil permeability (m/s)

i = Hydraulic gradient

A =cross sectional area is perpendicular to the flow direction (m^2)

Permeability is a really important for geotechnical engineering and;

1. Permeability effects settlement under the load in saturated soils.
2. Slopes and retaining structures of stability influences permeability of soils.
3. Filters of soils are designed based on permeability.

Figure 3.8. presents soil permeabilities values for each soil types.

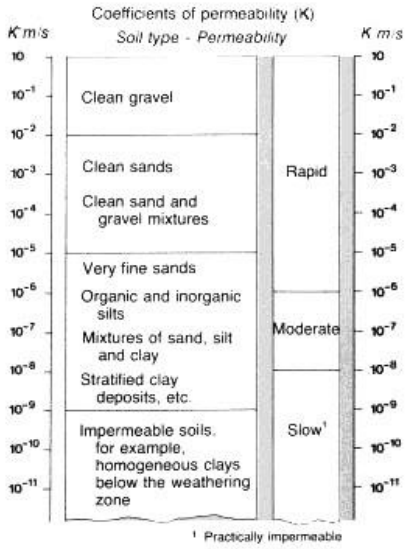

Figure 3.8 Soil permeability classes (Source: Das 1999)

3.4.3. Empirical Relations for Hydraulic Conductivity

There are several empirical relations to determine hydraulic conductivity. These empirical relations are applied coarse-granular soils and fine-grained soils.

3.4.3.1. Coarse-Granular Soils

Permeability is influenced by some of the factors such as grain size, void ratio etc. The smaller the grain size, the smaller the voids which induce the reduced size of flow channels and lower permeability. Seepage prevention methods are important for levees. Filter sands is which has several permeability calculations for seepage prevention elements of levees. Hazen (1892) developed extensive investigation of filter sands. The hydraulic conductivity of filter sands can be determined using equation 3.34.

$$k\ (\text{m/s}) = c.D_{10}^2 \tag{3.34}$$

where;

k =hydraulic conductivity

D_{10} =effective grain size (mm)

$c = 10^{-2}$

Chapius (2004) developed extensive investigation of sands. Accordingly Chapius, the hydraulic conductivity of sands can be determined using equation 3.35.

$$k\ (\text{cm/sec}) = 2.4622.(D_{10}^2.\frac{e^3}{1+e})^{0.7825} \tag{3.35}$$

where;

k =hydraulic conductivity

D_{10} =effective grain size (mm)

e = void ratio

Figure 3.9 presents Hazen equation and data relating hydraulic conductivity of granular soils.

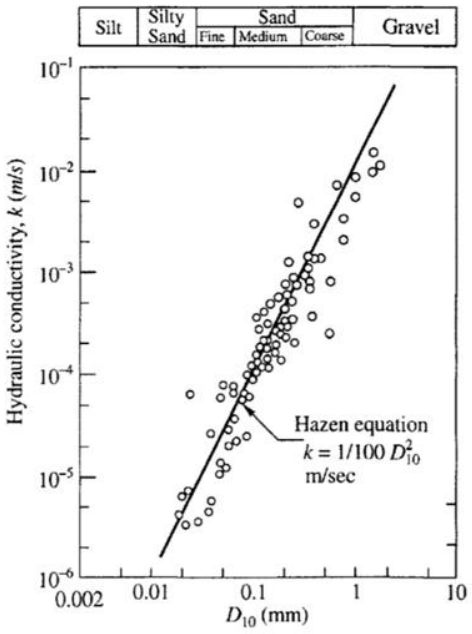

Figure 3.9 Hazen equation and data relating hydraulic conductivity and D_{10} of granular soils (Source: Louden 1952)

3.4.3.1.1. Hydraulic Conductivity as a Function of Void Ratio for Granular Soils

There are three types of relationships between permeability and void ratio in granular soils. These relations are presented in Figure 3.10.

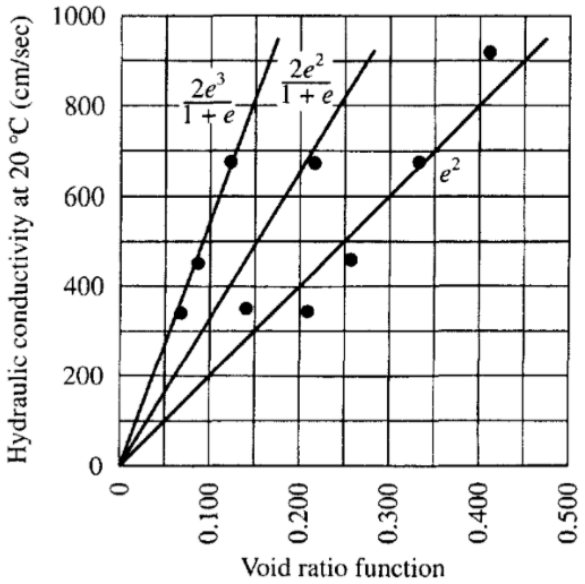

Figure 3.10 Relationship between void ratio and permeability for coarse grained Soils (Source: Das 1999)

3.4.3.1.2. Fine-Grained Soils

Hydraulic conductivity of very fine grained soils does not depend on void ratio due to a rapid decrease in the value of k for clays below the plastic limit as Figure 3.11 and Figure 3.12. Equation (3.36) shows how calculates soil permeability according to fine-grained soils.

$$k = c.\left(e^n / \left(1+e\right)\right) \tag{3.36}$$

where;

c and n = constant determined experimentally

e = void ratio

k= soil permeability

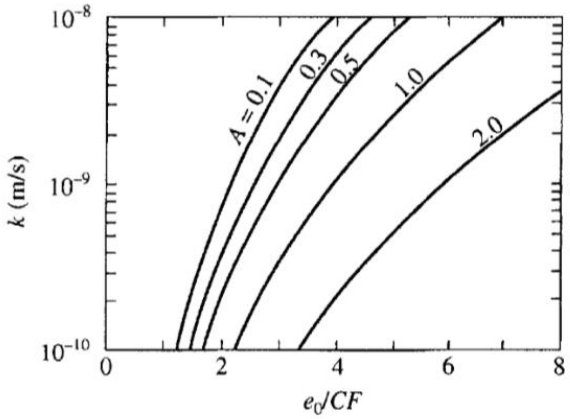

Figure 3.11 In situ permeability of soft clays in relation to initial void ratio, e_o; clay fraction; CF; and activity A (Source: Mesri *et al*. 1994)

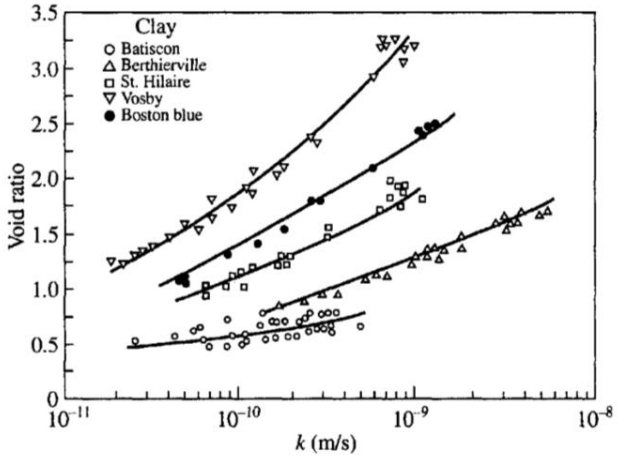

Figure 3.12 Results of falling-head and constant-head permeability tests on undisturbed samples of soft clays (Source: Terzaghi *et* al. 1996)

3.5. Seepage and Erosion

There are several analyses on levees and that is a seepage analyses. Seepage analyses may be solved numerical or analytical methods.

3.5.1. Seepage

The interaction between soils and percolating water influences the design of foundations and earth slopes and the quantity of water that lost by leakage through some

hydraulic structures. Foundation failures happens due to excess pressure of water which tries to lift up the soil on downstream sides of some hydraulic structures.

3.5.1.1. Mathematical Appreciation of Seepage

Mathematical appreciation of seepage is a analytical methods for seepage problems. One of the this method is a Laplace Equation.

3.5.1.1.1. Laplace Equation

Some assumptions were made in the Laplace Equation. These;

1- Darcy's Law is valid.
2- Soil is homogenous and saturated.
3- Soil and water aren't compressed.
4- Volume change is not occured.

Soil prism (Fig. 3.13) is created at A point to obtain the continuity equation of flow. The incoming flow is given to the prism in x, y and z directions according to Darcy's Law.

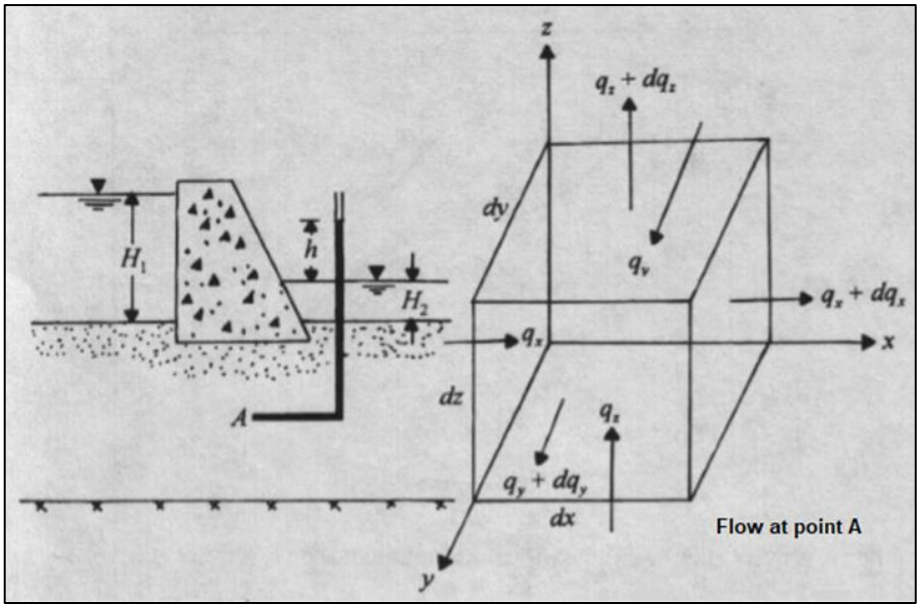

Figure 3.13 Formation of the Continuity Equation (Source: Das 1999)

$$q_x = k_x.i_x.A_x = k_x.\frac{\delta h}{\delta x}.dy.dz \qquad (3.37)$$

$$q_y = k_y.i_y.A_y = k_y.\frac{\delta h}{\delta y}.dx.dz \tag{3.38}$$

$$q_z = k_z.i_z.A_z = k_z.\frac{\delta h}{\delta z}.dx.dy \tag{3.39}$$

The flows in the x,y,z directions from the prism.

$$q_x + d.q_x = k_x.\left(i_x.d.i_x\right).A_x = k_x\left(\frac{\partial h}{\partial x} + \frac{\partial^2 h}{\partial x^2}.d_x\right).d_y.d_z \tag{3.40}$$

$$q_y + d.q_y = k_y.\left(i_y.d.i_y\right).A_y = k_y\left(\frac{\partial h}{\partial y} + \frac{\partial^2 h}{\partial y^2}.d_y\right).d_x.d_z \tag{3.41}$$

$$q_z + d.q_z = k_z.\left(i_z.d.i_z\right).A_z = k_z\left(\frac{\partial h}{\partial z} + \frac{\partial^2 h}{\partial z^2}.d_z\right).d_x.d_y \tag{3.42}$$

Laminar flow in a incompressible environment, the flow entering and leaving the prism is equal to each other.

$$q_x + q_y + q_z = \left(q_x + d.q_x\right) + \left(q_y + d.q_y\right) + \left(q_z + d.q_z\right) \tag{3.43}$$

By combining the equations;

$$k_x.\left(\frac{\partial^2 h}{\partial x^2}\right) + k_y.\left(\frac{\partial^2 h}{\partial y^2}\right) + k_z.\left(\frac{\partial^2 h}{\partial z^2}\right) \tag{3.44}$$

For two-dimensional flow in the XZ plane, equation;

$$k_x.\left(\frac{\partial^2 h}{\partial x^2}\right) + k_z.\left(\frac{\partial^2 h}{\partial z^2}\right) = 0 \tag{3.45}$$

If soil is isotropic, the continuity equation is; $\left(k_x = k_z = k\right)$

$$\left(\frac{\partial^2 h}{\partial x^2}\right) + \left(\frac{\partial^2 h}{\partial z^2}\right) = 0 \tag{3.46}$$

This equation is generally called the Laplace equation.

3.5.2. Erosion

Erosion is called that soil particles are removed and carried with the water flow deu to the fact that erosion resistant forces are less than seepage forces. The soil erosion problems may occur in river banks and factors affecting soil erosion are the erodibility of the soil, the water velocity inside the soil mass or the water velocity on a river and geometry of levee. Figure 3.14 shows evidences of instability in river embenkments caused by erosion.

Figure 3.14 Evidences of instability in river embenkments caused by erosion
(Source: Jeanmonod and Rebecca 2018)

If the hydraulic gradient reaches the critical hydraulic gradient, the balance in the soil mass is distorted and it moves up. The soil surface floots and the soil – water mixture exit on the surface. This is called piping or internal erosion. Heaving observes when seepage forces push the substrata upward. Figure 3.15 presents heave potential at the toe of an levee. Heave, piping and erosion were classified as seepage erosion failures by Zyl and Harr (1981). Exit gradient is called that is the hydraulic gradient at the downstream end of the flow line where percolating water leaves the soil mass and emerges into the free water at the downstream(Whitman *et* al. 1979). Terzaghi(1921) developed an exit gradient approach to seepage forces exerted by the upward flow of water and the vertical downward weight of the submerged soil. It is given as;

$$i_c = \frac{\gamma'}{\gamma_w} = \frac{G_s - 1}{1 + e} \tag{3.47}$$

where;

i_c = critical hydraulic gradient

γ_{sub} = submerged unit weight of soil

γ_w = unit weight of water

G_s = specific gravity of soil

e = void ratio of soil

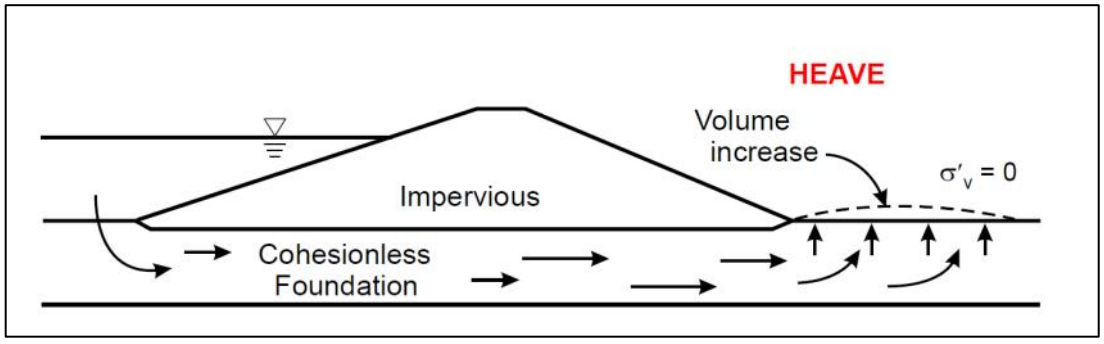

Figure 3.15 Heave Potential (Source: Pabst *et* al. 2012)

If i_{exit} is higher than $i_{critical}$, soil grain is washed and piping occurs for granular soils. According to Casagrande (1937), Khosla (1936), Harr (1962), Khilar (1985) presented the following equation as a measure of the critical gradient to cause piping;

$$i_c = \frac{\tau_c}{2.878.\gamma_w}.\left(\frac{n_o^{0.5}}{K_o}\right) \tag{3.48}$$

where;

τ_c =critical tractive shear stress (kN/m^2)

n_0 =initial porosity

K_0 =initial intrinsic permeability (a typical value is, $K_0 = 10^{-10}$ cm^2)

Sherard et al. (1963) studied the mechanics of piping in earth-rock dams. If the erosion resisting forces are lower than the seepage erosive forces, the soil particles are washed away, resulting in the initiation of piping. According to Zyl and Harr (1981), analysis of piping erosion was impossible because of the mechanism by discontinuities. Bligh (1927) and Lane (1935) developed global gradient approaches that are used in the design of dams and levees. Several studies were done about protecting to soil erosion so, a creep coefficient is obtained to choose available filter material. Bligh (1927) defined a creep coefficient as;

$$C = L / h \tag{3.49}$$

L = length of seepage path

h = total head less

Another creep coefficient equation is at below. According to Lane (1935) investigated a weight creep ratio as;

$$c_w = \frac{\frac{L_h}{3} + L_v}{h} \tag{3.50}$$

where;

L_h = distance along horizontal contacts ($< 45^\circ$ measured from the horizontal)

L_v = distance along vertical contacts ($> 45^\circ$ measured from the vertical)

Values of weighted creep ratio are 8.5 to 5.0 for very fine to coarse sand, 4.0 to 2.5 for fine gravel to boulders and 1.8 for hard clay (Lane 1938). Internal erosion begins when fine particles move, resulting in the formation of cavities. This in turn causes the collapse, and thus failure occurs due to the internal erosion. Figure 3.16 shows internal erosion due to migration of fine material into coarse meterial. Table 3.3 presents erosion resistance of soils against to sand boils.

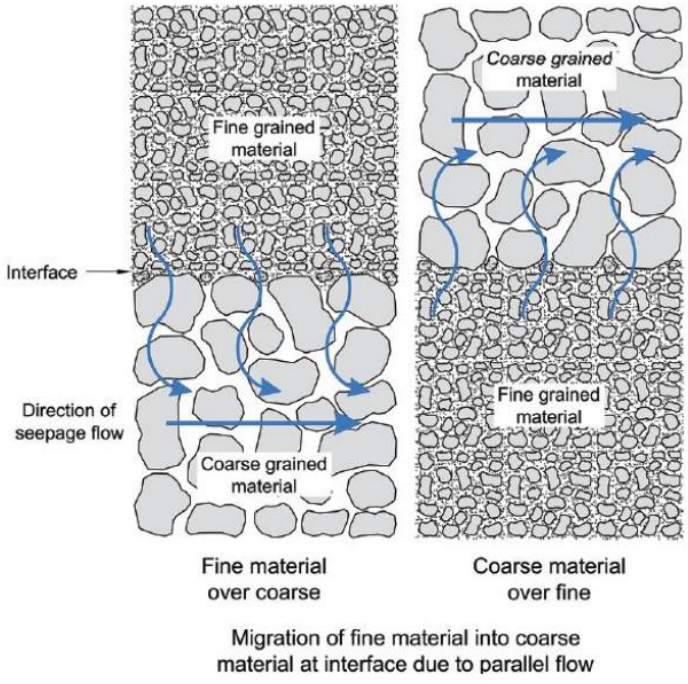

Figure 3.16 Migration of Fine into Coarse Material
(Source: US Department of the Interior Bureau of Reclamation 2015)

Table 3.3 Erosion Resistance of Soils
(Source: US Department of the Interior Bureau of Reclamation 2015)

Erosion	Soil Properties
1. Extremely erodible	All dispersive soils and SM with FC < 30%
2. Highly erodible	SM with FC > 30%, ML, SC, and CL-ML
3. Moderately erodible	CL, CL-CH, MH, and CH with LL < 65
4. Erosion resistant	CH with LL > 65

Critical tractive shear stress may be found from d_{50} size for granular materials (Lane 1935) ($\tau_c(dynes/cm^2) = 10.d_{50}(mm)$. The soil type, rate of head increasing water and flow condition induce seepage erosion failure (Zyl and Harr 1981). Heave leads to cracks and it generally occurs in granular soil with a large percentage of fines in case of flow and piping. Tomlinson and Vaid (2000) stated an experimental study of piping erosion. The critical gradient gradually decreases if the head rapidly increases. The choice of permeability function is important for determining the piping model because the permeability functions depend on grain size and porosity. Eroded sections are generally protected with levees of clay material, rock fill, concrete bags, breakwaters and sheetpile walls etc.

3.5.3. Development of Underseepage and Sand Boils

During a flood, holes or cracks under the levee structure occur due to increase in water pressure. Thus; piping through sand, silty sand, sandy silt and silty soils happens because of underseepage at the levee. A sand boil forms that water seeps through pipes from the water side to the land side of the levee and carries levee foundation material out from under the levee. The critical gradient is the important parameter to cause sand boils or heaving and it estimates by equation (3.51). Critical gradients for silty clay and clay is 0.8 and for silty sands and silts are 0.85 (Turnbull and Mansur 1961). In the field, the critical gradient is determined by;

$$i_c = h_x / z_t \tag{3.51}$$

where;

h_x = head beneath top stratum at distance x landward from landside toe of the levee

z_t = thickness of landside top stratum.

Sand boil formation is influenced by some factors as;

(i) Geological features,

(ii) Properties and thickness of the topsoil,

(iii) Man-made works such as post holes, borrow pits and seismic shot holes,

(iv) Cracks and fissures formed by natural causes,

(v) Organic events such as decay of roots, uprooting of trees and animal burrows.

Seepage was classified as heavy, medium and light by Mansur *et* al. (1956). Mansur observed sand boils in a hydraulic gradient range of 0.5 to 0.8 Table 3.4 shows seepage condition according to different exit gradients of soils.

Table 3.4 Seepage Conditions and Exit Gradients During the 1950 High Water (Source: Turnbull and Mansur 1961)

Seepage Condition	**Amount of Seepage (Q/H)**	**Exit Gradient**
Light to no seepage	< 5 gal/min/100 ft of levee	0-0.5
Medium seepage	5 - 10 gal/min/100 ft of levee	0.2-0.6
Heavy seepage	> 10 gal/min/100 ft of levee	0.4-0.7

Figure 3.17 shows underseepage and through seepage of the levee during high water level. Table 3.5 shows approximate permeability coefficient values for various types of sandy soil.

Table 3.5 Permeability coefficient values of Sandy Soil (Source: Rowe 2001)

Type of Sand	**k(cm/sec)**
Sandy Silt	0,0005~0,0002
Silty Sand	0,0002~0,005
Very Fine Sand	0,005~0,02
Fine Sand	0,02~0,05

(cont. on next page)

Table 3.5 (cont.)

Fine-Middle Sand	0,05~0,1
Middle Sand	0,1~0,15
Middle-Coarse Sand	0,15~0,2
Coarse Sand - Gravel	0,2~0,5

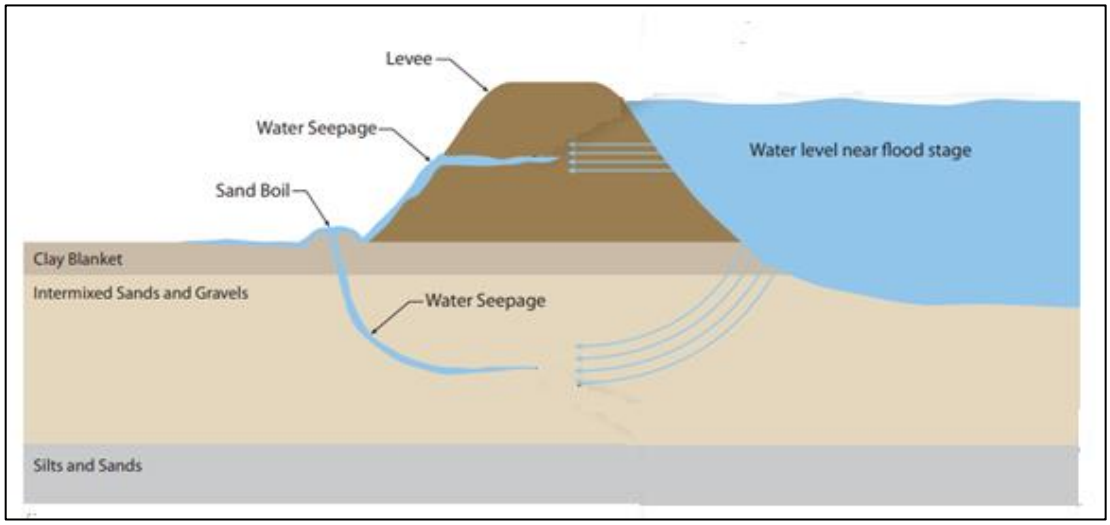

Figure 3.17 Underseepage and through seepage of the levee (Source: USACE 1993)

3.5.4. Investigation Soil Properties for Piping

Peter (1974) presented that grain size distribution curves are the most important tools to determine the danger of piping problems. The coefficient of uniformity, C_u, and the coefficient of curvature, C_c of soils are determined to quantify the danger of piping problems.

$$C_u = \frac{d_{60}}{d_{10}} \tag{3.52}$$

$$C_c = \frac{d_{30}^2}{d_{10}.d_{60}} \tag{3.53}$$

Where;

d_{60} = 60 % of the soil particles are finer than this size

d_{30} =30% of the particles are finer than this size.

d_{10} =10% of the particles are finer than this size.

Piping observes in sandy gravelly soils and this soil has in small quantities of fine particles and values of these soils are d_{10}=0,25 mm, $C_u > 20$, $C_c > 3$ for piping. According to Wit *et al.*(1981), for laboratory research on piping on scale models are fine, medium or coarse sand. In general, higher critical exit gradients observed for the coarser and the denser sand. Li *et al.*(1993) observed that 98 % by weight of eroded grains were smaller than 0.125 mm in diameter for sand boil formation during Mississippi River Flood of 1993. Sherard *et al.*(1972) showed that non cohesive silt, rock flour and very fine sands disperse in water and may be higly erosive.

Harza (1935) investigated the safety of levees against piping. According to these studies, the number of safety against piping is G_s;

$$G_s = \frac{i_{cr}}{i_{exit}} \tag{3.54}$$

where;

i_{cr} = critical hydraulic gradient

i_{exit} = max exit hydraulic gradient

It is recommended that the number of safety is 3-4 for the safety hydraulic sutructures (Das 1997). This number of safety can be taken as 1.5-2 for temporary structures (Das 1999).

3.5.5. Difference Between Steady-State and Transient Seepage Analysis

A steady-state seepage occurs when hydraulic head, flow rate or given soil hydraulic properties are not changing with time. In transient flows, the variables depend on time. Some studies show steady-state seepage as a ‘‘saturated’’ flow condition and transient seepage as a ‘‘partially saturated or unsaturated ’’ flow condition. The soil is partially saturated at and/or above the phreatic surface and saturated below the phreatic surface. Figure 3.18 shows the levees cross section of unconfined steady-state seepage.

Riverside and flood side water level is at the elevation for a finite period of time when a steady-state seepage analysis applies on a dam or levee. Put it differently, flow is constant, although time is not a component of the analysis. Figure 3.19 shows examples of steady-state and transient boundary conditions on riverside of levee.

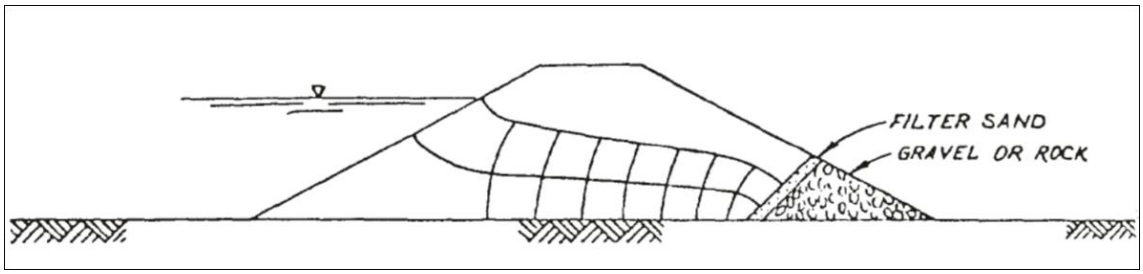

Figure 3.18 Cross section of unconfined steady-state seepage (Source: USACE 1993)

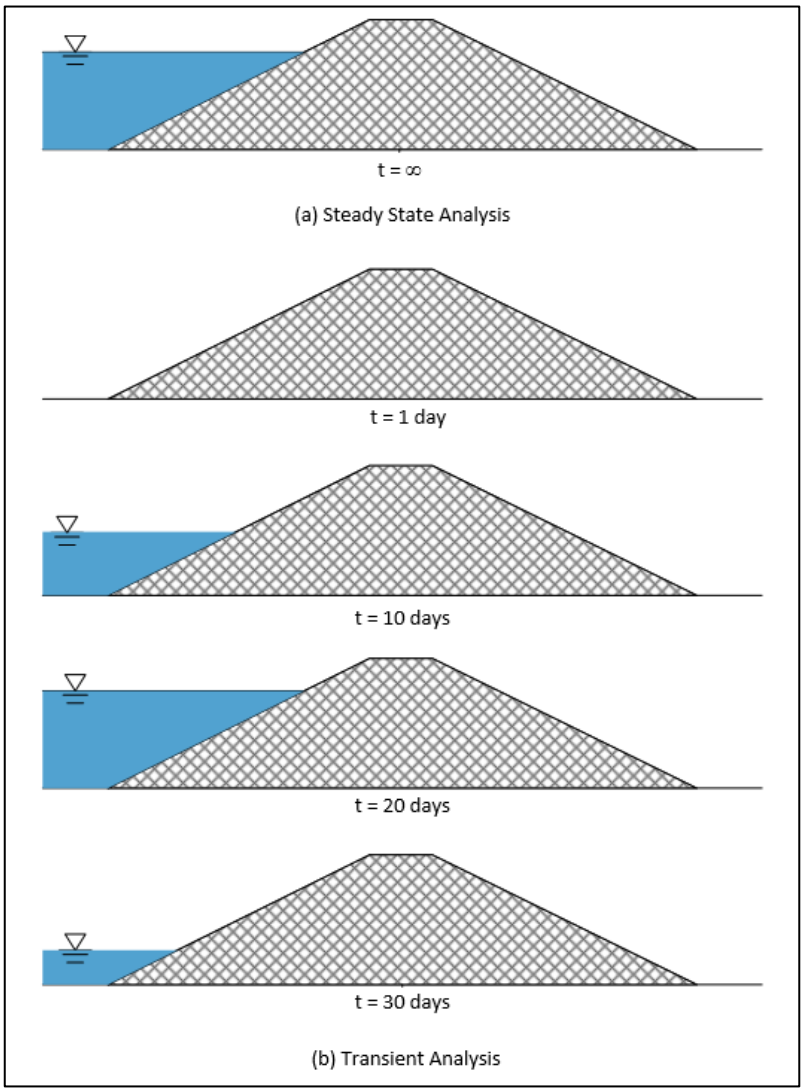

Figure 3.19 Steady-state and transient boundary conditions on riverside of levee.
(Source: Tracy *et* al. 2016)

Transient analyses can be successful to estimate the development of the uplift forces, exit gradients for the factor of safety against uplift, or the heave pressures acting on the base of a top stratum in regard to hydrograph for the flood event.

Transient flow is determined in an isotropic and homogeneous soil domain by the following partial differential equation.

$$div\left[kgrad\left(h\right)\right]+c\frac{\partial h}{\partial t}=Q \tag{3.55}$$

where;

k =hydraulic conductivity of soil

h =hydraulic head

c =specific capacity of soil

t =elapsed time

Q =discharge quantity

The equation includes Darcy's Law and the continuity and represent the flow in heterogeneous and anisotropic soils. Specific capacity depends on porosity and degree of saturation for partially saturated soils. According to Van Genuchten (1980), the degree of saturation and permeability depend on local pressure.

The methods used for transient flow conditions due to changing hydraulic head phenomenon include;

- Analytical solution of partial differential equations (Alberro 2006).

- Approximate graphical method named transient flow nets (Cedergren 1989).

- Numerical techniques such as finite element method (e.g. Plaxflow, Delft University of Technology 2007), or finite differences (*e.g.* Flac3D, ITASCA Consulting Group Inc. 2009).

Numerical methods are commonly used ones. Transient flow analysis is investigated in two different ways: (a) step-wise condition and (b) time-dependent condition.

CHAPTER 4

LEVEE DESIGN

4.1. Levee Design

Levees are embankments constructed of compacted earthen material (Figure 4.1). These materials can be impervious and sempervious but sometimes they may be pervious levee fill such as sands or gravels (Figure 4.2). Levess are generally constructed for floods of range of frequencies 50 years (avarage between 25 or 100 years). Slope of levee outline is choosen equal slope of water surface during flood. Phreatic line of filling determines size of levee. Drain dike is constructed as paralel to levee to collect and remove seepage water from levee. Table 4.1 presents average size of levees.

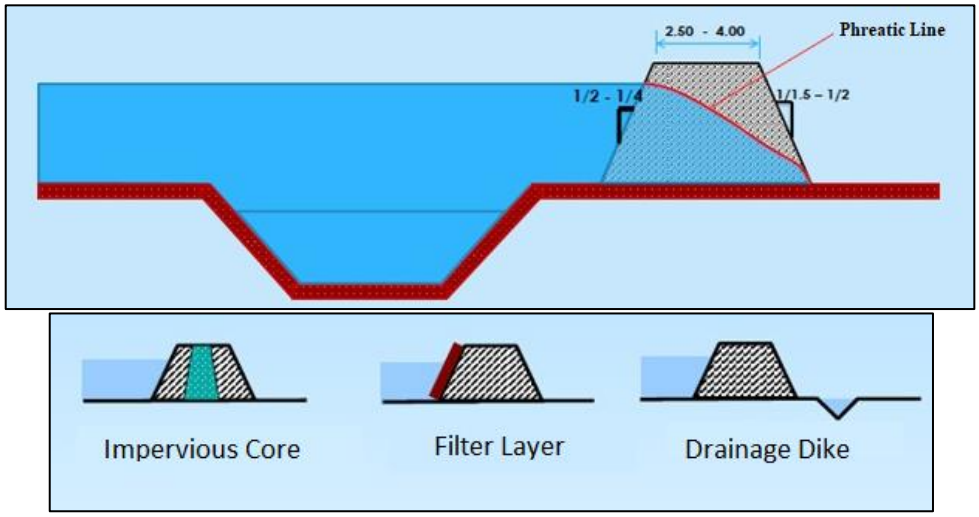

Figure 4.1 Seepage protection methods of levee body (Source: Onusluel 2010)

There are several terms about levees and some of these are;

1. Phreatic line is that the top flow line of a saturated soil mass below which seepage takes place.

2. There are seepage protection methods of levee body such as impervious core materials are clayey materials and filter layer is generally uniform sand materials.
3. Drainage dike is called that is a natural or artificial slope or wall to regulate water levels during flood. It is recommended that a drainage hatch be made parallel to the levee to collect the waters leaking from the levee.

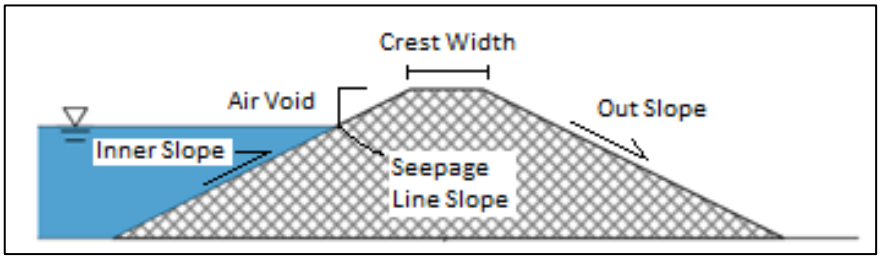

Figure 4.2 Terms of Levee (Source: Tracy *et*. al. 2016)

Table 4.1 Average Size of Levee (Source: Onusluel 2010)

Average Size of Levee	
Inner Slope	1/3 , 1/4
Out Slope	1/5 , 1/10
Crest Width	1-2 m
Air Void	0,3 – 0,6 m
Seepage Line Slope	1/3 , 1/5

Levee stability is important during flood so, some of problems may occur in the levee. Circular wedge slip, local erosion, piping etc. are generally problems.

- Overtopping is called that floodwaters exceed the height of a levee and flow over its crown (Figure 4.3).

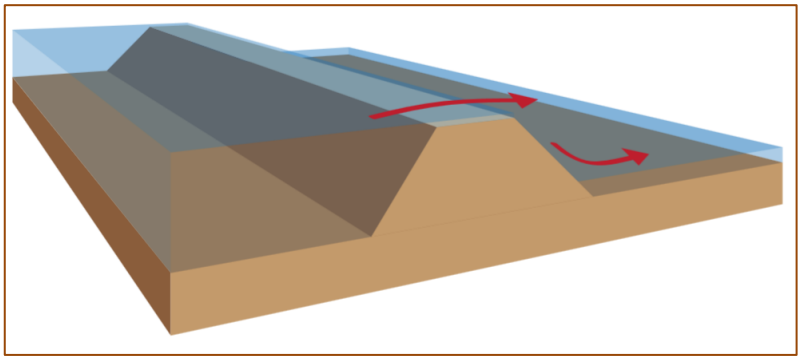

Figure 4.3 Problem: Floodwater overtopping the levee (Source: Sherman 2008)

- Seepage might occur through the levees based on levee materials during flood, so piping, erosion may observe levee body. (Figure 4.4).

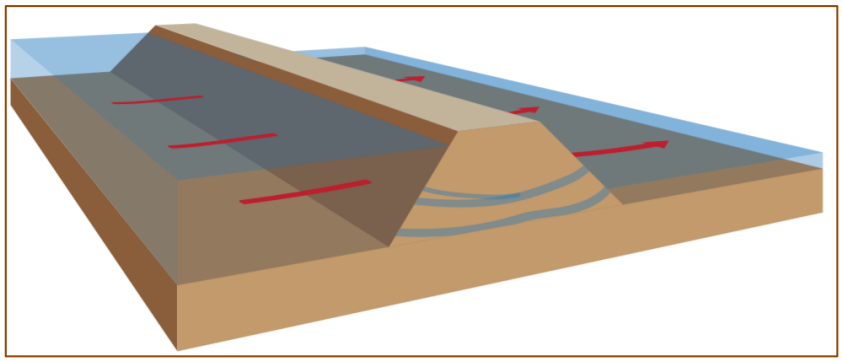

Figure 4.4 Problem: Seepage water exiting from a point on the levee's land-side batter (Source: Sherman 2008)

- Underseepage may occur through the levee foundation based on levee materials during flood, so sand boil may observe under the levee. (Figure 4.5).

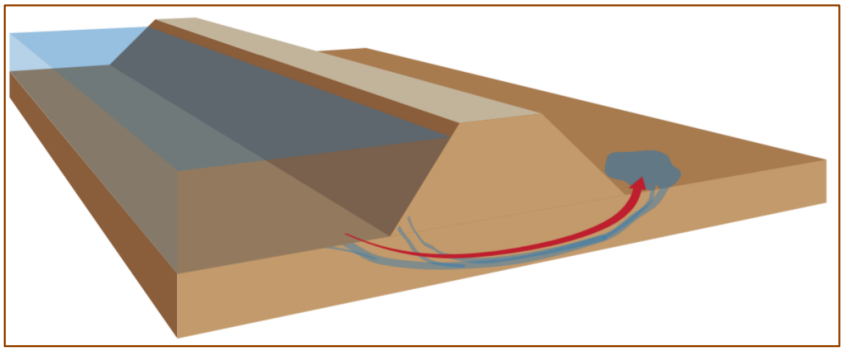

Figure 4.5 Problem: Seepage water exiting from the foundation (Source: Sherman 2008)

- Stability problems may occurs at levee body due to erosion and piping (Figure 4.6).

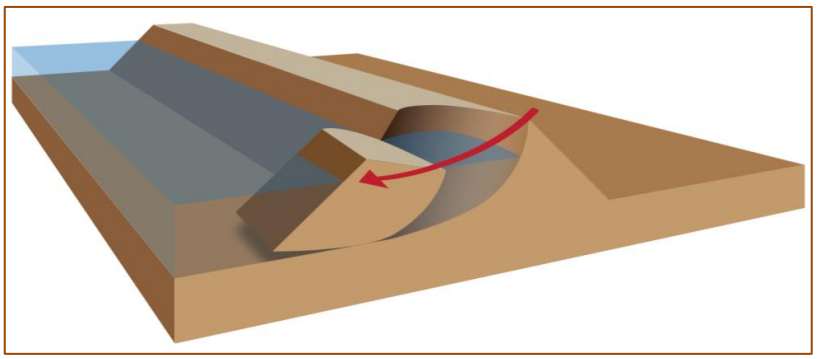

Figure 4.6 Problem: Slide, slump or slip (Source: Sherman 2008)

4.2. Geosynthetic Drainage Layer of Levee Surface

Geosynhetics often use civil engineering, geotechnical engineering, transportation, hydraulic and environmental projects nowadays. There are several functions of geosynhetics such as filter, drainage, protecting, erosion control seperation, reinforcement and impermeability. Types of geosynhetic are geotextiles, geonets, geocomposites, geogrids and geosynhetics clay layers etc. Figure 4.7 shows how geocomposites create.

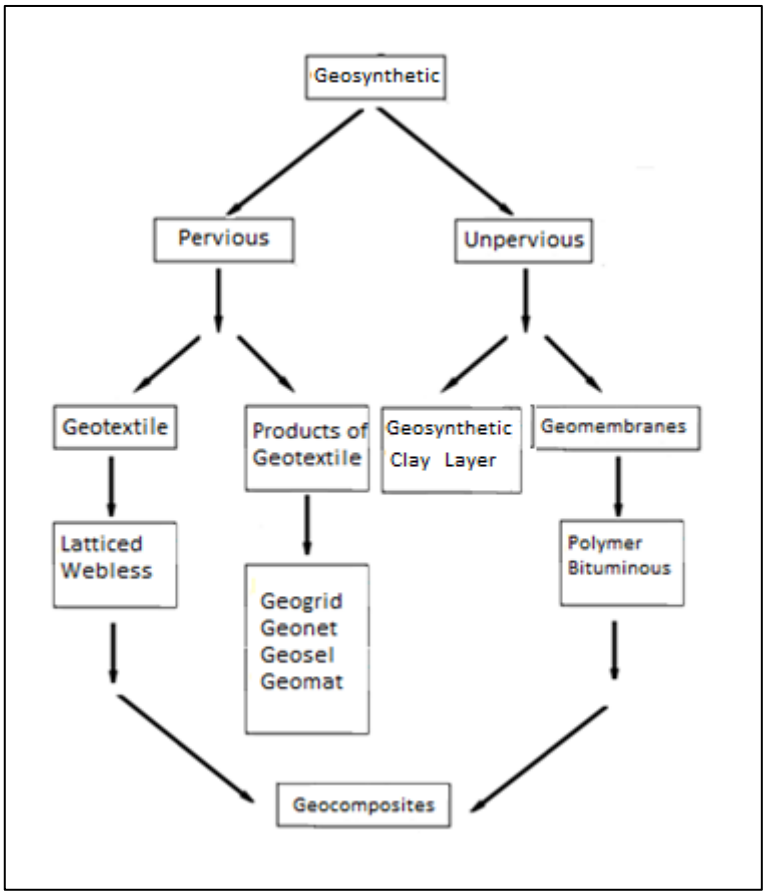

Figure 4.7 Geocomposite

4.2.1. Geocomposites

Geocomposites (Figure 4.8 through 4.16) made by together two or more layers of flexible synthetic materials. ASTM (2005) is defined that a geocomposite is " a product composed two or more materials, at least one of which is geosynthetic.

The following are illustrative examples:

- Geomembrane/Geotextile Composite
- Geonet/Geotextile Composite
- Geogrid/Geotextile Composite
- Geomat/Geotextile Composite

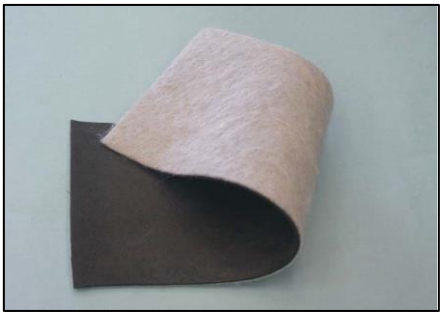

Figure 4.8 Single-Sided Geocomposite Geomembrane.

- It is made by bonding a geotextile (grey colored layer) to one side of a geomembrane.

Figure 4.9 A Double-Sided Geocomposite Geomembrane

- It is made by bonding geotextiles to both sides of a geomembrane (black colored core).

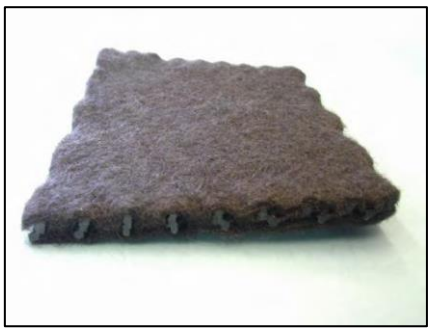

Figure 4.10 Geocomposite Geonet Drain

- It is made by bonding a geotextile to each side of a bi-planar geonet.

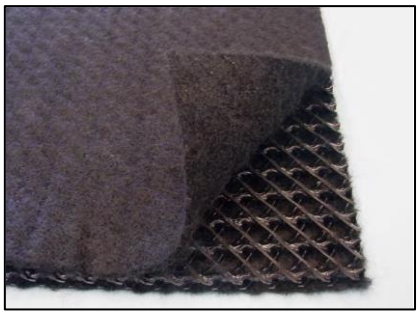

Figure 4.11 Geocomposite Geonet Drain

- It is made by bonding a geotextile to each side of a tri-planar geonet. One corner of the upper geotextile layer has been peeled back to show the underlying geonet core.

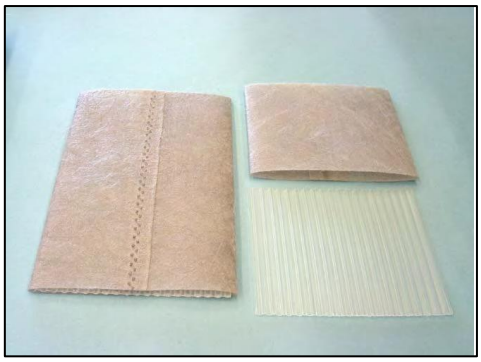

Figure 4.12 Example of a 4-inch-wide wick drain composed of a polymeric corrugated core and outer geotextile

- The core (Figure 4.12) is shown in the lower right part of the photograph and the nonwoven geotextile is in the upper right. The assembled wick drain is shown in the left side of the photograph.

Figure 4.13 Geocomposite Edge Drain

- It is made by wrapping a geotextile tube around a vacuum-formed drainage core.

Figure 4.14 Geocomposite drain formed by enclosing a row of perforated geopipes inside a geotextile tube.

Figure 4.15 Geocomposite edge drain

- It is made by placing a perforated geosynthetic core inside a geotextile tube. The core functions as a flat-shaped pipe.

Figure 4.16 Photograph showing a close-up view of a portion of the geocomposite drain

Geosynthetic products gain favor solving problems of geotechnical engineering. Figure 4.17 and Figure 4.18 show several function of geotextiles.

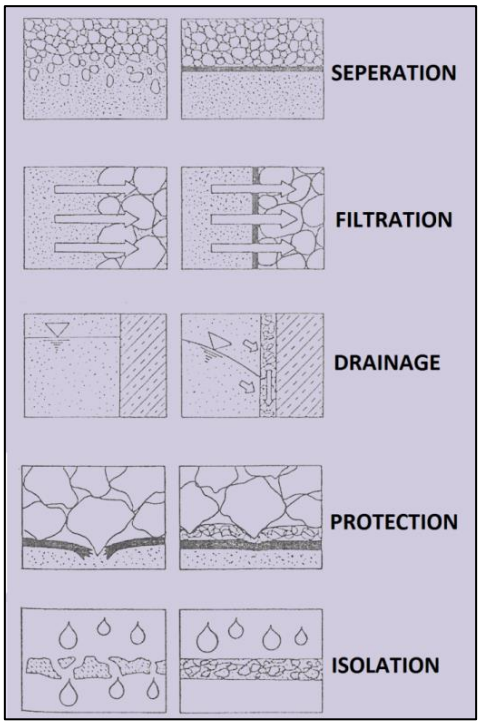

Figure 4.17 Functions of Geotextiles (Source: Yılmaz and Eskisar 2007)

Type of Geosynthetic	Separation	Reinforcement	Fitration	Drainage	Containment
Geotextile	■	■	■	■	
Geogrid		■			
Geonet				■	
Geomembrane					■
Geosynthetic clay liner					■
Geopipe				■	
Geofoam	■				
Geocomposite	■	■	■	■	■

■ : It has a this property.

Figure 4.18 Functions of Geosynthetics (Source: Zornberg *et* al. 1999)

The foundation washed out and slip surface occurs at levees, so available levee covering types are choosen for surfaces of levees. Table 4.2 and Figure 4.19 and Figure 4.20 present levee covering types.

Table 4.2 Levee Covering Types (Source: Civelek 2013)

Levee Coverings	Riprap Coverings	Dry Riprap Coverings
		Mortared Riprap Coverings
	Rock Fills	Disordered Rock Fills
		Ordered Rock Fills

- Riprap covering have good granulometry and rock material should be diameter of grain max 90 mm and grain volume max 0.75 meter cubic. It has a mixture of hard, solid and durable rock fragments.
- Sand gravel filter criteria should be compared between the aquifers producing seepage and the soil being protected.
- Composite Geomembrane has lowest permeability value, so this material prevent. Figure 4.19 and Figure 4.20 show examples of levee covering types.

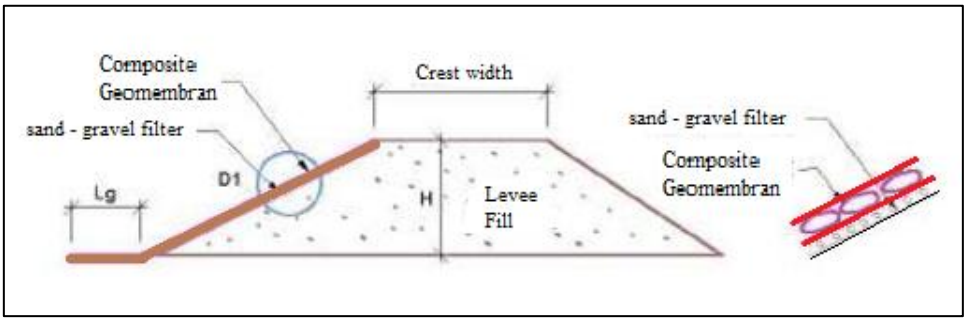

Figure 4.19 Composite Geomembrane Covering (Source: Civelek 2013)

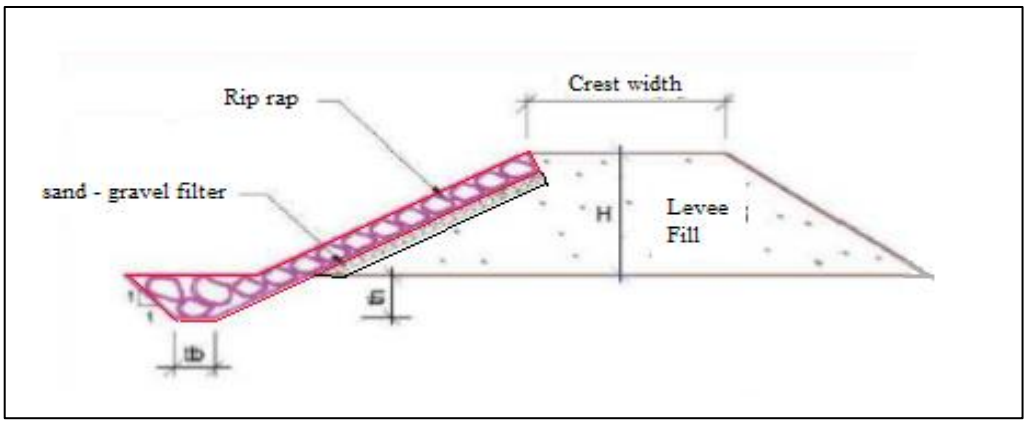

Figure 4.20 Riprap Covering (Source: Civelek 2013)

Figure 4.21 and Figure 4.22 present cross section of Filyos Levee and content of Geocomposite layer.

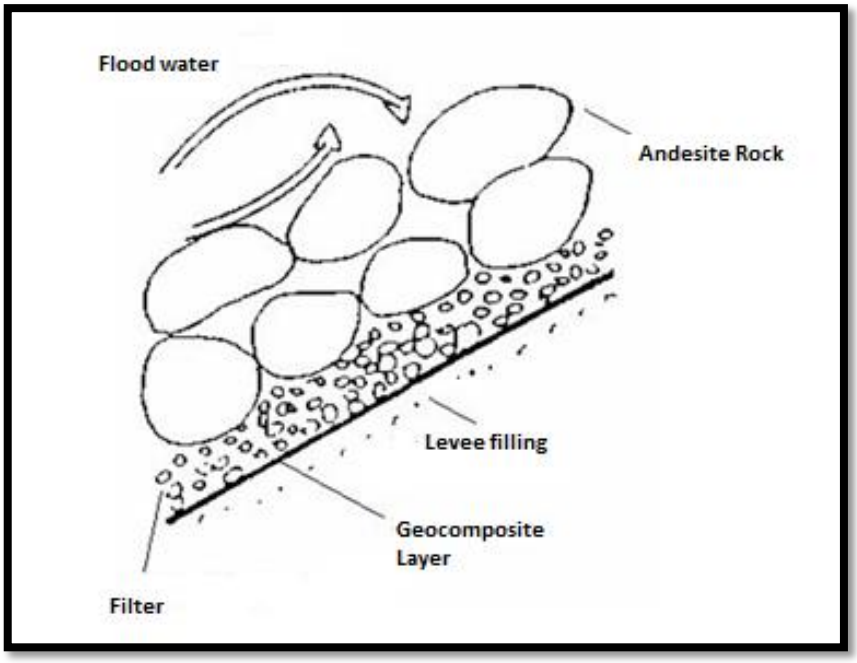

Figure 4.21 Cross section of Filyos Levee

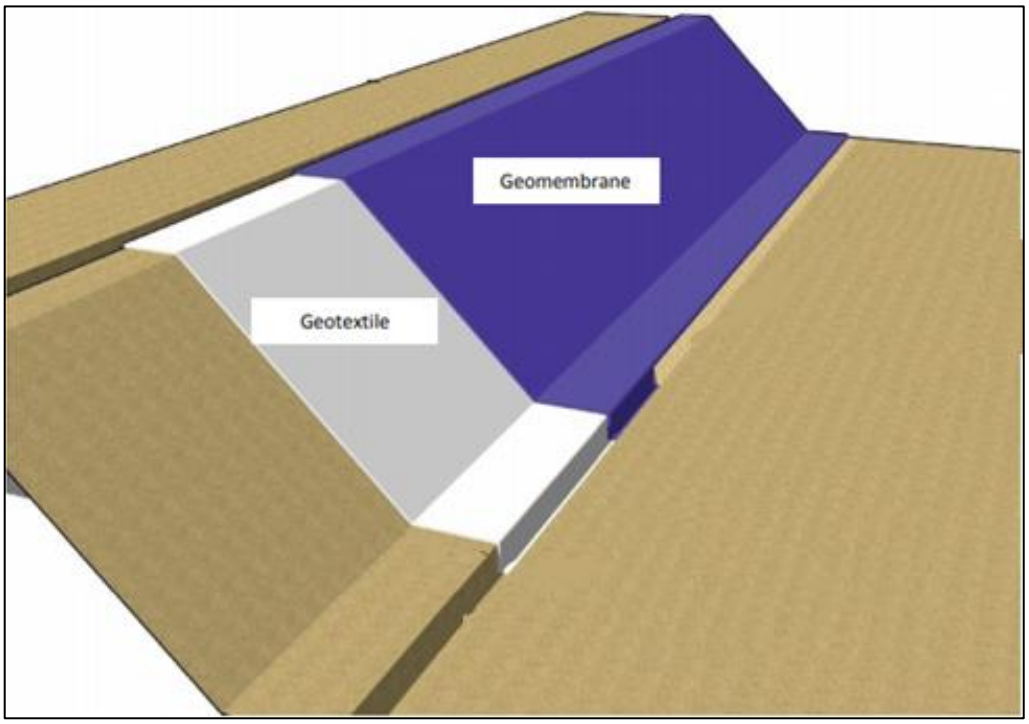

Figure 4.22 Geocomposite Covering

4.3. Fem Model of Plaxis

One of the Plaxis products is Plaxflow. Plaxflow is a finite element software for groundwater flow analysis in geotechnical engineering.

4.3.1. Introduction

One of the Plaxis products is Plaxflow. Plaxflow is a finite element software for groundwater flow analysis in geotechnical engineering. Plaxflow produces quick generation of complex finite element models. It presents output facilities with detailed presentation of computational results. Levee analysis offers more possibilities using of FEM model with coupled modelling of seepage and stability. Hamdhan (2013) studied changes in water level around and in the levee, infiltration into the levee effects of drowdown, etc. Using Plaxis FEM model is more realistically than conventional methods. Seepage analysis may be investigated in volume change prediction, groundwater contamination control, slope stability analysis and design of earth structures such as dams or levees. The currrent software package Plaxflow solves groundwater flow program and this program includes transient flow, steady-state flow, unsaturated behavior and time-dependent boundary conditions, deformation and/or stress analysis and stability. Plaxfow involves different models for saturated/unsaturated groundwater flow, using ‘Van Genuchten’ relations between pore pressures, saturation and permeability. Plaxflow is equipped with advanced features to solve various aspects of the complex geotechnical flow problems.

Van Genuchten (1980) is a well known model that simulates unsaturated soil behavior. The basis of common soil classification systems (Hypres, USDA, Staring) can be selected for various types of soil and also, different types of soil are created using user-defined models relationships between groundwater head, permeability, and saturation. The groundwater flow calculation allows for steady-state and transient groundwater flow calculations. The other important parameter is the time-dependent conditions. It can be created by linear or harmonic function or by means of an input table. Output feauteres are distributions of the groundwater head pore pressure, degree of saturation and Darcy Flux.

4.3.2. Plaxflow Model

Saturated and unsaturated soil behavior is presented in three different options such as standard, advanced, and expert. Standard option enables a simple means for the identification of soil materials. Advanced option provides several soil materials based on three standardised soil classification series such as Hypres, USDA, and Staring (Figure 4.24). The other option is the Expert option and it requires experience with (un)saturated groundwater flow modelling (Figure 4.25). Both saturated and unsaturated properties are defined manually by using the expert option.

4.3.2.1. Standard Option

Standard option (Figure 4.23) includes most common soil types: non-organic coarse material, medium, medium fine, fine, very fine and organic material. This category presents Approximate Van Genuchten Model. The model consists of a linear relationship between the relative saturation and the unsaturated zone. Approximate Van Genuchten model for unsaturated soil behavior is standard series for this option.

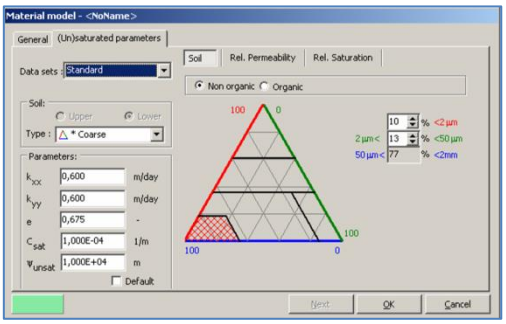

Figure 4.23 Standard series soil tab sheet (Source: Waterman *et* al. 2009)

4.3.2.2. Advanced Option

The Advenced option uses for an extended selection of soil types based on different soil classification systems. Van Genuchten and Approximate Van Genuchten model are available for this category. Data sets of advanced option are standard series, Hypres, USDA and Staring series. Approximate Van Genuchten model is applied by standard series. The standard series includes coarse, medium, medium fine, fine, very fine and organic soils.

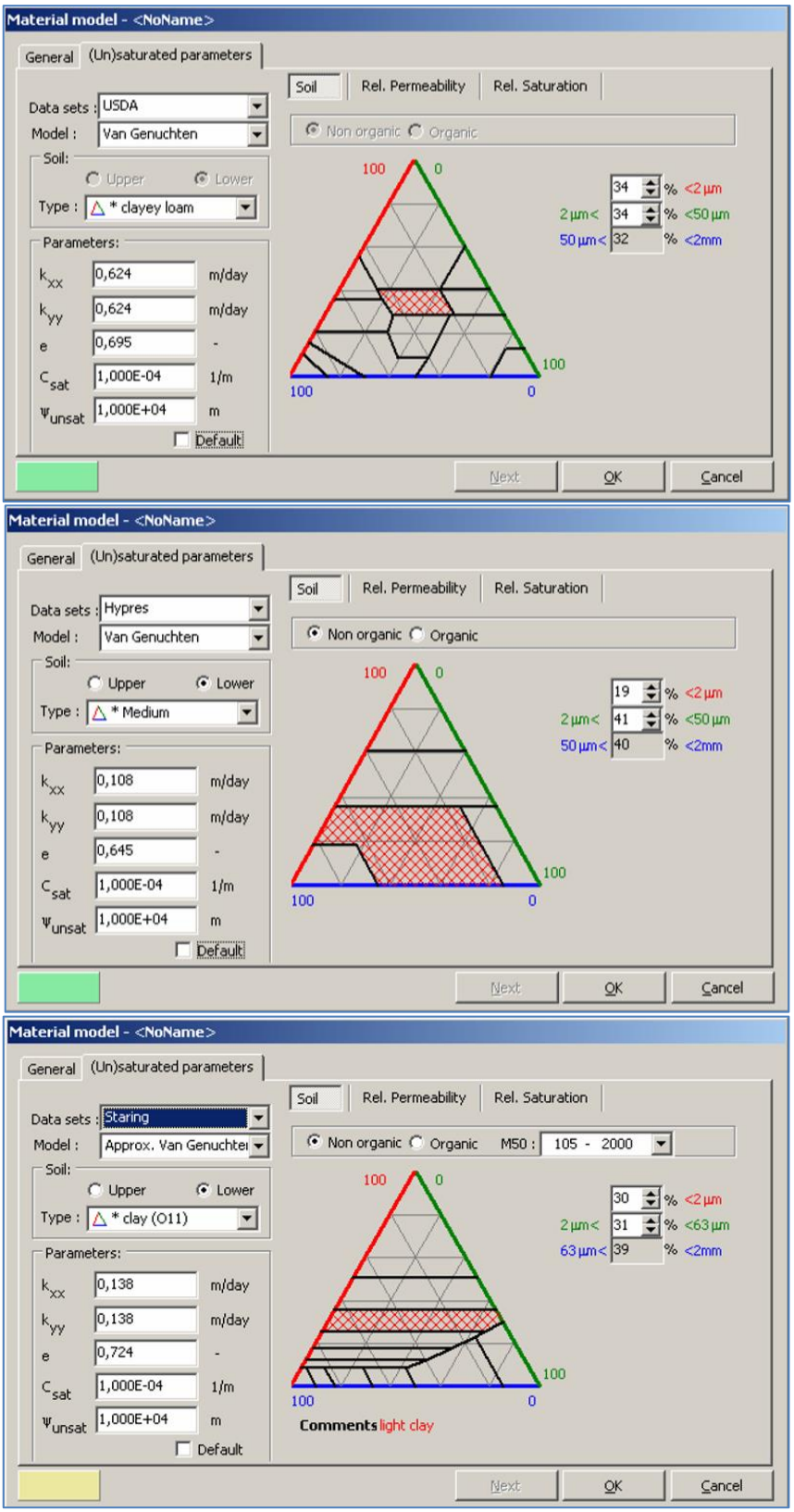

Figure 4.24 USDA, Hypres, Staring series soil tab sheet
(Source: Waterman *et. al.* 2009)

4.3.2.3. Expert Option

The user can choose the expert option to define both saturated and unsaturated properties manually. The model parameter includes Van Genuchten model, the linear model (Approximate Van Genuchten), a spline function or fully saturated soil behavior. When the saturated option is choosen, no extra data input is needed. Plaxflow will use the saturated permeabilities for soil layers.

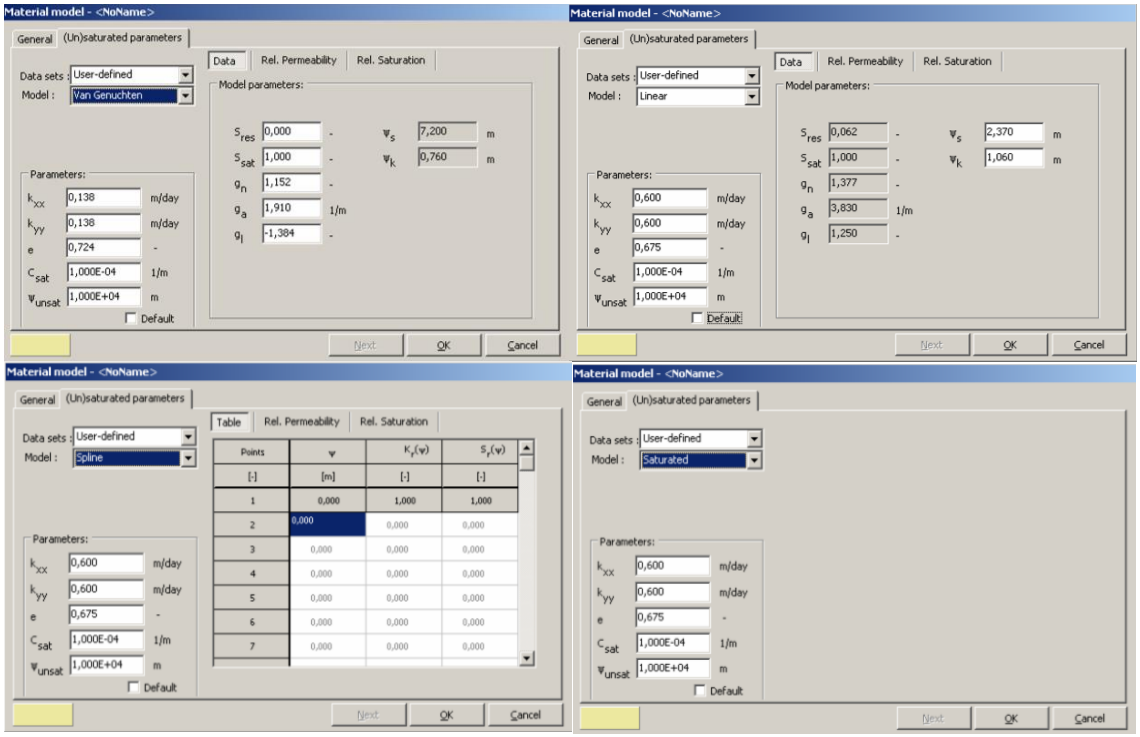

Figure 4.25 Expert Van Genuchten, Linear, Spline and Saturated data tab sheet (Source: Waterman *et. al.* 2009)

4.3.2.4. Time-Dependent Conditions

Plaxflow enables many features for analysis of transient groundwater flow problems with several conditions in time. Also, time-dependent conditions are only used for transient analysis. Irregular variations in water levels are modelled using harmonic, linear or user-defined time distributions to enable time-dependent water level. The other time-dependent conditions are inflow, outflow and infiltration based on boundary conditions.

4.3.2.4.1. Linear

This option describes the increase or decrease of a condition linearly in time. For a linear variation of groundwater head, input parameters are Δt , y_0 , Δy .

where;

Δt = the time interval for the calculation phase,

y_0 = actual height of water level

Δy = increase or decrease of the water level in the time interval

For a linear variation of infiltration, inflow or outflow, input are parameters;

Q_0 = the initial specific discharge

ΔQ = increase or decrease of the specific discharge in the time interval

4.3.2.4.2. Harmonic

If the condition varies harmonically in time, this option can be used.

$$y(t) = y_0 + 0.5.H.\sin(w_0.t + \varphi_0) \text{ with } w_0 = 2\pi / T \quad (4.1)$$

where;

$y(t)$ = the harmonic variation of the water level,

H = wave heght (in unit of height)

T = wave period

φ_0 = initial phase angle

4.3.2.4.3. Table

User-defined time series option can be used to describe increase or decrease of water level. PlaxFlow provides the options to enter user-defined time series. These options are Table button and Import Table button. The time value should remains with each new line and it is not necessary to use constant time intervals.

4.3.3. Previous Studies of Plaxflow

López-Acosta *et al*.(2010) investigated the transient flow caused by rapid filling and drawdown in typical levees of Villhermosa city in Tabasco Mexico in 2007. Analyses were performed by FEM of Plaxflow. From results of analysis, some general conslusions can be drawn. Figure 4.26 shows that the highest hydraulic gradients and velocities take place at the downstream slope of levee. Particularly, the gradient values of those areas greater than critical gradient (>1) and global piping could observed through the body of levee or through the foundation soil.

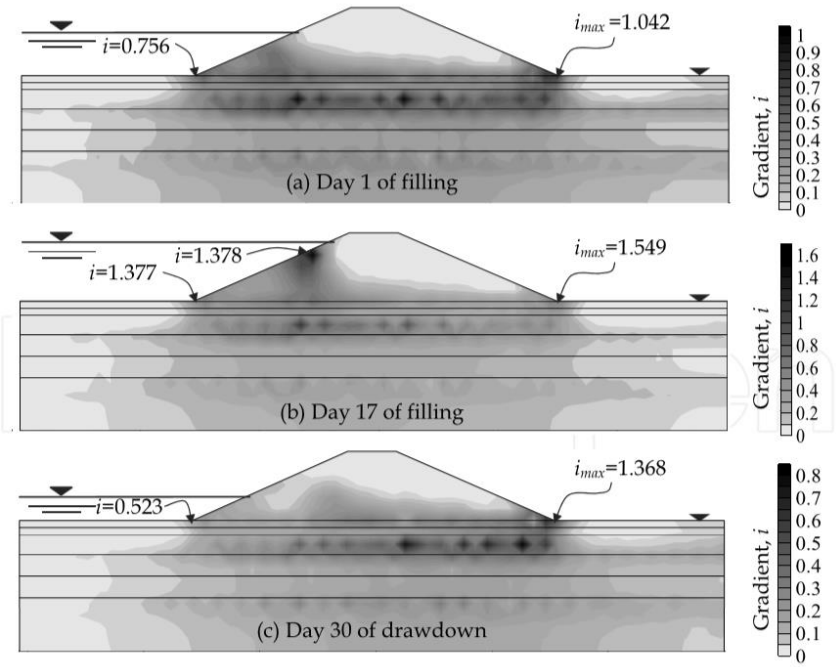

Figure 4.26 Hydraulic gradients (magnitude) for three different times during rapid filling and drawdown (Source: Lopez-Acosta *et. al.,* 2010)

In Figure 4.27 it is observed that in general the highest values of flow velocity occur in the more pervious materials of the investigated domain.

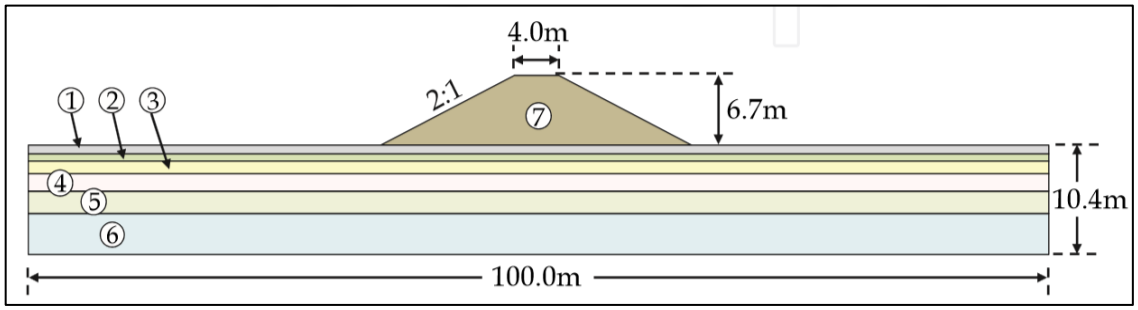

(a)

N°	Material	Hydraulic conductivity, k	Void ratio, e
1	Clay sand (SC)	0.0864 m/d (1×10^{-6} m/s)	0.43
2	Sandy clay of low plasticity (CL)	0.0864 m/d (1×10^{-6} m/s)	0.50
3	Organic sandy-clay silt of high plasticity (OH)	0.00864 m/d (1×10^{-7} m/s)	0.90
4	Clay sand (SC)	0.0864 m/d (1×10^{-6} m/s)	0.43
5	Silty sand (SM)	0.0864 m/d (1×10^{-6} m/s)	0.43
6	Organic clay of high plasticity (OH)	0.00864 m/d (1×10^{-7} m/s)	0.90
7	Clay levee	0.00864 m/d (1×10^{-7} m/s)	0.70

(b)

Figure 4.27 Simplified geometry and material number of the studied domain a.) Figure b.) Table (Source: Lopez-Acosta *et al.*2010)

According to Figure 4.28, the maximum values of flow velocities are observed at toe of upstream slope of levee for higher filling rate. In contrast, Figure 4.29 present that maximum values of flow velocities are observed at toe of downstream slope of levee for lower filling rate.

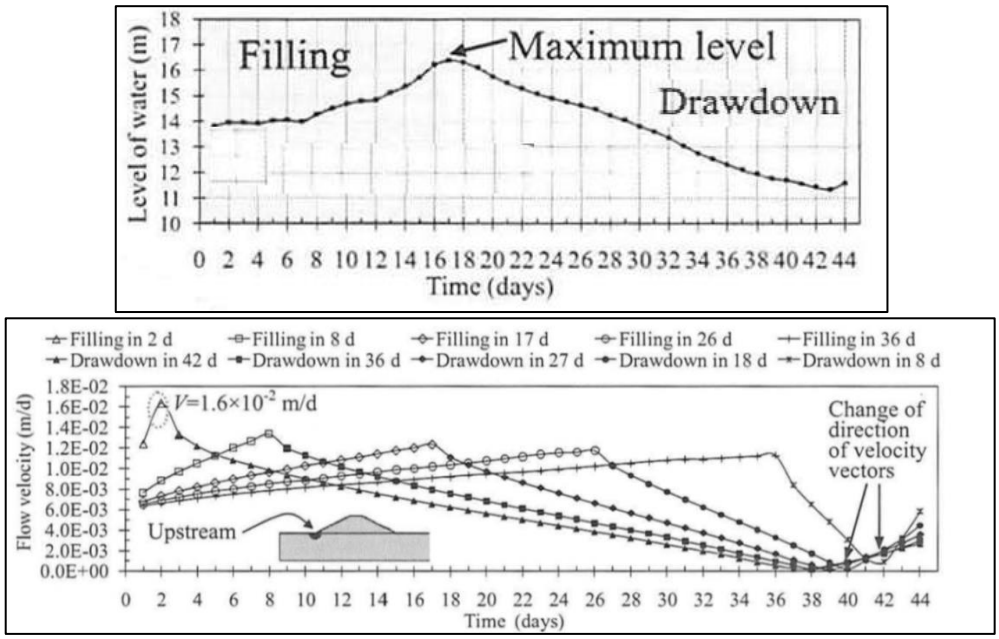

Figure 4.28 Flow velocity as a function of time for different filling and drawdown rates (at toe of upstream slope of levee) (Source: Lopez-Acosta *et. al* 2010)

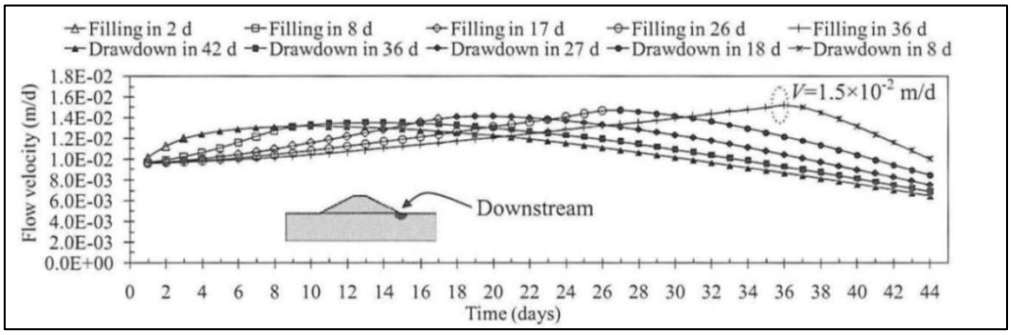

Figure 4.29 Flow velocity as a function of time for different filling and drawdown rates (at toe of downstream slope of levee) (Source: Lopez-Acosta *et. al.*2010)

CHAPTER 5

A CASE STUDY: FILYOS RIVER LEVEES

5.1. General

Filyos River Basin covers area of 13.300 km^2 in the Western Black Sea region in Zonguldak. (Figure 5.1). The project area is 203 km at the east-west direction, at 120 km north-south direction and the slope of the river is quite small. Project area is located at the Filyos river in the north of the area of rainfall and Filyos River flood plain of a north-south direction is 33.35 km long. Filyos river and tributaries of the river as Yenice, Devrek, Soganlı and Arac river form water sources of project area (Figure 5.2). Yenice River is the biggest tributary of the Filyos river side. Number of 1335 Filyos river – Derecikviran flow observation station represents flow measurement of Filyos River (Figure 5.3). The Filyos Basin gets more rain in winter and spring and according to number of 1335 Filyos river – Derecikviran flow observation station, annual average flow of Filyos River is 3085 hm^3.

Figure 5.1 Filyos River (Source: Cetinkaya 2010)

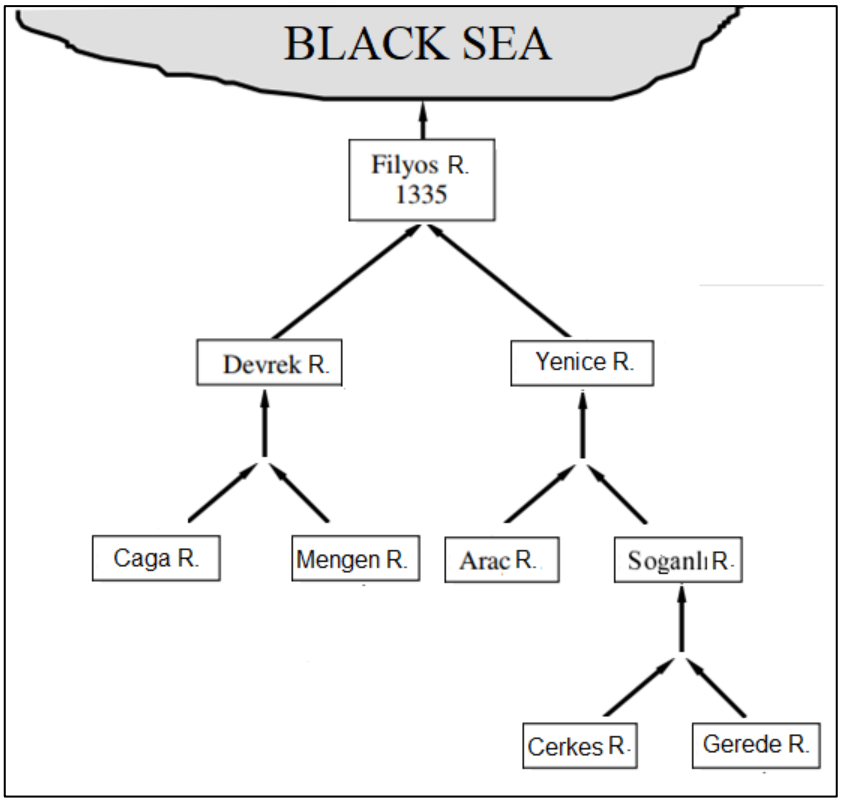

Figure 5.2 Tributaries of the Filyos river side

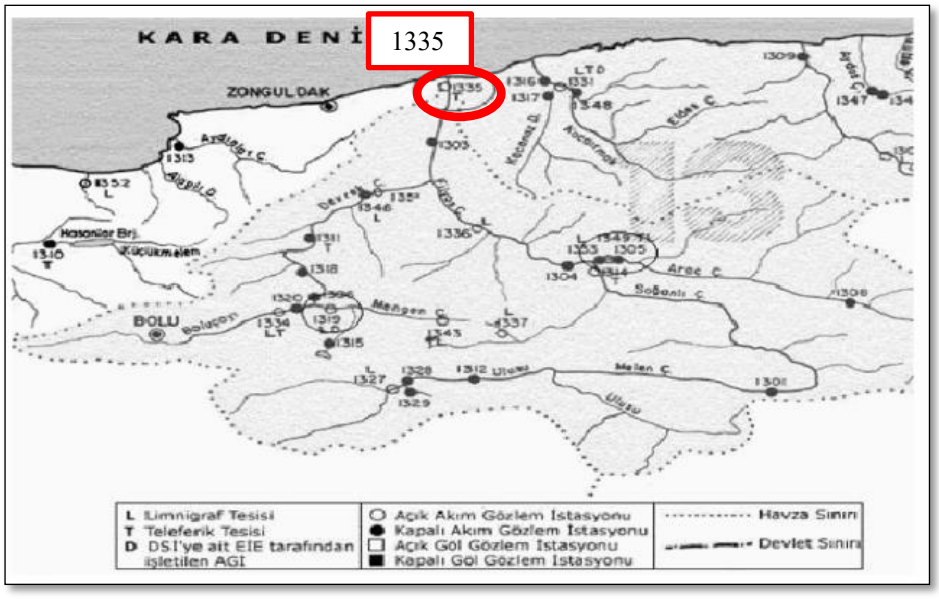

Figure 5.3 Number of 1335 Filyos River – Derecikviran flow observation station

5.2. Filyos River Levees

The flood protection project of Filyos River included the construction of a total 7 km of levee, and these levees are 3.5 km long along the right and left shore at the exit the sea. Distance of between the two levees is approximately 300 m and levee height is 6.7 m. Because alluvial soils was very variable in the soil layers, more shallow and frequent foundation drillings were made. In this study, Filyos levees were modelled as including geotextile material, riprap and at last this levees were projected that used to steady state model of software by private company. Fill and excavation can be applied to the levee floor to provide similar levels (Between the Figure 5.4-5.6). Between the Figure 5.7-5.12 show cover materials upstream of the filyos levee to protect seepage and it presents detail drawings of cover materials of levees.

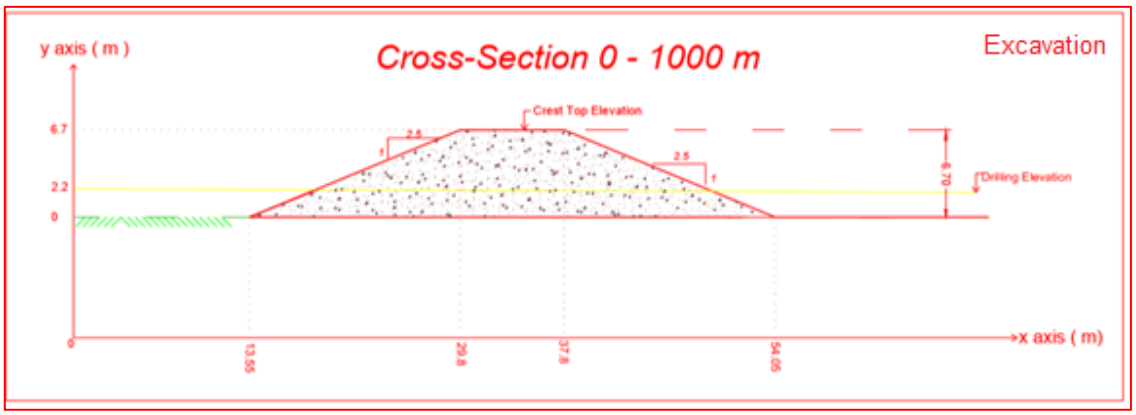

Figure 5.4 Uncovered materials Filyos Levee sections (excavation)

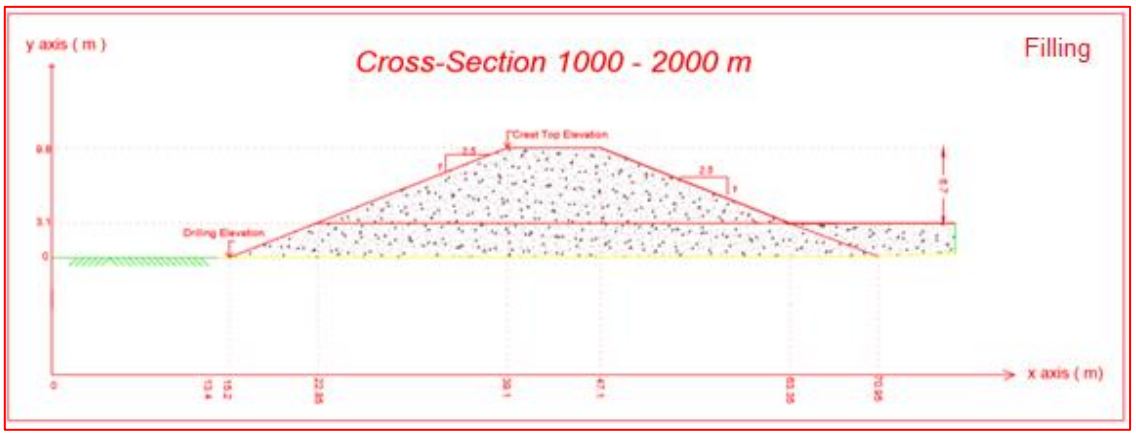

Figure 5.5 Uncovered materials Filyos Levee sections (filling)

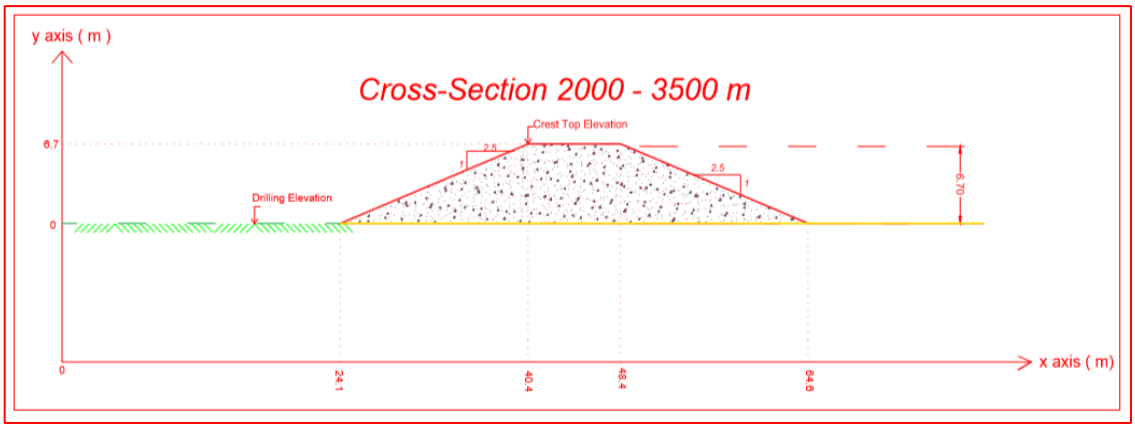

Figure 5.6 Uncovered materials Filyos Levee sections (2000-3500 m)

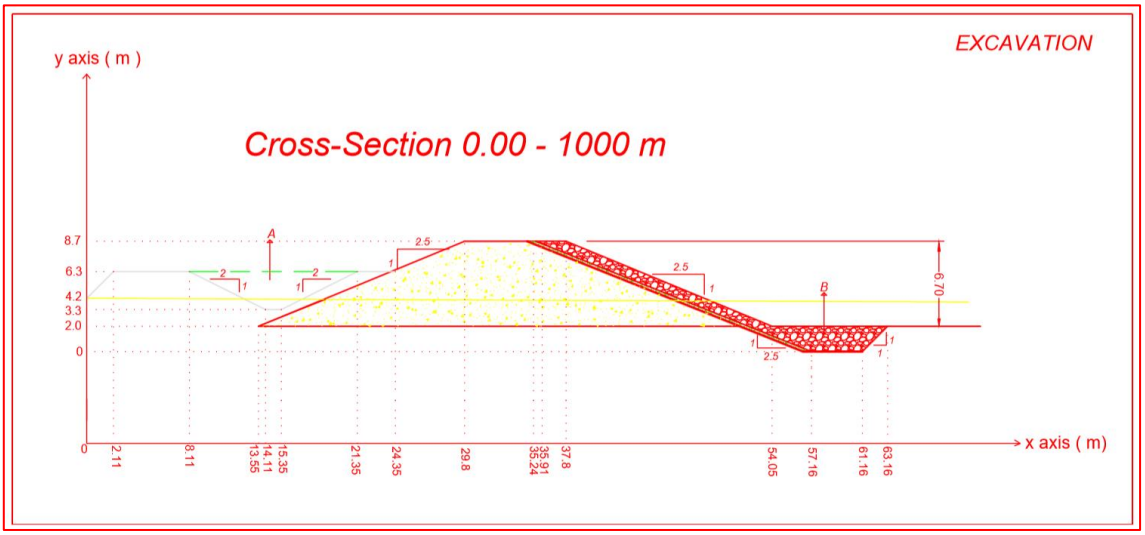

Figure 5.7 Covered materials Filyos Levee sections (0-1000 m)

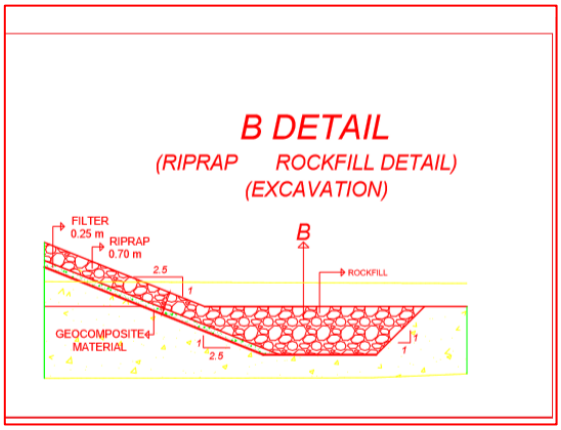

Figure 5.8 Covered materials Filyos Levee sections (excavation)

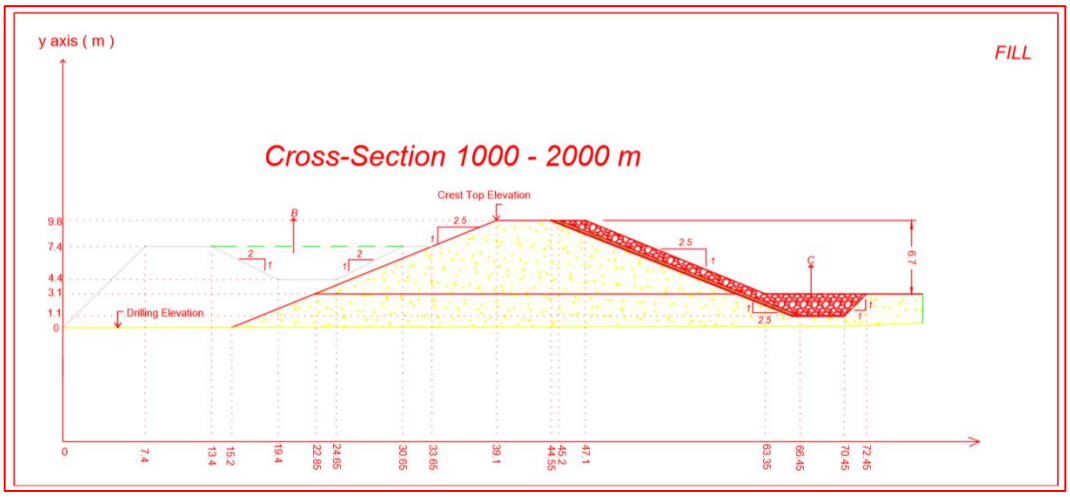

Figure 5.9 Covered materials Filyos Levee sections (1000-2000 m)

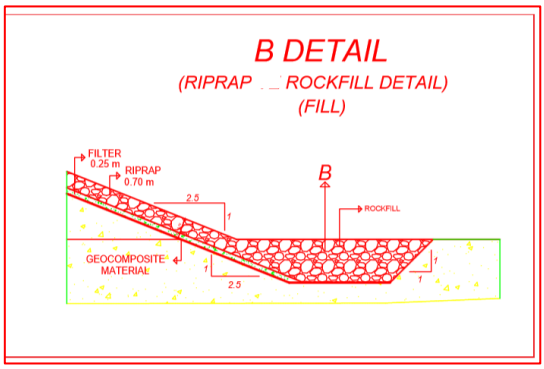

Figure 5.10 Covered materials Filyos Levee sections (fill)

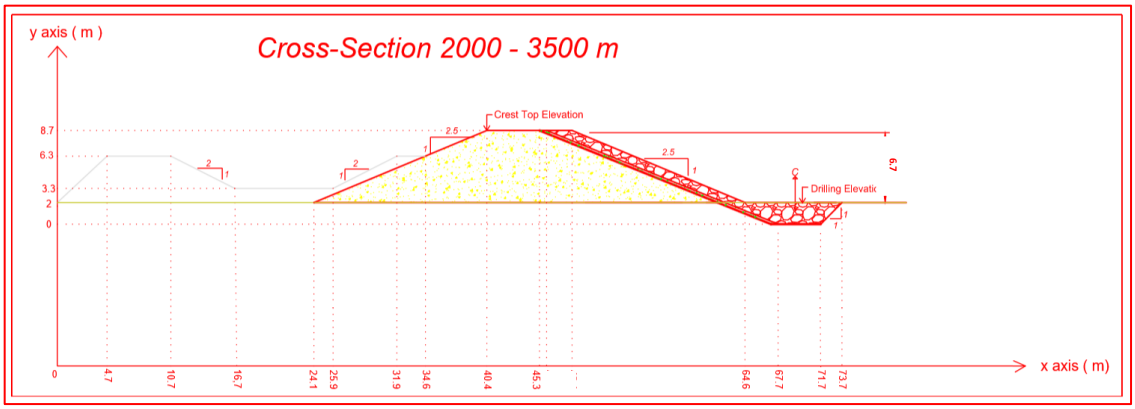

Figure 5.11 Covered materials Filyos Levee sections (2000-3500 m)

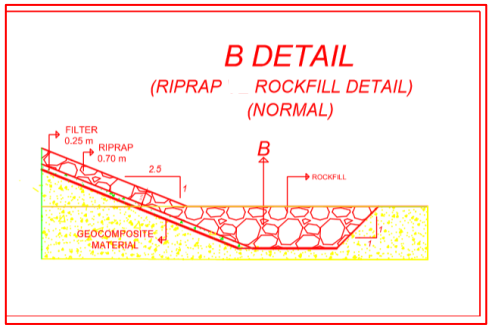

Figure 5.12 Covered materials Filyos Levee sections (normal)

CHAPTER 6

DATA COLLECTION: FILYOS RIVER LEVEES

6.1. Datas

There are some of datas to be solved groundwater seepage analysis on Filyos levee. These datas are unit hydrograph and soil properties of Filyos basin.

6.1.1. Unit Hydrograph

Unit hydrograph is the most popular method and widely used method for predicting flood hydrograph. A hydrograph that results in 1 cm excess rainfall Flood Basin gets the most rain in summer. There are widely used for flood estimation such as statistical, rational, Mockus and Synder methods. Every method has some significant limited conditions and these methods give different results for same place. A suitable method should be selected according to meteorological, hydrologic, topogrophic conditions of a basin. Synder method uses due to the fact that Flood basin of Filyos river is larger than 1000 km^2. This is one of the synthetic methods to obtain unit hydrograph which was developed by Synder in USA in 1938. The basin characteristics which are area, shape, topography, channel slope, stream density are affected the shape of unit hydrograph is the main idea of this method. Figure 6.1 shows a relation between the flow and hours and Figure 6.2 presents relation river level and hours during the flood.

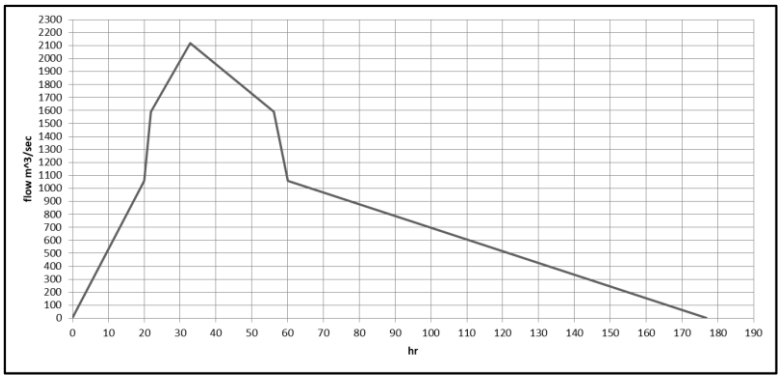

Figure 6.1 Unit Hydrograph

Peak discharge is 2120 m^3 / s at 6.5 meter high of levee and the time of duration for peak discharge (T_p) completed 32.8 hours The fall time of the flood level is 144 hours. Time of duration of unit hydrograph of Filyos River approximately completed 7.5 days.

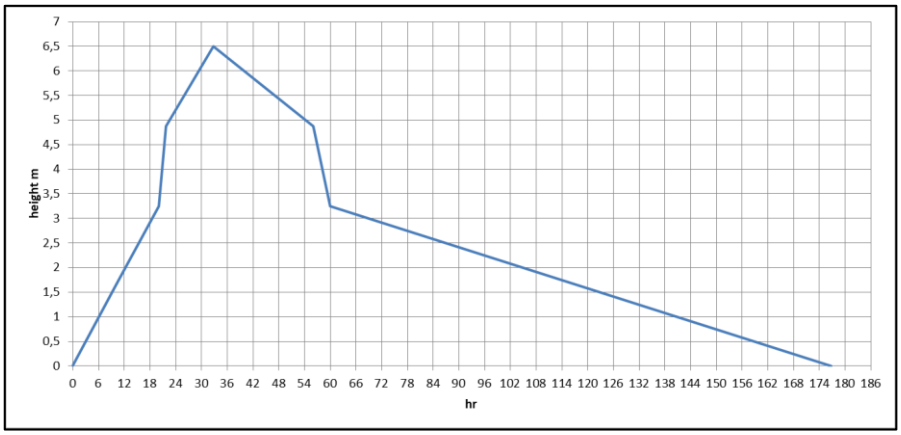

Figure 6.2 Relation river height and hour

6.1.2. Soil Properties of Filyos Basin

The soil has a cellular structure and includes minerals, humus, plant roots, microorganisms and air gaps. The soil is often compressed as it descends from the ground and it is limited to impermeable rock layers.

Drilling must be made in order to know the soil properties. Since the alluvium forming the basement floor is very variable in Filyos basin, it is better to perform shallower and frequent foundation drilling. Six drillings drilled at 30 meters deep on the left shore. On the right shore, a total of five drillings drilled at depths of 30 m.

Table 6.1 Depth and location properties of foundation drilling wells

No	Drilling No	Well Point	Locations (km)	Depth (m)
1	**TSK-1**	Left Shore	**0+044.24**	30
2	**TSK-2**	Left Shore	**0+511.29**	30
3	**TSK-3**	Left Shore	**1+010.63**	30
4	**TSK-4**	Left Shore	**1+513.22**	30
5	**TSK-5**	Left Shore	**2+005.66**	30
6	**TSK-6**	Left Shore	**2+501.94**	30
7	**TSK-9**	Right Shore	**0+271.05**	30
8	**TSK-10**	Right Shore	**0+758.18**	30
9	**TSK-11**	Right Shore	**1+256.40**	30
10	**TSK-12**	Right Shore	**1+762.17**	30
11	**TSK-13**	Right Shore	**2+327.64**	30

The general information about soil properties are defined at Table 6.2 and used inputs are permeability (k), specific gravity (G_s) and void ratio (e) that are important for both levee and under seepage of levee. Samples of drilling wells and soil properties of TSK-1 are seen Figure 6.3. and Table 6.2. The other informations about soil properties are available in Appendix A.

(1)-TSK-1

Figure 6.3 Sample drilling well of TSK-1 at 44.24 m

Table 6.2 Soil Properties of TSK-1

Depth(m)	**Soil Type**	**Permeability(k) (m/sec)**	**Specific Gravity (G_s)**	**Void Ratio (e)**
0.0-6.0	Clayey Silt	$1x10^{-7}$	2.70	0.90
6.0-27.5	Silty Clay	$5x10^{-8}$	2.75	1.78
27.5-29.0	Clayey Silt	$1x10^{-7}$	2.70	0.90
29.0-30.0	Silty Clay	$5x10^{-8}$	2.75	1.78

Filyos levee has covered along rising water level. The covered members are filter, riprap and geocomposite materials. Table 6.3 and Table 6.4 shows properties of covered materials and levee.

Table 6.3 Soil Properties of levee members

	Soil Type / Material	**Permeability(k) (m/sec)**	**Specific Gravity (G_s)**	**Void Ratio (e)**
Levee	Gravelly Sand	$5x10^{-4}$	2.66	0.62
Filter	Uniform Sand	$1x10^{-3}$	2.67	0.70
Riprap	Andesite Rock	0.645	2.65	0.34
Geocomposite Material	Geotextile and Geomembrane	$1x10^{-13}$	-	0.02

Table 6.4 Soil Properties

Soil Type	**G_S**	**e**	**γ_{sat} (kN/m^3)**	**γ_s (kN/m^3)**
Clayey Silt	2.70	0.90	18.6	26.5
Silty Clay	2.75	1.78	16.0	27.0
Clayey Sand	2.67	0.43	21.3	26.2
Sand	2.68	0.55	20.4	26.3
Gravelly Sand	2.66	0.62	19.9	26.1
Gravel	2.65	0.27	22.6	26.0
Silty Sand	2.69	0.43	21.4	26.4
Sandy Silt	2.68	0.85	18.7	26.3
Sandy Clay	2.72	0.47	21.3	26.7
Sandy Gravel	2.65	0.50	20.6	26.0
Clay	2.80	1.85	16.0	27.5
Silt	2.70	1.10	17.8	26.5
Gravelly Clay	2.71	0.80	19.1	26.6
Gravelly Silt	2.69	0.75	19.3	26.4

CHAPTER 7

ANALYSIS: FILYOS RIVER LEVEES

7.1. Introduction

If the hydraulic gradient is low, the water may seep out slowly and soil erosion does not observe in wet conditions. However, if the hydraulic gradient is large enough, the underseepage may conclude erosion of the foundation soils.

Soil erosion caused by underseepage may occur due to several mechanism. Firstly, the seepage exits the soil (exit gradient) is larger than the gradient required to cause erosion of the soil at the location (critical gradient). The soil particles will be eroded from the exit location. This mechanism are commonly named as piping. A second mechanism may observe when high-hydraulic conductivity soils on the landside of the levee are overlain by a soil layer having lower hydraulic conductivity. Due to the lower hydraulic conductivity, water pressure creates at the base of the top layer. If the water pressure grows into great enough, it may lift the top layer upward a mechanism are generally called as heave. And then, the top layer may crack, sand boil formation can become at there. According to Salem (2010), boiling occurs sand soil types in case quick condition and heave observes clay soil types.

In the first failure mechanism case is the factor of safety against to erosion piping.

$$F_{bep} = \frac{i_c}{i_e} > 3-4 \tag{7.1}$$

Where;

F_{bep} = factor of safety against to erosion piping

i_e = exit graident calculated at the ground surface in the finite-element analyses

i_c = critical gradient of the eroding soil

Calculated using hydraulic head data from the top two to three rows of elements below the ground surface is exit gradient. In the second failure mechanism case is the factor of safety against heave.

$$F_{heave} = \frac{H.\gamma_{sat}}{h_m.\gamma_w} > 3.0 \tag{7.2}$$

$$i_{\max} = \frac{h_m}{H} \tag{7.3}$$

H = thickness of overlying top layer(m)

γ_{sat} = saturated unit weight of overlying top layer(kN/m^2)

h_m = average hydraulic head at the point(m)

γ_w = water unit wight(kN/m^2)

$i_{\max}$ = maximum exit gradient

7.2. Filyos Levee at 44.24 m on Left Shore of Filyos River

Location of Filyos levee at 44.24 m on left shore is seen Figure 7.1 and the schematic representation of Filyos Levee and soil profile is given in Figure 7.2 Filyos levee includes gravelly sand soil type. There is a clayey silt layer under the levee and this layer is 4 m thick.

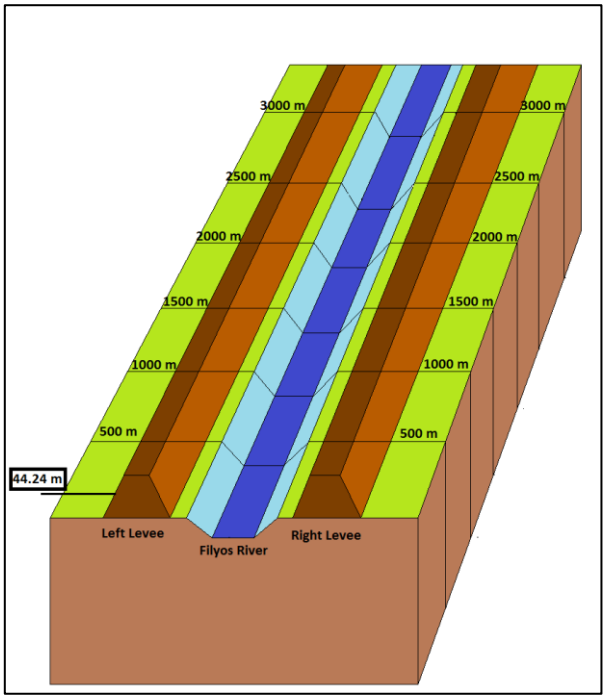

Figure 7.1 Locations of Filyos levee at 44.24 m on left shore of Filyos River

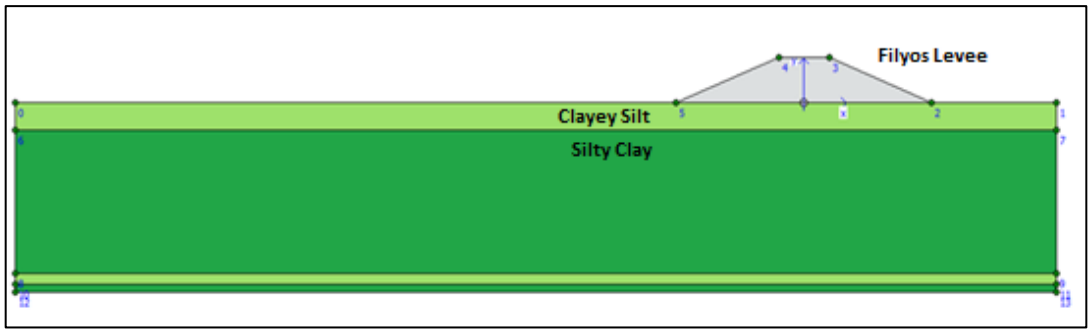

Figure 7.2 Filyos Levee at 44.24 m on left shore of Filyos River

Figure 7.3 shows that each soil layers have saturated unit weight under the levee for transient analysis and area of under the flow line is saturated during $h_{max.}$

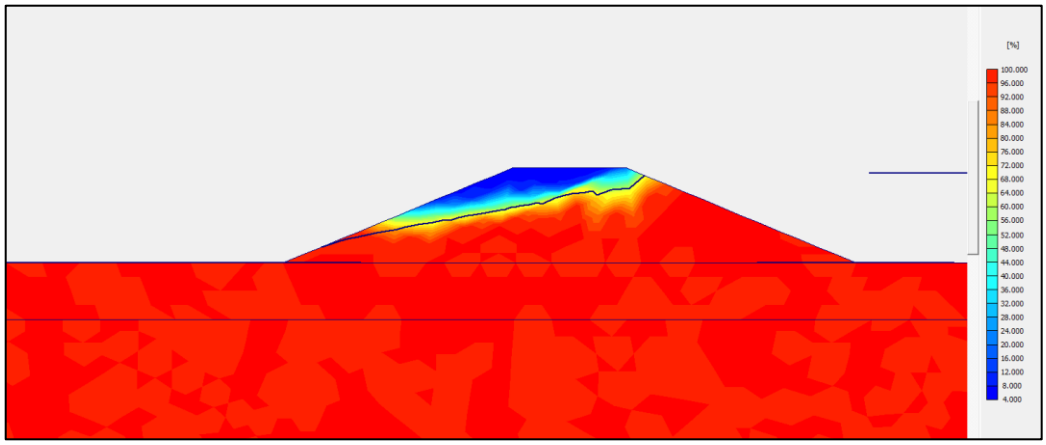

Figure 7.3 Degree of Saturation of Filyos Levee at 44.24 m on left shore of Filyos River during h_{max}

It is seen that flow values are high at the red area in case h_{max} under the flow line according to Plaxflow2D (Figure 7.4.a). There is a risk that is observed piping at these areas.

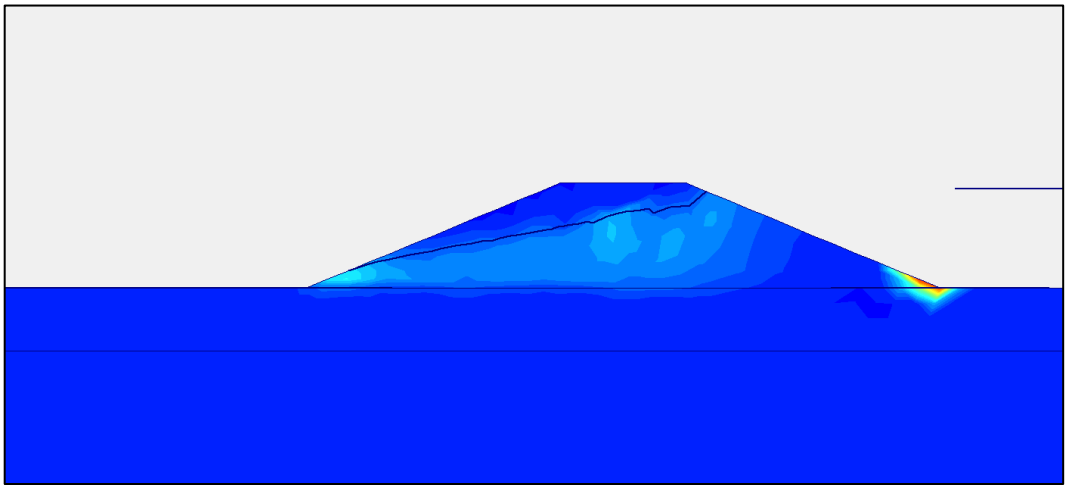

(a)

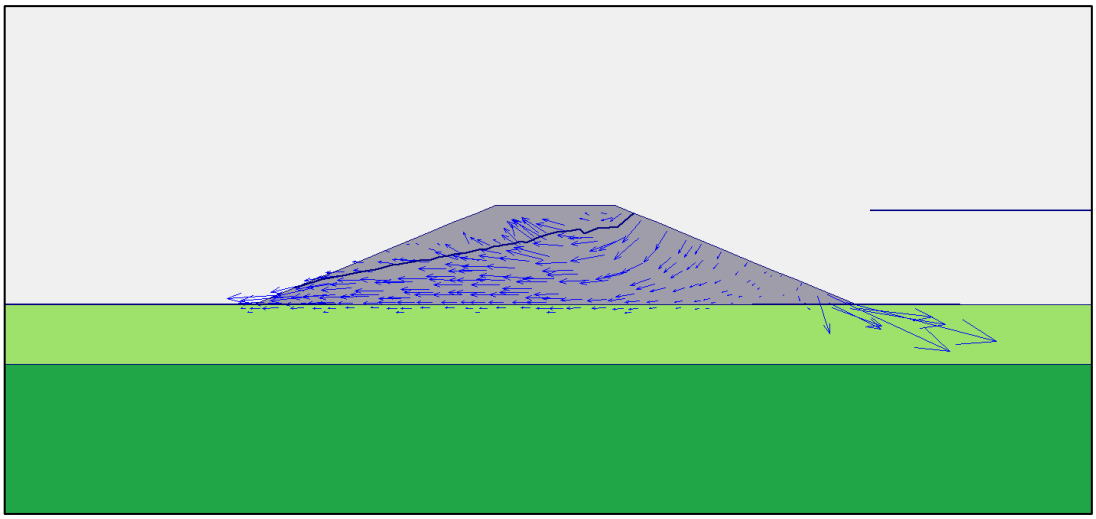

(b)

Figure 7.4. Flow field at 44.24 m on left shore of Filyos River during h_{max} a.) Shadings view b.) Arrows view

Figure 7.4. (b) is other notation that is vector stage in case h_{max}. That is called arrows in Plaxflow2D literature. If the vectors values are higher than others, there will be observing piping formations. There are not flow above the phreatic line because this area is unsaturated.

Analysis of clayey silt at under the levee ;

Figure 7.5 shows that location of points near the ground surface for finding extreme velocity and Figure 7.6 presents that results of flow velocity at K, L, M, N, O, P, Q and R.

One of the most important point is M points. M point is levee toe and K point is located upstream face region. L point is under the levee.

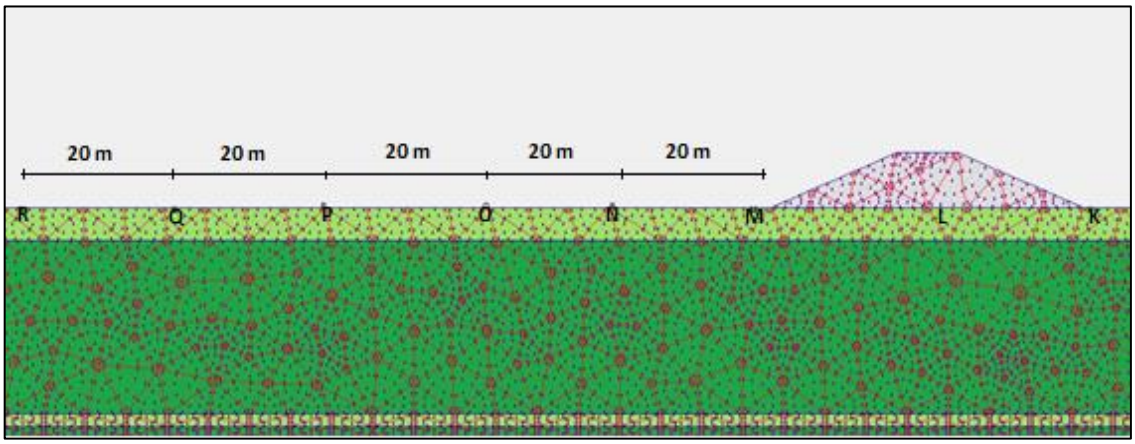

Figure 7.5 Location of points near the ground surface for finding extreme velocity

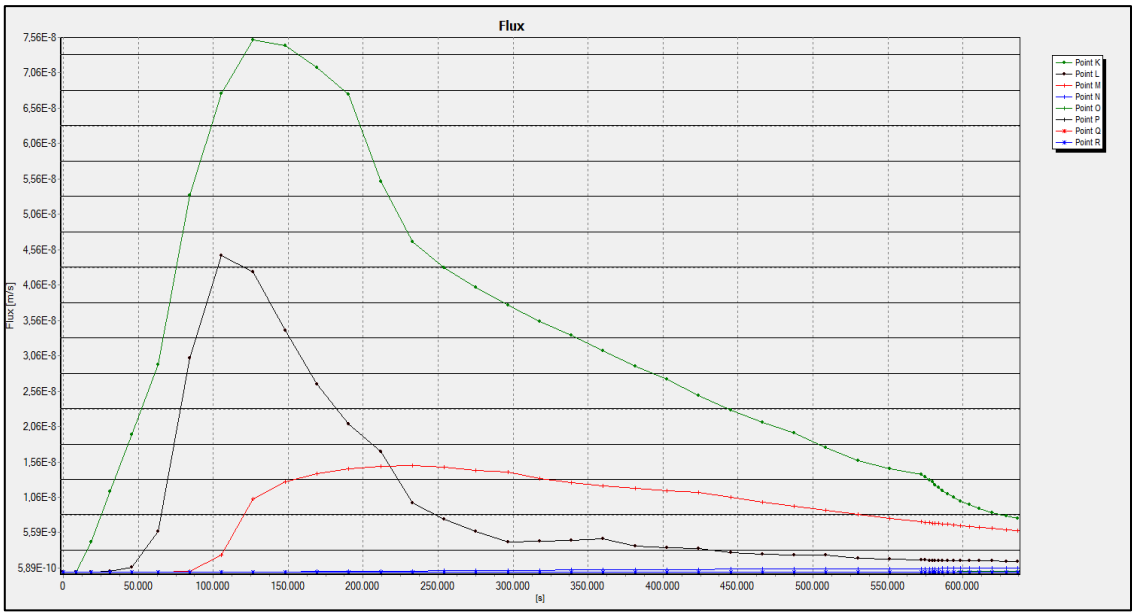

Figure 7.6 Extreme velocity graph relation time to seepage velocity

According to Figure 7.6, max values of flow are K=7.6x10^{-8} m/s at time=38.9 hours; L=4.6x10^{-8} m/s at time=30.6 hours; M=1.6x10^{-8} m/s at time=66.7 hours; N, O, P, Q and R= 5.4x10^{-10} m/s at time=152.8 hours.

Piping formations are simply compate as;

$$v = k.i\,; \tag{7.4}$$

$$i_c = \frac{G_s - 1}{1+e} = \frac{2.70-1}{1+0.9} = 0.89; \tag{7.5}$$

Where;

v = flow velocity (m/sec)

k = permeabilty (m/sec)

i = hydraulic gradient

i_c = critical hydraulic gradient

G_s = specific gravity; 2.70 for clayey silt

e = void ratio; 0.90 for clayey silt

Critical hydraulic gradients is 0.89 for clayey silt. According to max flow velocity, piping is investigated these points. Table 7.1 shows that piping is not observed at any points due to $i_{exit} < i_c$.

Table 7.1 Piping Status

Symbol	Max Seepage Velocity (m/s)	Permeability (m/s) (k)	Exit Gradient (*i*)	Piping
K	7.6×10^{-8}	1×10^{-7}	0.76	**NaN**
L	4.6×10^{-8}	1×10^{-7}	0.46	**NaN**
M	1.6×10^{-8}	1×10^{-7}	0.16	**NaN**
N	5.4×10^{-10}	1×10^{-7}	0	**NaN**
O	5.4×10^{-10}	1×10^{-7}	0	**NaN**
P	5.4×10^{-10}	1×10^{-7}	0	**NaN**
Q	5.4×10^{-10}	1×10^{-7}	0	**NaN**
R	5.4×10^{-10}	1×10^{-7}	0	**NaN**

NaN:Not a Number

In order for the sand boiling to occur, the piping must take place. As can be seen in the Table 7.2. Critical hydraulic gradient is 0.89 for clayey silt and it did not reach critical hydraulic gradient for the formation of boiling.

Table 7.2 Sand Boil Status

Symbol	Max Seepage Velocity (m/s)	Permeability (m/s) (k)	Exit Gradient (*i*)	Sand Boil
M	1.6×10^{-8}	1×10^{-7}	0.16	**NaN**
N	5.4×10^{-10}	1×10^{-7}	0	**NaN**
O	5.4×10^{-10}	1×10^{-7}	0	**NaN**
P	5.4×10^{-10}	1×10^{-7}	0	**NaN**
Q	5.4×10^{-10}	1×10^{-7}	0	**NaN**
R	5.4×10^{-10}	1×10^{-7}	0	**NaN**

NaN:Not a Number

The analysis above the levee for gravelly sand soil type ;

Piping can only observe K, L and M point because these points only are under the phreatic line. K, L, M etc. points on the ground surface or levee are different from other analyses. K, L and M points are investigated in terms of piping formation and Figure 7.7 shows K, L and M points on downstream face of Filyos levee.

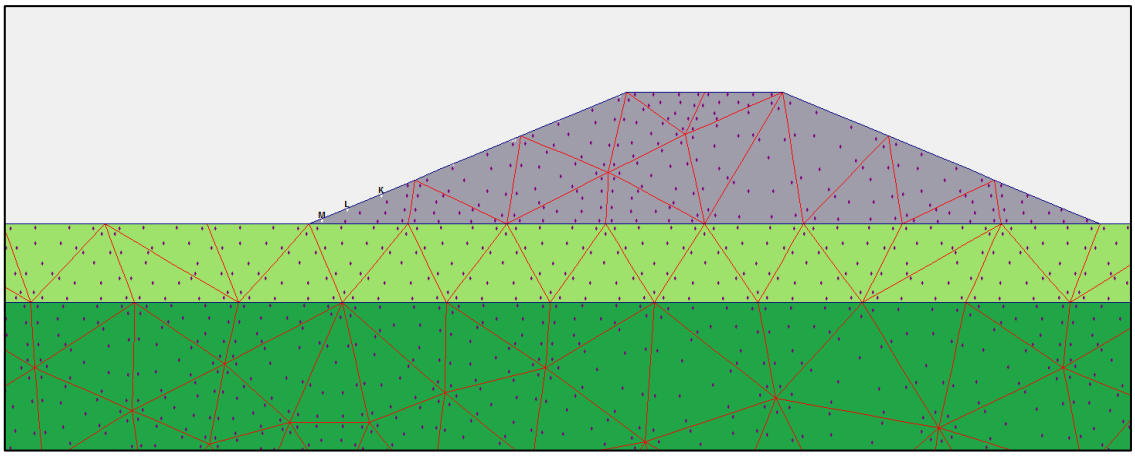

Figure 7.7 Location of points above the levee for finding extreme velocity

Extreme velocities of K, L and M point are Figure 7.8 and piping formations are investigated for these points.

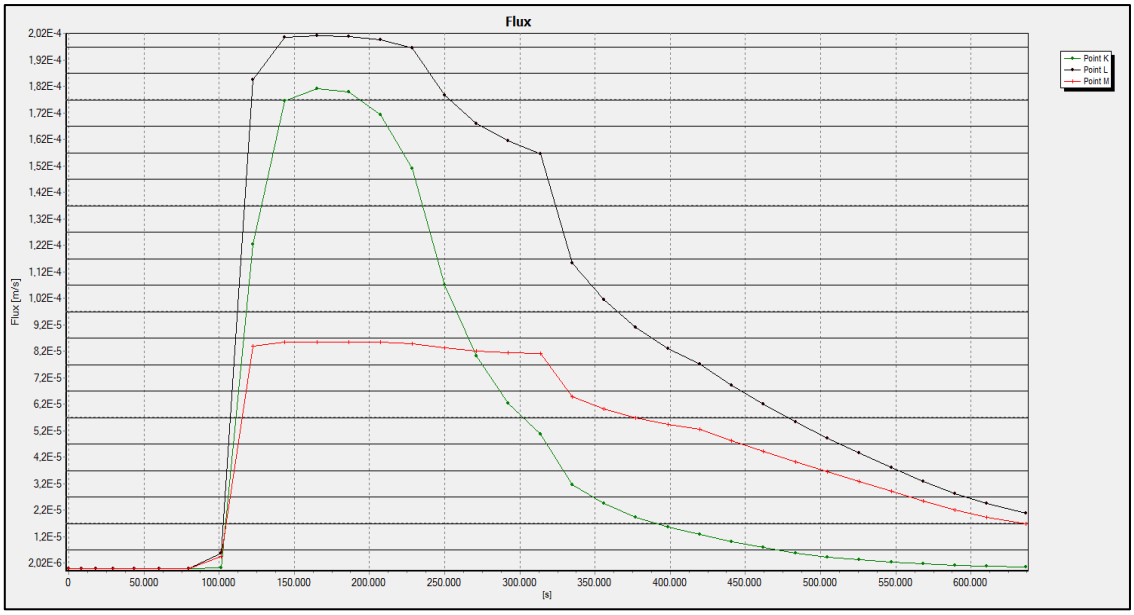

Figure 7.8 Extreme velocity graph relation time above the levee

According to Figure 7.8, max values of flow are K=1.8x10^{-4}m/s at time=48.6 hours; L=2x10^{-4}m/s at time=48.6 hours; M=8.7 x 10^{-5}m/s at time=55.6 hours.

Piping formations are simply compate as;

$$v = k.i\,; \tag{7.6}$$

$$i_c = \frac{G_s - 1}{1+e} = \frac{2.66-1}{1+0.62} = 1.02\,; \tag{7.7}$$

Where;

v = flow velocity (m/sec)

k = permeabilty (m/sec)

i = hydraulic gradient

i_c = critical hydraulic gradient

G_s = specific gravity; 2.66 for gravelly sand

e = void ratio; 0.62 for gravelly sand

Table 7.3. shows that piping is not observed at any points due to $i_{exit} < i_c$.

Table 7.3 Piping Status

Symbol	Max Seepage Velocity (m/s)	Permeability (m/s) (k)	Exit Gradient (*i*)	Piping
K	1.8×10^{-4}	5×10^{-4}	0.36	**NaN**
L	2.0×10^{-4}	5×10^{-4}	0.40	**NaN**
M	8.7×10^{-5}	5×10^{-4}	0.17	**NaN**

NaN:Not a Number

The factor of safety against heave analysis for top layer ;

Equation 7.8 and 7.9 are used to determine the factor of safety against heave analysis for top layer. Heaving potential are only observed ground surface hence a point are investigated at 1 m below the top layer like Figure 7.9.

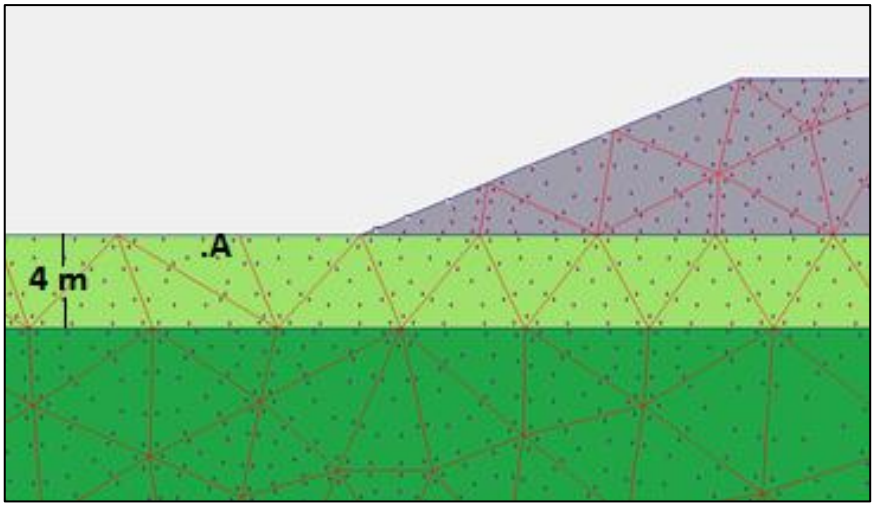

Figure 7.9 Analysis against to heave at A point 1 m below the top layer

$$F_{heave} = \frac{H.\gamma_{sat}}{h_m.\gamma_w} > 3.0 \tag{7.8}$$

$$i_{\max} = \frac{h_m}{H} \tag{7.9}$$

Where;

H = thickness of overlying top layer (m)

γ_{sat} = saturated unit weight of overlying top layer (kN/m^2)

h_m = average hydraulic head at the point (m)

γ_w = water unit wight (kN/m^2)

$i_{\max}$ = maximum exit gradient

$$0.16 = \frac{h_m}{1.0} \Rightarrow h_m = 0.16 \;;\; F_{heave} = \frac{1.0x18.6}{0.16x10.0} = 3.2 > 3.0$$

It is not observed heave due to the fact that F_{heave} is higher than 3.0 .

7.3. Filyos Levee at 44.24 m on the Left Shore of Filyos River with Covered along Upstream of River(Upstream face is covered)

The schematic representation of Filyos Levee and soil profile is given in Figure 7.10. Filyos levee includes gravelly sand soil type and cover materials against piping and sand boil formations. The cover materials are riprap which is andesite, uniform sand filter layer and geocomposite layer. There is a clayey silt layer under the levee and this layer is 4 m thick.

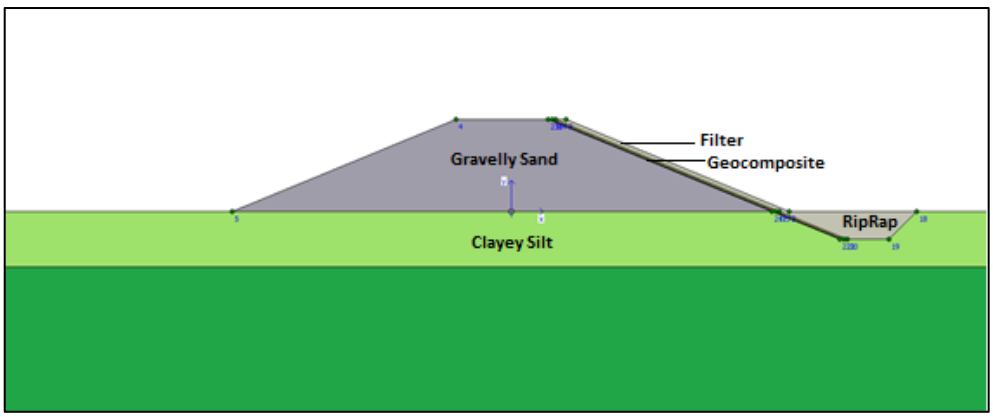

Figure 7.10 Filyos Levee with cover materials at 44.24 m on left shore of Filyos River

Filyos levee has covered along rising water level. The covered members are filter, riprap and geocomposite materials. Table 7.4 shows properties of covered materials and levee.

Table 7.4 Soil Properties of levee members

	Soil Type / Material	**Permeability(k) (m/sec)**	**Specific Gravity (G_s)**	**Void Ratio (e)**	**Thickness (m)**
Filter	Uniform Sand	$1x10^{-3}$	2.67	0.70	0.25
Riprap	Andesite Rock	0.645	2.65	0.34	0.70
Geocomposite Material	Geotextile and Geomembrane	$1x10^{-13}$	-	0.02	0.30

Figure 7.11 shows that each soil layers have saturated unit weight under the levee with cover materials for transient analysis and area of under the flow line is saturated during h_{max}. Saturation rates of red areas are high and saturation rates of other areas are almost zero with riprap, filter and geocomposites.

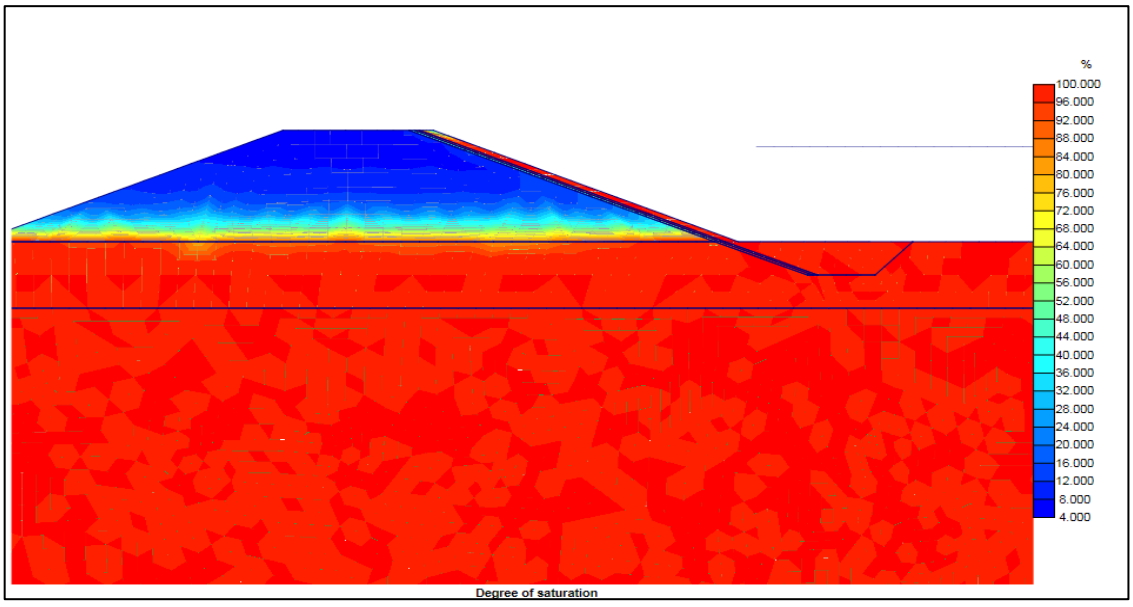

Figure 7.11 Degree of Saturation of Filyos Levee with cover materials at 44.24 m on left shore of Filyos River during h_{max}

It is seen that flow values are high at the red area in case h_{max} under the flow line according to Plaxflow2D (Figure 7.12.a). There is not a risk that is observed piping into through levee.

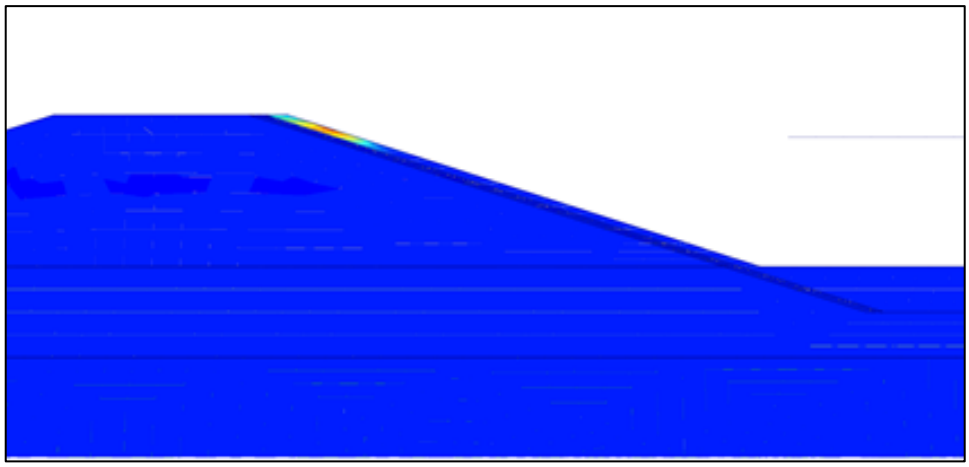

(a)

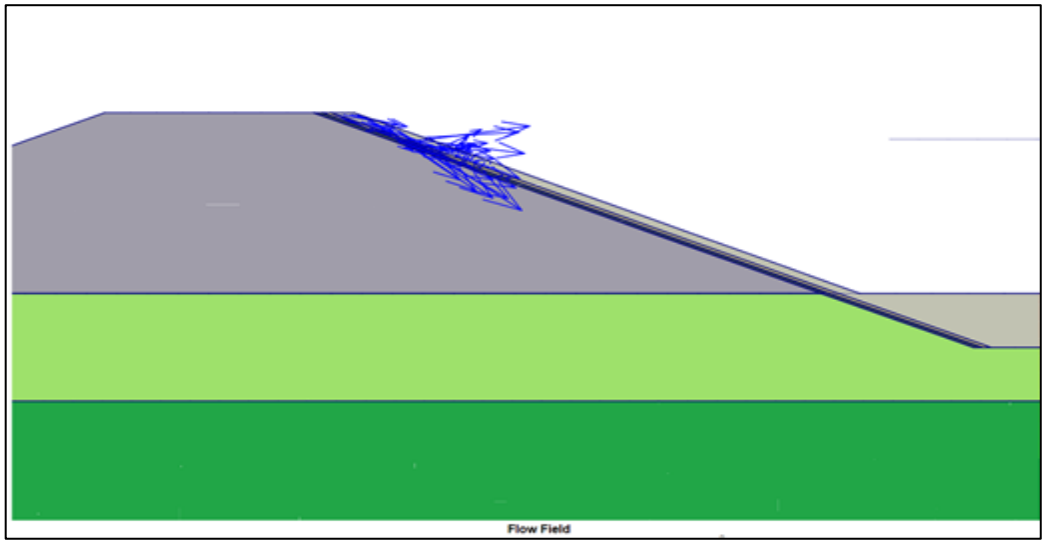

(b)

Figure 7.12. Flow field at 44.24 m on left shore of Filyos River during h_{max} a.) Shadings view b.) Arrows view

Figure 7.12. (b) is other notation that is vector stage in case h_{max}. That is called arrows in Plaxflow2D literature and there is not risk into through levee.

Analysis of clayey silt at under the levee;

Figure 7.13 shows that location of points near the ground surface for finding extreme velocity and Figure 7.14 presents that results of flow velocity at K, L, M, N, O, P and Q. K point is on the Filyos levee and this point is under the phreatic line and piping formation is observed this point. L point is at levee toe and the other points are under the levee. Piping formations, sand boil formations and heaving potential are observed these points.

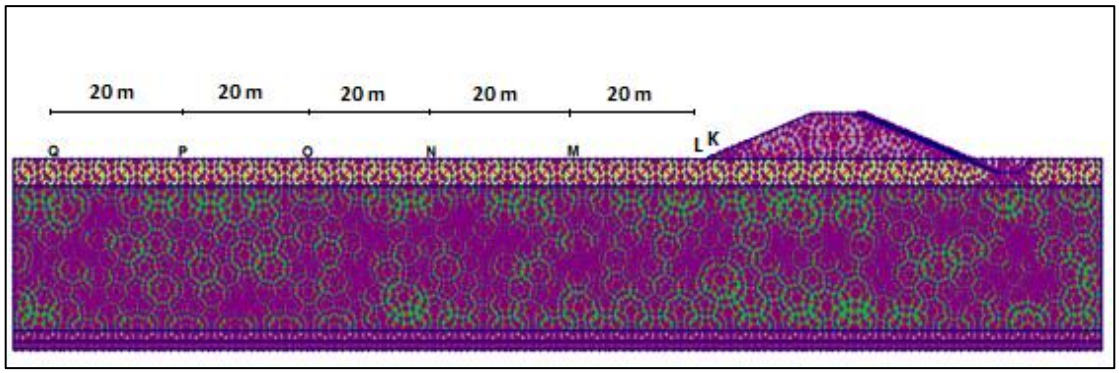

Figure 7.13 Location of points near the ground surface for finding extreme velocity

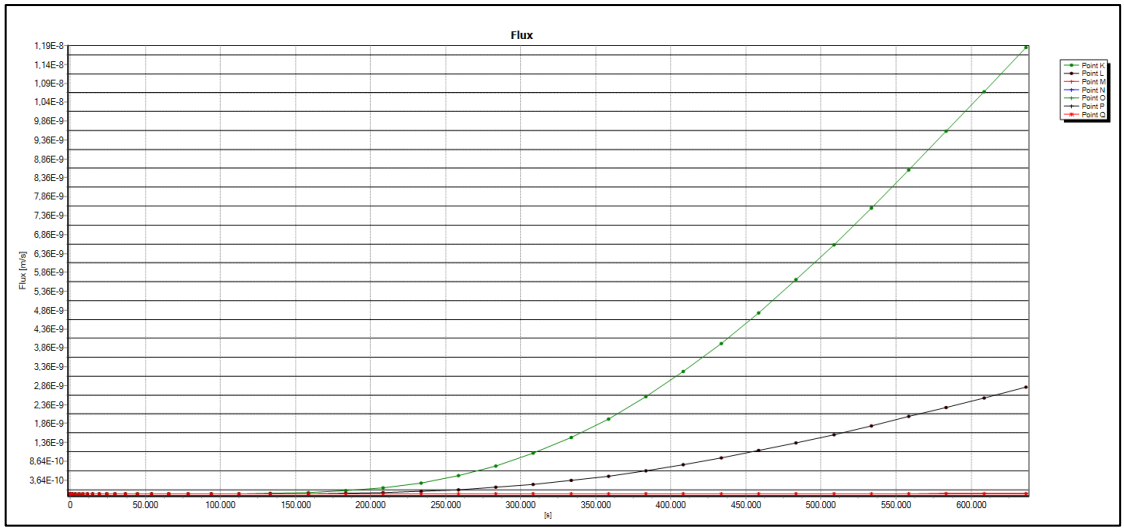

Figure 7.14 Extreme velocity graph relation time Filyos Levee

Table 7.5 shows that piping is not observed at any points due the fact that to exit gradient is zero. See equations 7.4, 7.5, 7.6 and 7.7 for calculated critical hydraulic gradients.

Table 7.5 Piping Status

Symbol	Max Seepage Velocity (m/s)	Permeability (m/s) (k)	Exit Gradient (*i*)	Piping
K	1.2×10^{-8}	1×10^{-7}	0	**NaN**
L	2.8×10^{-9}	1×10^{-7}	0	**NaN**
M	3.5×10^{-10}	1×10^{-7}	0	**NaN**
N	3.0×10^{-10}	1×10^{-7}	0	**NaN**
O	3.0×10^{-10}	1×10^{-7}	0	**NaN**
P	3.0×10^{-10}	1×10^{-7}	0	**NaN**
Q	3.0×10^{-10}	1×10^{-7}	0	**NaN**

NaN:Not a Number

In order for the sand boiling to occur, the piping must take place. As can be seen in the Table 7.6, it did not reach critical gradient for the formation of boiling. See equations 7.4, 7.5, 7.6 and 7.7 for calculated critical hydraulic gradients.

Table 7.6 Sand Boil Status

Symbol	Max Seepage Velocity (m/s)	Permeability (m/s) (k)	Exit Gradient (*i*)	Sand Boil
L	2.8×10^{-9}	1×10^{-7}	0.03	**NaN**
M	3.5×10^{-10}	1×10^{-7}	0	**NaN**
N	3.0×10^{-10}	1×10^{-7}	0	**NaN**
O	3.0×10^{-10}	1×10^{-7}	0	**NaN**
P	3.0×10^{-10}	1×10^{-7}	0	**NaN**
Q	3.0×10^{-10}	1×10^{-7}	0	**NaN**

NaN:Not a Number

- Heaving potential is not observed that levee has cover materials along river since the exit gradients approach zero.

7.4. Filyos Levee at 271.05 m on Right Shore of Filyos River

Location of Filyos levee at 271.05 m on right shore is seen Figure 7.16 and the schematic representation of Filyos levee and soil profile is given in Figure 7.15 Filyos levee includes gravelly sand soil type. There is a clayey sand layer under the levee and this layer is 2 m thick.

Piping formation is investigated on levees and under levees. Sand boil and heaving potential are investigated on ground surface.

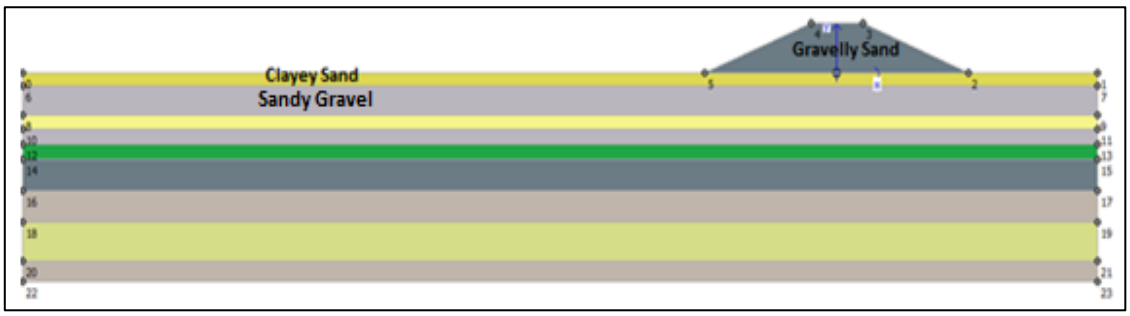

Figure 7.15 Filyos Levee at 271.05 m on right shore of Filyos River

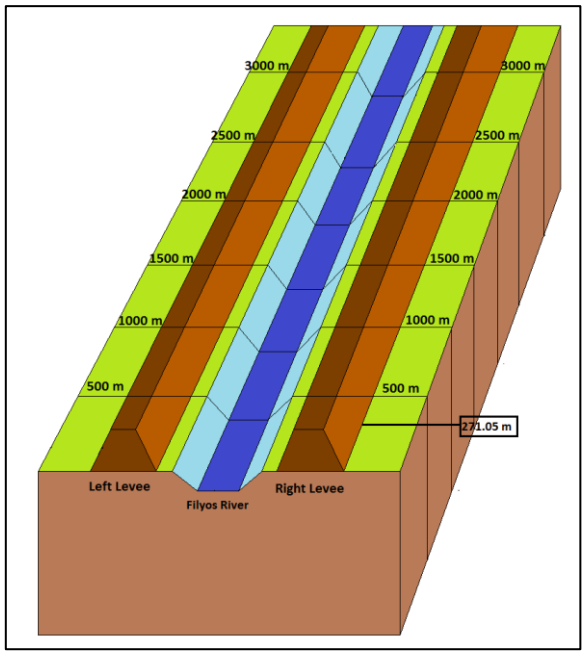

Figure 7.16 Filyos Levee at 271.05 m on right shore of Filyos River

Figure 7.17 shows that each soil layers have saturated unit weight under the levee for transient analysis and area of under the flow line is saturated during h_{max}.

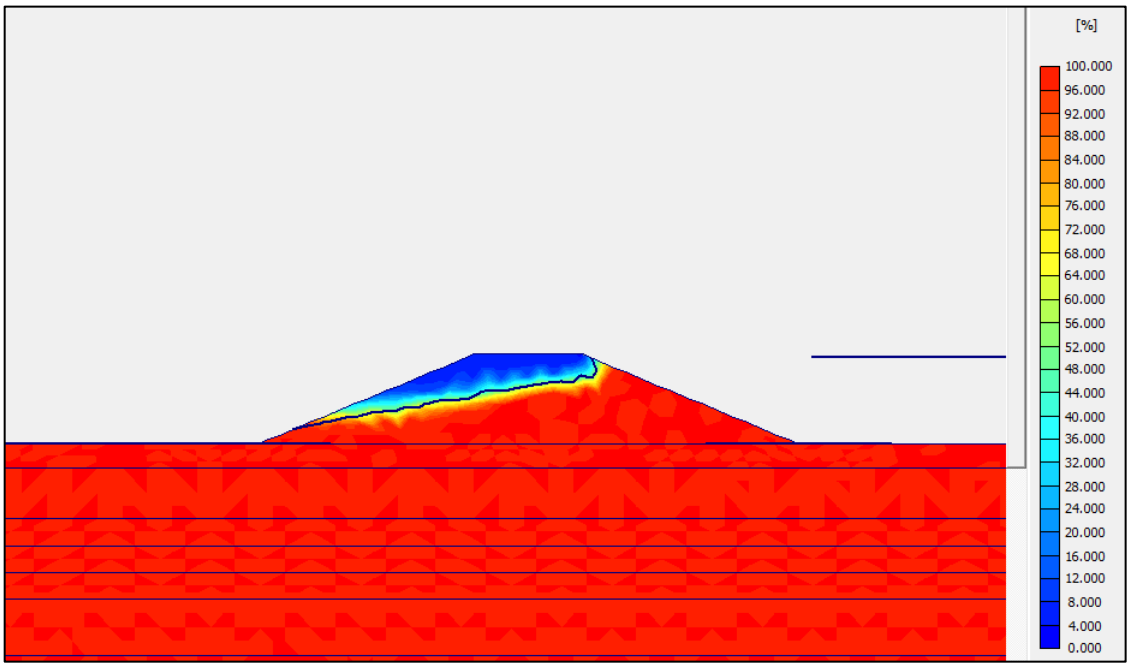

Figure 7.17 Degree of Saturation of Filyos Levee at 271.05 m on right shore of Filyos River during h_{max}

It is seen that flow values are high at the red area in case h_{max} under the flow line according to Plaxflow2D (Figure 7.18.a). There is a risk that is observed piping at these areas.

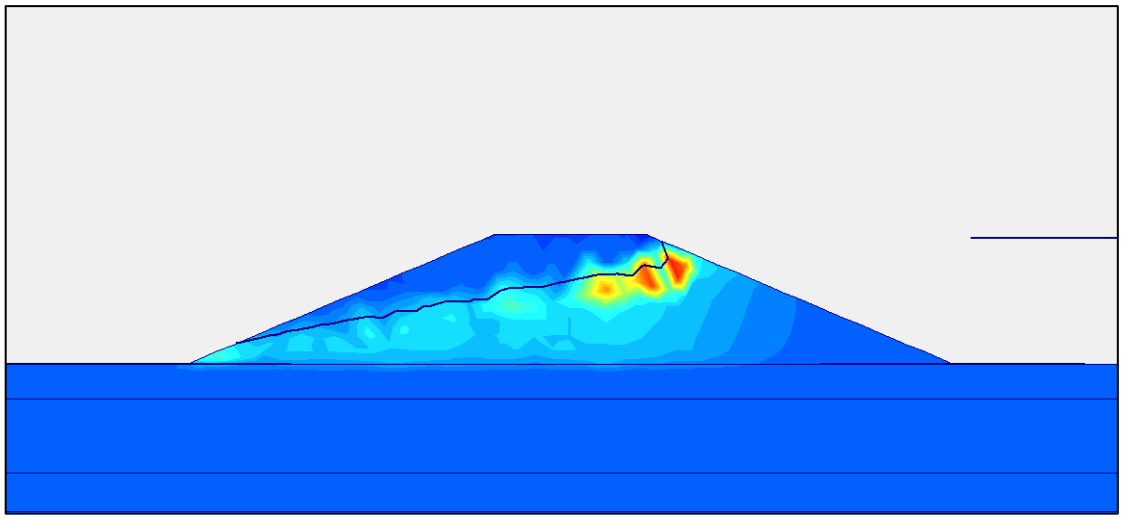

(a)

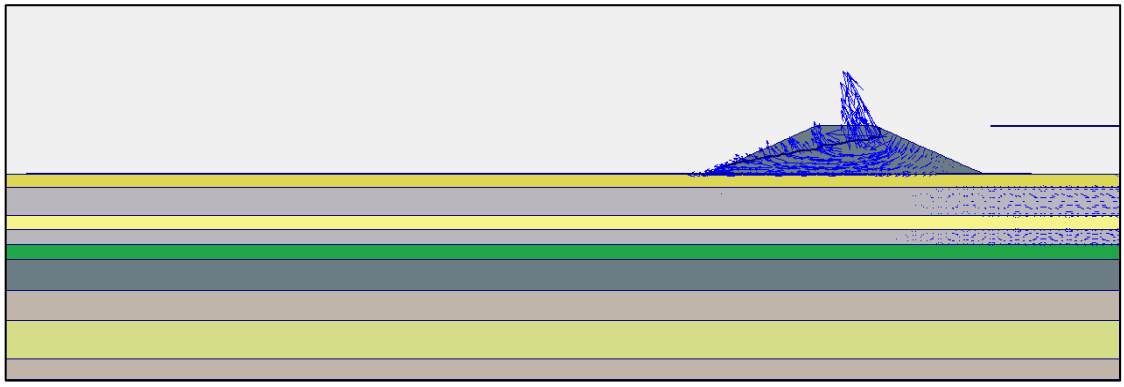

(b)

Figure 7.18. Flow field at 271.05 m on right shore of Filyos River during h_{max}
a.) Shadings view b.) Arrows view

Figure 7.18. (b) is other notation that is vector stage in case h_{max}. That is called arrows in Plaxflow2D literature. If the vectors values are higher than others, there will be observing piping formations.

Analysis of clayey sand at under the levee;

Figure 7.19 shows that location of points near the ground surface for finding extreme velocity and Figure 7.20 presents that results of flow velocity at K, L, M, N, O, P, Q and R. K, L, M etc. points on the ground surface or levee are different from other analyses.

One of the most important point is R points. R point is levee toe and K point is located upstream face region. L point is under the levee. Sand boil and heaving potential are investigated for other points.

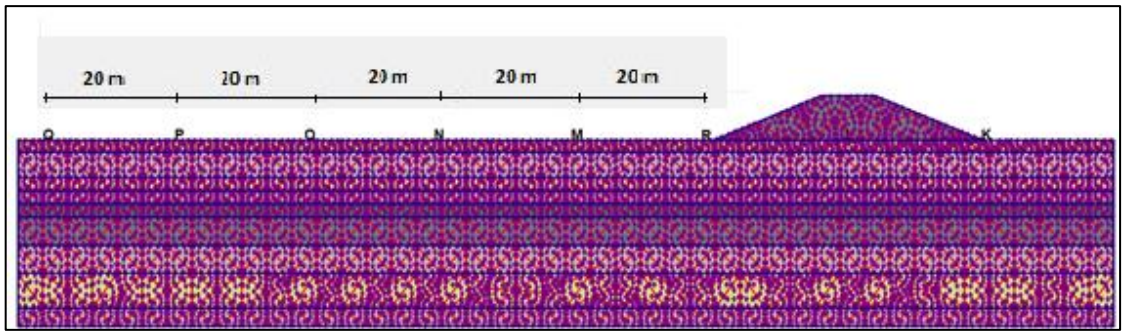

Figure 7.19 Location of points near the ground surface for finding extreme velocity

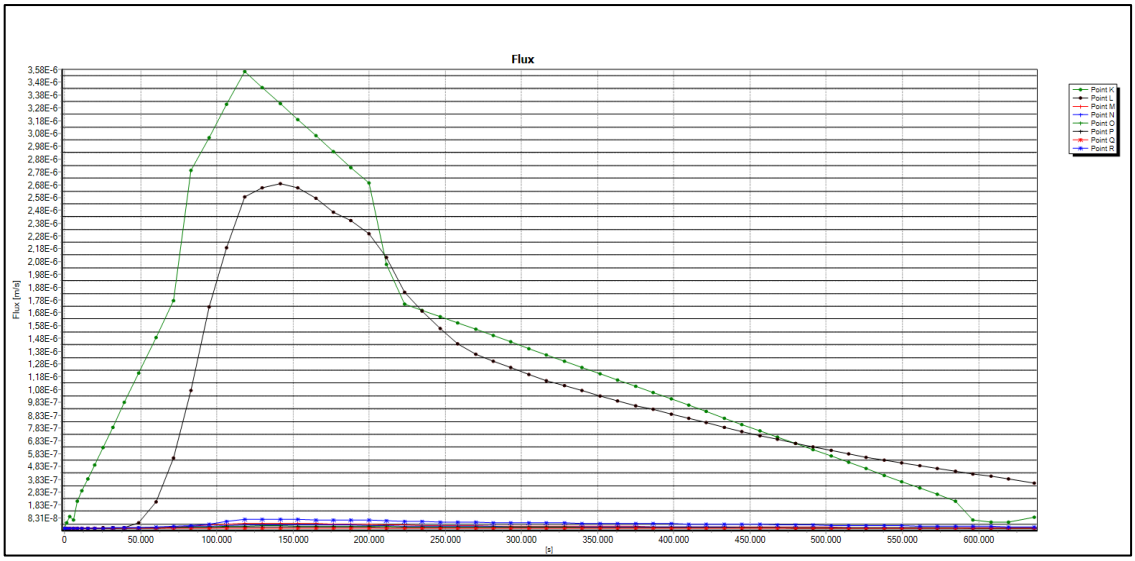

Figure 7.20 Extreme velocity graph relation time to seepage velocity

According to Figure 7.20, max values of flow are K=3.6x10^{-6}m/s at time=34.7 hours; L=2.7x10^{-6}m/s at time=40.3 hours; M=7 x 10^{-8}m/s at time=40.3 hours; N=6x10^{-8}m/s at time=40.3 hours; O, P and Q=5x10^{-8}m/s at time=40.3 hours; R=8.3 x 10^{-8}m/s at time=40.3 hours.

Piping formations are simply compate as;

$$v = k.i\,; \tag{7.10}$$

$$i_c = \frac{G_s - 1}{1+e} = \frac{2.67-1}{1+0.43} = 1.2\,; \tag{7.11}$$

Where;

v = flow velocity (m/sec)

k = permeabilty (m/sec)

i = hydraulic gradient

i_c = critical hydraulic gradient

G_s = specific gravity; 2.67 for clayey sand

e = void ratio; 0.43 for clayey sand

Table 7.7 shows that piping is observed at some points due to $i_{exit} > i_c$ but it is not insufficient piping formation because it does not occur piping at levee toe (Point R).

Table 7.7 Piping Status

Symbol	Max Seepage Velocity (m/s)	Permeability (m/s) (k)	Exit Gradient (i)	Piping
K	3.6×10^{-6}	1×10^{-6}	3.60	$i_{exit} > i_c$
L	2.7×10^{-6}	1×10^{-6}	2.70	$i_{exit} > i_c$
M	7.0×10^{-8}	1×10^{-6}	0.07	**NaN**
N	6.0×10^{-8}	1×10^{-6}	0.06	**NaN**
O	5.0×10^{-8}	1×10^{-6}	0.05	**NaN**
P	5.0×10^{-8}	1×10^{-6}	0.05	**NaN**
Q	5.0×10^{-8}	1×10^{-6}	0.05	**NaN**
R	8.3×10^{-8}	1×10^{-6}	0.08	**NaN**

NaN:Not a Number

In order for the sand boiling to occur, the piping must take place. As can be seen in the Table 7.8. Critical hydraulic gradient is 1.2 for clayey sand so, it did not reach critical hydraulic gradient for the formation of boiling.

Table 7.8 Sand Boil Status

Symbol	Max Seepage Velocity (m/s)	Permeability (m/s) (k)	Exit Gradient (i)	Sand Boil
M	7.0×10^{-8}	1×10^{-6}	0.07	**NaN**
N	6.0×10^{-8}	1×10^{-6}	0.06	**NaN**
O	5.0×10^{-8}	1×10^{-6}	0.05	**NaN**
P	5.0×10^{-8}	1×10^{-6}	0.05	**NaN**
Q	5.0×10^{-8}	1×10^{-6}	0.05	**NaN**
R	8.3×10^{-8}	1×10^{-6}	0.08	**NaN**

NaN:Not a Number

The analysis above the levee for gravelly sand soil type;

Piping can only observe K, L and M point because these points only are under the phreatic line. K, L, M etc. points on the ground surface or levee are different from other analyses.

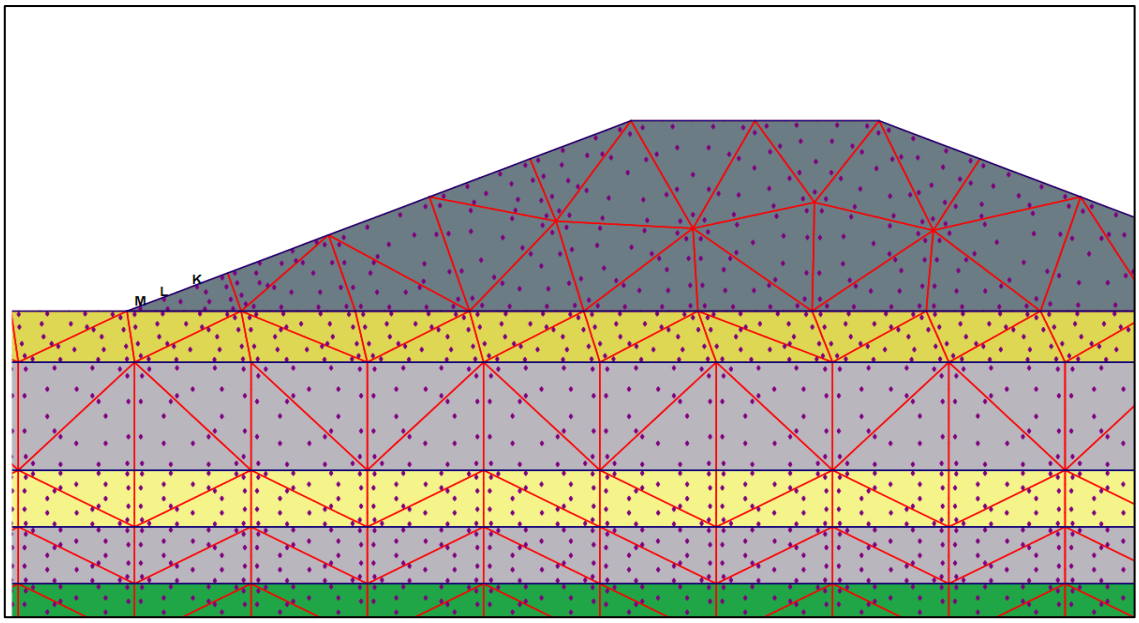

Figure 7.21 Location of points above the levee for finding extreme velocity

Extreme velocities of K, L and M point are Figure 7.22 and piping formations are investigated for these points.

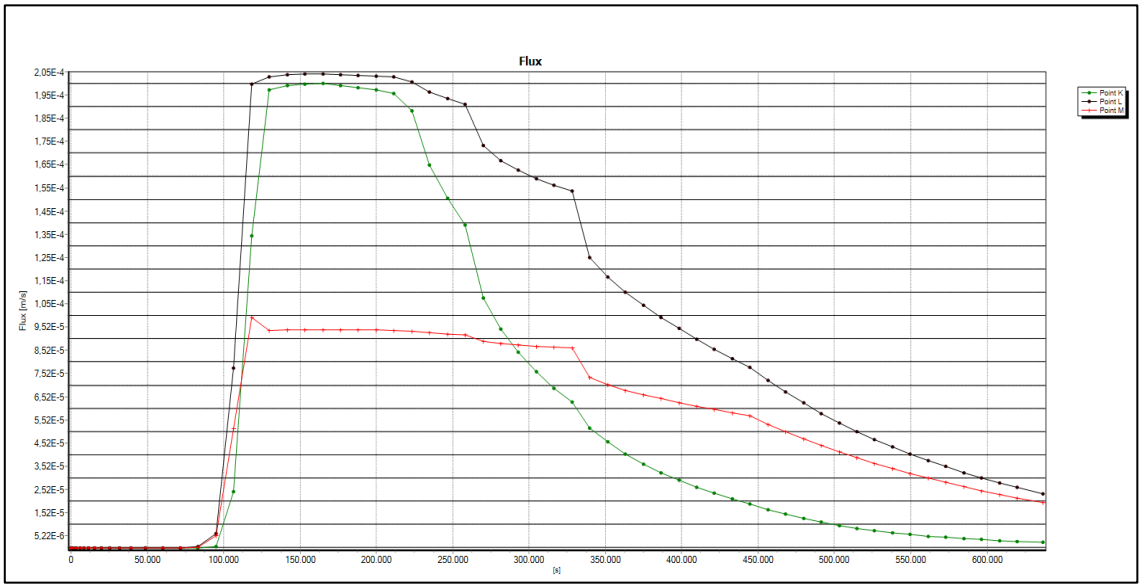

Figure 7.22 Extreme velocity graph relation time above the levee

According to Figure 7.22, max values of flow are K=2.0x10^{-4}m/s at time=41.7 hours; L=2.1x10^{-4}m/s at time=41.7 hours; M=1.0 x 10^{-6}m/s at time=34.7 hours.
Piping formations are simply compate as;

$$v = k.i\,; \tag{7.12}$$

$$i_c = \frac{G_s - 1}{1 + e} = \frac{2.66 - 1}{1 + 0.62} = 1.02\,; \tag{7.13}$$

Where;

v = flow velocity (m/sec)

k = permeabilty (m/sec)

i = hydraulic gradient

i_c = critical hydraulic gradient

G_s = specific gravity; 2.66 for gravelly sand

e = void ratio; 0.62 for gravelly sand

Critical hydraulic gradients is 1.02 for gravelly sand. According to max flow velocity, piping is investigated these points. Table 7.9. shows that piping is not observed at any points due to $i_{exit} < i_c$.

Table 7.9 Piping Status

Symbol	Max Seepage Velocity (m/s)	Permeability (m/s) (k)	Exit Gradient (*i*)	Piping
K	2.0 x 10^{-4}	5 x 10^{-4}	0.40	**NaN**
L	2.1 x 10^{-4}	5 x 10^{-4}	0.42	**NaN**
M	1.0 x 10^{-4}	5 x 10^{-4}	0.20	**NaN**

NaN:Not a Number

The factor of safety against heave analysis for top layer;

Equation 7.13 and 7.14 are used to determine the factor of safety against heave analysis for top layer. Heaving potential are only observed ground surface hence a point are investigated at 1 m below the top layer like Figure 7.23.

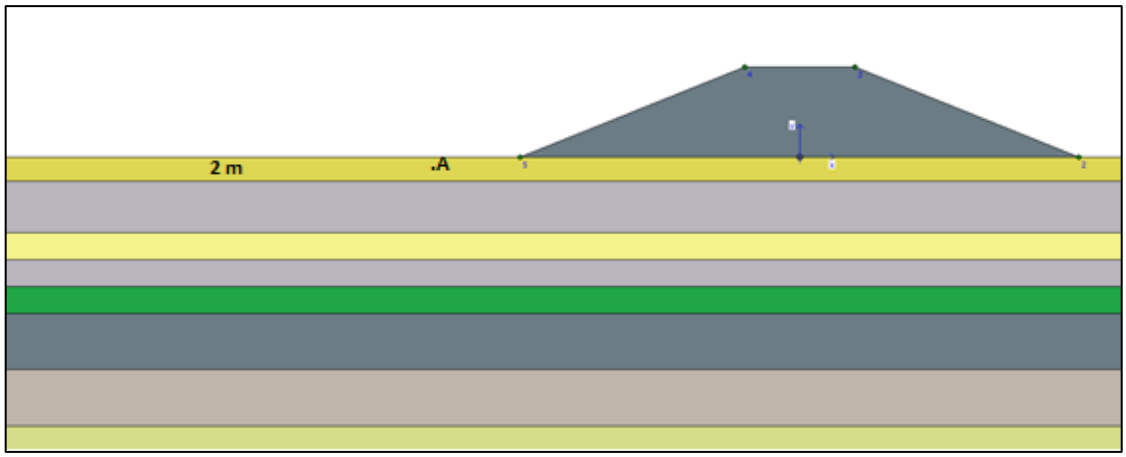

Figure 7.23 Analysis against to heave at A point 1 m below the top layer

$$F_{heave} = \frac{H.\gamma_{sat}}{h_m.\gamma_w} > 3.0 \tag{7.13}$$

$$i_{\max} = \frac{h_m}{H} \tag{7.14}$$

Where;

H = thickness of overlying top layer (m)

γ_{sat} = saturated unit weight of overlying top layer (kN/m^2)

h_m = average hydraulic head at the point (m)

γ_w = water unit wight (kN/m^2)

$i_{\max}$ = maximum exit gradient

$$0.08 = \frac{h_m}{1.0} \Rightarrow h_m = 0.08 \;;\; F_{heave} = \frac{1.0x21.3}{0.1x10.0} = 3.2 > 3.0$$

It is not observed heave due to the fact that F_{heave} is higher than 3.0 .

7.5. Filyos Levee at 271.05 m on Right Shore of Filyos River along Upstream of River(Upstream face is covered)

The schematic representation of Filyos Levee and soil profile is given in Figure 7.24. Filyos levee includes gravelly sand soil type and cover materials against piping and sand boil formations. The cover materials are riprap which is andesite, uniform sand

filter layer and geocomposite layer. There is a clayey sand layer under the levee and this layer is 2 m thick.

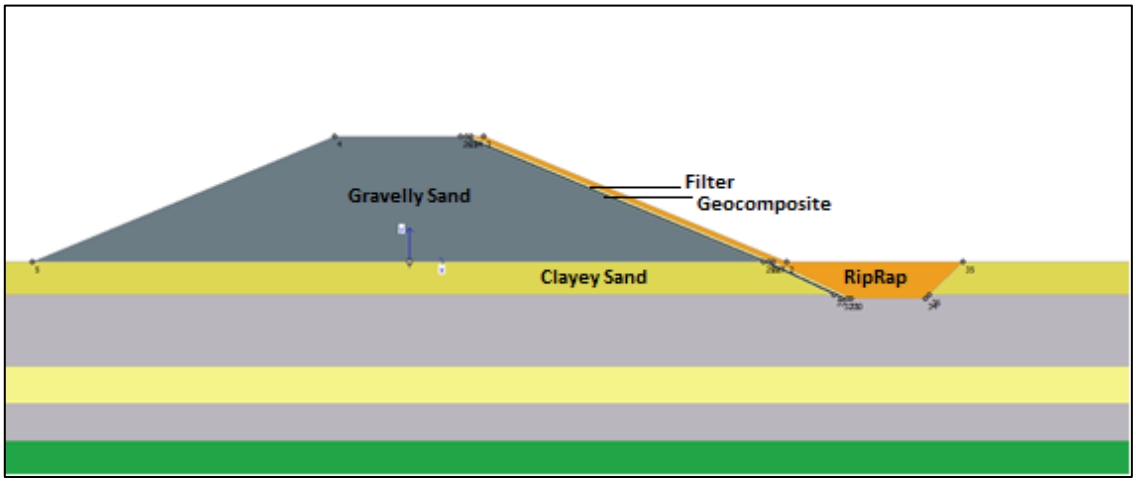

Figure 7.24 Filyos Levee with cover materials at 271.05 m on right shore of Filyos River

Filyos levee has covered along rising water level. The covered members are filter, riprap and geocomposite materials. Table 7.10 shows properties of covered materials and levee.

Table 7.10 Soil Properties of levee members

	Soil Type / Material	**Permeability(k) (m/sec)**	**Specific Gravity (G_s)**	**Void Ratio (e)**
Levee	Gravelly Sand	$5x10^{-4}$	2.66	0.62
Filter	Uniform Sand	$1x10^{-3}$	2.67	0.70
Riprap	Andesite Rock	0.645	2.65	0.34
Geocomposite Material	Geotextile and Geomembrane	$1x10^{-13}$	-	0.02

Figure 7.25 shows that each soil layers have saturated unit weight under the levee with cover materials for transient analysis and area of under the flow line is saturated during h_{max}. Saturation rates of red areas are high and saturation rates of other areas are almost zero with riprap, filter and geocomposites.

It is seen that flow values are high at the red area in case h_{max} under the flow line according to Plaxflow2D (Figure 7.26.a). There is not a risk that is observed piping into through levee.

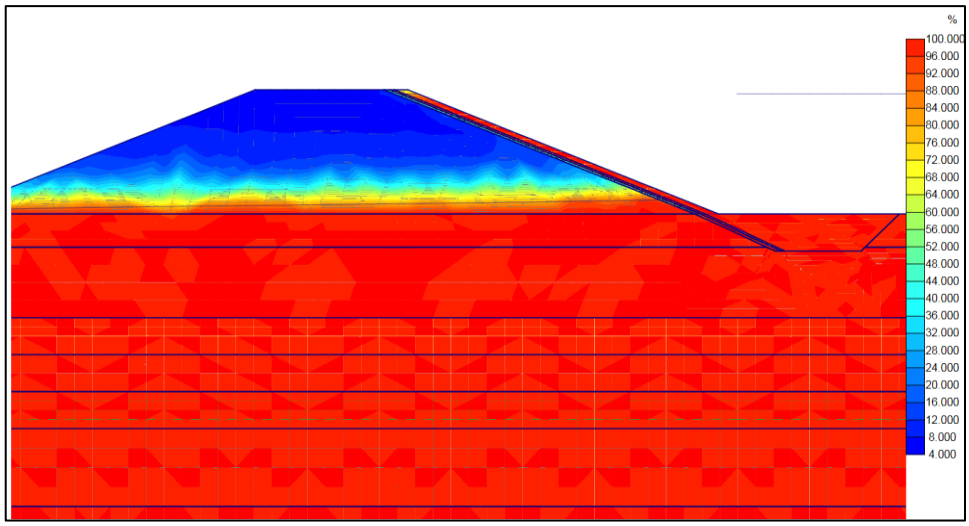

Figure 7.25 Degree of Saturation of Filyos Levee with cover materials at 271.05 m on right shore of Filyos River during h_{max}

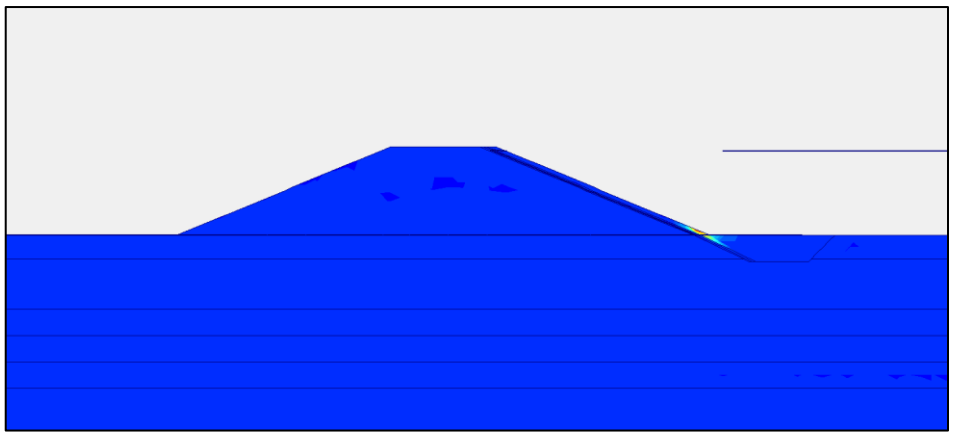

(a)

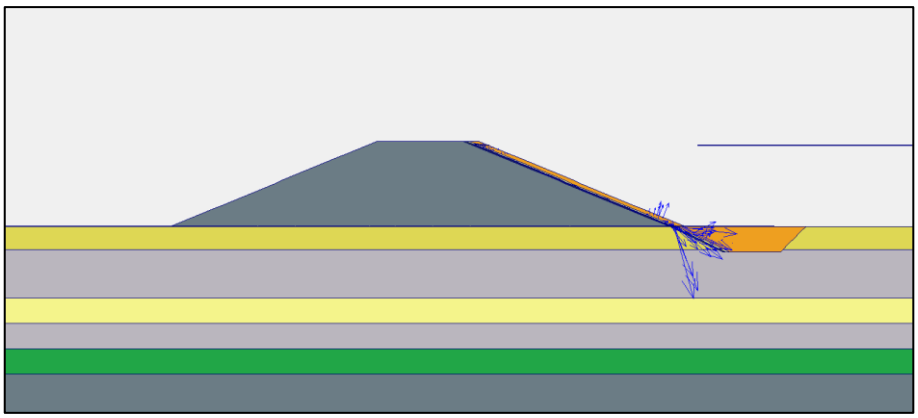

(b)

Figure 7.26. Flow field at 271.05 m on right shore of Filyos River during h_{max} a.)Shadings view b.) Arrows view

Figure 7.26. (b) is other notation that is vector stage in case h_{max}. That is called arrows in Plaxflow2D literature and there is not risk into through levee.

Analysis of clayey silt at under the levee;

Figure 7.27 shows that location of points near the ground surface for finding extreme velocity and Figure 7.28 presents that results of flow velocity at K, L, M, N, O, P and Q. K point is on the Filyos levee and this point is under the phreatic line and piping formation is observed this point. L point is at levee toe and the other points are under the levee. Piping formations, sand boil formations and heaving potential are observed these points.

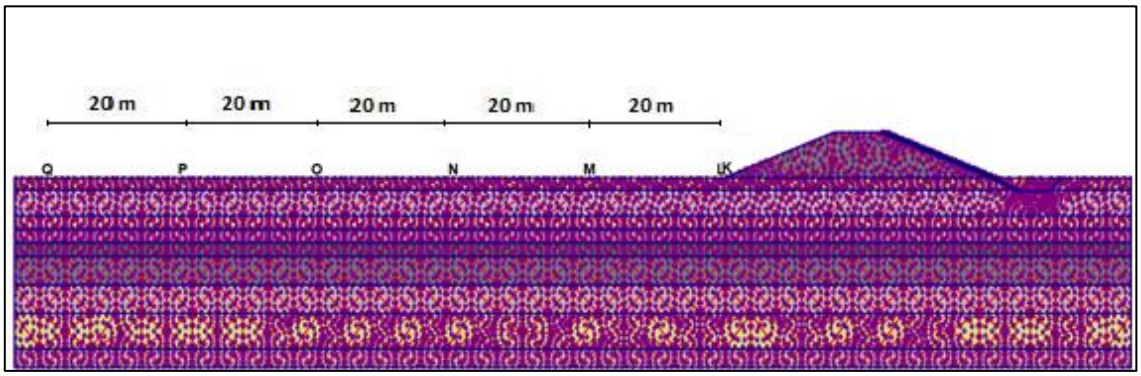

Figure 7.27 Location of points near the ground surface for finding extreme velocity

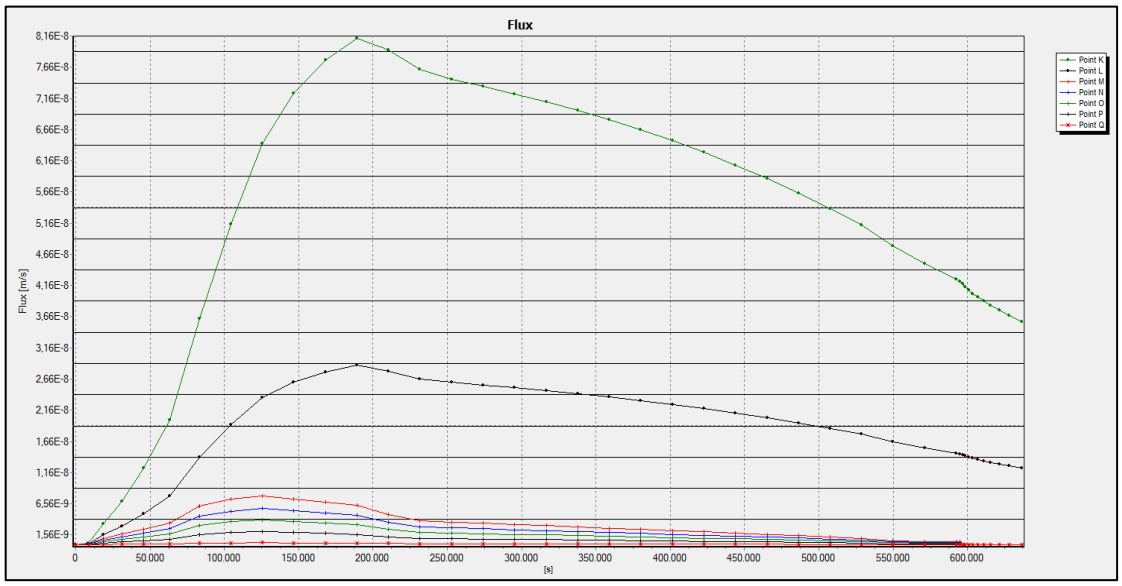

Figure 7.28 Extreme velocity graph relation time Filyos Levee

Table 7.11 shows that piping is not observed at any points due the fact that exit gradient is zero. See equations 7.11, 7.13 for calculated critical hydraulic gradients. In order for the sand boiling to occur, the piping must take place. As can be seen in the Table 7.12, it did not reach critical gradient for the formation of boiling.

Table 7.11 Piping Status

Symbol	Max Seepage Velocity (m/s)	Permeability (m/s) (k)	Exit Gradient (*i*)	Piping
K	8.2×10^{-8}	5×10^{-4}	0	**NaN**
L	2.9×10^{-8}	1×10^{-6}	0.03	**NaN**
M	6.7×10^{-9}	1×10^{-6}	0	**NaN**
N	6.6×10^{-9}	1×10^{-6}	0	**NaN**
O	6.4×10^{-9}	1×10^{-6}	0	**NaN**
P	1.5×10^{-9}	1×10^{-6}	0	**NaN**
R	1.0×10^{-9}	1×10^{-6}	0	**NaN**

NaN:Not a Number

Table 7.12 Sand boil Status

Symbol	Max Seepage Velocity (m/s)	Permeability (m/s) (k)	Exit Gradient (*i*)	Sand Boil
L	2.9×10^{-8}	1×10^{-6}	0.03	**NaN**
M	6.7×10^{-9}	1×10^{-6}	0	**NaN**
N	6.6×10^{-9}	1×10^{-6}	0	**NaN**
O	6.4×10^{-9}	1×10^{-6}	0	**NaN**
P	1.5×10^{-9}	1×10^{-6}	0	**NaN**
R	1.0×10^{-9}	1×10^{-6}	0	**NaN**

NaN:Not a Number

Heaving potential is not observed that levee has cover materials along river since the exit gradients approach zero and other analyses are in Appendix B.

CHAPTER 8

DISCUSSION OF RESULTS

8.1. Discussion of Results

Two dimensional transient seepage through into levee was simulated using variably saturated flow theory. It shows that proposed approaches are not only a theoretical exercise but it is suitable procedure to be used in engineering applications. It is known hydraulic gradients to compare each points for piping, sand boil and heaving potential. The hydraulic gradients are not the direct outputs of the Plaxflow model, but can be easily calculated from the flow velocity. Table 8.1 presents the results of the various approaches according to several autors.

Table 8.1 Approaches piping, heave and boiling

Autors	***Approaches***
Daniel (1985)	▪ i_{exit} = 0.5-1.02 for sand boil
Van Zyl and Harr (1981)	▪ Classified seepage erosion failures into three modes: heave, piping and internal erosion.
Terzaghi (1929)	▪ He defined the critical gradient to cause heaving as approximately 1.0.
Turnbull and Mansur (1961)	• Critical gradient required to cause sand boils is 0.85 for silty sands and silts, is 0.8 for silty clay and clay. • Exit Gradients are according to seepage conditions; Light to no seepage 0-0.5, Medium seepage 0.2-0.6, Heavy seepage 0.4-0.7 • Sand boils observe in a hydraulic gradient range of 0.5 to 0.8.
Peter (1974)	▪ Piping occurs very permeable sandy gravel. Properties of this soil are d_{10}=0,25 mm, C_u>20, C_c>3 and lack of grains 0.5 to 2 mm
De Wit *et al.* (1981)	▪ They observed higher critical exit gradients for the coarser and the denser sand.

(cont. on next page)

Table 8.1 (cont.)

Sherard *et al.* (1972)	▪ Some natural clay soils disperse in the presence of water and become highly susceptible to erosion and piping. ▪ Non-cohesive silt, rock flour, and very fine sands also disperse in water and may be highly erosive.
Li *et al.* (1996)	▪ There was no significant evidence of surface seepage beyond 100 m from the levee North of Cairo, Illinois after the 1993 high water.

CHAPTER 9

CONCLUSION

9.1. Conclusions

Filyos river base is often exposed to floods so seepages induced flood observe through into levee and underseepage. The study is part of the research with the aim to reveal a methodology the simulate soil mechanical behavior of levees during flood. There are available inputs of hydrological and soil properties datas for transient analysis using PlaxFlow V.9. According to steady state analysis, riprap, filter, geocomposite layer were applied to Filyos levees along upstream. Filyos river was designed the case steady state but this study investigated transient effects of seepage flow on Filyos levees and under levees associated sand boil, piping and heaving formation. Cover and uncover cases of levees were compared through into levee, levee toe, underseepage and at beyond 100 m from levee to for sand boil, piping and heaving formations.

Fallowing conclusions are drawn from this study:

1- Maximum exit gradient doesn't exceed critical hydraulic gradient, so sand boil formations do not observed at levee toe. The possible danger is completely removed with cover materials such as riprap, filter and geocomposite.
2- Piping formations do not observed at under levee. The possible danger is completely removed with cover materials such as riprap, filter and geocomposite.
3- The maximum exit gradient are respectively 0.78 and 1.0 through into levee and into through filling(silty sand layer), so piping formations do not observed in here. The possible danger is completely removed with cover materials such as riprap, filter and geocomposite.
4- Since factor of safety is heigher than 3-4, heaving potential do not observed at ground surface. The possible danger is completely removed with cover materials such as riprap, filter and geocomposite.

Overall, silty and sandy soils with finer have piping potential at K, L points under the levee. If the top layer is thin, it increases the risk of piping. The designs of levee made for the steady state flow are valid within transient flow.

REFERENCES

ADRIAN D.D. et al, Transient head development due to flood induced seepage under levees, USA, 2006.

AKI S. and MODELLEMES H, Sel kontrolunda hidroloji, 2018, pp.1-28.

ALBERTO F, A topology on inequalities, 2006, No. 85, pp.1-22.

ASKIN H, Kaplamasız yolların geotekstil ile tasarımında analitik çözümle basitleştirilmiş yaklaşımların karşılaştırılması ve geotekstillerde enerji emilim potansiyelinin önemi, Fen Bilimleri Enstitüsü, Post graduate, İstanbul, 2011.

Average Specific Gravity of Various Rock Types; <http://www.edumine.com/xtoolkit/tables/sgtables.htm>

BAJLAN F. G. F, Sonlu elemanlar kullanılarak bir barajın güvenliğinin yeniden incelenmesi, Dicle Üniversitesi Fen Bilimleri Enstitüsü, Diyarbakır, 2016.

BERILGEN S.A, Zemin suyu, Yıldız Teknik Üniversitesi, İstanbul

BLIGH W.G, The Practical Design of Irrigation Works, Van Nostr and Co, New York, 1972, pp.425.

BRINKGREVE R.B.J. et al, PlaxFlow-Version 1.4, Delft University of Technology & Plaxis bv, The Netherlands, 2006.

CEDERGREN H. R, Seepage, drainage and flow nets, *3 rd ed., John Wiley and Sons, New York,* N. Y. 1989.

CELİK H. E, Sel kontrolünde hidroloji, Hidroloji, Istanbul, 2012.

CICEK C, kil zemin üzerine inşa edilen granüler yol dolgusu şevlerinin geogrid donatıyla iyileştirilmesi, Fen Bilimleri Enstitüsü, Post graduate, Ankara, 2014.

CIVELEK, C.V. *et al,* Effects of temperature on larval swimming patterns regulate vertical distribution relative to thermoclines in Asterias rubens, *Journal of Experimental Marine Biology and Ecology 445. Elsevier B.V,*2013, pp.1–12.

DAS B, Soil Mechaics and Foundations Lecture 5.1, 2010.

DAS Braja M, Advanced Soil Mechanics, Second Edition, *Taylor&Francis,* Washington, 1997.

EKINCI C.E. and ORAKOGLU M.E, Zeminlerinin mühendislik özelliklerinin belirlenmesi üzerine bir çalışma, Journal of Advanced Technology Sciences, Turkey, 2012, pp.1-6.

Geotextiles in Embankment Dams, Federal Emergency Management Agency, 2008.

GHADA Ellithy and AIGEN Zhao, Using Help Model For Designing Geocomposite Drainage Systems in Landfills, USA.

GULBAHAR N, A Comparison Study of Some Flood Estimation Methods in terms of Design of Water Structures, 2016, pp.8-13.

HAMDHAN I.N, A contribution to slope stability analysis with finite element method, *Technische Universität Graz*, 2013.

HONG Yung-Shan et al, The load type ınfluence on the filtration behavior of soil-nonwoven geotextile composite, Tamkang Journal of Science and Engineering, Taiwan, 2011.

Internal Erosion, US Department of the Interior Breau of Reclamation, 2010.

Introduction to unit hydrograph, NPTEL, <https://nptel.ac.in/courses/105101002/downloads/module3/lecture4.pdf>.

JOHN D. R, Reliability-Based Underseepage Analysis in Levees Using a Response Surface–Monte Carlo Simulation Method, 2012.

JOHN E. et al, Evaluation of Leakage Rates through Geomembrane Liners beneath Phosphogypsum Disposal Facilities, USA.

KUTOGLU H. Yaşar, Taşkınlar Hidrolojisi, yüksek lisans tezi, Ankara, 2008.

LAM et al, Transient seepage model for saturated-unsaturated soil systems: a geotechnical engineering approach, Can. Geotech. J, Canada, 1987, pp.565-580.

LANE E.W, Security from Under - Seepage: Masonry Dam son Earth Foundation, *Trans. ASCE* pp.1235-1272.

Levee Construction, US Army Corps of Engineers, <www.fema.gov.tr>.

LI Y. et al, Sand Boils Induced by the 1993 Mississippi River Flood: Could They One Day be Misinterpreted as EarthquakeInduced Liquefaction. *Geology, 24 (2)*, 1993, pp. 171-174.

LINDEBOOM R, Design Flood Estimation, Kharagpur, 2011.

LÓPEZ-ACOSTA N. P. et al, Study of transient flow caused by rapid filling and drawdown in protection levees, Mexico, pp.316-325.

LÓPEZ-ACOSTA N. P. et al, Effects of groundwater seepage in steady-state conditions in deep tunnel shafts, Pan-Am CGS Geotechnical conferance, Mexico, 2011.

LÓPEZ-ACOSTA N. P. et al, Internal erosion due to water flow through earth dams and earth structures, Mexico.

LÓPEZ-ACOSTA N.P. et al, Assessment of exit hydraulic gradients at the toe of levees in water drawdown conditions, London, 2015.

MANSUR C.I. et al, Investigation of Underseepage and Its Control, Lower Mississippi River Levees, *2 vols. USACE Waterways Experiment Station, Technical Memo,* Vicksburg, MS, 1956, pp.3-424.

MESRI G. et al, Permeability characteristics of soft clays, *XIIII CSMFE,* New Delhi, 1994.

NIX Pete, Levee Seepage: Concerns, Evaluations, and Solutions, 2011.

OLSEN H.W, Hydraulic flows through saturated clays, MIT, USA, 2013.

ONUSLUEL G, Taşkın Kontrol Önlemleri, 2010.

OTHMAN Maidiana, Interface Behaviour And Stability Of Geocomposite Drain/Soil Systems, Doctor of Philosophy of Loughborough University, Doctoral thesis, 2016.

OZBEK Tülay, Sulama Kurutma, Gazi Üniversitesi, Basın Yayın Yüksek Okulu Matbaası Mühendislik ve Mimarlık Fakültesi, Ankara, 1987, pp.130-135.

OZKAN Senda, Analytical study on flood induced seepage under river levees, USA, 2003.

PETER P, Canal and River Levees. Developments of Civil Engineering 29, *Elsevier/North-Holland*, Bratislava, Slovakia,1982.

PIETRO D. P, Geocomposites for Drainage Experiences and Applications, Helsinki, 2013.

RICE J. D. and POLANCO L, Reliability-based underseepage analysis in levees using a response surface–monte carlo simulation method, J. Geotech. Geoenviron. Eng., 2012, M.ASCE.

RINALDI M. and CASAGLI N, Stability of streambanks formed in partially saturated soils and effects of negative pore water pressures: the Sieve River, *Italy Geomorphology*, 26(4), Italy, 1999. pp.253-277.

RINALDI Massimo and CASAGLI Nicola, Stability of streambanks formed in partially saturated soils and effects of negative pore water pressures, 1999.

ROWE R. K, Combined effect of reinforcement and prefabricated vertical drains on embankment performance, *Can. Geotech. J. 38(6)*, 2001, pp.1266-1282.

ROWE R. K, Geotechnical and Geoenvironmental Engineering Handbook, 2001.

SALEM M.A, Soil Permeability and Seepage, 2010-2011.

SANDERS M. P.M and VAN BER SCHRIER J.S, Tide induced piping risk assessed by transient groundwater flow, Netherlands.

SHERMAN L. K, Streamflow from rainfall by the unit hydrograph method, *Eng. News-Record*, 1932, pp.501-505.

SHERMAN Leroy K, The relation of hydrographs of runoff to size and character of drainage-basins, 1932.

SIVRIKAYA Osman, Soil Mechanics, Soil flownets, Niğde, 2010.

Soil Permeabilty and void ratio, <www.geotechdata.info>.

SONMEZ O, OZTURK M. and DOGAN E, Istanbul derelerinin taşkın debilerinin tahmini, Fen Bilimleri Dergisi, Sakarya, 2012.

Standards soil void ratios, 1985-2018, <www.zsoil.com>.

STARK T.D. et al, Soil compressibility in transient unsaturated seepage analyses, Can Geatech. J, USA, 2014, pp.858-868.

SZEPESHAZI Robert et al, Hydraulical and mechanical modelling of levees, Hungary, 2015.

TERZAGHİ K.et al, (1996). Soil Mechanics in Engineering Practice, *3rd Edition, John Wiley&Sons, Inc*, New York, 1996, pp.549.

THIEU N.T.M. et al, Seepage modelling in a saturated/unsaturated soil systems, Internation Conferance MLWR, 2001, Vietnam.

TOMLINSON S.S. and VADI Y.P, Seepage forces and confining pressure effects on piping erosion, *Can. Geotech. J. 37(1)*, 2000, pp.1–13.

TRACY F. et al, Transient Seepage Analyses in Levee Engineering Practice Engineer Research and Development, 2016.

TRACY F.T. and CORCORAN M.K, Effect of changes in hydraulic conductivity on exit gradient at selected levee systems using numerical models, The Open Hyd. Journal, USA, 2014, pp.27-40.

TURNBULL W.J. and MANSUR C.I, Investigation of Underseepage-Mississippi River Levees, *Transactions, ASCE, 126 (1)*, 1961, pp. 1429-1485.

US Department of the Interior Bureau of Reclamation, Internal Erosion Risks for Embankments and Foundations, 2015, pp.1-134.

USUL Nurünnisa, Engineering Hydrology, ODTU Yayıncılık, Ankara, 2008.

VAN GENUCHTEN M.T. and ALVES W. J, Analytical Solutions of the One Dimensional Convective-Dispersive Solute Transport Equation, *Technical Bulletin 1661, U. S. Department of Agriculture, Agricultural Research Service,* Washington, 1980.

VISWANADHAM B.V.S, Advanced Geotechnical Engineering, IIT Bombay.

WATERMAN D. et al, *Plaxis 2D - Version 8. Delft: Plaxis bv. P.O. Box 572*, 2006.

WHITMAN V et al, Exit gradient, 1979.

YANG et al, Factors affecting drying and wetting soil-water characteristic curves of sandy soils, Can. Geotech. J. 41, pp.908-920, 2004.

YILMAZ H.R. and ESKİSAR T, Usage of Geosynthetic Products to Solve Geotechnical Problems and Their Advantages, 2010, pp.437-453.

ZORNBERG Jorge G. and CHRISTOPHER Barry R , Geosynthetics, The Handbook of Groundwater Engineering, 1999.

ZUMR D. and CISLEROVA M, Soil moisture Dynamics in levee during flood events-variably saturated approach, J.Hydrol. Hydromech, Czech Republic, 2010.

ZYL Van D. and HARR M. E, Seepage erosion analyses of structures, USA, 1981.

APPENDIX A

DRILLING WELLS AND SOIL PROPERTIES

A.1. TSK-2

The information on soil samples obtained from drilling wells is defined Figure A.1. Table A.1 shows parameter values, such as Permeability (k), Specific Gravity (G_s) and Void Ratio (e) of the soil samples. These values were used to perform transient analysis of Filyos Levees.

Figure A.1 Sample drilling well of TSK-2 at 511.29 m

Table A.1 Soil Properties of TSK-2

Depth(m)	Soil Type	Permeability(k) (m/sec)	Specific Gravity (G_s)	Void Ratio (e)
0.0-2.0	Clayey Sand	$1x10^{-6}$	2.67	0.43
2.0-3.0	Silty Clay	$5x10^{-8}$	2.75	1.78
3.0-3.5	Clayey Sand	$1x10^{-6}$	2.67	0.43
3.5-10.0	Silty Clay	$5x10^{-8}$	2.75	1.78
10.0-10.5	Sand	$1x10^{-4}$	2.68	0.55
10.5-12.0	Silty Clay	$5x10^{-8}$	2.75	1.78

(cont. on next page)

Table A.1 (cont.)

12.0-12.5	Clayey Sand	$1x10^{-6}$	2.67	0.43
12.5-13.5	Silty Clay	$5x10^{-8}$	2.75	1.78
13.5-14.0	Clayey Sand	$1x10^{-6}$	2.67	0.43
14.0-14.50	Silty Clay	$5x10^{-8}$	2.75	1.78
14.5-18.5	Gravelly Sand	$5x10^{-4}$	2.66	0.62
18.5-19.0	Silty Clay	$5x10^{-8}$	2.75	1.78
19.0-20.0	Gravelly Sand	$5x10^{-4}$	2.66	0.62
20.0-20.5	Silty Clay	$5x10^{-8}$	2.75	1.78
20.5-23.0	Gravelly Sand	$5x10^{-4}$	2.66	0.62
23.0-23.5	Gravel	$1x10^{-2}$	2.65	0.27
23.5-30.0	Gravelly Sand	$5x10^{-4}$	2.66	0.62

A.2. TSK-3

The information on soil samples obtained from drilling wells is defined Figure A.2. Table A.2 shows parameter values, such as Permeability (k), Specific Gravity (G_s) and Void Ratio (e) of the soil samples. These values were used to perform transient analysis of Filyos Levees.

Figure A.2 Sample drilling well of TSK-3 at 1010.63 m

Table A.2 Soil Properties of TSK-3

Depth (m)	Soil Type	Permeability(k) (m/sec)	Specific Gravity (G_s)	Void Ratio (e)
0.0-0.6	Silty Clay	$5x10^{-8}$	2.75	1.78
0.6-4.0	Silty Sand	$1x10^{-6}$	2.69	0.43
4.0-8.0	Gravel	$1x10^{-2}$	2.65	0.27
8.0-10.0	Silty Sand	$1x10^{-6}$	2.69	0.43
10.0-20.0	Sand	$1x10^{-4}$	2.68	0.55
20.0-28.0	Clayey Silt	$1x10^{-7}$	2.70	0.90
28.0-29.0	Silty Clay	$5x10^{-8}$	2.75	1.78
29.0-30.0	Clayey Silt	$1x10^{-7}$	2.70	0.90

A.3. TSK-4

The information on soil samples obtained from drilling wells is defined Figure A.3. Table A.3 shows parameter values, such as Permeability (k), Specific Gravity (G_s) and Void Ratio (e) of the soil samples. These values were used to perform transient analysis of Filyos Levees.

Figure A.3 Sample drilling well of TSK-4 at 1513.22 m

Table A.3 Soil Properties of TSK- 4

Depth(m)	Soil Type	Permeability(k) (m/sec)	Specific Gravity (G_s)	Void Ratio (e)
0.0-2.0	Sand	$1x10^{-4}$	2.68	0.55
2.0-2.5	Sandy Silt	$1x10^{-7}$	2.68	0.85
2.5-3.5	Sandy Clay	$1x10^{-6}$	2.72	0.47
3.5-7.0	Gravelly Sand	$5x10^{-4}$	2.66	0.62
7.0-10.0	Sand	$1x10^{-4}$	2.68	0.55
10.0-12.0	Gravelly Sand	$5x10^{-4}$	2.66	0.62
12.0-14.0	Silty Sand	$1x10^{-6}$	2.69	0.43
14.0-17.5	Silty Clay	$5x10^{-8}$	2.75	1.78
17.5-18.5	Sandy Clay	$1x10^{-6}$	2.72	0.47
18.5-20.5	Clayey Sand	$1x10^{-6}$	2.67	0.43
20.5-23.0	Sand	$1x10^{-4}$	2.68	0.55
23.0-24.0	Silty Clay	$5x10^{-8}$	2.75	1.78
24.0-24.5	Sand	$1x10^{-4}$	2.68	0.55
24.5-25.5	Silty Clay	$5x10^{-8}$	2.75	1.78
25.5-28.5	Sand	$1x10^{-4}$	2.68	0.55
28.5-30.0	Silty Clay	$5x10^{-8}$	2.75	1.78

A.4. TSK-5

The information on soil samples obtained from drilling wells is defined Figure A.4. Table A.4 shows parameter values, such as Permeability (k), Specific Gravity (G_s) and Void Ratio (e) of the soil samples. These values were used to perform transient analysis of Filyos Levees.

Table A.4 Soil Properties of TSK-5

Depth(m)	Soil Type	Permeability(k) (m/sec)	Specific Gravity (G_s)	Void Ratio (e)
0.0-4.0	Sandy Silt	$1x10^{-7}$	2.68	0.85
4.0-8.0	Silty Sand	$1x10^{-6}$	2.69	0.43
8.0-28.0	Silty Clay	$5x10^{-8}$	2.75	1.78
28.0-30.0	Clayey Silt	$1x10^{-7}$	2.70	0.90

Figure A.4 Sample drilling well of TSK-5 at 2005.66 m

A.5. TSK-6

The information on soil samples obtained from drilling wells is defined Figure A.5. Table A.5 shows parameter values, such as Permeability (k), Specific Gravity (G_s) and Void Ratio (e) of the soil samples. These values were used to perform transient analysis of Filyos Levees.

Figure A.5 Sample drilling well of TSK-6 at 2501.94 m

Table A.5 Soil Properties of TSK-6

Depth(m)	Soil Type	Permeability(k) (m/sec)	Specific Gravity (G_s)	Void Ratio (e)
0.0-2.0	Silty Sand	$1x10^{-6}$	2.69	0.43
2.0-3.0	Silty Clay	$5x10^{-8}$	2.75	1.78
3.0-4.0	Gravel	$1x10^{-2}$	2.65	0.27
4.0-12.0	Gravelly Sand	$5x10^{-4}$	2.66	0.62
12.0-12.5	Gravel	$1x10^{-2}$	2.65	0.27
12.5-15.5	Gravelly Sand	$5x10^{-4}$	2.66	0.62
15.5-16.5	Gravel	$1x10^{-2}$	2.65	0.27
16.5-23.0	Gravelly Sand	$5x10^{-4}$	2.66	0.62
23.0-28.5	Silty Clay	$5x10^{-8}$	2.75	1.78
28.5-30.0	Silty Sand	$1x10^{-6}$	2.69	0.43

A.6. TSK-9

The information on soil samples obtained from drilling wells is defined Figure A.6. Table A.6 shows parameter values, such as Permeability (k), Specific Gravity (G_s) and Void Ratio (e) of the soil samples. These values were used to perform transient analysis of Filyos Levees.

Figure A.6 Sample drilling well of TSK-6 at 271.05 m

Table A.6 Soil Properties of TSK-9

Depth(m)	Soil Type	Permeability(k) (m/sec)	Specific Gravity (G_s)	Void Ratio (e)
0.0-2.5	Silty Clay	$5x10^{-8}$	2.75	1.78
2.5-4.0	Silty Sand	$1x10^{-6}$	2.69	0.43
4.0-8.0	Sandy Gravel	$5x10^{-3}$	2.65	0.50
8.0-10.0	Sand	$1x10^{-4}$	2.68	0.55
10.0-12.0	Sandy Gravel	$5x10^{-3}$	2.65	0.50
12.0-14.0	Silty Clay	$5x10^{-8}$	2.75	1.78
14.0-15.0	Gravelly Silt	$5x10^{-6}$	2.69	0.75
15.0-18.0	Gravelly Sand	$5x10^{-4}$	2.66	0.62
18.0-20.0	Silty Clay	$5x10^{-8}$	2.75	1.78
20.0-28.0	Clayey Silt	$1x10^{-7}$	2.70	0.90
28.0-30.0	Clayey Sand	$1x10^{-6}$	2.67	0.43

A.7. TSK-10

The information on soil samples obtained from drilling wells is defined Figure A.7. Table A.7 shows parameter values, such as Permeability (k), Specific Gravity (G_s) and Void Ratio (e) of the soil samples. These values were used to perform transient analysis of Filyos Levees.

Figure A.7 Sample drilling well of TSK-10 at 758.18 m

Table A.7 Soil Properties of TSK-10

Depth(m)	Soil Type	Permeability(k) (m/sec)	Specific Gravity (G_s)	Void Ratio (e)
0.0-4.0	Clayey Silt	$1x10^{-7}$	2.70	0.90
4.0-6.0	Gravel	$1x10^{-2}$	2.65	0.27
6.0-8.0	Silty Sand	$1x10^{-6}$	2.69	0.43
8.0-13.0	Silty Clay	$5x10^{-8}$	2.75	1.78
13.0-14.0	Clayey Silt	$1x10^{-7}$	2.70	0.90
14.0-15.0	Silty Clay	$5x10^{-8}$	2.75	1.78
15.0-23.5	Clayey Silt	$1x10^{-7}$	2.70	0.90
23.5-30.0	Silty Clay	$5x10^{-8}$	2.75	1.78

A.8. TSK-11

The information on soil samples obtained from drilling wells is defined Figure A.8. Table A.8 shows parameter values, such as Permeability (k), Specific Gravity (G_s) and Void Ratio (e) of the soil samples. These values were used to perform transient analysis of Filyos Levees.

Figure A.8 Sample drilling well of TSK-11 at 1256.4 m

Table A.8. Soil Properties of TSK-11

Depth(m)	Soil Type	Permeability(k) (m/sec)	Specific Gravity (G_s)	Void Ratio (e)
0.0-4.0	Clayey Silt	$1x10^{-7}$	2.70	0.90
4.0-6.0	Gravel	$1x10^{-2}$	2.65	0.27
6.0-8.0	Silty Sand	$1x10^{-6}$	2.69	0.43
8.0-13.0	Silty Clay	$5x10^{-8}$	2.75	1.78
13.0-14.0	Clayey Silt	$1x10^{-7}$	2.70	0.90
14.0-15.0	Silty Clay	$5x10^{-8}$	2.75	1.78
15.0-23.5	Clayey Silt	$1x10^{-7}$	2.70	0.90
23.5-30.0	Silty Clay	$5x10^{-8}$	2.75	1.78

A.9. TSK-12

The information on soil samples obtained from drilling wells is defined Figure A.9. Table A.9 shows parameter values, such as Permeability (k), Specific Gravity (G_s) and Void Ratio (e) of the soil samples. These values were used to perform transient analysis of Filyos Levees.

Figure A.9 Sample drilling well of TSK-12 at 1762.17 m

Table A.9 Soil Properties of TSK-12

Depth(m)	Soil Type	Permeability(k) (m/sec)	Specific Gravity (G_s)	Void Ratio (e)
0.0-4.0	Clayey Silt	$1x10^{-7}$	2.70	0.90
4.0-8.0	Sandy Gravel	$5x10^{-3}$	2.65	0.50
8.0-10.0	Silty Clay	$5x10^{-8}$	2.75	1.78
10.0-14.0	Sandy Clay	$1x10^{-6}$	2.72	0.47
14.0-18.0	Clay	$1x10^{-8}$	2.80	1.85
18.0-20.0	Silty Clay	$5x10^{-8}$	2.75	1.78
20.0-22.0	Gravelly Clay	$5x10^{-7}$	2.71	0.80
22.0-30.0	Clay	$1x10^{-8}$	2.80	1.85

A.10. TSK-13

The information on soil samples obtained from drilling wells is defined Figure A.10. Table A.10 shows parameter values, such as Permeability (k), Specific Gravity (G_s) and Void Ratio (e) of the soil samples. These values were used to perform transient analysis of Filyos Levees.

Figure A.10. Sample drilling well of TSK-13 at 2327.64 m

Table A.10. Soil Properties of TSK-13

Depth(m)	**Soil Type**	**Permeability(k) (m/sec)**	**Specific Gravity (G_s)**	**Void Ratio (e)**
0.0-2.0	Clayey Silt	$1x10^{-7}$	2.70	0.90
2.0-4.0	Sand	$1x10^{-4}$	2.68	0.55
4.0-6.0	Gravel	$1x10^{-2}$	2.65	0.27
6.0-14.0	Sand	$1x10^{-4}$	2.68	0.55
14.0-18.0	Clayey Silt	$1x10^{-7}$	2.70	0.90
18.0-20.0	Silt	$5x10^{-7}$	2.70	1.10
20.0-24.0	Sand	$1x10^{-4}$	2.68	0.55
24.0-30.0	Silty Clay	$5x10^{-8}$	2.75	0.90

APPENDIX B

TRANSIENT ANALYSES WİTH PLAXFLOW-2D

B.1. Filyos Levee at 511.29 m on Left Shore of Filyos River

Location of Filyos levee at 511.29 m on left shore is seen Figure B.1 and the schematic representation of Filyos Levee and soil profile is given in Figure B.2 Filyos levee includes gravelly sand soil type. There is a silty clay layer under the levee and this layer is 1 m thick.

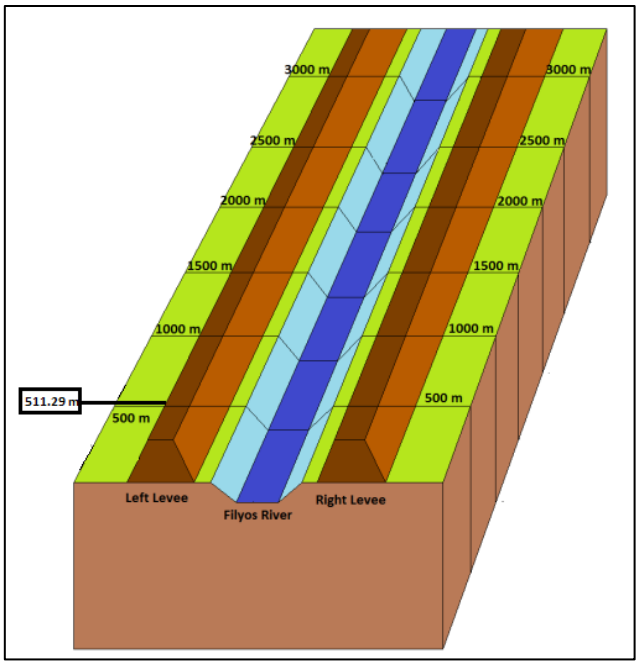

Figure B.1 Filyos Levee at 511.29 m m on left shore of Filyos River

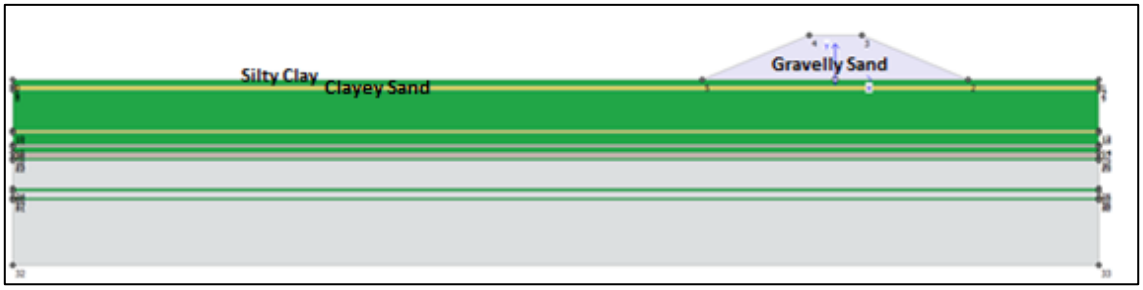

Figure B.2 Filyos Levee at 511.29 m m on left shore of Filyos River

Figure B.3 shows that each soil layers have saturated unit weight under the levee for transient analysis and area of under the flow line is saturated during h_{max}.

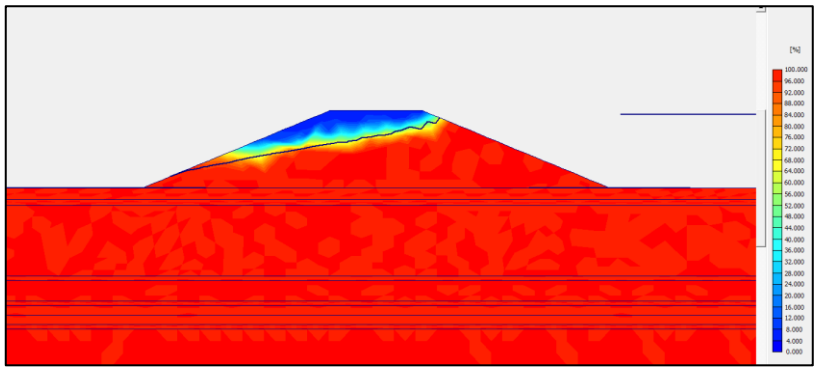

Figure B.3 Degree of Saturation of Filyos Levee at 511.29 m on left shore of Filyos River during h_{max}

It is seen that flow values are high at the red area in case h_{max} under the flow line according to Plaxflow2D (Figure B.4.a). There is a risk that is observed piping at these areas.

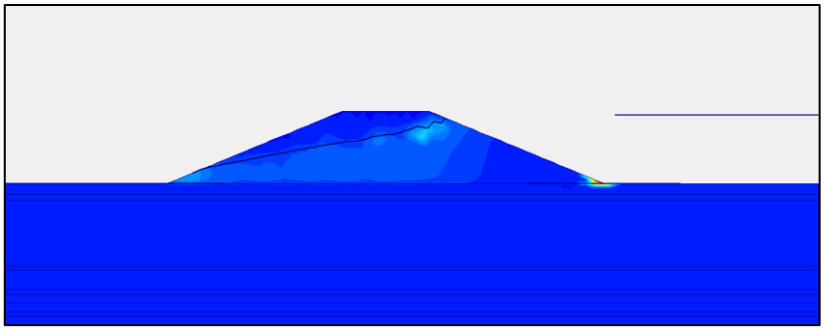

(a)

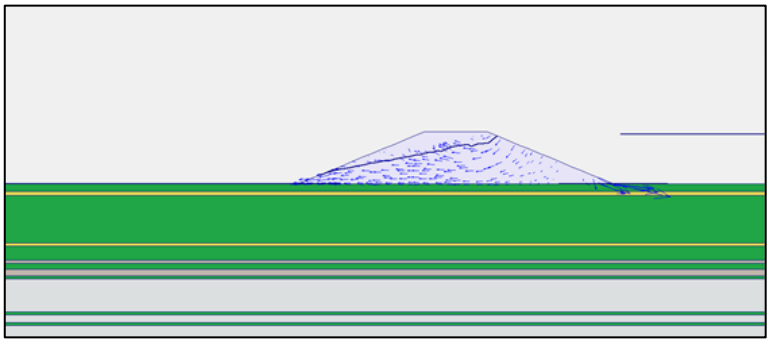

(b)

Figure B.4. Flow field at 511.29 m on left shore of Filyos River during h_{max} a.) Shadings view b.) Arrows view

Figure B.4. (b) is other notation that is vector stage in case h_{max}. That is called arrows in Plaxflow2D literature. If the vectors values are higher than others, there will be observing piping formations.

Analysis of silty clay at under the levee;

Figure B.5 shows that location of points near the ground surface for finding extreme velocity and Figure B.6 presents that results of flow velocity at K, L, M, N, O, P, Q and R.

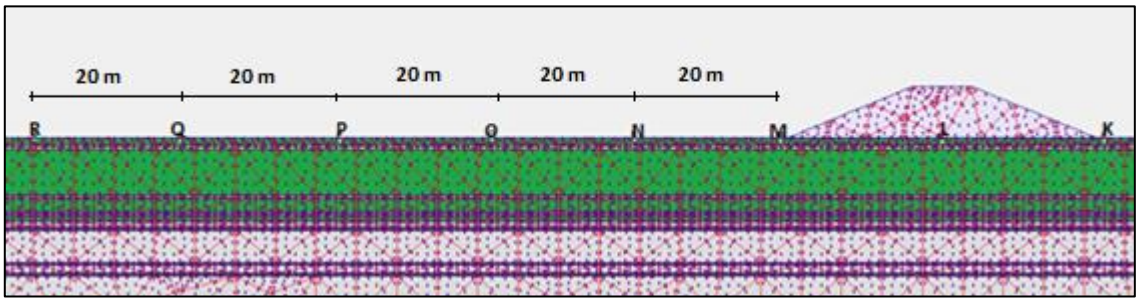

Figure B.5 Location of points near the ground surface for finding extreme velocity

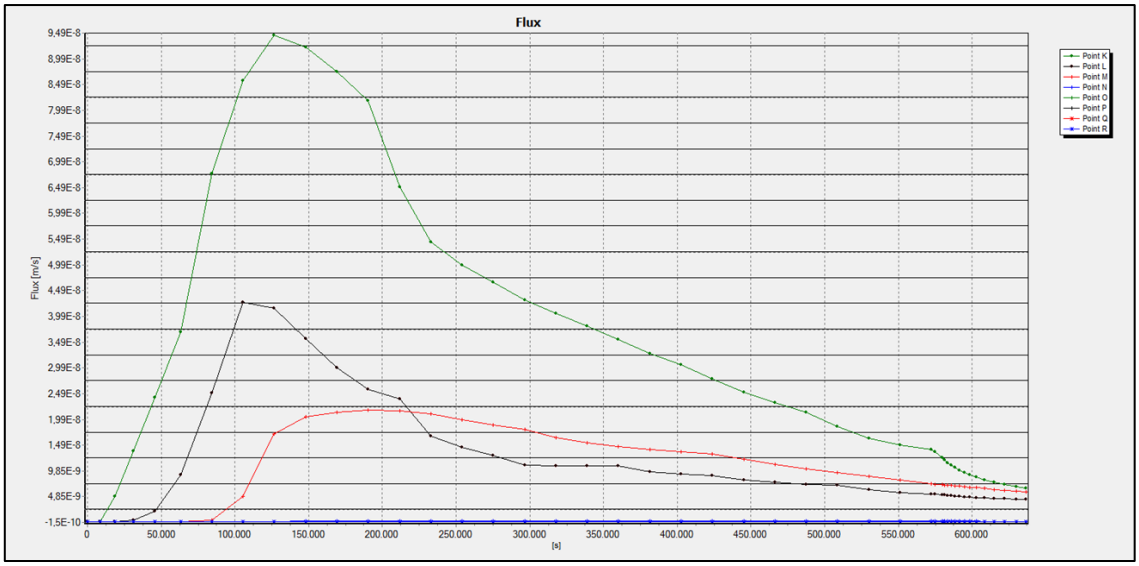

Figure B.6. Extreme velocity graph relation time to seepage velocity

According to Figure B.6, max values of flow are K=9.5x10^{-8} m/s at time=39.4 hours; L=4.25x10^{-8} m/s at time=26.4 hours; M=2.25x10^{-8} m/s at time=55.6 hours; N, O, P, Q, R= 1.5x10^{-10} m/s at time=152.8 hours.

Piping formations are simply compate as;

$$v = k.i\,; \tag{B.1}$$

$$i_c = \frac{G_s - 1}{1+e} = \frac{2.75-1}{1+1.78} = 0.63\ ; \tag{B.2}$$

Where;

v = flow velocity (m/sec)

k = permeabilty (m/sec)

i = hydraulic gradient

i_c = critical hydraulic gradient

G_s = specific gravity; 2.75 for silty clay

e = void ratio; 1.78 for silty clay

Table B.1. shows that piping is observed at some points due to $i_{exit} > i_c$ but it is not insufficient piping formation bucause it does not occur piping at levee toe (Point M).

Table B.1 Piping Status

Symbol	Max Seepage Velocity (m/s)	Permeability (m/s) (k)	Exit Gradient (*i*)	Piping
K	9.5 x 10^{-8}	5 x 10^{-8}	1.90	$i_{exit} > i_c$
L	4.25 x 10^{-8}	5 x 10^{-8}	0.85	$i_{exit} > i_c$
M	2.25 x 10^{-8}	5 x 10^{-8}	0.45	**NaN**
N	1.5 x 10^{-10}	5 x 10^{-8}	0	**NaN**
O	1.5 x 10^{-10}	5 x 10^{-8}	0	**NaN**
P	1.5 x 10^{-10}	5 x 10^{-8}	0	**NaN**
Q	1.5 x 10^{-10}	5 x 10^{-8}	0	**NaN**
R	1.5 x 10^{-10}	5 x 10^{-8}	0	**NaN**

NaN:Not a Number

Table B.2 shows that sand boil is not observed at any points because max exit gradient is smaller than 0.85 and it is not exceed to critical hydraulic gradient at levee toe.

Table B.2 Sand Boil Status

Symbol	Max Seepage Velocity (m/s)	Permeability (m/s) (k)	Exit Gradient (*i*)	Sand Boil
M	2.25 x 10^{-8}	5 x 10^{-8}	0.45	**NaN**
N	1.5 x 10^{-10}	5 x 10^{-8}	0	**NaN**
O	1.5 x 10^{-10}	5 x 10^{-8}	0	**NaN**
P	1.5 x 10^{-10}	5 x 10^{-8}	0	**NaN**
Q	1.5 x 10^{-10}	5 x 10^{-8}	0	**NaN**
R	1.5 x 10^{-10}	5 x 10^{-8}	0	**NaN**

NaN:Not a Number

The analysis above the levee for gravelly sand soil type;

Piping can only observe K, L and M point because these points only are under the phreatic line. K, L, M etc. points on the ground surface or levee are different from other analyses.

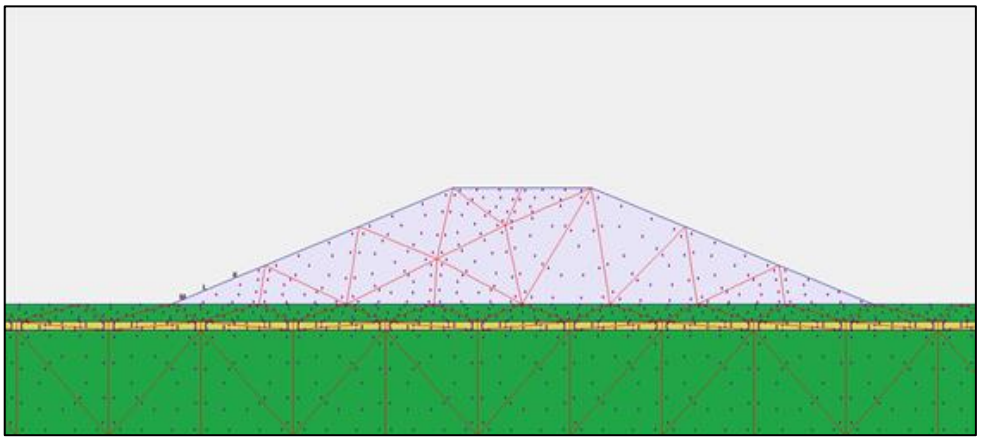

Figure B.7 Location of points above the levee for finding extreme velocity

Extreme velocities of K, L and M point are Figure B.8 and piping formations are investigated for these points.

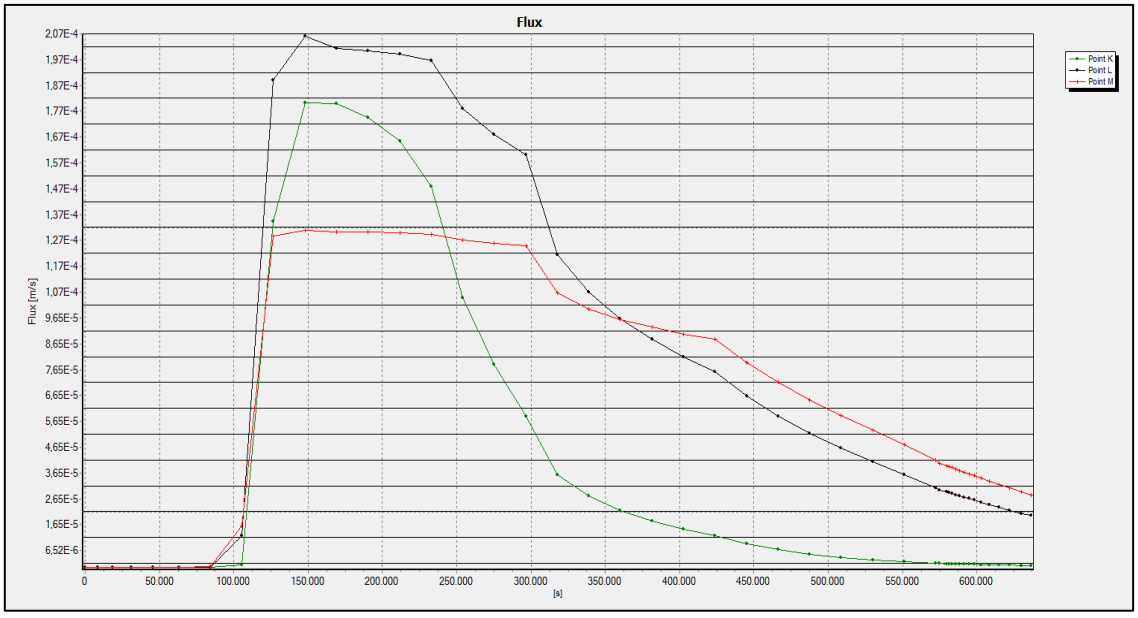

Figure B.8 Extreme velocity graph relation time above the levee

According to Figure 7.8, max values of flow are K=1.8x10^{-4}m/s at time=41.7 hours; L=2.1x10^{-4}m/s at time=41.7 hours; M=1.3 x 10^{-5}m/s at time=41.7 hours.

Piping formations are simply compate as;

$$v = k.i\,; \tag{B.3}$$

$$i_c = \frac{G_s - 1}{1 + e} = \frac{2.66 - 1}{1 + 0.62} = 1.02\,; \tag{B.4}$$

Where;

v = flow velocity (m/sec)

k = permeabilty (m/sec)

i = hydraulic gradient

i_c = critical hydraulic gradient

G_s = specific gravity; 2.66 for gravelly sand

e = void ratio; 0.62 for gravelly sand

Table B.3. shows that piping is not observed at any points due to $i_{exit} < i_c$.

Table B.3. Piping Status

Symbol	Max Seepage Velocity (m/s)	Permeability (m/s) (k)	Exit Gradient (*i*)	Piping
K	1.8×10^{-4}	5×10^{-4}	0.36	**NaN**
L	2.1×10^{-4}	5×10^{-4}	0.42	**NaN**
M	1.3×10^{-5}	5×10^{-4}	0.26	**NaN**

NaN:Not a Number

The factor of safety against heave analysis for top layer;

Equation B.5 and B.6 are used to determine the factor of safety against heave analysis for top layer. Heaving potential are only observed ground surface hence a point are investigated at 0.5 m below the top layer like Figure B.9.

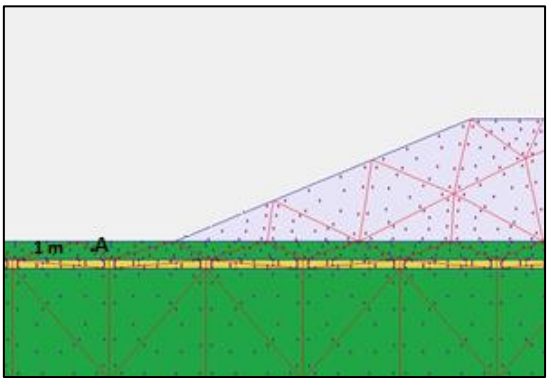

Figure B.9 Analysis against to heave at A point 0.5 m below the top layer

$$F_{heave} = \frac{H.\gamma_{sat}}{h_m.\gamma_w} > 3.0 \quad \text{(B.5)}$$

$$i_{\max} = \frac{h_m}{H} \quad \text{(B.6)}$$

Where;

H = thickness of overlying top layer (m)

γ_{sat} = saturated unit weight of overlying top layer (kN/m^2)

h_m = average hydraulic head at the point (m)

γ_w = water unit wight (kN/m^2)

$i_{\max}$ = maximum exit gradient

$$0.45 = \frac{h_m}{0.5} \Rightarrow h_m = 0.23 \;;\; F_{heave} = \frac{0.5x16}{0.23x10} = 3.5 > 3.0$$

It is not observed heave due to the fact that F_{heave} is higher than 3.0 .

B.1.1. Filyos Levee at 511.29 m on Left Shore of Filyos River according to Current Situation (Upstream face is covered)

The schematic representation of Filyos Levee and soil profile is given in Figure B.10. Filyos levee includes gravelly sand soil type and cover materials against piping and sand boil formations. The cover materials are riprap which is andesite, uniform sand filter layer and geocomposite layer. There is a silty clay layer under the levee and this layer is 1 m thick.

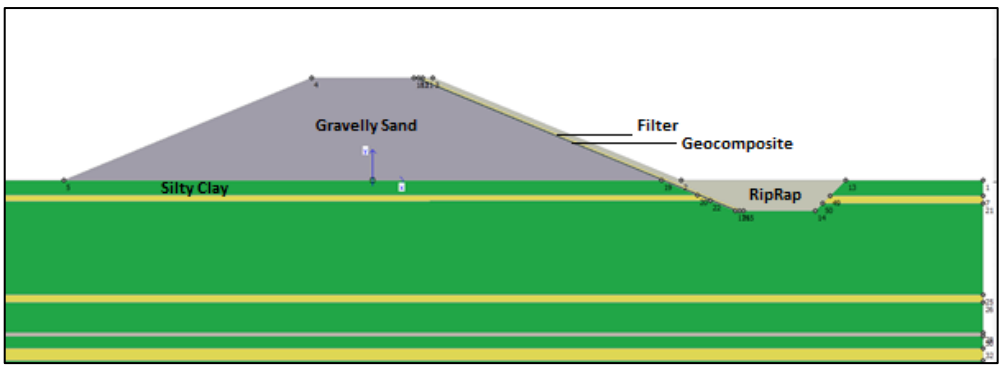

Figure B.10 Filyos Levee with cover materials at 511.29 m m on left shore of Filyos River

Filyos levee has covered along rising water level. The covered members are filter, riprap and geocomposite materials. Table B.4 shows properties of covered materials and levee.

Table B.4 Soil Properties of levee members

	Soil Type / Material	**Permeability(k) (m/sec)**	**Specific Gravity (G_s)**	**Void Ratio (e)**	**Thickness (m)**
Filter	Uniform Sand	$1x10^{-3}$	2.67	0.70	0.25
Riprap	Andesite Rock	0.645	2.65	0.34	0.70
Geocomposite Material	Geotextile and Geomembrane	$1x10^{-13}$	-	0.02	0.30

Figure B.11 shows that each soil layers have saturated unit weight under the levee with cover materials for transient analysis and area of under the flow line is saturated during h_{max}. Saturation rates of red areas are high and saturation rates of other areas are almost zero without riprap, filter, and areas under levee.

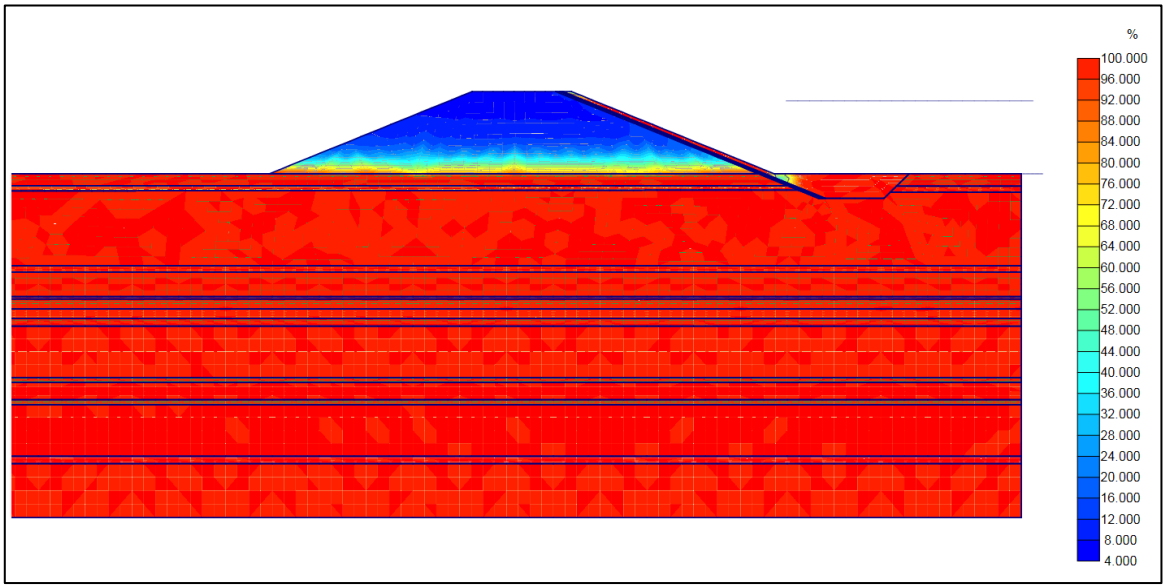

Figure B.11. Degree of Saturation of Filyos Levee with cover materials at 511.29 m on left shore of Filyos River during h_{max}

It is seen that flow values are high at the red area in case h_{max} under the flow line according to Plaxflow2D (Figure B.12.a). There is not a risk that is observed piping into through levee.

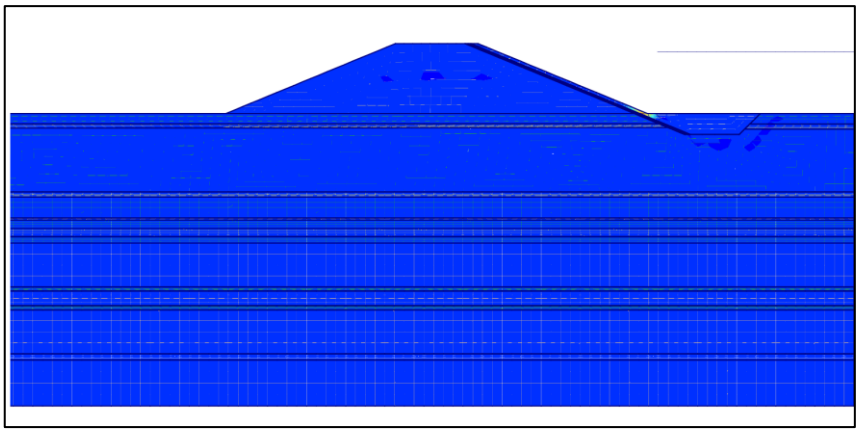

(a)

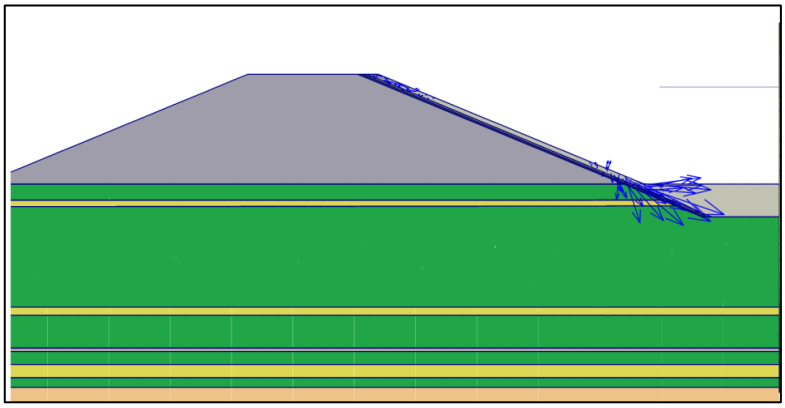

(b)

Figure B.12. Flow field at 511.29 m on left shore of Filyos River during h_{max}
a.) Shadings view b.) Arrows view

Figure B.12. (b) is other notation that is vector stage in case h_{max}. That is called arrows in Plaxflow2D literature and there is not risk into through levee.

Analysis of silty clay at under the levee;

Figure B.13 shows that location of points near the ground surface for finding extreme velocity and Figure B.14 presents that results of flow velocity at K, L, M, N, O, P and Q.

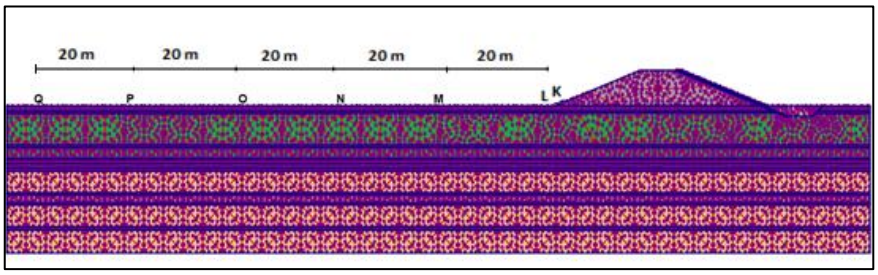

Figure B.13 Location of points near the ground surface for finding extreme velocity

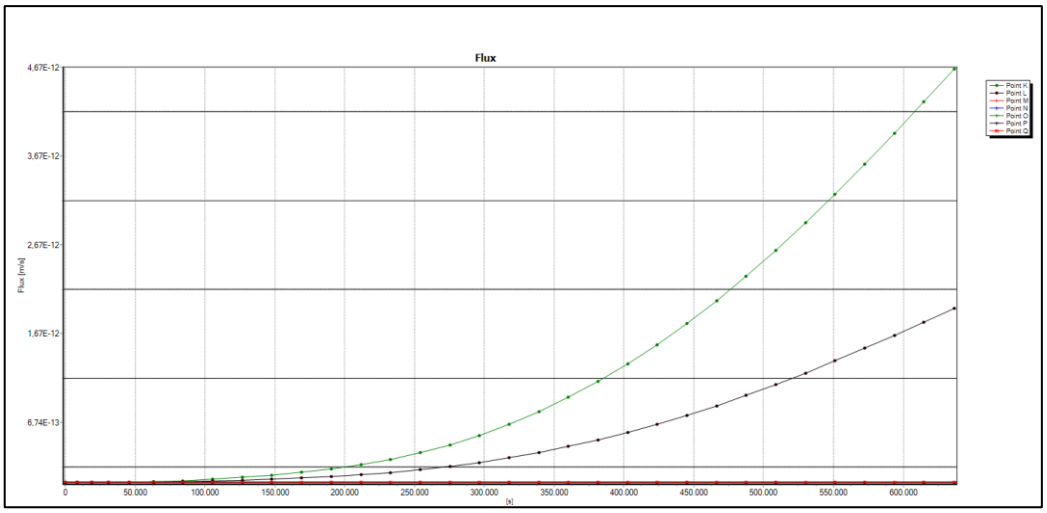

Figure B.14 Extreme velocity graph relation time Filyos Levee

Table B.5 shows that piping is not observed at any points due the fact that to exit gradient is zero. See equations B.1, B.2, B.3 and B.4 for calculated critical hydraulic gradients.

Table B.5 Piping Status

Symbol	Max Seepage Velocity (m/s)	Permeability (m/s) (k)	Exit Gradient (*i*)	Piping
K	4.7×10^{-12}	5×10^{-4}	0	**NaN**
L	2.1×10^{-12}	5×10^{-8}	0	**NaN**
M	7×10^{-13}	5×10^{-8}	0	**NaN**
N	7×10^{-13}	5×10^{-8}	0	**NaN**
O	7×10^{-13}	5×10^{-8}	0	**NaN**
P	7×10^{-13}	5×10^{-8}	0	**NaN**
Q	7×10^{-13}	5×10^{-8}	0	**NaN**

NaN:Not a Number

In order for the sand boiling to occur, the piping must take place. As can be seen in the Table B.6, it did not reach critical gradient for the formation of boiling. See equations B.1, B.2, B.3 and B.4 for calculated critical hydraulic gradients.

Table B.6 Sand Boil Status

Symbol	Max Seepage Velocity (m/s)	Permeability (m/s) (k)	Exit Gradient (*i*)	Sand Boil
L	2.1×10^{-12}	5×10^{-8}	0	**NaN**
M	7×10^{-13}	5×10^{-8}	0	**NaN**
N	7×10^{-13}	5×10^{-8}	0	**NaN**
O	7×10^{-13}	5×10^{-8}	0	**NaN**
P	7×10^{-13}	5×10^{-8}	0	**NaN**
Q	7×10^{-13}	5×10^{-8}	0	**NaN**

NaN:Not a Number

- Heaving potential is not observed that levee has cover materials along river since the exit hydraulic gradients approach zero.

B.2. Filyos Levee at 1+010.63 km on Left Shore of Filyos River

The schematic representation of Filyos levee and soil profile is given in Figure B.16. Filyos levee includes gravelly sand soil type. Also, location of this levee is Figure B.15 There is a silty clay layer under the levee and this layer is approximately 1 m thick. Also, silty sand material is used for this layer to need filling under the levee.

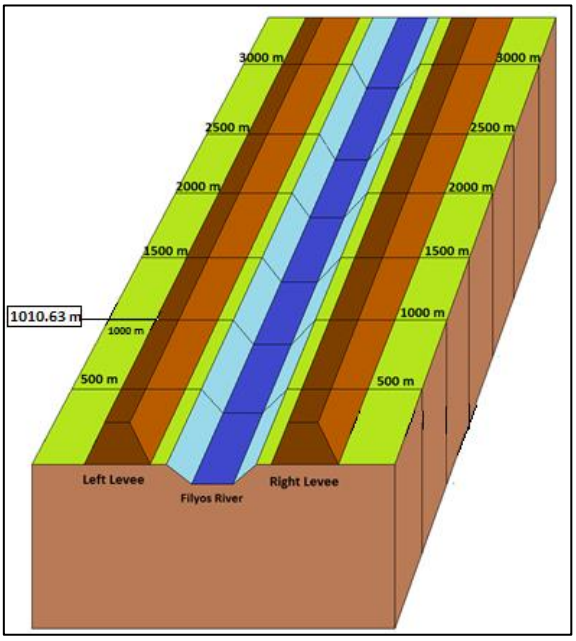

Figure B.15 Filyos Levee at 1010.63 m on left shore of Filyos River

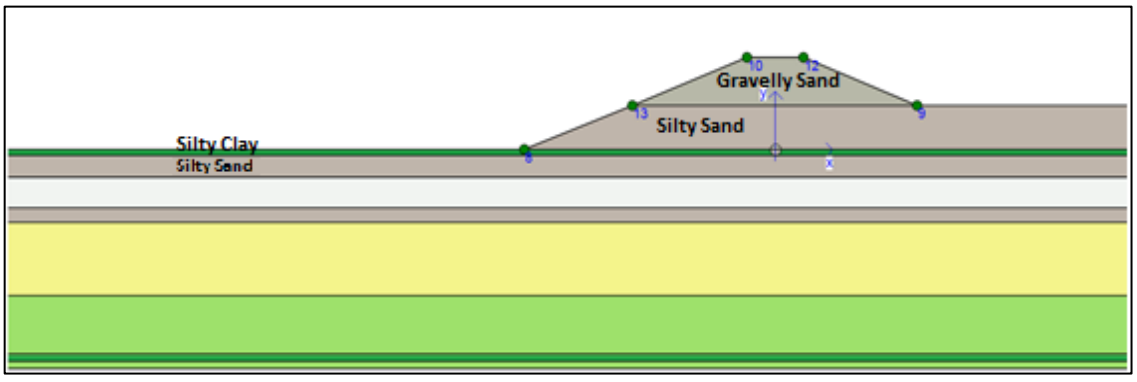

Figure B.16 Filyos Levee at 1+010.63 km on left shore of Filyos River

Figure B.17. shows that each soil layers have saturated unit weight under the levee for transient analysis and area of under the flow line is saturated during $h_{max.}$

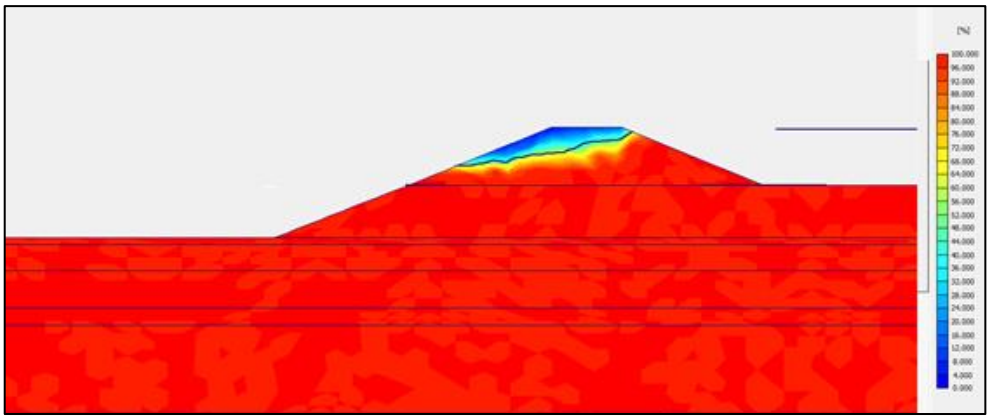

Figure B.17 Degree of Saturation of Filyos Levee at 1+010.63 km on left shore of Filyos River during h_{max}

It is seen that flow values are high at the red area in case h_{max} under the flow line according to Plaxflow2D (Figure B.18.a). There is a risk that is observed piping at these areas.

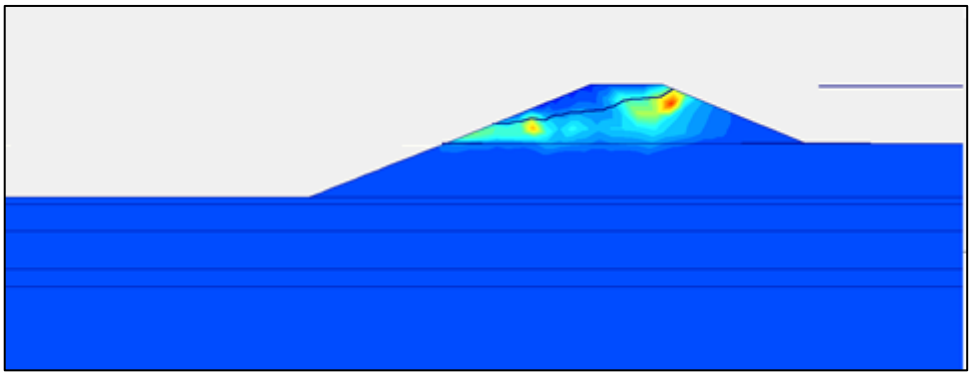

(a)

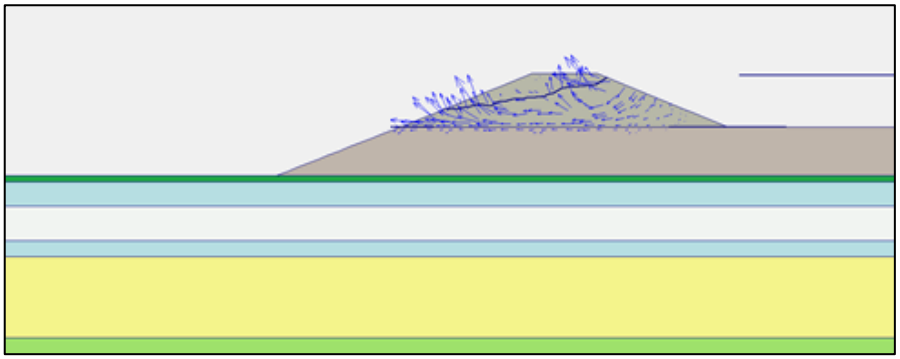

(b)

Figure B.18. Flow field at 1+010.63 km on left shore of Filyos River during h_{max} a.)Shadings view b.) Arrows view

Figure B.18. (b) is other notation that is vector stage in case h_{max}. That is called arrows in Plaxflow2D literature. If the vectors values are higher than others, there will be observing piping formations.

Analysis of silty clay at under the levee;

Figure B.19. shows that location of points near the ground surface for finding extreme velocity and Figure B.18. presents that results of flow velocity at K, L, M, N, O and P.

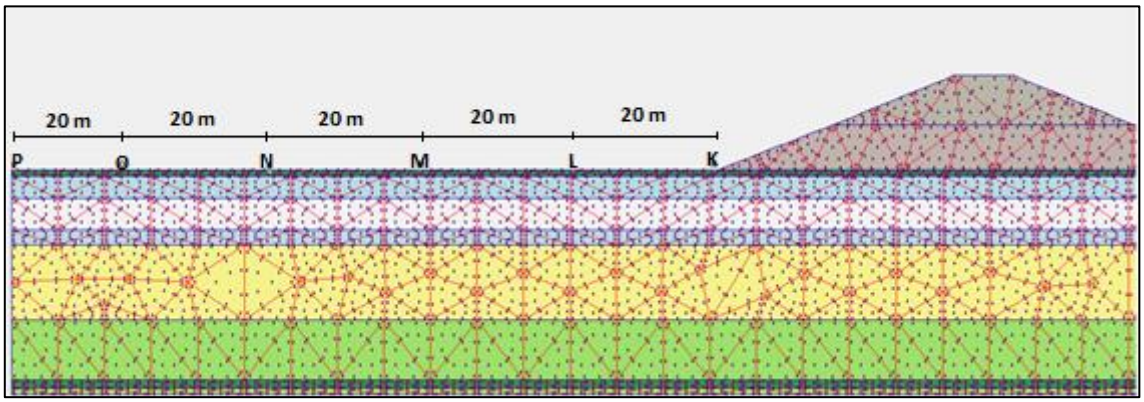

Figure B.19 Location of points near the ground surface for finding extreme velocity

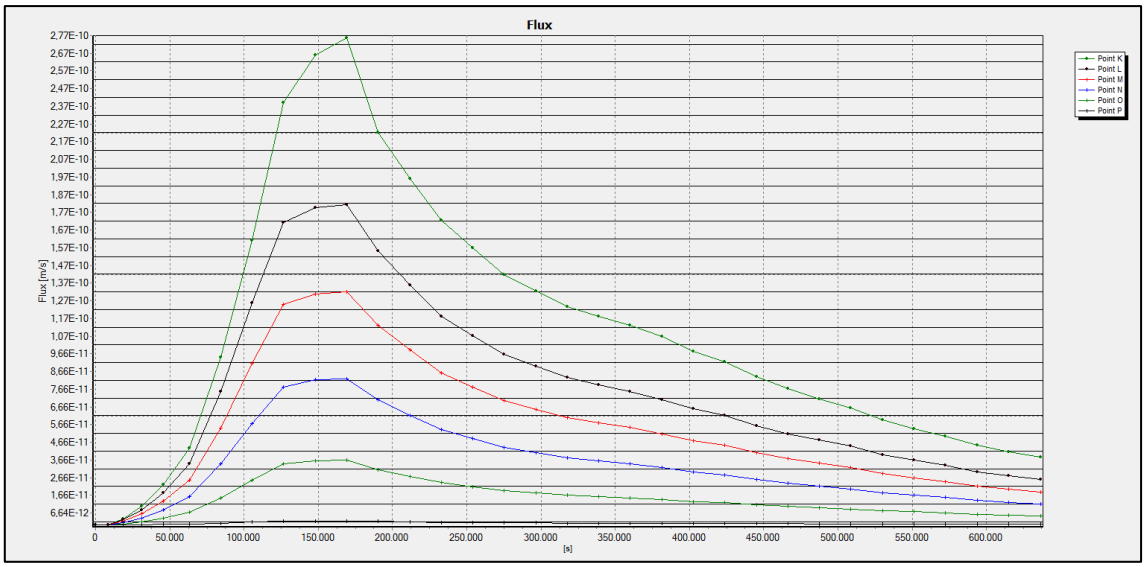

Figure B.20 Extreme velocity graph relation time to seepage velocity

According to Figure B.20, max values of flow are K=2.8x10^{-10} m/s at time=48.6 hours; L=1.82x10^{-10} m/s at time=48.6 hours; M=1.32x10^{-10} m/s at time=48.6 hours; N=8.2x 10^{-11} m/s at time=48.6 hours, O=3.7x 10^{-11} m/s at time=48.6 hours, P=6.5x 10^{-12} m/s at time=48.6 hours.

Piping formations are simply compate as;

$$v = k.i\,; \qquad \text{(B.7)}$$

$$i_c = \frac{G_s - 1}{1 + e} = \frac{2.75 - 1}{1 + 1.78} = 0.63; \quad \text{(B.8)}$$

Where;

v = flow velocity (m/sec)

k = permeabilty (m/sec)

i = hydraulic gradient

i_c = critical hydraulic gradient

G_s = specific gravity; 2.75 for silty clay

e = void ratio; 1.78 for silty clay

Table B.7 shows that piping is not observed at any points due to $i_{exit} < i_c$.

Table B.7. Piping Status

Symbol	Max Seepage Velocity (m/s)	Permeability (m/s) (k)	Exit Gradient (i)	Piping
K	2.8×10^{-10}	5×10^{-8}	0	**NaN**
L	1.82×10^{-10}	5×10^{-8}	0	**NaN**
M	1.32×10^{-10}	5×10^{-8}	0	**NaN**
N	8.2×10^{-11}	5×10^{-8}	0	**NaN**
O	3.7×10^{-11}	5×10^{-8}	0	**NaN**
P	6.5×10^{-12}	5×10^{-8}	0	**NaN**

NaN:Not a Number

In order for the sand boiling to occur, the piping must take place. As can be seen in the Table B.8. Critical hydraulic gradient is 0.63 for silty clay and it did not reach critical gradient for the formation of boiling.

Table B.8. Sand Boil Status

Symbol	Max Seepage Velocity (m/s)	Permeability (m/s) (k)	Exit Gradient (i)	Sand Boil
K	2.8×10^{-10}	5×10^{-8}	0	**NaN**
L	1.82×10^{-10}	5×10^{-8}	0	**NaN**
M	1.32×10^{-10}	5×10^{-8}	0	**NaN**
N	8.2×10^{-11}	5×10^{-8}	0	**NaN**
O	3.7×10^{-11}	5×10^{-8}	0	**NaN**
P	6.5×10^{-12}	5×10^{-8}	0	**NaN**

NaN:Not a Number

The analysis above the levee for gravelly sand and silty sand fill soil type;

Piping can only observe K, L and M point because these points only are under the phreatic line. K, L, M etc. points on the ground surface or levee are different from other analyses.

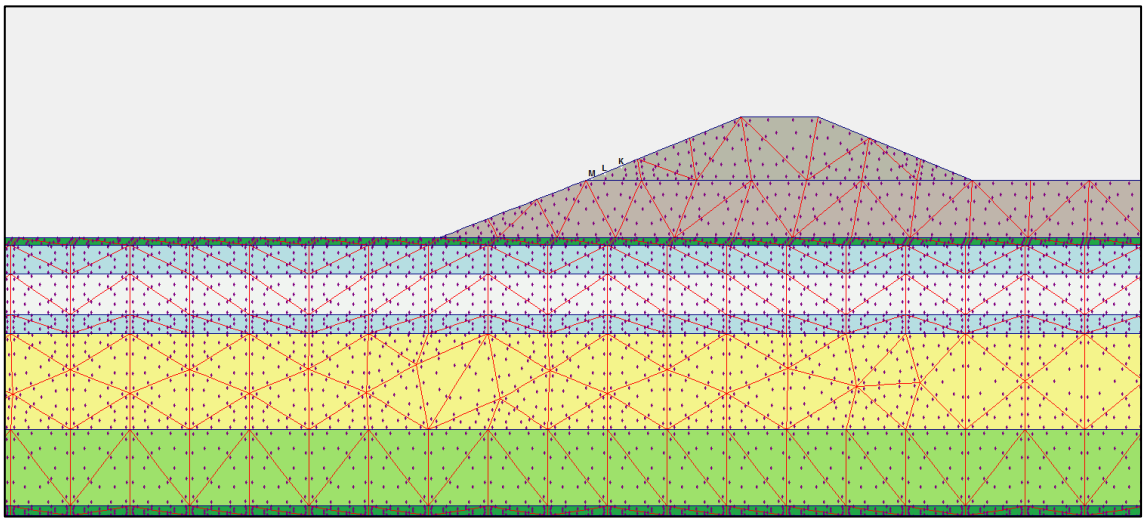

Figure B.21 Location of points above the levee for finding extreme velocity

Extreme velocities of K, L and M point are Figure B.22 and piping formations are investigated for these points.

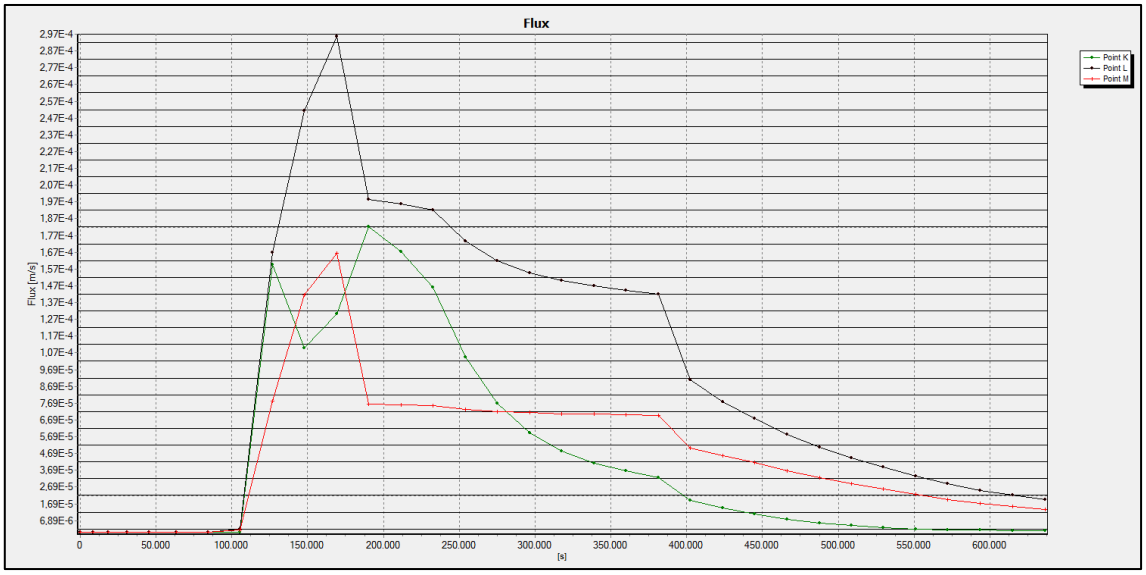

Figure B.22 Extreme velocity graph relation time above the levee

According to Figure 7.8, max values of flow are K=1.82x10^{-4}m/s at time=48.6 hours; L=3x10^{-4}m/s at time=61.1 hours; M=1.7 x 10^{-4}m/s at time=48.6 hours.

Piping formations are simply compate as;

$$v = k.i\,; \tag{B.9}$$

$$i_c = \frac{G_s - 1}{1 + e} = \frac{2.66 - 1}{1 + 0.62} = 1.02\,; \tag{B.10}$$

Where;

v = flow velocity (m/sec)

k = permeabilty (m/sec)

i = hydraulic gradient

i_c = critical hydraulic gradient

G_s = specific gravity; 2.66 for gravelly sand

e = void ratio; 0.62 for gravelly sand

Table B.9. shows that piping is not observed at any points due to $i_{exit} < i_c$.

Table B.9. Piping Status

Symbol	Max Seepage Velocity (m/s)	Permeability (m/s) (k)	Exit Gradient (*i*)	Piping
K	1.82×10^{-4}	5.0×10^{-4}	0.36	**NaN**
L	3.0×10^{-4}	5.0×10^{-4}	0.60	**NaN**
M	1.7×10^{-4}	5.0×10^{-4}	0.34	**NaN**

NaN:Not a Number

Piping can only observe K, L and M point because these points only are under the phreatic line. K, L, M etc. points on the ground surface or levee are different from other analyses.

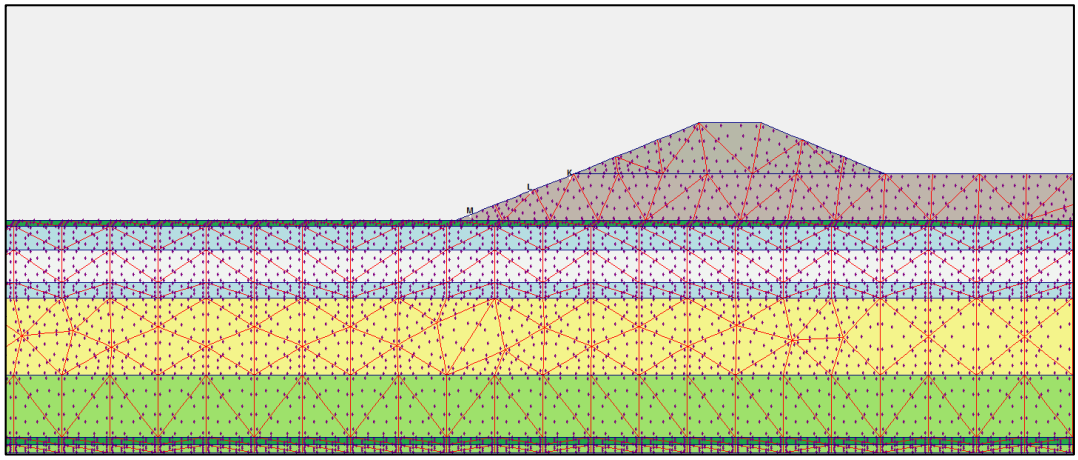

Figure B.21. Location of points above the levee for finding extreme velocity

Extreme velocities of K, L and M point are on the silty sand soil layer. Figure B.23 and piping formations are investigated for these points.

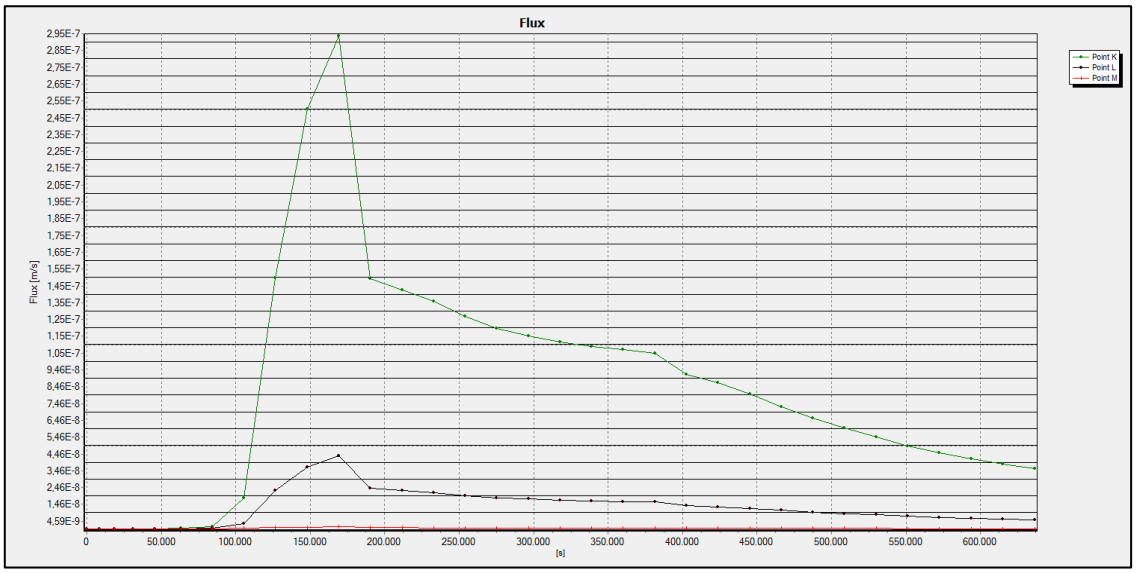

Figure B.23 Extreme velocity graph relation time above the levee

According to Figure B.23, max values of flow are K=3x10^{-7}m/s at time=48.6 hours; L=4.5x10^{-8}m/s at time=48.6 hours; M=4.6x 10^{-9}m/s at time=48.6 hours.

Piping formations are simply compate as;

$$v = k.i\,; \tag{B.11}$$

$$i_c = \frac{G_s - 1}{1+e} = \frac{2.69-1}{1+0.43} = 1.2\,; \tag{B.12}$$

Where;

$v =$ flow velocity (m/sec)

$k =$ permeabilty (m/sec)

$i =$ hydraulic gradient

$i_c =$ critical hydraulic gradient

$G_s =$ specific gravity; 2.69 for silty sand

$e =$ void ratio; 0.43 for silty sand

Critical hydraulic gradients is 1.2 for silty sand. Table B.10. shows that piping is not observed at any points due to $i_{exit} < i_c$.

Table B.10. Piping Status

Symbol	Max Seepage Velocity (m/s)	Permeability (m/s) (k)	Exit Gradient (*i*)	Piping
K	3.0×10^{-7}	1.0×10^{-6}	0.3	**NaN**
L	4.5×10^{-8}	1.0×10^{-6}	0.05	**NaN**
M	4.6×10^{-9}	1.0×10^{-6}	0	**NaN**

NaN:Not a Number

The factor of safety against heave analysis for top layer;

Equation B.13 and B.14 are used to determine the factor of safety against heave analysis for top layer. Heaving potential are only observed ground surface hence a point are investigated at 0.5 m below the top layer like Figure B.24.

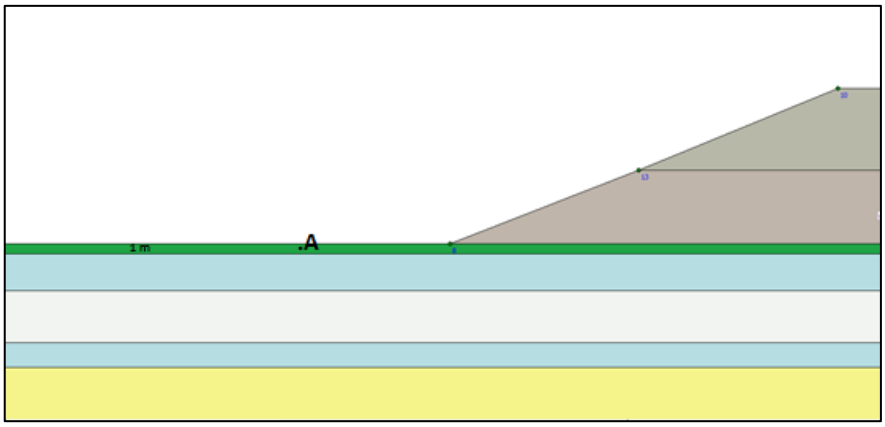

Figure B.24 Analysis against to heave at A point 0.5 m below the top layer

$$F_{heave} = \frac{H.\gamma_{sat}}{h_m.\gamma_w} > 3.0 \qquad \text{(B.13)}$$

$$i_{\max} = \frac{h_m}{H} \qquad \text{(B.14)}$$

H = thickness of overlying top layer(m)

γ_{sat} = saturated unit weight of overlying top layer(kN/m^2)

h_m = average hydraulic head at the point(m)

γ_w = water unit wight(kN/m^2)

$i_{\max}$ = maximum exit gradient

Since $i_{\max}$ =0, heaving is not likely to occur.

B.2.1. Filyos Levee at 1+010.63 km on Left Shore of Filyos River according to Current Situation(Upstream face is covered)

The schematic representation of Filyos levee and soil profile is given in Figure B.25. Filyos levee includes gravelly sand soil type and cover materials against piping and sand boil formations. The cover materials are riprap which is andesite, uniform sand filter layer and geocomposite layer. There is a silty clay layer under the levee and this layer is 1 m thick.

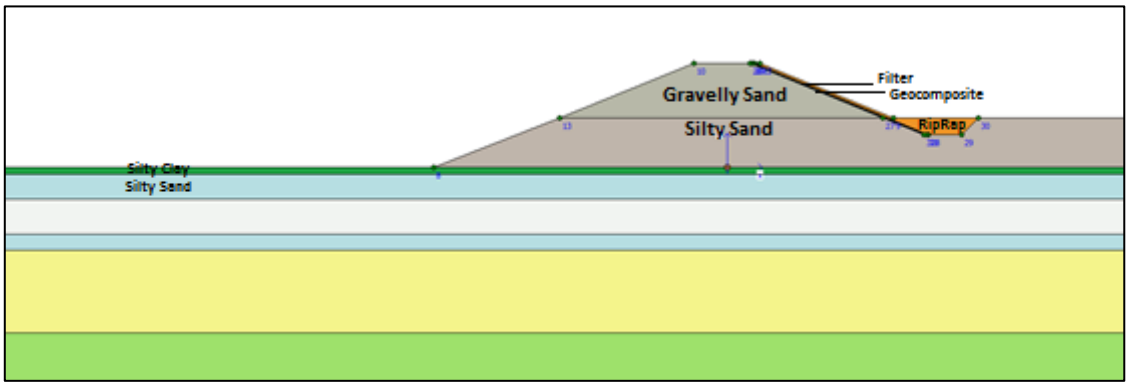

Figure B.25 Filyos Levee with cover materials at 1+010.63 km on left shore of Filyos River

Filyos levee has covered along rising water level. Table B.15 shows properties of covered materials and levee.

Table B.15 Soil Properties of levee members

	Soil Type / Material	**Permeability(k) (m/sec)**	**Specific Gravity (G_s)**	**Void Ratio (e)**	**Thickness (m)**
Filter	Uniform Sand	$1x10^{-3}$	2.67	0.70	0.25
Riprap	Andesite Rock	0.645	2.65	0.34	0.70
Geocomposite Material	Geotextile and Geomembrane	$1x10^{-13}$	-	0.02	0.30

Figure B.26 shows that each soil layers have saturated unit weight under the levee with cover materials for transient analysis and area of under the flow line is saturated during h_{max}. Saturation rates of red areas are high and saturation rates of other areas are almost zero without riprap, filter, and areas under levee.

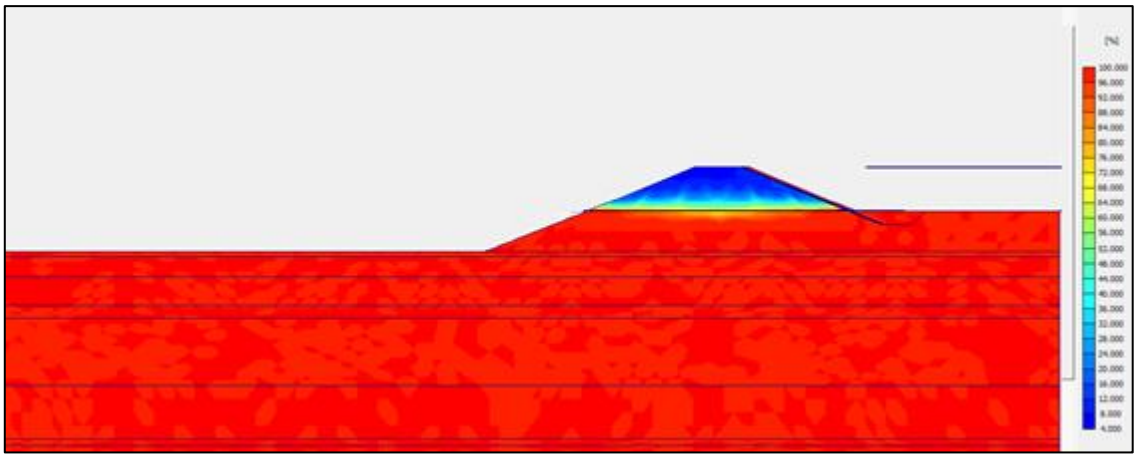

Figure B.26 Degree of Saturation of Filyos Levee with cover materials at 1+010.33 km on left shore of Filyos River during h_{max}

It is seen that flow values are high at the red area in case h_{max} under the flow line according to Plaxflow2D (Figure B.27.a). There is not a risk that is observed piping into through levee.

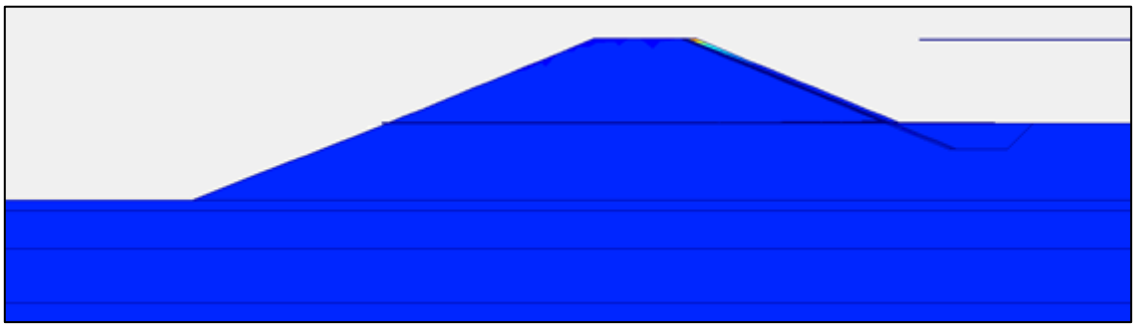

(a)

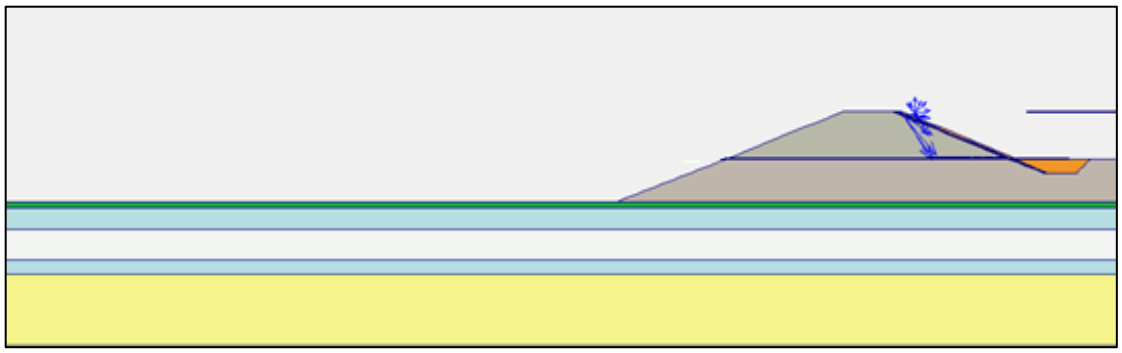

(b)

Figure B.27. Flow field at 1+010.63 km on left shore of Filyos River during h_{max} a.) Shadings view b.) Arrows view

Figure B.27. (b) is other notation that is vector stage in case h_{max}. That is called arrows in Plaxflow2D literature and there is not risk into through levee.

Analysis of silty clay at under the levee;

Figure B.28 shows that location of points near the ground surface for finding extreme velocity and Figure B.29 presents that results of flow velocity at K, L, M, N, O and P.

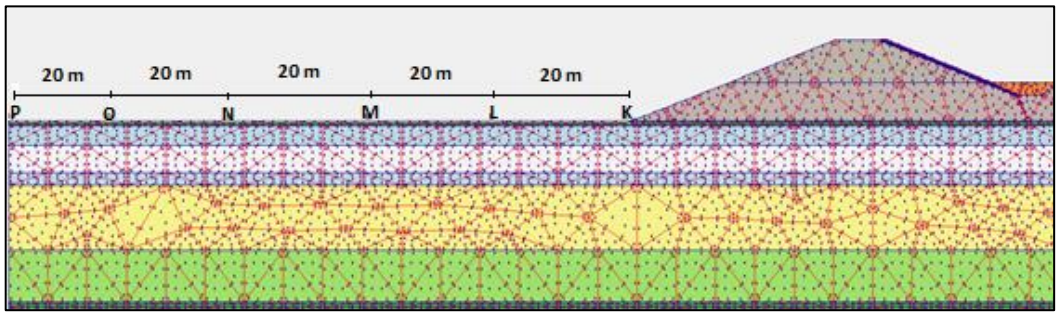

Figure B.28 Location of points near the ground surface for finding extreme velocity

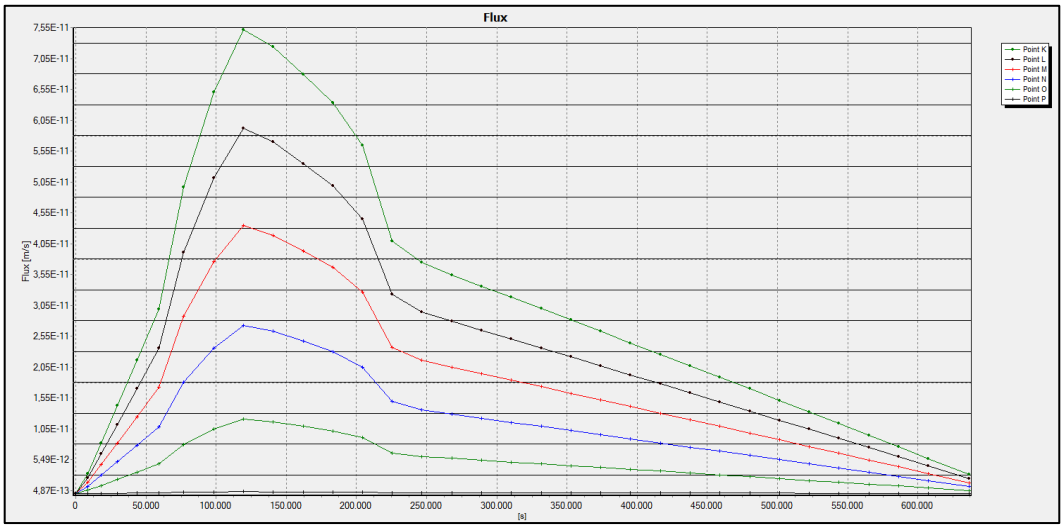

Figure B.29 Extreme velocity graph relation time Filyos Levee

Table B.12 shows that piping is not observed at any points due the fact that to exit gradient is zero. See equations B.7 and B.8 for calculated critical hydraulic gradients.

Table B.16 Piping Status

Symbol	Max Seepage Velocity (m/s)	Permeability (m/s) (k)	Exit Gradient (*i*)	Piping
K	7.6×10^{-11}	5×10^{-8}	0	**NaN**
L	6.0×10^{-11}	5×10^{-8}	0	**NaN**
M	4.3×10^{-11}	5×10^{-8}	0	**NaN**
N	2.8×10^{-11}	5×10^{-8}	0	**NaN**
O	1.3×10^{-11}	5×10^{-8}	0	**NaN**
P	4.9×10^{-13}	5×10^{-8}	0	**NaN**

NaN:Not a Number

In order for the sand boiling to occur, the piping must take place. As can be seen in the Table B.16, it did not reach critical gradient for the formation of boiling. See equations B.7 and B.8 for calculated critical hydraulic gradients.

Table B.17 Sand Boil Status

Symbol	Max Seepage Velocity (m/s)	Permeability (m/s) (k)	Exit Gradient (*i*)	Sand Boil
K	7.6×10^{-11}	5×10^{-8}	0	**NaN**
L	6.0×10^{-11}	5×10^{-8}	0	**NaN**
M	4.3×10^{-11}	5×10^{-8}	0	**NaN**
N	2.8×10^{-11}	5×10^{-8}	0	**NaN**
O	1.3×10^{-11}	5×10^{-8}	0	**NaN**
P	4.9×10^{-13}	5×10^{-8}	0	**NaN**

NaN:Not a Number

- Heaving potential is not observed that levee has cover materials along river since the exit gradients approach zero.

The analysis above the levee for gravelly sand and silty sand fill soil type;

Piping can only observe K, L and M point because these points only are under the phreatic line. K, L, M etc. points on the ground surface or levee are different from other analyses.

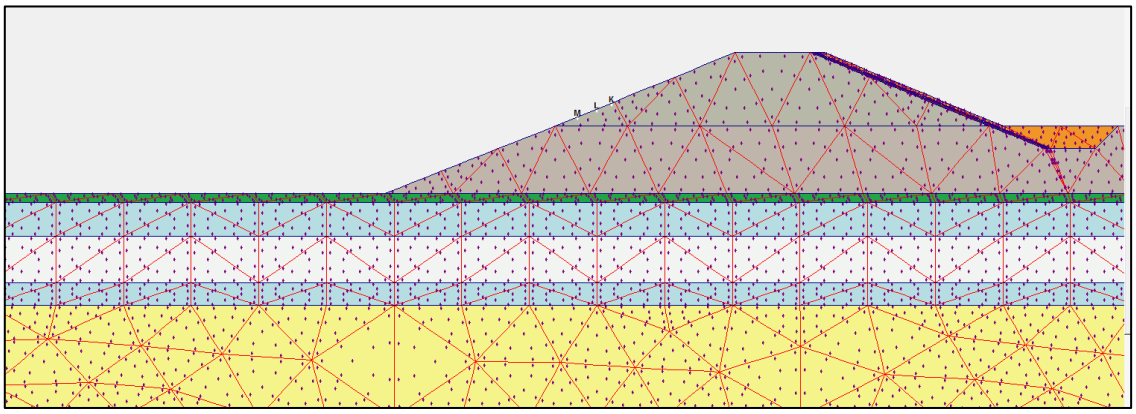

Figure B.30 Location of points above the levee for finding extreme velocity

Extreme velocities of K, L and M point are below and piping formations are investigated for these points. Filyos levee includes gravelly sand soil type and filling layer includes silty sand soil type so, K, L and M points are different from each soil layer.

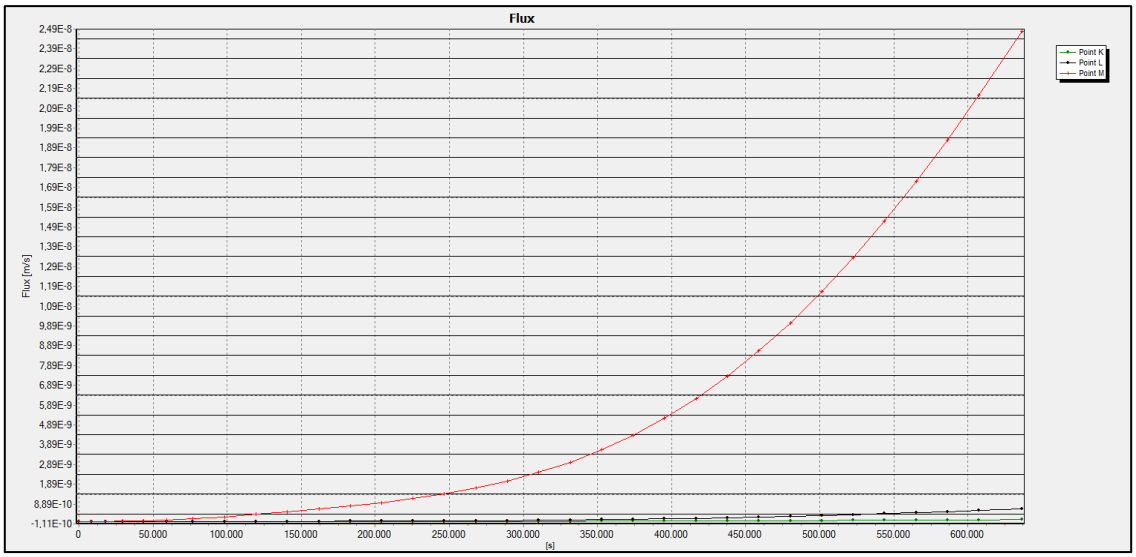

Figure B.31 Extreme velocity graph relation time to seepage velocity

Table B.18 shows that piping is not observed at any points due the fact that to exit gradient is zero. See equations B.9 and B.10 for calculated critical hydraulic gradients.

Table B.18 Piping Status

Symbol	Max Seepage Velocity (m/s)	Permeability (m/s) (k)	Exit Gradient (*i*)	Piping
K	8.0×10^{-10}	$5x10^{-4}$	0	**NaN**
L	9.0×10^{-10}	$5x10^{-4}$	0	**NaN**
M	2.5×10^{-8}	$5x10^{-4}$	0	**NaN**

NaN:Not a Number

K, L, M etc. points on the ground surface or levee are different from other analyses. (Figure B.32).

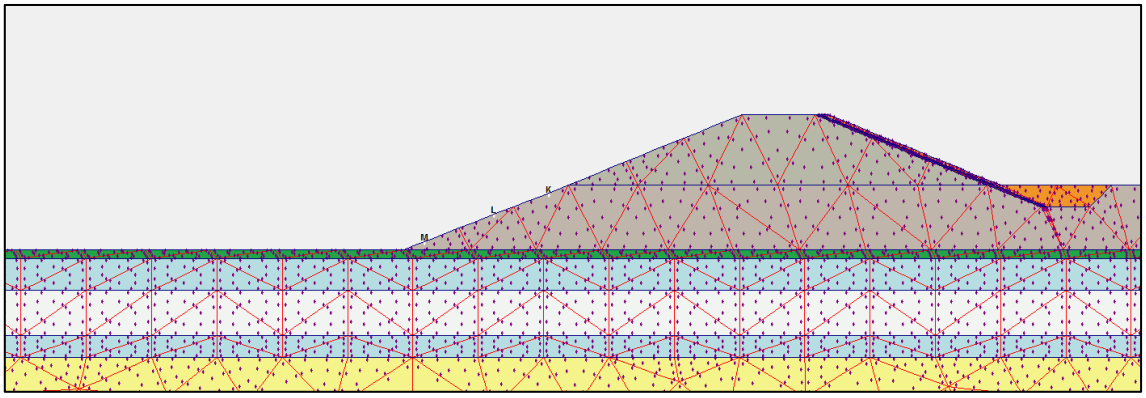

Figure B.32 Location of points above the levee for finding extreme velocity

Extreme velocities of K, L and M point are below and piping formations are investigated for these points.

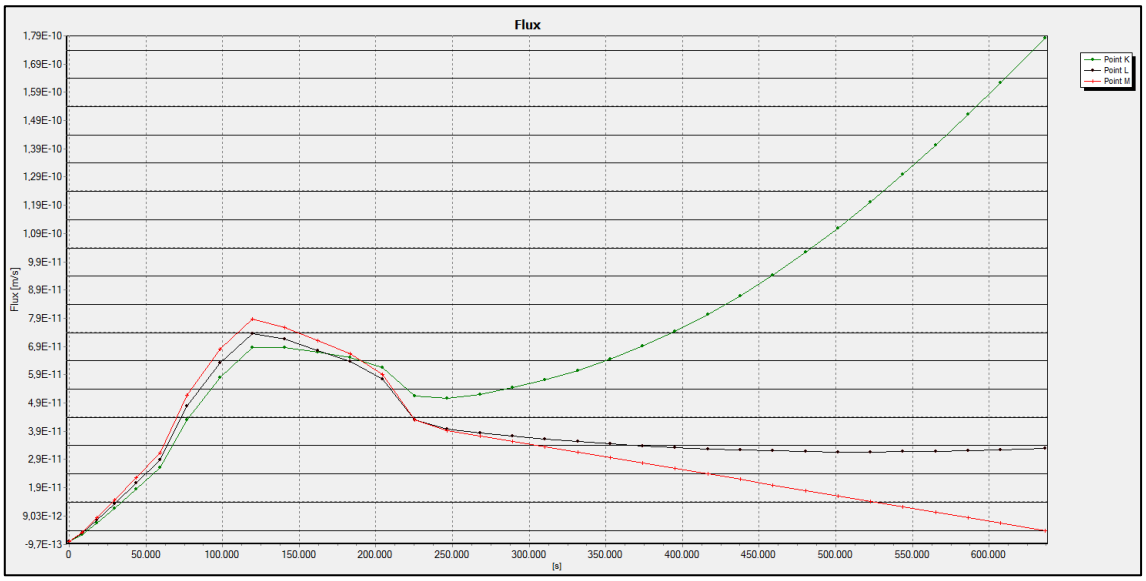

Figure B.33 Extreme velocity graph relation time above the levee

Table B.19 shows that piping is not observed at any points due the fact that to exit gradient is zero. See equations B.11 and B.12 for calculated critical hydraulic gradients.

Table B.19 Piping Status

Symbol	Max Seepage Velocity (m/s)	Permeability (m/s) (k)	Exit Gradient (*i*)	Piping
K	1.8×10^{-10}	1×10^{-6}	0	**NaN**
L	7.4×10^{-11}	1×10^{-6}	0	**NaN**
M	6.9×10^{-11}	1×10^{-6}	0	**NaN**

NaN:Not a Number

B.3. Filyos Levee at 1+513.22 km on Left Shore of Filyos River

Location of Filyos levee at 1513.22 m on left shore is seen Figure B.34 and the schematic representation of Filyos levee and soil profile is given in Figure B.35. Filyos levee includes gravelly sand soil type. There is a sand layer under the levee and this layer is 2 m thick. Also, silty sand material is used for this layer to need filling under the levee.

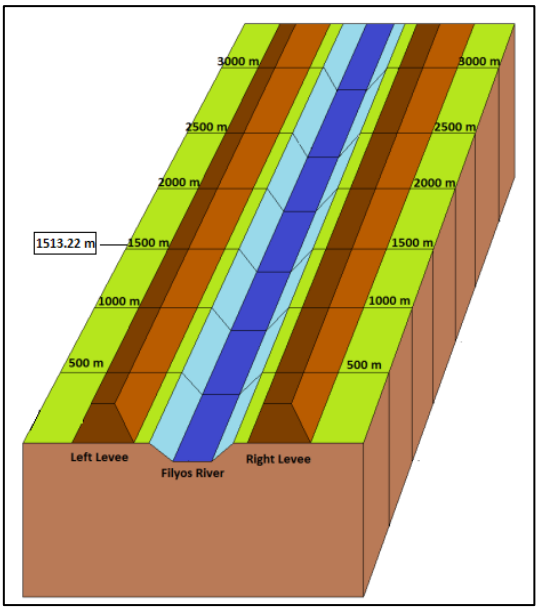

Figure B.34 Locations of Filyos levee at 1513.22 m on left shore of Filyos River

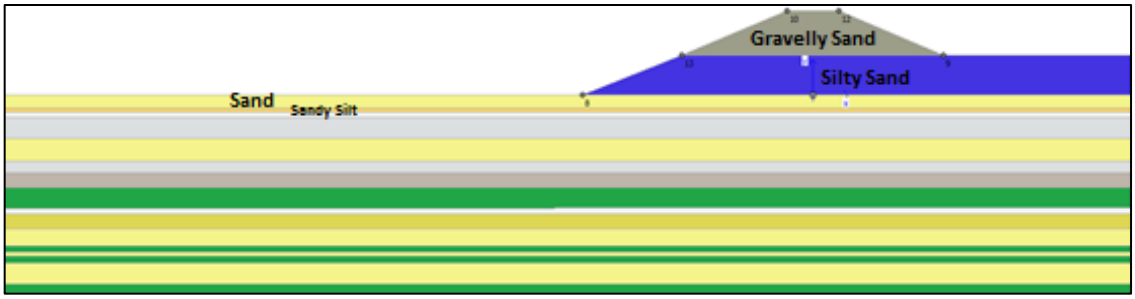

Figure B.35 Filyos Levee at 1+513.22 km on left shore of Filyos River

Figure B.36 shows that each soil layers have saturated unit weight under the levee for transient analysis and area of under the flow line is saturated during h_{max}.

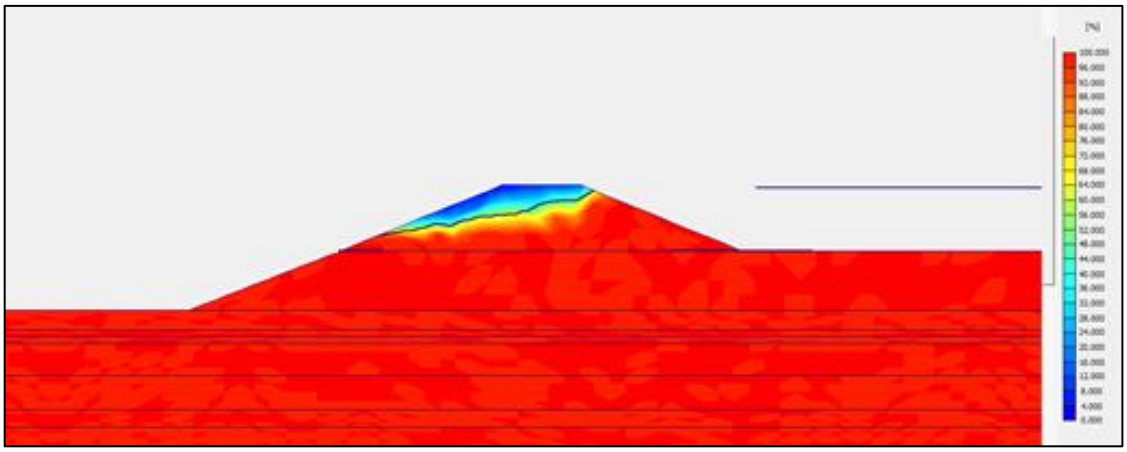

Figure B.36 Degree of Saturation of Filyos Levee at 1+513.22 km on left shore of Filyos River during h_{max}

It is seen that flow values are high at the red area in case h_{max} under the flow line according to Plaxflow2D (Figure B.37.a). There is a risk that is observed piping at these areas.

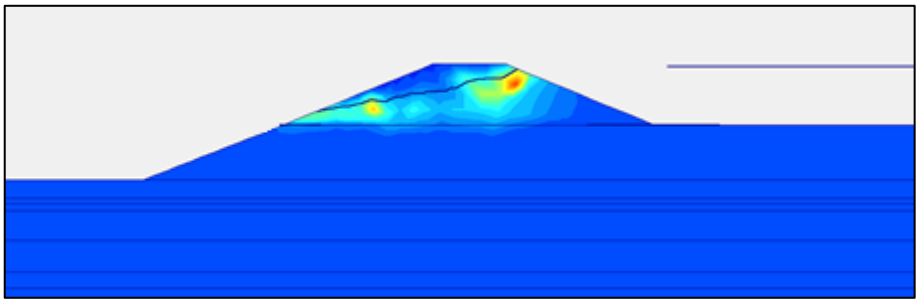

(a)

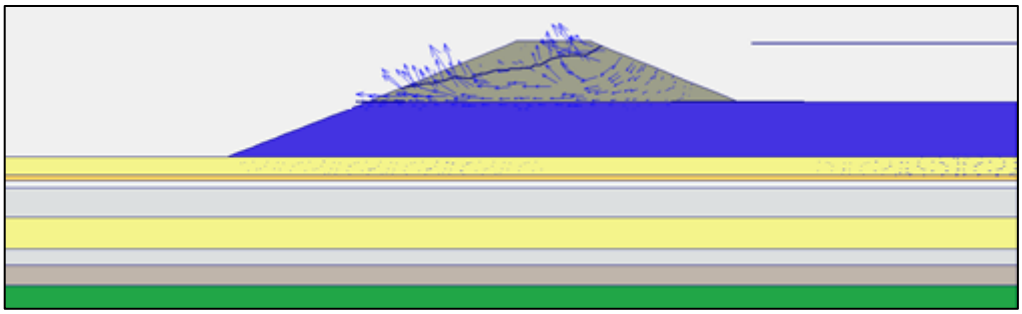

(b)

Figure B.37. Flow field at 1+513.22 km on left shore of Filyos River during h_{max}
a.) Shadings view b.) Arrows view

Figure B.37. (b) is other notation that is vector stage in case h_{max}. That is called arrows in Plaxflow2D literature. If the vectors values are higher than others, there will be observing piping formations.

Analysis of sand at under the levee;

Figure B.38 shows that location of points near the ground surface for finding extreme velocity and Figure B.39 presents that results of flow velocity at K, L, M, N, O, P.

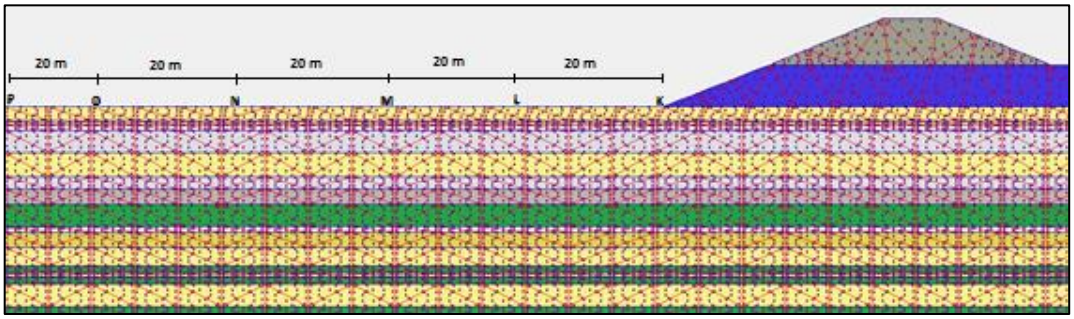

Figure B.38 Location of points near the ground surface for finding extreme velocity

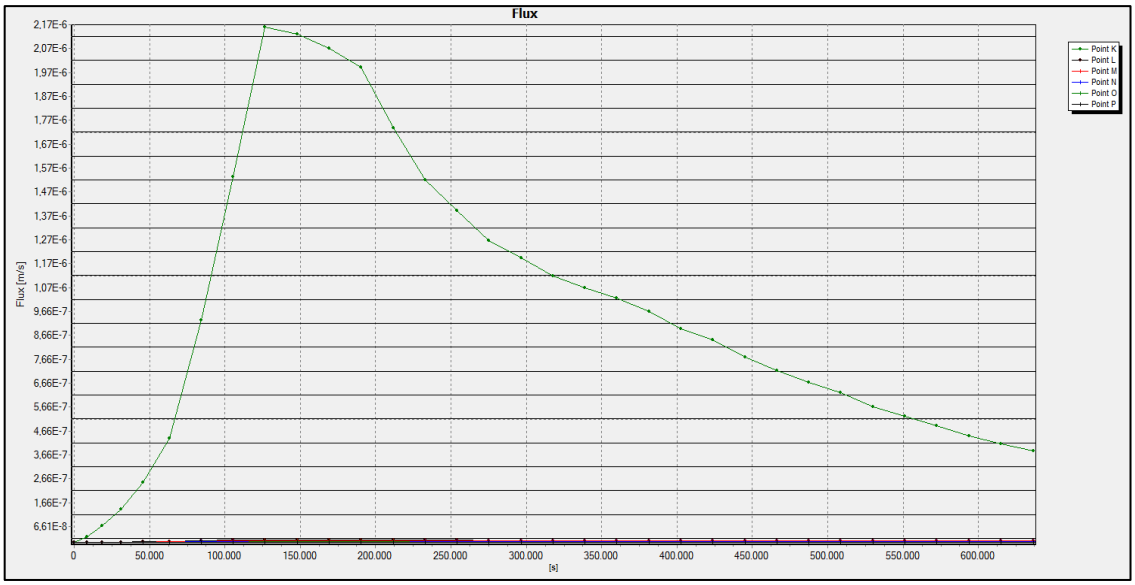

Figure B.39 Extreme velocity graph relation time to seepage velocity

According to Figure B.31, max values of flow are K=2.2x10^{-6}m/s at time=34.7 hours; L=5x10^{-8}m/s at time=34.7 hours; M=4x10^{-8}m/s at time=34.7 hours; N=3x10^{-8}m/s at time=34.7 hours; O=2x10^{-8}m/s at time=34.7 hours; P=1x10^{-8}m/s at time=34.7 hours.

Piping formations are simply compate as;

$$v = k.i\,; \tag{B.15}$$

$$i_c = \frac{G_s - 1}{1+e} = \frac{2.68-1}{1+0.55} = 1.1\,; \tag{B.16}$$

Where;

v = flow velocity (m/sec)

k = permeabilty (m/sec)

i = hydraulic gradient

i_c = critical hydraulic gradient

G_s = specific gravity; 2.68 for sand

e = void ratio; 0.55 for sand

Critical hydraulic gradients is 1.1 for sand so, Table B.20 shows that piping is not observed at any points due the fact that to exit gradient is zero. In order for the sand boiling to occur, the piping must take place.

Table B.20 Piping Status

Symbol	Max Seepage Velocity (m/s)	Permeability (m/s) (k)	Exit Gradient (*i*)	Piping
K	2.2×10^{-6}	1×10^{-4}	0.02	**NaN**
L	5×10^{-8}	1×10^{-4}	0	**NaN**
M	4×10^{-8}	1×10^{-4}	0	**NaN**
N	3×10^{-8}	1×10^{-4}	0	**NaN**
O	2×10^{-8}	1×10^{-4}	0	**NaN**
P	1×10^{-8}	1×10^{-4}	0	**NaN**

NaN:Not a Number

In order for the sand boiling to occur, the piping must take place. As can be seen in the Table B.21, it did not reach critical gradient for the formation of boiling.

Table B.21 Sand Boil Status

Symbol	Max Seepage Velocity (m/s)	Permeability (m/s) (k)	Exit Gradient (*i*)	Sand Boil
K	2.2×10^{-6}	1×10^{-4}	0.02	**NaN**
L	5×10^{-8}	1×10^{-4}	0	**NaN**
M	4×10^{-8}	1×10^{-4}	0	**NaN**
N	3×10^{-8}	1×10^{-4}	0	**NaN**
O	2×10^{-8}	1×10^{-4}	0	**NaN**
P	1×10^{-8}	1×10^{-4}	0	**NaN**

NaN:Not a Number

The analysis above the levee for gravelly sand and silty sand soil fill type;

Piping can only observe K, L and M point because these points only are under the phreatic line. K, L, M etc. points on the ground surface or levee are different from other analyses.

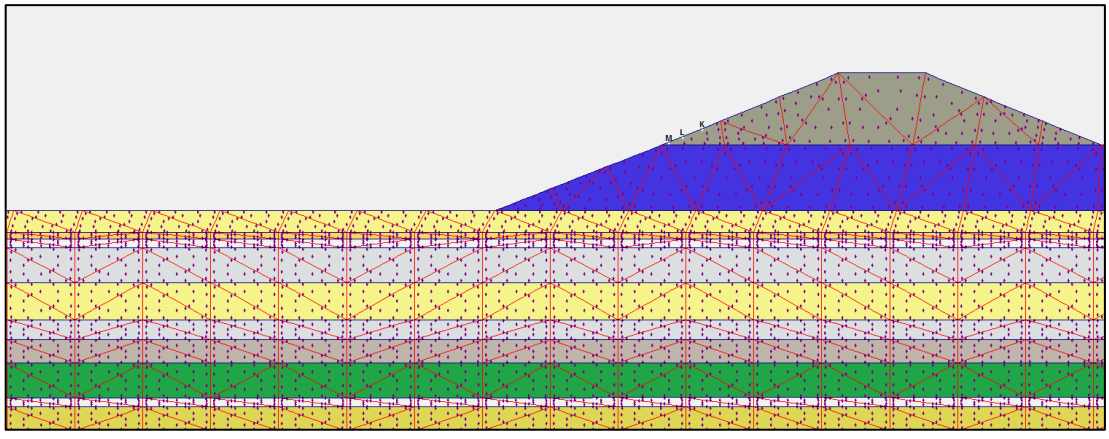

Figure B.40 Location of points above the levee for finding extreme velocity

Extreme velocities of K, L and M point are below and piping formations are investigated for these points.

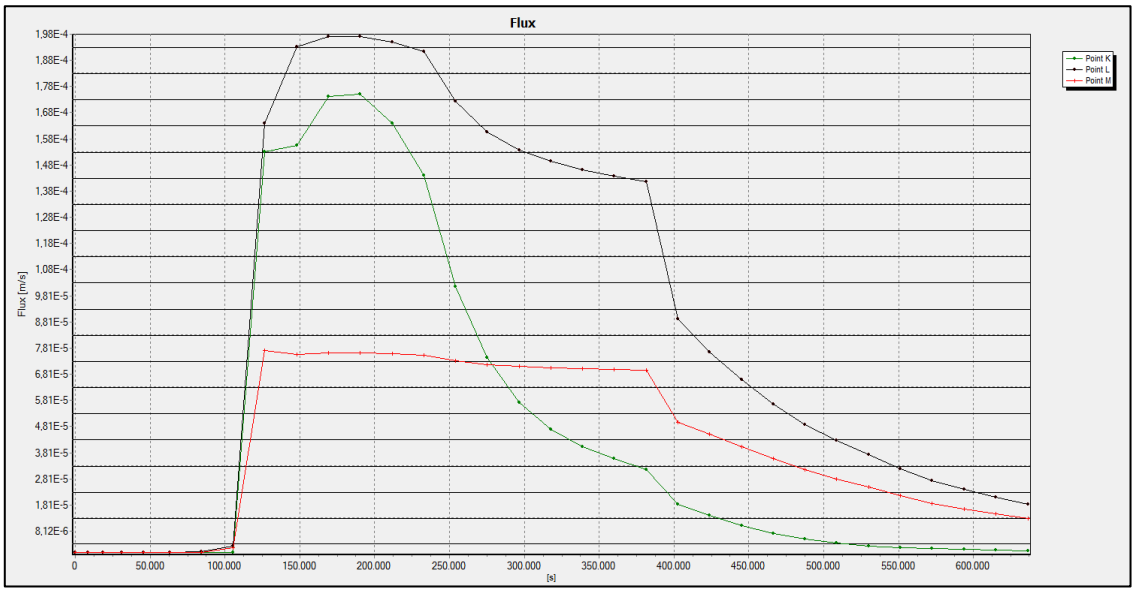

Figure B.41 Extreme velocity graph relation time above the levee

According to Figure B.41, max values of flow are K=1.8x10^{-4}m/s at time=44.4 hours; L=2x10^{-4}m/s at time=44.4 hours; M=7.5x10^{-8}m/s at time=34.7 hours.

Piping formations are simply compate as;

$$v = k.i\,; \tag{B.17}$$

$$i_c = \frac{G_s - 1}{1+e} = \frac{2.66-1}{1+0.62} = 1.02\,; \tag{B.18}$$

Where;

v = flow velocity (m/sec)

k = permeabilty (m/sec)

i = hydraulic gradient

i_c = critical hydraulic gradient

G_s = specific gravity; 2.66 gravelly sand

e = void ratio; 0.62 for gravelly sand

Critical hydraulic gradient is 1.02 for gravelly sand so, Table B.22 shows that piping is not observed at any points due to $i_{exit} < i_c$.

Table B.22 Piping Status

Symbol	Max Seepage Velocity (m/s)	Permeability (m/s) (k)	Exit Gradient (*i*)	Piping
K	1.8×10^{-4}	5×10^{-4}	0.36	**NaN**
L	2.0×10^{-4}	5×10^{-4}	0.40	**NaN**
M	7.5×10^{-8}	5×10^{-4}	0.78	**NaN**

NaN:Not a Number

Piping can only observe K, L and M point because these points only are under the phreatic line. K, L, M etc. points on the ground surface or levee are different from other analyses.

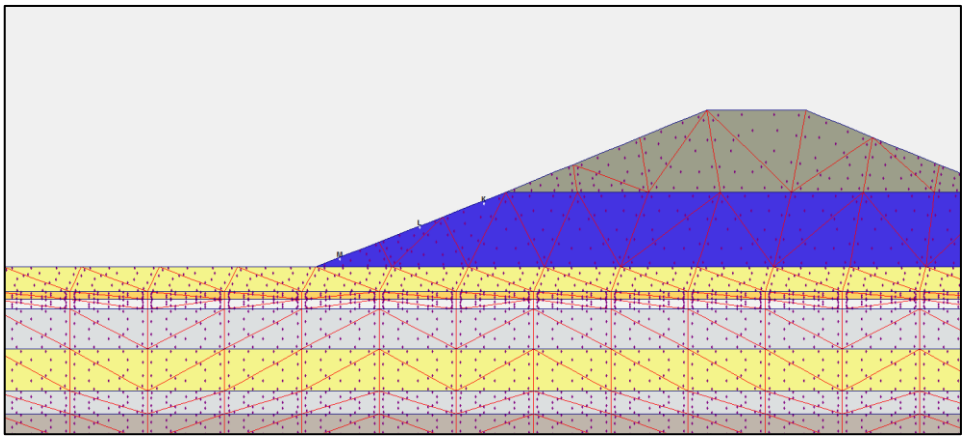

Figure B.42 Location of points above the levee for finding extreme velocity

Extreme velocities of K, L and M point are below and piping formations are investigated for these points.

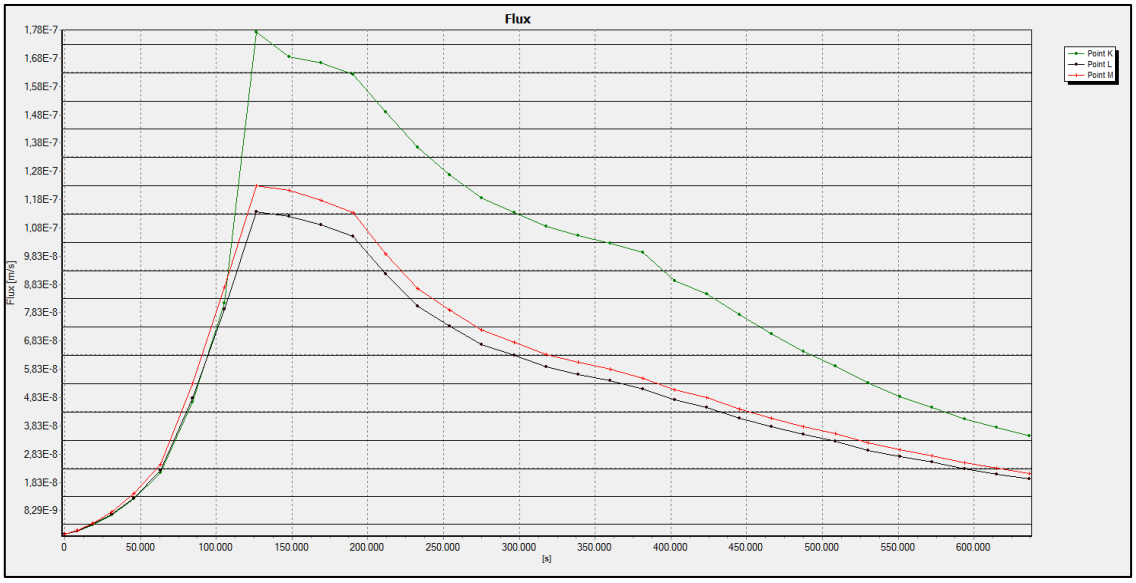

Figure B.43. Extreme velocity graph relation time above the levee

According to Figure B.41, max values of flow are K=1.8x10^{-7}m/s at time=34.7 hours; L=1.13x10^{-7}m/s at time=34.7 hours; M=1.12x10^{-7}m/s at time=34.7 hours.

Piping formations are simply compate as;

$$v = k.i\,; \tag{B.19}$$

$$i_c = \frac{G_s - 1}{1+e} = \frac{2.69-1}{1+0.43} = 1.2\,; \tag{B.20}$$

Where;

v = flow velocity (m/sec)

k = permeabilty (m/sec)

i = hydraulic gradient

i_c = critical hydraulic gradient

G_s = specific gravity; 2.69 for silty sand

e = void ratio; 0.42 for silty sand

Table B.24. shows that piping is not observed at any points due to $i_{exit} < i_c$.

Table B.24 Piping Status

Symbol	Max Seepage Velocity (m/s)	Permeability (m/s) (k)	Exit Gradient (*i*)	Piping
K	1.8 x 10^{-7}	1x10^{-6}	0.18	**NaN**
L	1.13 x 10^{-7}	1x10^{-6}	0.11	**NaN**
M	1.12 x 10^{-7}	1x10^{-6}	0.11	**NaN**

NaN:Not a Number

The factor of safety against heave analysis for top layer;

Equation B.21 and B.22 are used to determine the factor of safety against heave analysis for top layer. Heaving potential are only observed ground surface hence a point are investigated at 1 m below the top layer like Figure B.44.

$$F_{heave} = \frac{H.\gamma_{sat}}{h_m.\gamma_w} > 3.0 \tag{B.21}$$

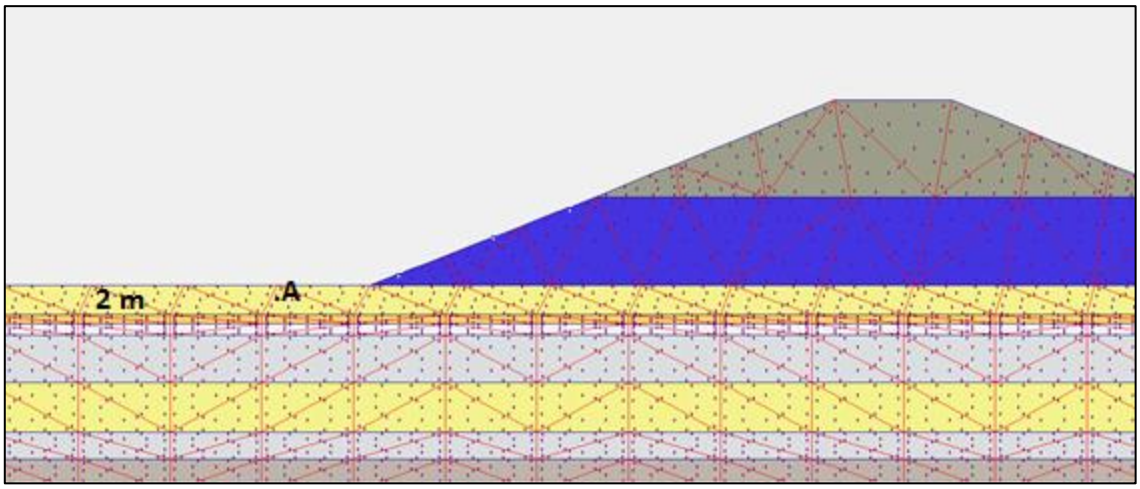

Figure B.44 Analysis against to heave at A point 1 m below the top layer

$$i_{\max} = \frac{h_m}{H} \tag{B.22}$$

Where;

H = thickness of overlying top layer

γ_{sat} = saturated unit weight of overlying top layer

h_m = average hydraulic head at the point

γ_w = water unit wight

$i_{\max}$ = maximum exit gradient

$$0.02 = \frac{h_m}{1} \Rightarrow h_m = 0.02 \;;\; F_{heave} = \frac{1x20.4}{0.02x10} > 3.0$$

It is not observed heave due to the fact that F_{heave} is higher than 3.0 .

B.3.1. Filyos Levee at 1+513.22 km on Left Shore of Filyos River according to Current Situation(Upstream face is covered)

The schematic representation of Filyos Levee and soil profile is given in Figure B.45 Filyos levee includes gravelly sand soil type and cover materials against piping and sand boil formations. The cover materials are riprap which is andesite, uniform sand filter layer and geocomposite layer. There is a sand layer under the levee and this layer is 4 m thick.

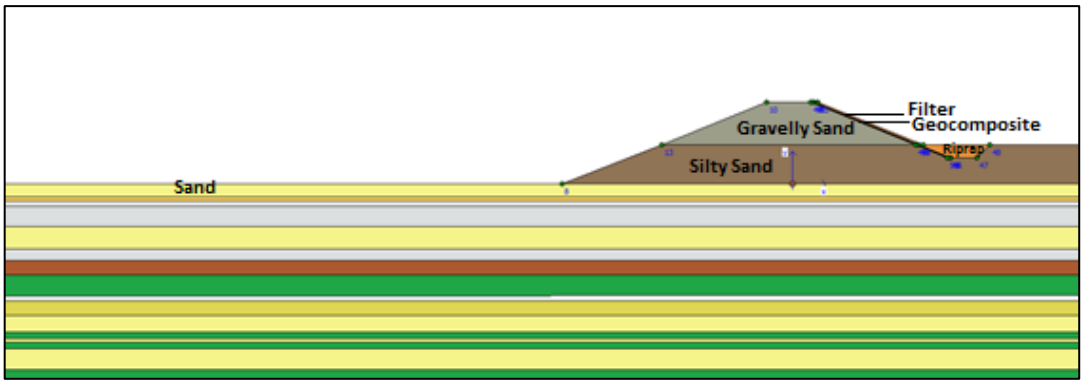

Figure B.45 Filyos Levee with cover materials at 1+513.22 km on left shore of Filyos River

Filyos levee has covered along rising water level. Table B.25 shows properties of covered materials and levee.

Table B.25 Soil Properties of levee members

	Soil Type / Material	**Permeability(k) (m/sec)**	**Specific Gravity (G_s)**	**Void Ratio (e)**	**Thickness (m)**
Filter	Uniform Sand	$1x10^{-3}$	2.67	0.70	0.25
Riprap	Andesite Rock	0.645	2.65	0.34	0.70
Geocomposite Material	Geotextile and Geomembrane	$1x10^{-13}$	-	0.02	0.30

Figure B.46 shows that each soil layers have saturated unit weight under the levee with cover materials for transient analysis and area of under the flow line is saturated during h_{max}. Saturation rates of red areas are high and saturation rates of other areas are almost zero without riprap, filter, and areas under levee.

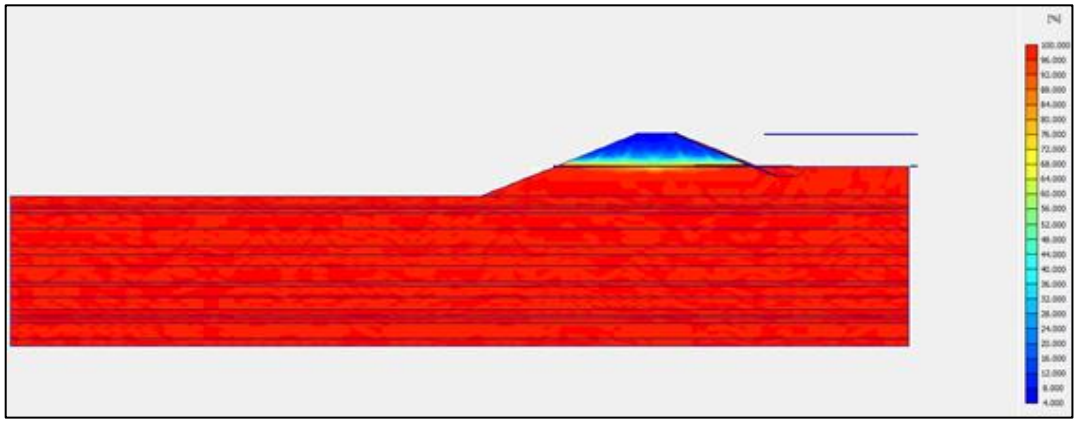

Figure B.46 Degree of Saturation of Filyos Levee with cover materials at 1+513.22 km on left shore of Filyos River during h_{max}

It is seen that flow values are high at the red area in case h_{max} under the flow line according to Plaxflow2D (Figure B.47.a). There is not a risk that is observed piping into through levee.

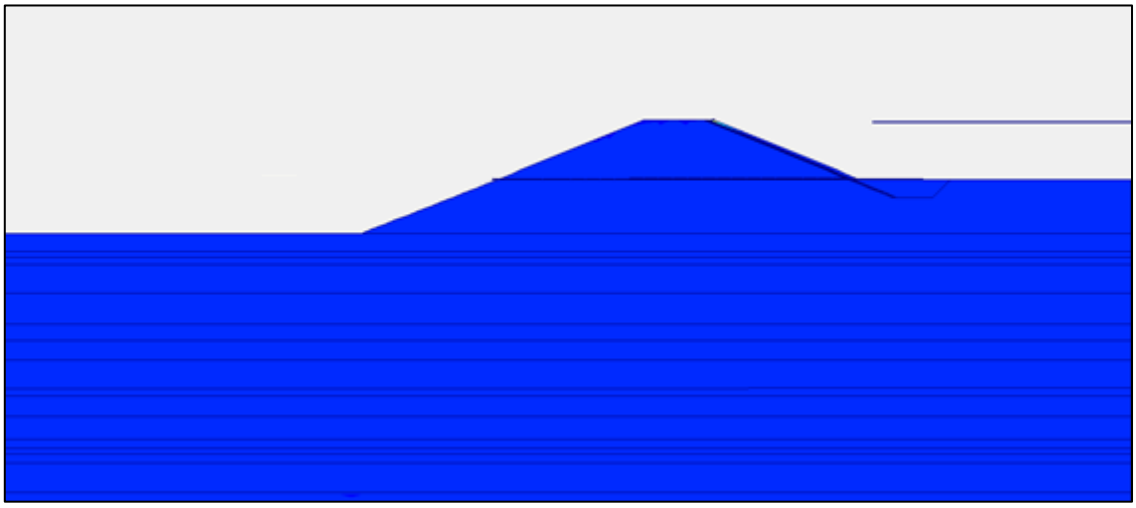

(a)

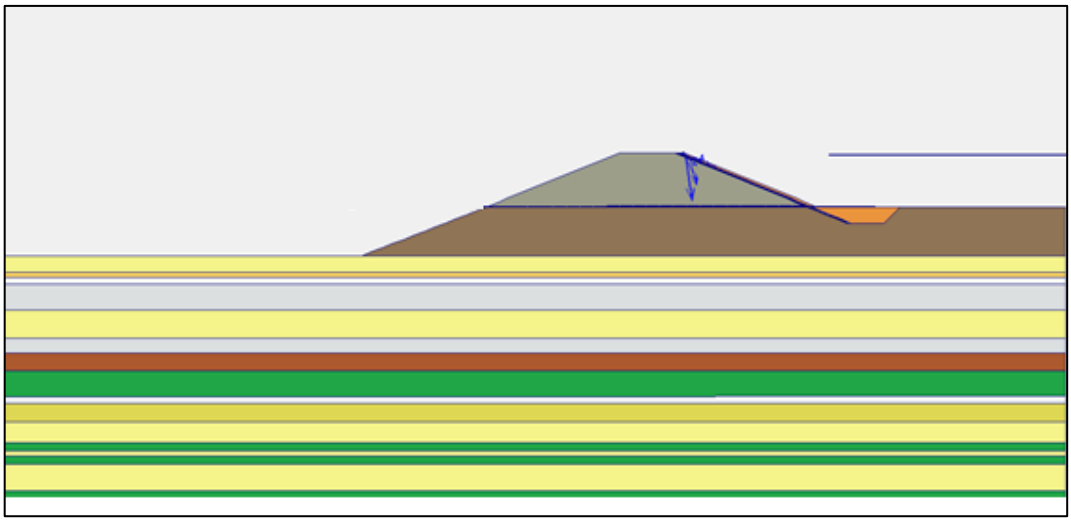

(b)

Figure B.47. Flow field at 1+513.22 km on left shore of Filyos River during h_{max} a.) Shadings view b.) Arrows view

Figure B.47. (b) is other notation that is vector stage in case h_{max}. That is called arrows in Plaxflow2D literature and there is not risk into through levee.

Analysis of sand at under the levee;

Figure B.48. shows that location of points near the ground surface for finding extreme velocity and Figure B.49 presents that results of flow velocity at K, L, M, N, O and P.

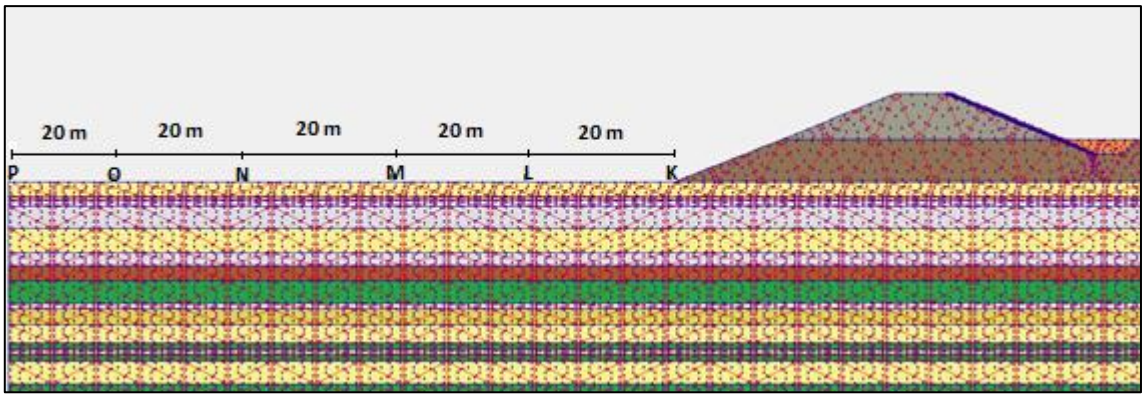

Figure B.48 Location of points near the ground surface for finding extreme velocity

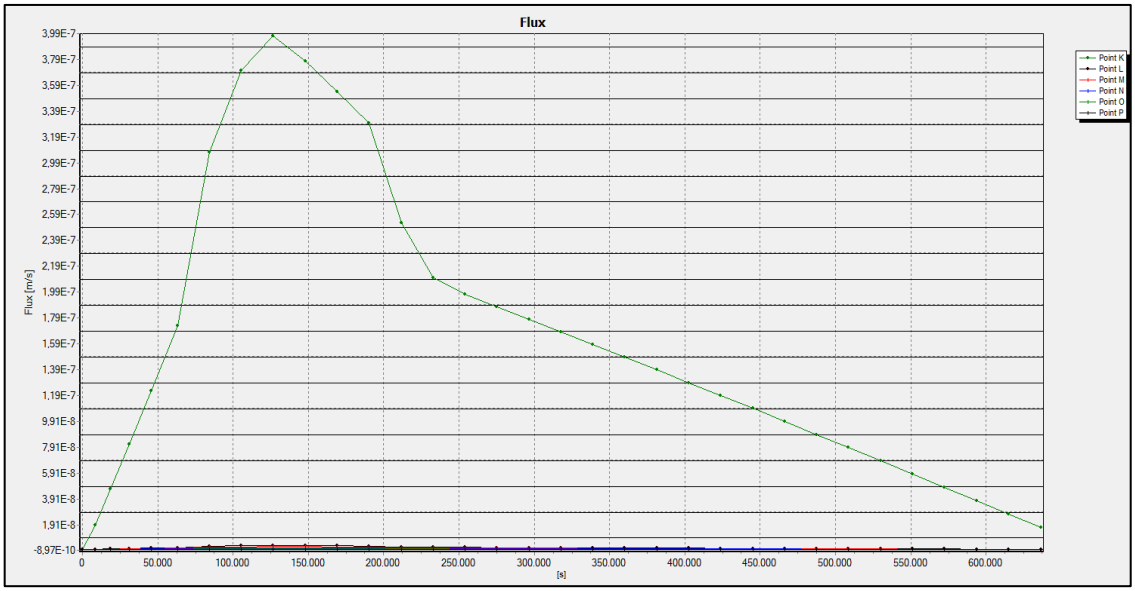

Figure B.49 Extreme velocity graph relation time Filyos Levee

Table B.26 shows that piping is not observed at any points due the fact that to exit gradient is zero. See equations B.15 and B.16 for calculated critical hydraulic gradients.

Table B.26 Piping Status

Symbol	Max Seepage Velocity (m/s)	Permeability (m/s) (k)	Exit Gradient (*i*)	Piping
K	4×10^{-7}	1×10^{-4}	0	**NaN**
L	1×10^{-8}	1×10^{-4}	0	**NaN**
M	1×10^{-9}	1×10^{-4}	0	**NaN**
N	1×10^{-10}	1×10^{-4}	0	**NaN**
O	1×10^{-10}	1×10^{-4}	0	**NaN**
P	1×10^{-10}	1×10^{-4}	0	**NaN**

NaN:Not a Number

In order for the sand boiling to occur, the piping must take place. As can be seen in the Table B.27, it did not reach critical gradient for the formation of boiling. See equations B.15 and B.16 for calculated critical hydraulic gradients.

Table B.27 Sand Boil Status

Symbol	Max Seepage Velocity (m/s)	Permeability (m/s) (k)	Exit Gradient (*i*)	Sand Boil
K	4×10^{-7}	1×10^{-4}	0	**NaN**
L	1×10^{-8}	1×10^{-4}	0	**NaN**
M	1×10^{-9}	1×10^{-4}	0	**NaN**
N	1×10^{-10}	1×10^{-4}	0	**NaN**
O	1×10^{-10}	1×10^{-4}	0	**NaN**
P	1×10^{-10}	1×10^{-4}	0	**NaN**

NaN:Not a Number

- Heaving potential is not observed that levee has cover materials along river since the exit gradients approach zero.

The analysis above the levee for gravelly sand and silty sand fill soil type;

Piping can only observe K, L and M point because these points only are under the phreatic line. K, L, M etc. points on the ground surface or levee are different from other analyses.

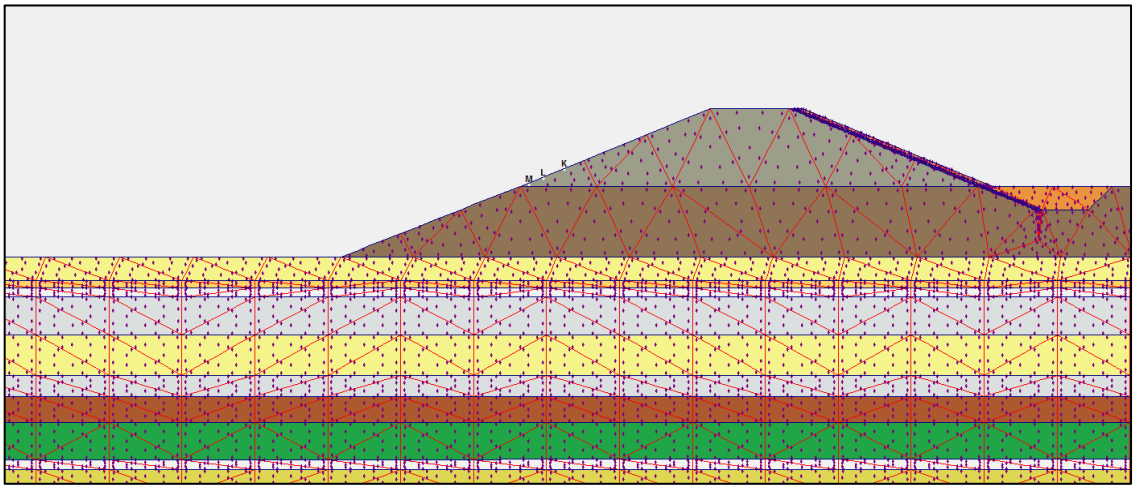

Figure B.50 Location of points above the levee for finding extreme velocity

Extreme velocities of K, L and M point are Figure B.51 and these extreme velocities generally observe during h_{max}. Filyos levee includes gravelly sand soil type and filling layer includes silty sand soil type so, K, L and M points are different from each soil layer.

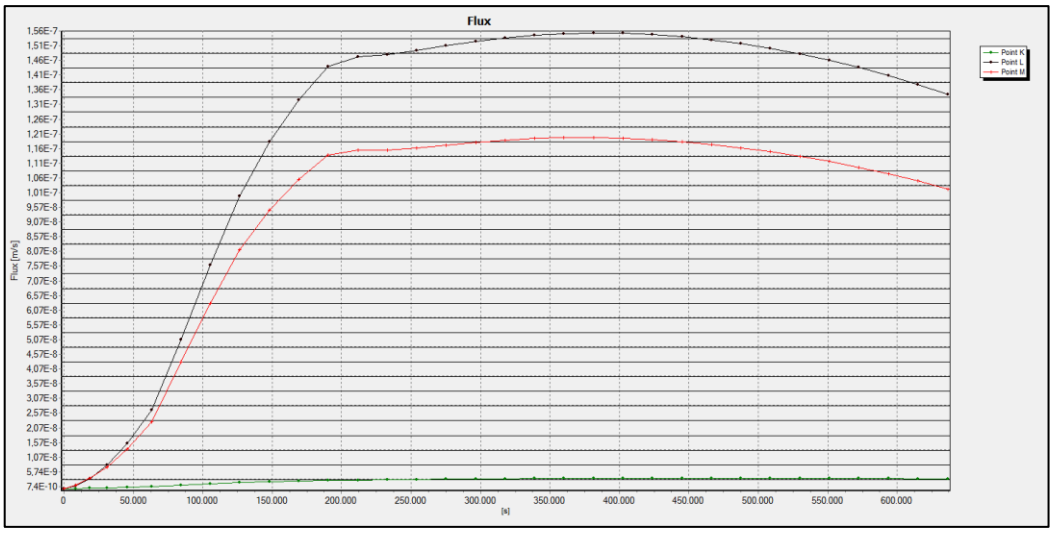

Figure B.51 Extreme velocity graph relation time to seepage velocity

Table B.28 shows that piping is not observed at any points due the fact that to exit gradient is zero. See equations B.17 and B.18 for calculated critical hydraulic gradients.

Table B.28 Piping Status

Symbol	Max Seepage Velocity (m/s)	Permeability (m/s) (k)	Exit Gradient (i)	Piping
K	7.4×10^{-10}	5×10^{-4}	0	**NaN**
L	1.6×10^{-7}	5×10^{-4}	0	**NaN**
M	1.2×10^{-7}	5×10^{-4}	0	**NaN**

NaN:Not a Number

Piping can only observe K, L and M point because these points only are under the phreatic line. K, L, M etc. points on the ground surface or levee are different from other analyses.

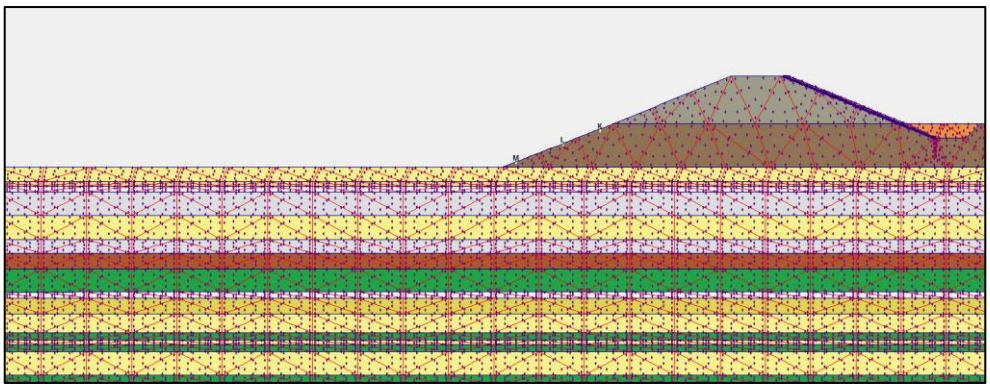

Figure B.53 Location of points above the levee for finding extreme velocity

Extreme velocities of K, L and M point are below and piping formations are investigated for these points.

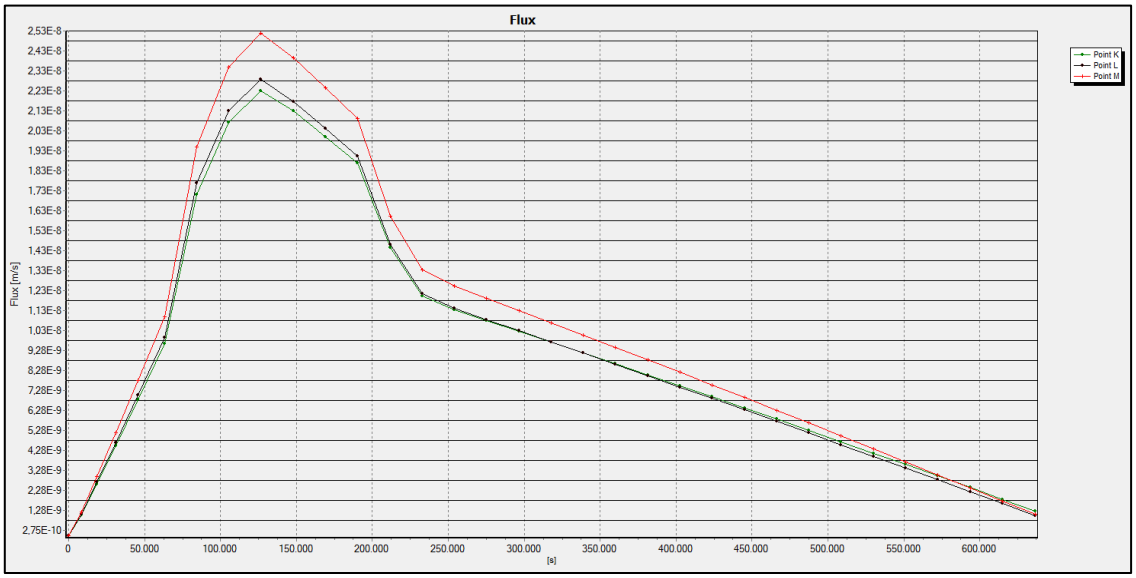

Figure B.54. Extreme velocity graph relation time above the levee

Table B.29 shows that piping is not observed at any points due to $i_{exit} < i_c$. See equations B.19 and B.20 for calculated critical hydraulic gradients.

Table B.29 Piping Status

Symbol	Max Seepage Velocity (m/s)	Permeability (m/s) (k)	Exit Gradient (*i*)	Piping
K	2.2×10^{-8}	1×10^{-6}	0.022	**NaN**
L	2.3×10^{-8}	1×10^{-6}	0.023	**NaN**
M	2.3×10^{-7}	1×10^{-6}	0.023	**NaN**

NaN:Not a Number

- Heaving potential is not observed that levee has cover materials along river since the exit gradients approach zero.

B.4. Filyos Levee at 2+005.66 km on Left Shore of Filyos River

Location of Filyos levee at 2+005.66 km on right shore is seen Figure B.55 and the schematic representation of Filyos Levee and soil profile is given in Figure B.56

Filyos levee includes gravelly sand soil type. There is a sandy silt layer under the levee and this layer is 4 m thick.

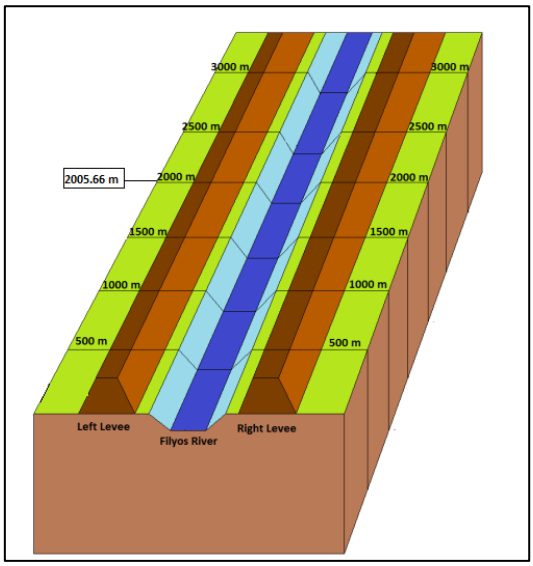

Figure B.55 Filyos Levee at 2+005.66 km on left shore of Filyos River

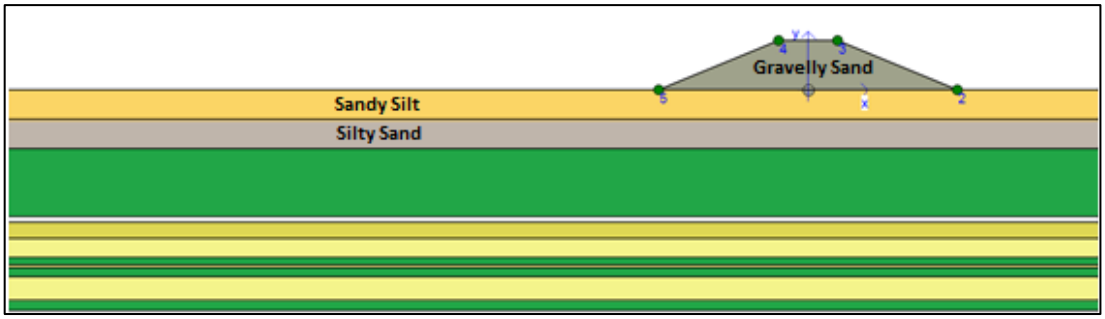

Fig. B.56 Filyos Levee at 2+005.66 km on left shore of Filyos River

Figure B.57 shows that each soil layers have saturated unit weight under the levee for transient analysis and area of under the flow line is saturated during h_{max}.

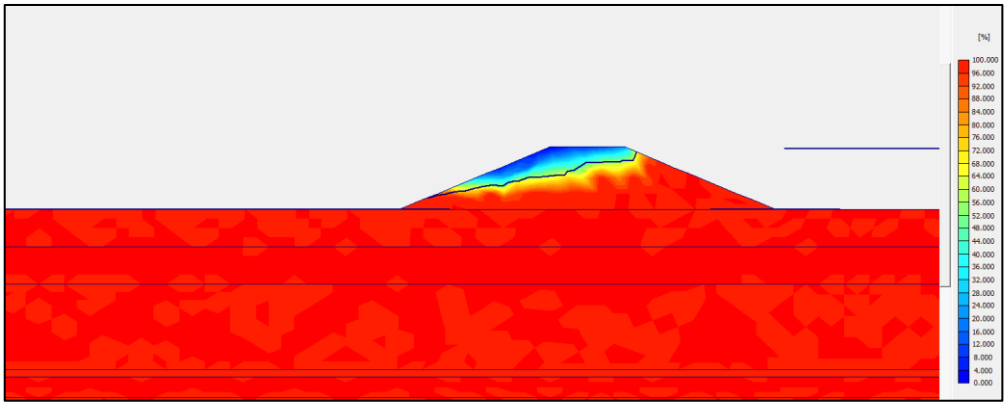

Figure B.57 Degree of Saturation of Filyos Levee at 2+005.66 km on left shore of Filyos River during h_{max}

It is seen that flow values are high at the red area in case h_{max} under the flow line according to Plaxflow2D (Figure B.58.a). There is a risk that is observed piping at these areas.

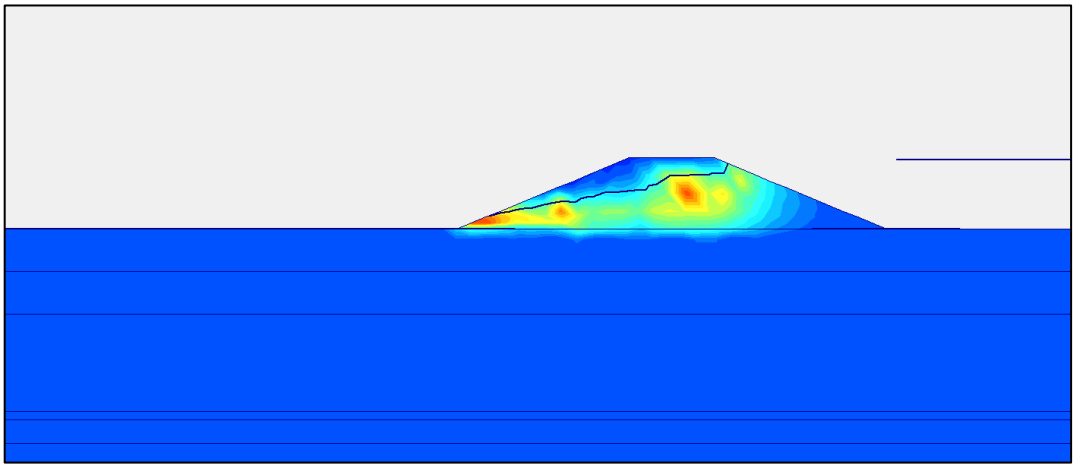

(a)

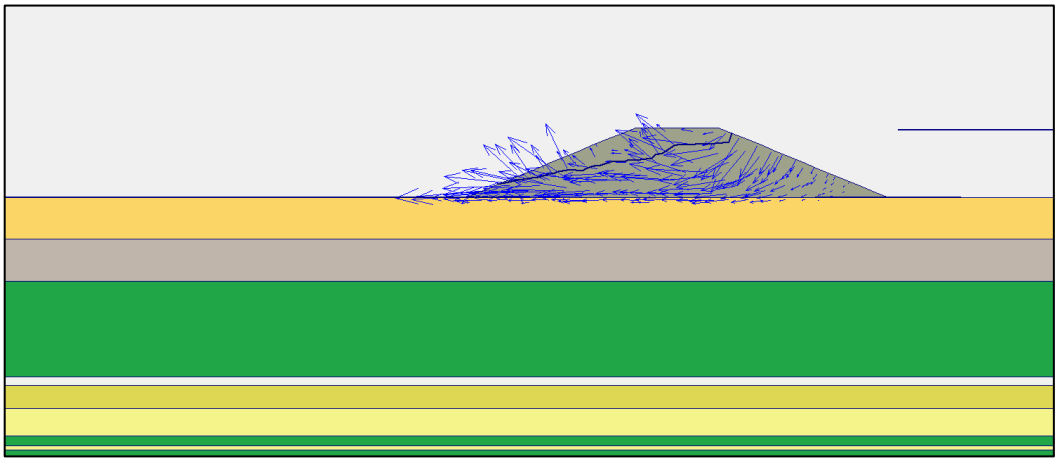

(b)

Figure B.58. Flow field at 2+005.66 km on left shore of Filyos River during h_{max} a.) Shadings view b.) Arrows view

Figure B.58. (b) is other notation that is vector stage in case h_{max}. That is called arrows in Plaxflow2D literature. If the vectors values are higher than others, there will be observing piping formations.

Analysis of sandy silt at under the levee;

Figure B.59 shows that location of points near the ground surface for finding extreme velocity and Figure B.60 presents that results of flow velocity at K, L, M, N, O, P, Q and R. K, L, M etc. points on the ground surface or levee are different from other analyses.

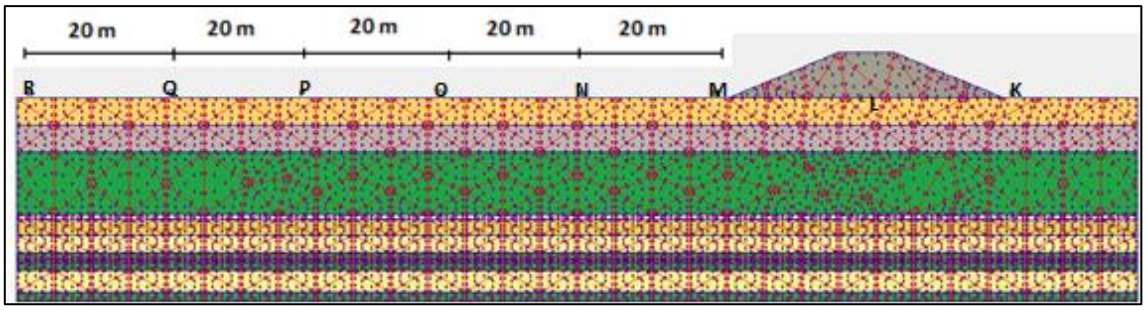

Figure B.59 Location of points near the ground surface for finding extreme velocity

Extreme velocities of K, L and M point are piping formations are investigated for these points.

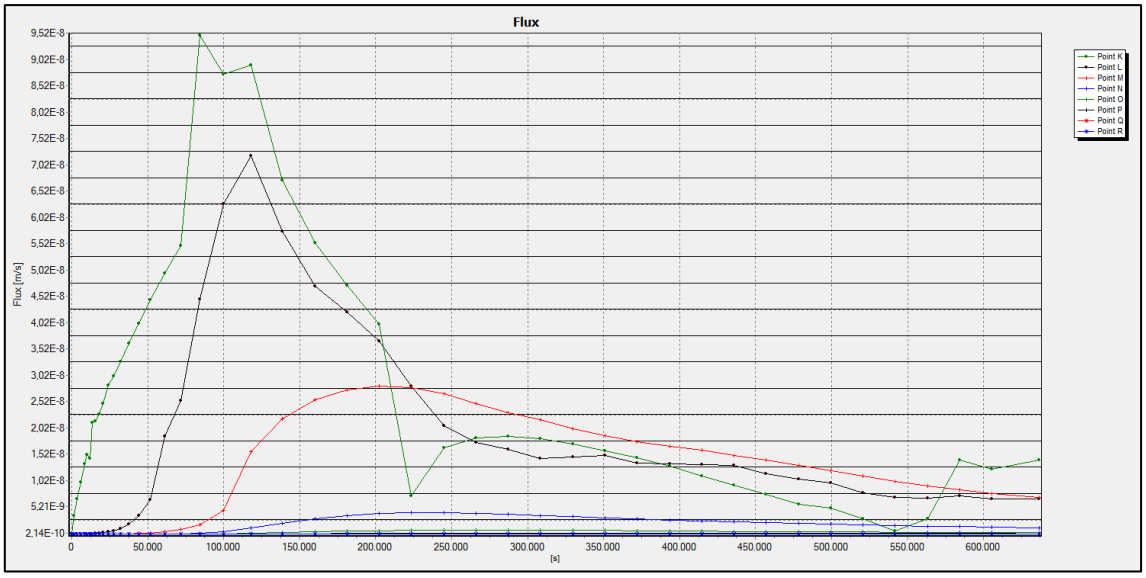

Figure B.60. Extreme velocity graph relation time to seepage velocity

According to Figure B.60, max values of flow are K=9.5x10^{-8}m/s at time=25 hours; L=7.3x10^{-8}m/s at time=33.4 hours; M=2.7x10^{-8}m/s at time=55.6 hours; N=5x10^{-9}m/s at time=55.6 hours; O, P, Q, R=2x10^{-10}m/s at time=55.6 hours.

Piping formations are simply compate as;

$$v = k.i\,; \tag{B.23}$$

$$i_c = \frac{G_s - 1}{1+e} = \frac{2.68-1}{1+0.55} = 0.91\,; \tag{B.24}$$

Where;

v = flow velocity (m/sec)

k = permeabilty (m/sec)

i = hydraulic gradient

i_c = critical hydraulic gradient

G_s = specific gravity; 2.68 for sandy silt

e = void ratio; 0.85 for sandy silt

Table B.30 shows that piping is not observed due to $i_{exit} < i_c$.

Table B.30 Piping Status

Symbol	Max Seepage Velocity (m/s)	Permeability (m/s) (k)	Exit Gradient (*i*)	Piping
K	9.5×10^{-8}	1×10^{-7}	0.95	$i_{exit} > i_c$
L	7.3×10^{-8}	1×10^{-7}	0.73	**NaN**
M	2.7×10^{-8}	1×10^{-7}	0.27	**NaN**
N	5×10^{-9}	1×10^{-7}	0.05	**NaN**
O	2×10^{-10}	1×10^{-7}	0	**NaN**
P	2×10^{-10}	1×10^{-7}	0	**NaN**
Q	2×10^{-10}	1×10^{-7}	0	**NaN**
R	2×10^{-10}	1×10^{-7}	0	**NaN**

NaN:Not a Number

In order for the sand boiling to occur, the piping must take place. As can be seen in the Table B.31. Critical hydraulic gradient is 0.91 for sandy silt so, it did not reach critical gradient for the formation of boiling.

Table B.31 Sand Boil Status

Symbol	Max Seepage Velocity (m/s)	Permeability (m/s) (k)	Exit Gradient (*i*)	Sand Boil
M	2.7×10^{-8}	1×10^{-7}	0.27	**NaN**
N	5×10^{-9}	1×10^{-7}	0.05	**NaN**
O	2×10^{-10}	1×10^{-7}	0	**NaN**
P	2×10^{-10}	1×10^{-7}	0	**NaN**
Q	2×10^{-10}	1×10^{-7}	0	**NaN**
R	2×10^{-10}	1×10^{-7}	0	**NaN**

NaN:Not a Number

The analysis above the levee for gravelly sand soil type;

Piping can only observe K, L and M point because these points only are under the phreatic line. K, L, M etc. points on the ground surface or levee are different from other analyses.

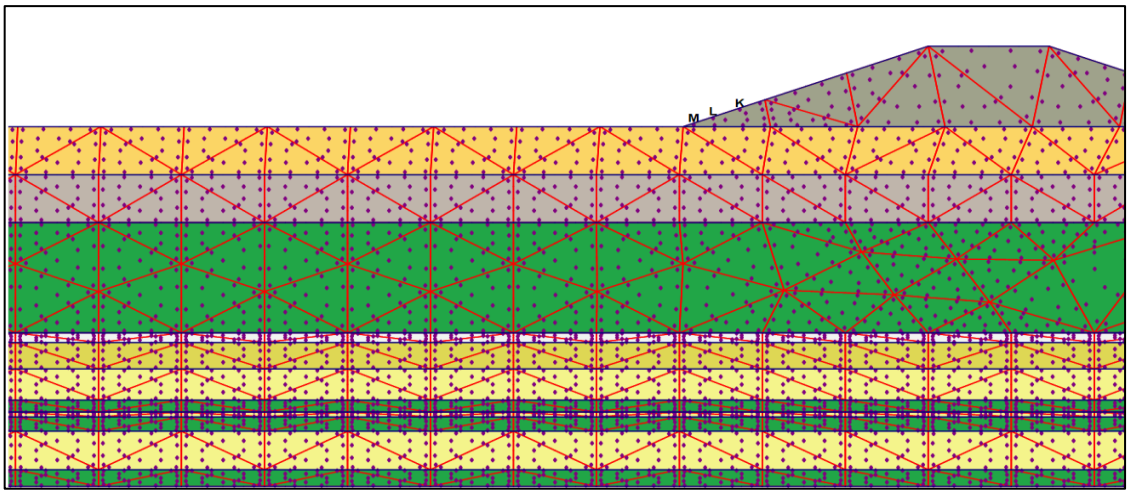

Figure B.61 Location of points above the levee for finding extreme velocity

Extreme velocities of K, L and M point are in Figure B.62 and piping formations are investigated for these points.

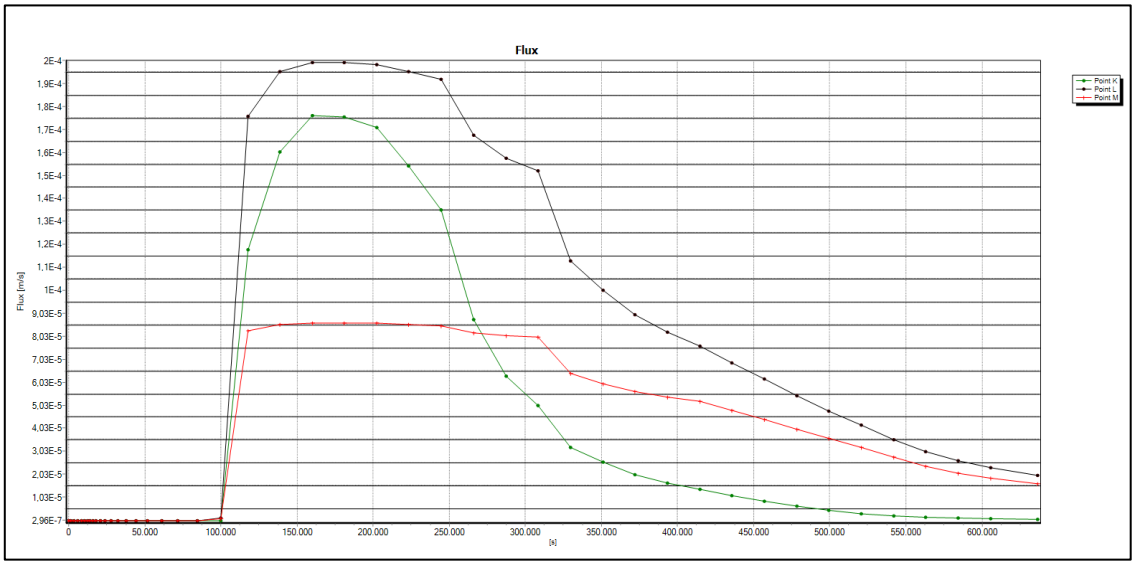

Figure B.62 Extreme velocity graph relation time above the levee

According to Figure B.62, max values of flow are K=1.75x10^{-4}m/s at time=34.7 hours; L=2x10^{-4}m/s at time=34.7 hours; M=8.5x10^{-5}m/s at time=34.7 hours.

Piping formations are simply compate as;

$$v = k.i\,; \tag{B.25}$$

$$i_c = \frac{G_s - 1}{1+e} = \frac{2.66-1}{1+0.62} = 1.02; \tag{B.26}$$

Where;

v = flow velocity (m/sec)

k = permeabilty (m/sec)

i = hydraulic gradient

i_c = critical hydraulic gradient

G_s = specific gravity; 2.66 for gravelly sand

e = void ratio; 0.62 for gravelly sand

Table B.32 shows that piping is not observed at any points due to $i_{exit} < i_c$.

Table B.32 Piping Status

Symbol	Max Seepage Velocity (m/s)	Permeability (m/s) (k)	Exit Gradient (*i*)	Piping
K	1.75×10^{-4}	5×10^{-4}	0.35	**NaN**
L	2×10^{-4}	5×10^{-4}	0.40	**NaN**
M	8.5×10^{-5}	5×10^{-4}	0.17	**NaN**

NaN:Not a Number

The factor of safety against heave analysis for top layer;

Equation B.35 and B.36 are used to determine the factor of safety against heave analysis for top layer. Heaving potential are only observed ground surface hence a point are investigated at 1 m below the top layer like Figure B.63.

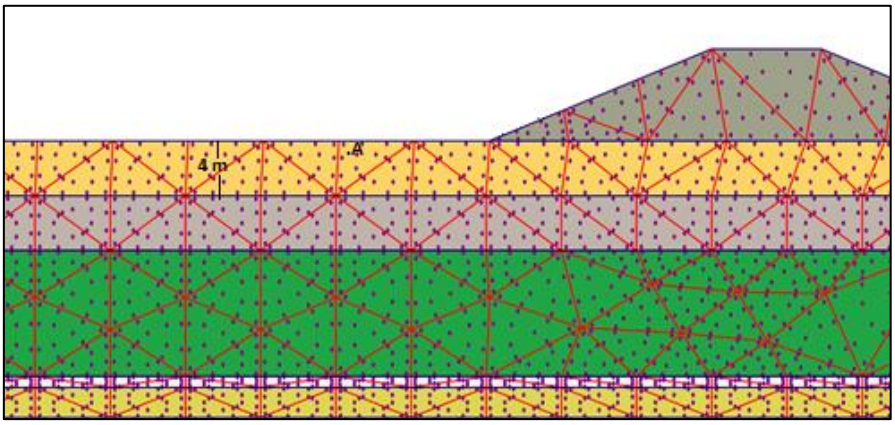

Figure B.63 Analysis against to heave at A point 0.5 m below the top layer

$$F_{heave} = \frac{H.\gamma_{sat}}{h_m.\gamma_w} > 3.0 \qquad \text{(B.27)}$$

$$i_{\max} = \frac{h_m}{H} \qquad \text{(B.28)}$$

Where;

H = thickness of overlying top layer (m)

γ_{sat} = saturated unit weight of overlying top layer (kN/m^2)

h_m = average hydraulic head at the point(m)

γ_w = water unit wight(kN/m^2)

$i_{\max}$ = maximum exit gradient

$$0.27 = \frac{h_m}{0.5} \Rightarrow h_m = 0.14 \ ; \ F_{heave} = \frac{0.5x18.7}{0.14x10} = 6.7 > 3.0$$

It is not observed heave due to the fact that F_{heave} is higher than 3.0 .

B.4.1. Filyos Levee at 2+005.66 km on Left Shore of Filyos River according to Current Situation(Upstream face is covered)

The schematic representation of Filyos Levee and soil profile is given in Figure B.64. Filyos levee includes gravelly sand soil type and cover materials against piping and sand boil formations. The cover materials are riprap which is andesite, uniform sand filter layer and geocomposite layer. There is a clayey silt layer under the levee and this layer is 4 m thick.

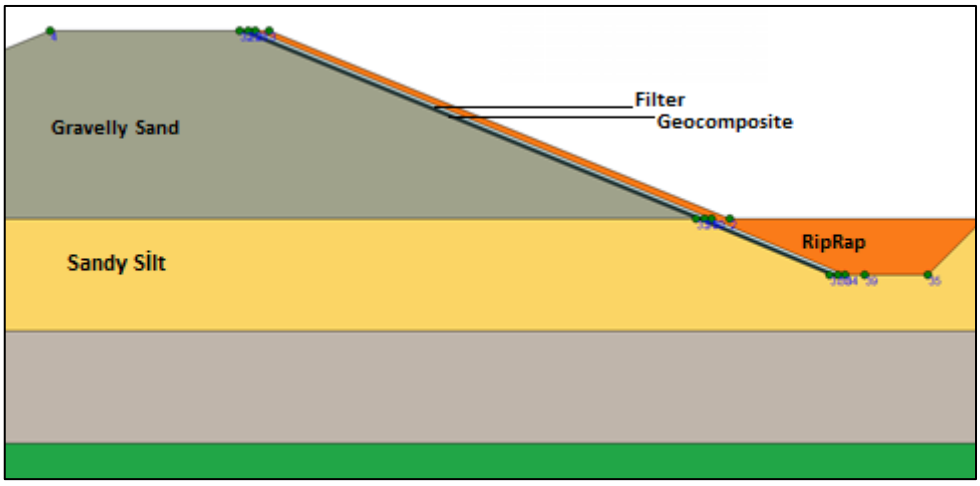

Figure B.64 Filyos Levee with cover materials at 2+005.66 km on left shore of Filyos River

Filyos levee has covered along rising water level. The covered members are filter, riprap and geocomposite materials. Table B.33 shows properties of covered materials and levee.

Table B.33 Soil Properties of levee members

	Soil Type / Material	Permeability(k) (m/sec)	Specific Gravity (G_s)	Void Ratio (e)	Thickness (m)
Filter	Uniform Sand	$1x10^{-3}$	2.67	0.70	0.25
Riprap	Andesite Rock	0.645	2.65	0.34	0.70
Geocomposite Material	Geotextile and Geomembrane	$1x10^{-13}$	-	0.02	0.30

Figure B.65 shows that each soil layers have saturated unit weight under the levee with cover materials for transient analysis and area of under the flow line is saturated during h_{max}. Saturation rates of red areas are high and saturation rates of other areas are almost zero without riprap, filter, and areas under levee.

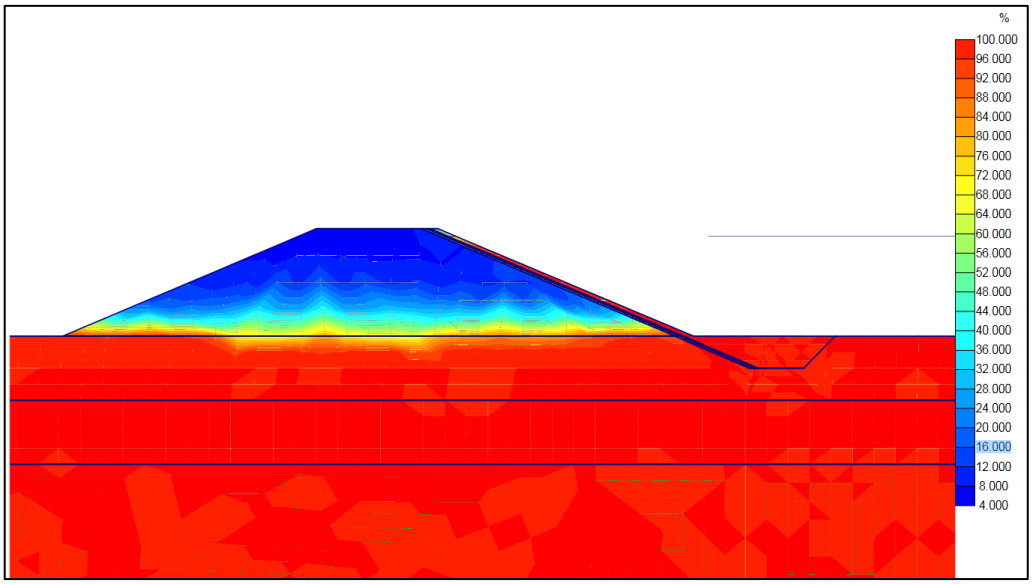

Figure B.65 Degree of Saturation of Filyos Levee with cover materials at 2+005.66 km on left shore of Filyos River during h_{max}

It is seen that flow values are high at the red area in case h_{max} under the flow line according to Plaxflow2D (Figure B.66.a). There is not a risk that is observed piping into through levee. The saturation rates are high in red areas and Filyos levee is protected from seepage problems thanks to covered materials.

Figure B.66. (b) is other notation that is vector stage in case h_{max}. That is called arrows in Plaxflow2D literature and there is not risk into through levee.

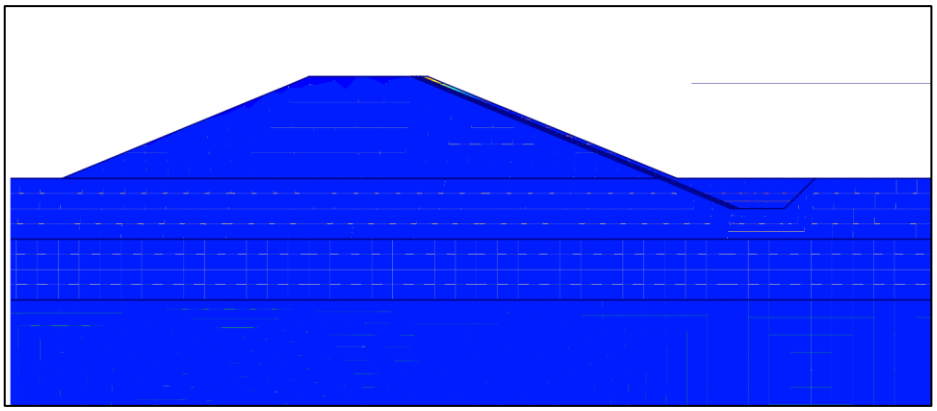

(a)

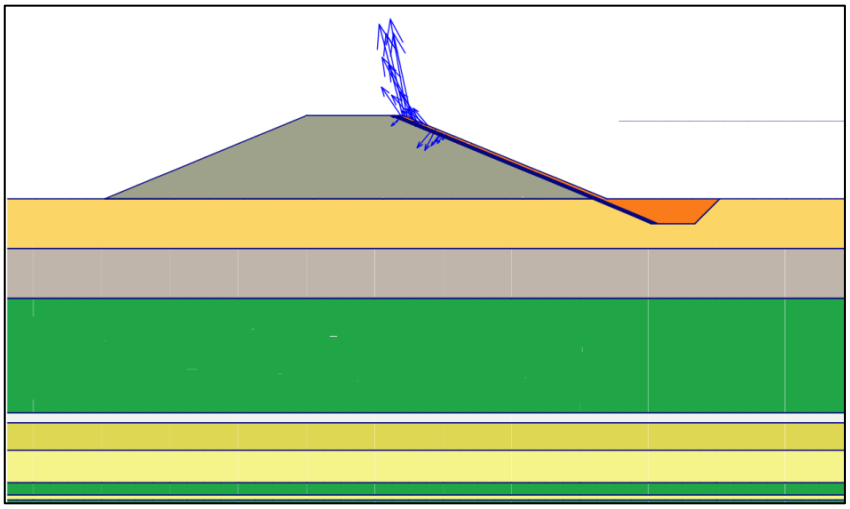

(b)

Figure B.66. Flow field at 2+005.66 km on left shore of Filyos River during h_{max}
a.) Shadings view b.) Arrows view

.**Analysis of sandy silt at under the levee;**

Figure B.67 shows that location of points near the ground surface for finding extreme velocity and Figure B.68 presents that results of flow velocity at K, L, M, N, O, P and Q.

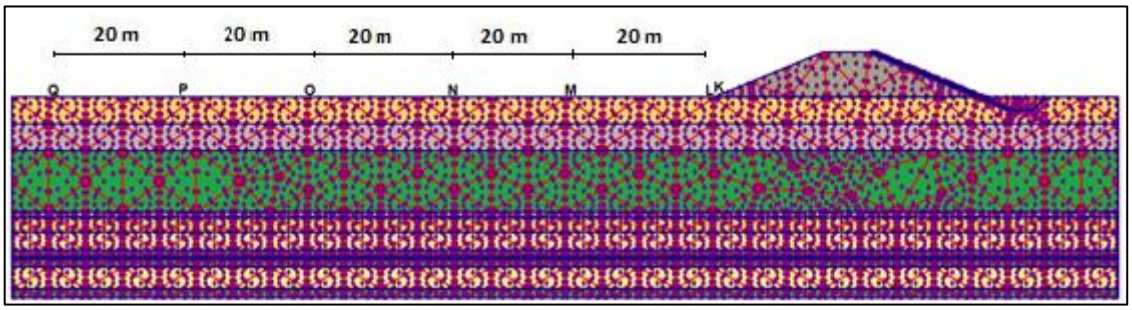

Fig. B.67.Location of points near the ground surface for finding extreme velocity

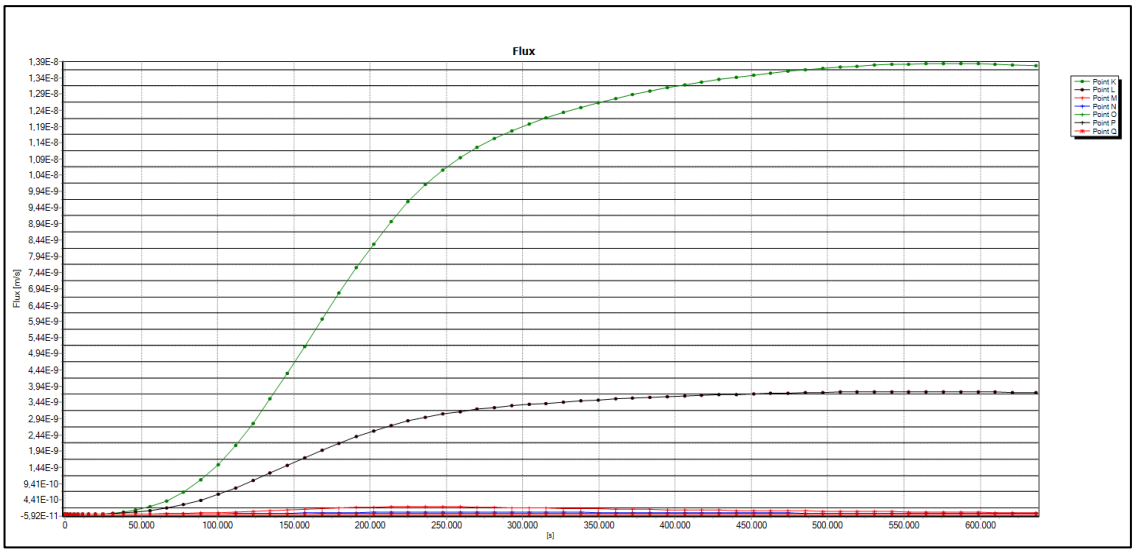

Figure B.68 Extreme velocity graph relation time Filyos Levee

Table B.34 shows that piping is not observed at any points due to $i_{exit} < i_c$. See equations B.23 and B.24 for calculated critical hydraulic gradients.

Table B.34 Piping Status

Symbol	Max Seepage Velocity (m/s)	Permeability (m/s) (k)	Exit Gradient (*i*)	Piping
K	1.4×10^{-8}	5×10^{-4}	0	**NaN**
L	3.65×10^{-9}	1×10^{-7}	0.04	**NaN**
M	6×10^{-11}	1×10^{-7}	0	**NaN**
N	6×10^{-11}	1×10^{-7}	0	**NaN**
O	6×10^{-11}	1×10^{-7}	0	**NaN**
P	6×10^{-11}	1×10^{-7}	0	**NaN**
Q	6×10^{-11}	1×10^{-7}	0	**NaN**

NaN:Not a Number

Table B.35 Sand Boil Status

Symbol	Max Seepage Velocity (m/s)	Permeability (m/s) (k)	Exit Gradient (*i*)	Sand Boil
L	3.65×10^{-9}	1×10^{-7}	0.04	**NaN**
M	6×10^{-11}	1×10^{-7}	0	**NaN**
N	6×10^{-11}	1×10^{-7}	0	**NaN**
O	6×10^{-11}	1×10^{-7}	0	**NaN**
P	6×10^{-11}	1×10^{-7}	0	**NaN**
Q	6×10^{-11}	1×10^{-7}	0	**NaN**

NaN:Not a Number

In order for the sand boiling to occur, the piping must take place. As can be seen in the Table B.35, it did not reach critical gradient for the formation of boiling. See equations B.23 and B.24 for calculated critical hydraulic gradients

- Heaving potential is not observed that levee has cover materials along river since the exit gradients approach zero.

B.5. Filyos Levee at 2+501.94 km on Left Shore of Filyos River

Location of Filyos levee at 2+501.94 km on left shore is seen Figure B.69 and the schematic representation of Filyos levee and soil profile is given in Figure B.70. Filyos levee includes gravelly sand soil type. There is a silty sand layer under the levee and this layer is 2.4 m thick.

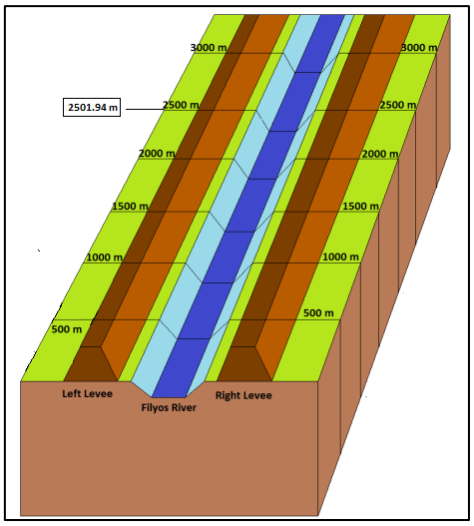

Figure B.69 Filyos Levee at 2+501.94 km on left shore of Filyos River

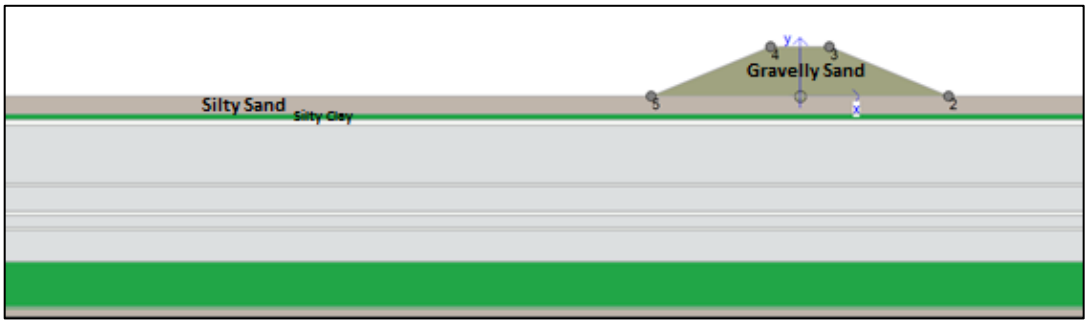

Figure B.70. Filyos Levee at 2+501.94 km on left shore of Filyos River

Figure B.71 shows that each soil layers have saturated unit weight under the levee for transient analysis and area of under the flow line is saturated during h_{max}.

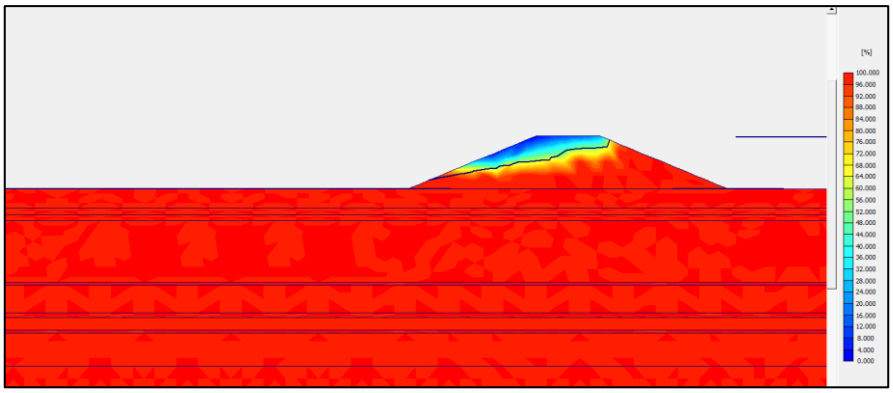

Figure B.71 Degree of Saturation of Filyos Levee at 2+501.94 km on left shore of Filyos River during h_{max}

It is seen that flow values are high at the red area in case h_{max} under the flow line according to Plaxflow2D (Figure B.72.a). There is a risk that is observed piping at these areas.

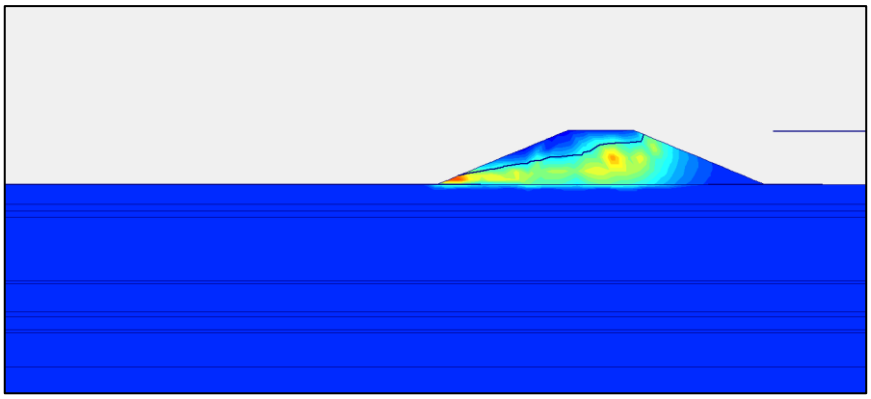

(a)

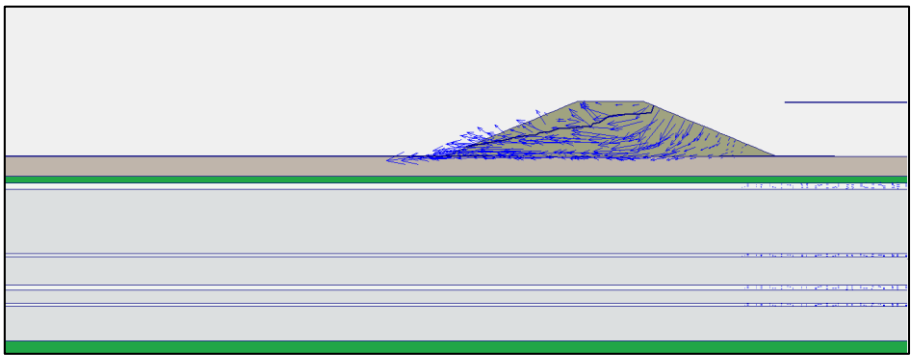

(b)

Figure B.72. Flow field at 2+501.94 km on left shore of Filyos River during h_{max} a.) Shadings view b.) Arrows view

Figure B.72. (b) is other notation that is vector stage in case h_{max}. That is called arrows in Plaxflow2D literature. If the vectors values are higher than others, there will be observing piping formations.

Analysis of silty sand at under the levee;

Figure B.73 shows that location of points near the ground surface for finding extreme velocity and Figure B.74 presents that results of flow velocity at K, L, M, N, O, P, Q and R.

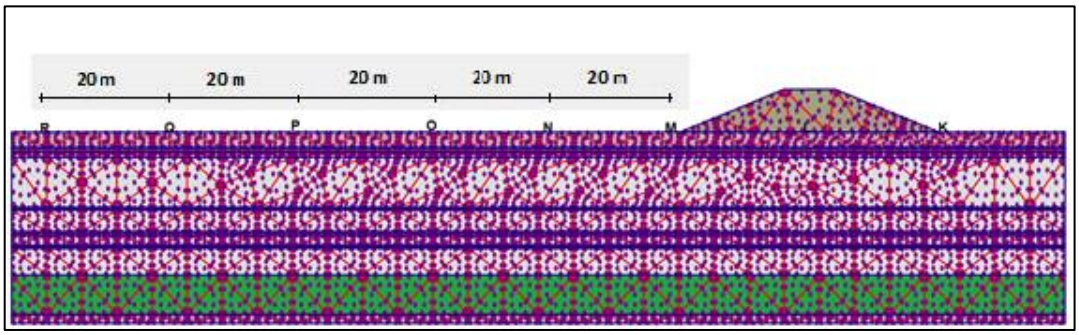

Figure B.73 Location of points near the ground surface for finding extreme velocity

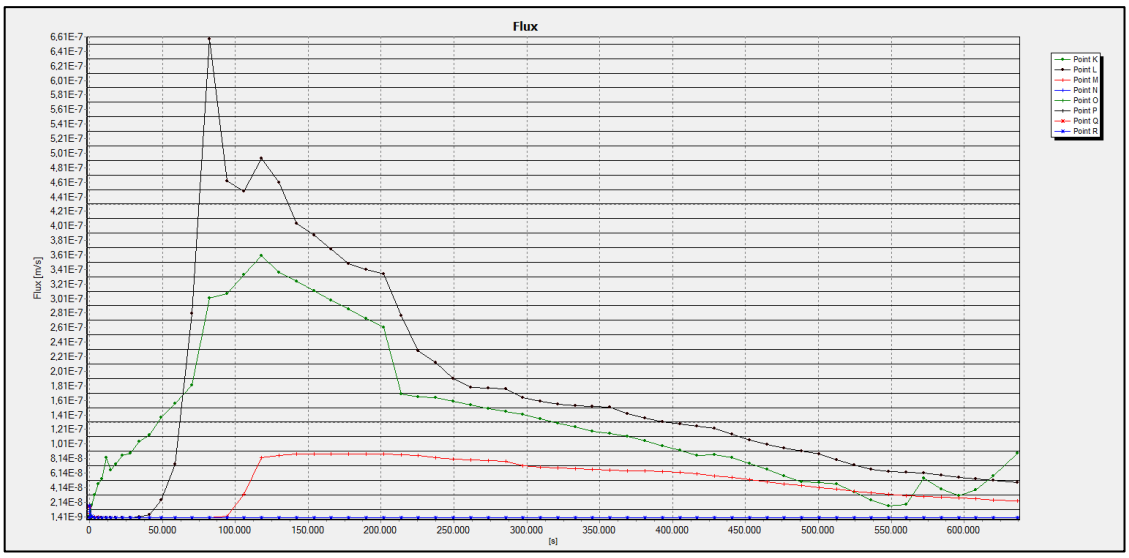

Figure B.74 Extreme velocity graph relation time to seepage velocity

According to Figure B.74, max values of flow are K=3.6x10^{-7} m/s at time=34.7 hours; L=6.6x10^{-7} m/s at time=25 hours; M=9x10^{-8} m/s at time=50 hours; N, O, P, Q, R= 1.4x10^{-9} m/s at time=50 hours.

Piping formations are simply compate as;

$$v = k.i\,; \tag{B.29}$$

$$i_c = \frac{G_s - 1}{1+e} = \frac{2.69-1}{1+0.43} = 1.2; \tag{B.30}$$

Where;

v = flow velocity (m/sec)

k = permeabilty (m/sec)

i = hydraulic gradient

i_c = critical hydraulic gradient

G_s = specific gravity; 2.69 for silty sand

e = void ratio; 0.43 for silty sand

Table B.35 shows that piping is not observed at any points due to $i_{exit} < i_c$.

Table B.35 Piping Status

Symbol	Max Seepage Velocity (m/s)	Permeability (m/s) (k)	Exit Gradient (*i*)	Piping
K	3.6×10^{-7}	1×10^{-6}	0.36	**NaN**
L	6.6×10^{-7}	1×10^{-6}	0.66	**NaN**
M	9×10^{-8}	1×10^{-6}	0.09	**NaN**
N	1.4×10^{-9}	1×10^{-6}	0	**NaN**
O	1.4×10^{-9}	1×10^{-6}	0	**NaN**
P	1.4×10^{-9}	1×10^{-6}	0	**NaN**
Q	1.4×10^{-9}	1×10^{-6}	0	**NaN**
R	1.4×10^{-9}	1×10^{-6}	0	**NaN**

NaN:Not a Number

In order for the sand boiling to occur, the piping must take place. As can be seen in the Table B.36, it did not reach critical slope for the formation of boiling.

Table B.36 Sand Boil Status

Symbol	Max Seepage Velocity (m/s)	Permeability (m/s) (k)	Exit Gradient (*i*)	Sand Boil
M	9×10^{-8}	1×10^{-6}	0.09	**NaN**
N	1.4×10^{-9}	1×10^{-6}	0	**NaN**
O	1.4×10^{-9}	1×10^{-6}	0	**NaN**
P	1.4×10^{-9}	1×10^{-6}	0	**NaN**
Q	1.4×10^{-9}	1×10^{-6}	0	**NaN**
R	1.4×10^{-9}	1×10^{-6}	0	**NaN**

NaN:Not a Number

The analysis above the levee for gravelly sand soil type;

Piping can only observe K, L and M point because these points only are under the phreatic line. K, L, M etc. points on the ground surface or levee are different from other analyses.

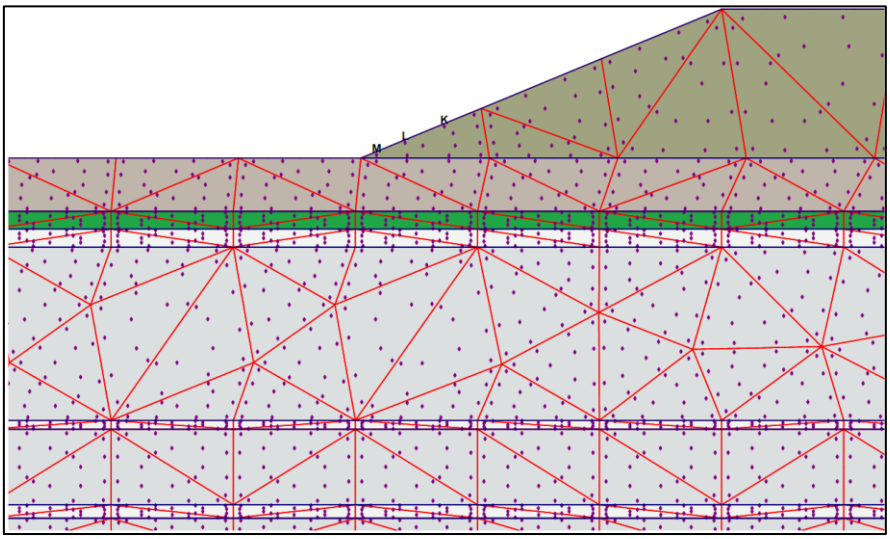

Figure B.75. Location of points above the levee for finding extreme velocity

Extreme velocities of K, L and M point are Figure B.76 and piping formations are investigated for these points.

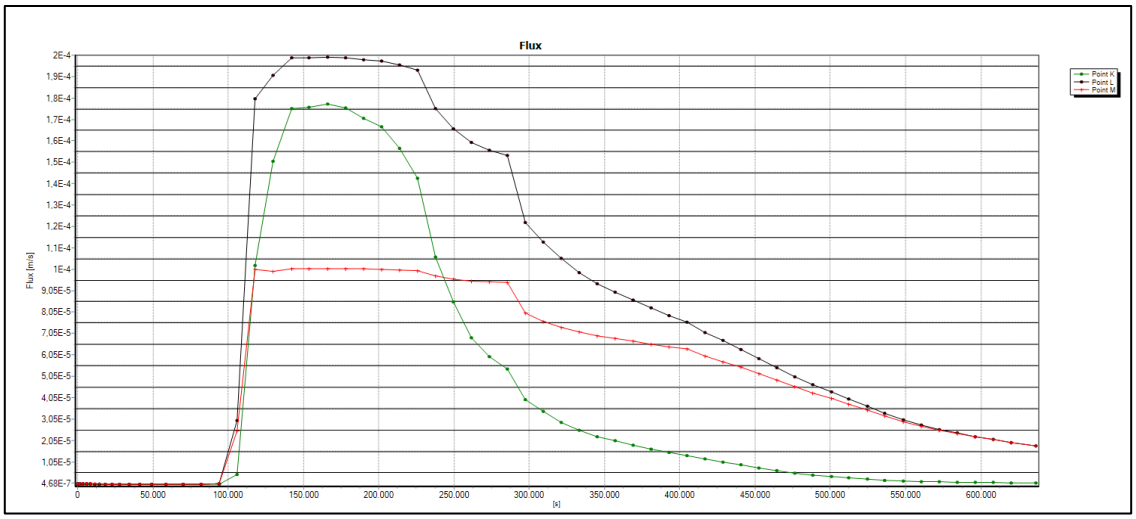

Figure B.76 Extreme velocity graph relation time above the levee

According to Fig. 7.8, max values of flow are K=1.8x10^{-4}m/s at time=38.8 hours; L=2.1x10^{-4}m/s at time=38.8 hours; M=1 x 10^{-4}m/s at time=38.8 hours.

Piping formations are simply compate as;

$$v = k.i\,; \tag{B.31}$$

$$i_c = \frac{G_s - 1}{1 + e} = \frac{2.66 - 1}{1 + 0.62} = 1.02\,; \tag{B.32}$$

Where;

v = flow velocity (m/sec)

k = permeabilty (m/sec)

i = hydraulic gradient

i_c = critical hydraulic gradient

G_s = specific gravity; 2.66 for gravelly sand

e = void ratio; 0.62 for gravelly sand

Table B.37 shows that piping is not observed at any points due to $i_{exit} < i_c$.

Table B.37 Piping Status

Symbol	Max Seepage Velocity (m/s)	Permeability (m/s) (k)	Exit Gradient (*i*)	Piping
K	1.8×10^{-4}	5×10^{-4}	0.36	**NaN**
L	2.1×10^{-4}	5×10^{-4}	0.42	**NaN**
M	1×10^{-4}	5×10^{-4}	0.20	**NaN**

NaN:Not a Number

The factor of safety against heave analysis for top layer;

Equation B.33 and B.34 are used to determine the factor of safety against heave analysis for top layer. Heaving potential are only observed ground surface hence a point are investigated at 1 m below the top layer like Figure B.77.

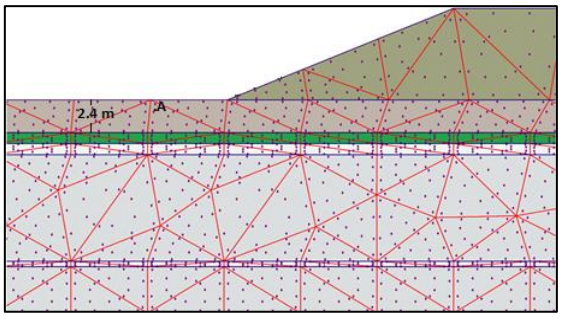

Figure B.77 Analysis against to heave at A point 1 m below the top layer

$$F_{heave} = \frac{H.\gamma_{sat}}{h_m.\gamma_w} > 3.0 \quad \text{(B.33)}$$

$$i_{\max} = \frac{h_m}{H} \quad \text{(B.34)}$$

Where;

H = thickness of overlying top layer(m)

γ_{sat} = saturated unit weight of overlying top layer(kN/m^2)

h_m = average hydraulic head at the point(m)

γ_w = water unit wight(kN/m^2)

$i_{\max}$ = maximum exit gradient

$$0.1 = \frac{h_m}{1} \Rightarrow h_m = 0.1 \;;\; F_{heave} = \frac{1x21.4}{0.1x10} = 21.4 > 3.0$$

It is not observed heave due to the fact that F_{heave} is higher than 3.0 .

B.5.1. Filyos Levee at 2+501.94 km on Left Shore of Filyos River according to Current Situation(Upstream face is covered)

The schematic representation of Filyos Levee and soil profile is given in Figure B.78. Filyos levee includes gravelly sand soil type and cover materials against piping and sand boil formations. The cover materials are riprap which is andesite, uniform sand filter layer and geocomposite layer. There is a silty sand layer under the levee and this layer is 2.4 m thick.

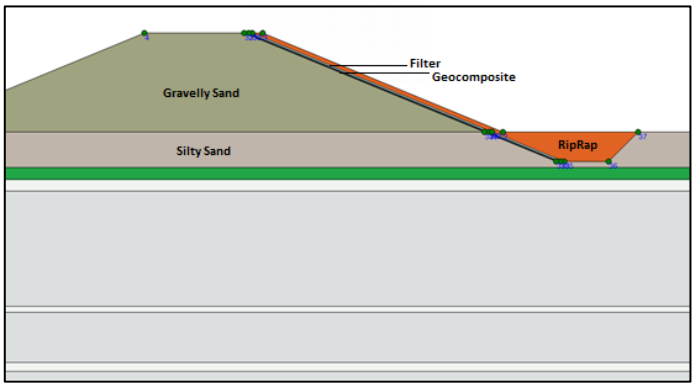

Figure B.78 Filyos Levee with cover materials at 2+501.94 km on left shore of Filyos River

Filyos levee has covered along rising water level. The covered members are filter, riprap and geocomposite materials. Table B.38 shows properties of covered materials and levee.

Table B.38 Soil Properties of levee members

	Soil Type / Material	**Permeability(k) (m/sec)**	**Specific Gravity (G_s)**	**Void Ratio (e)**	**Thickness (m)**
Filter	Uniform Sand	$1x10^{-3}$	2.67	0.70	0.25
Riprap	Andesite Rock	0.645	2.65	0.34	0.70
Geocomposite Material	Geotextile and Geomembrane	$1x10^{-13}$	-	0.02	0.30

Figure B.79 shows that each soil layers have saturated unit weight under the levee with cover materials for transient analysis and area of under the flow line is saturated during h_{max}. Saturation rates of red areas are high and saturation rates of other areas are almost zero without riprap, filter, and areas under levee.

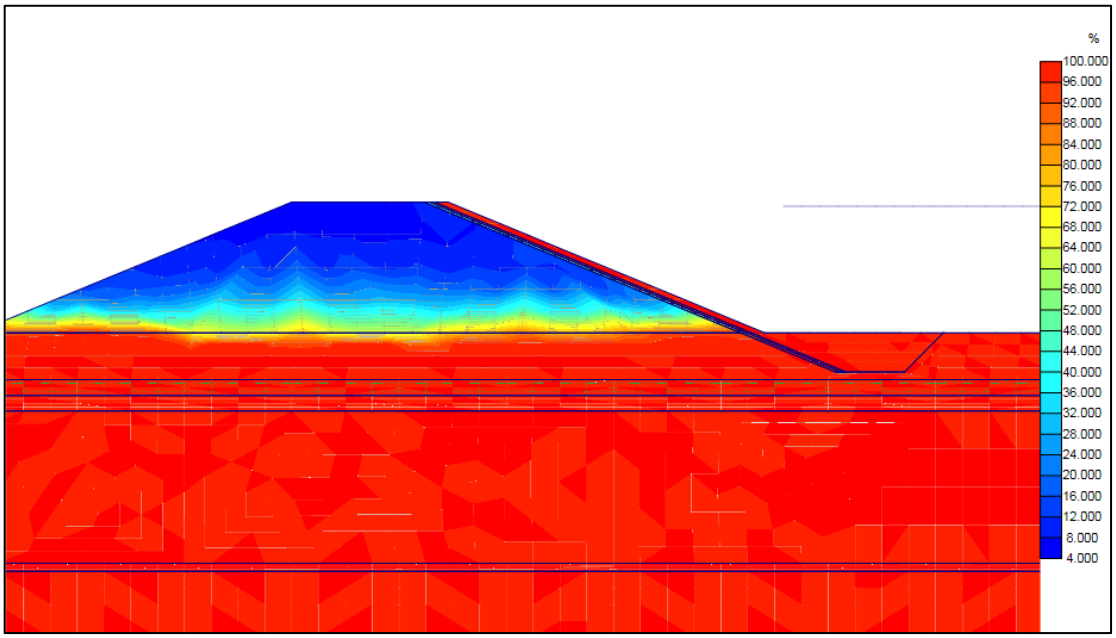

Figure B.79 Degree of Saturation of Filyos Levee with cover materials at 2+501.94 km on left shore of Filyos River during h_{max}

It is seen that flow values are high at the red area in case h_{max} under the flow line according to Plaxflow2D (Figure B.80.a). There is not a risk that is observed piping into through levee.

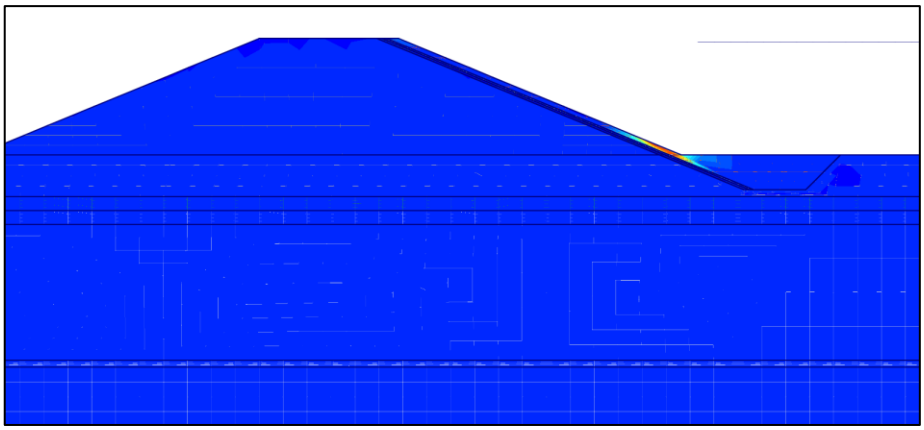

(a)

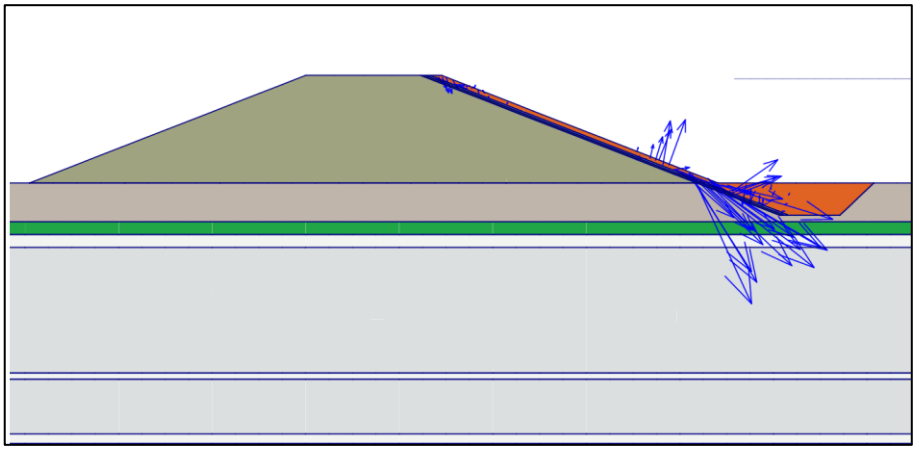

(b)

Figure B.80. Flow field at 2+501.94 km on left shore of Filyos River during h_{max}
a.) Shadings view b.) Arrows view

Figure B.80. (b) is other notation that is vector stage in case h_{max}. That is called arrows in Plaxflow2D literature and there is not risk into through levee.

Analysis of silty sand at under the levee;

Figure B.81 shows that location of points near the ground surface for finding extreme velocity and Figure B.82 presents that results of flow velocity at K, L, M, N, O, P and Q .

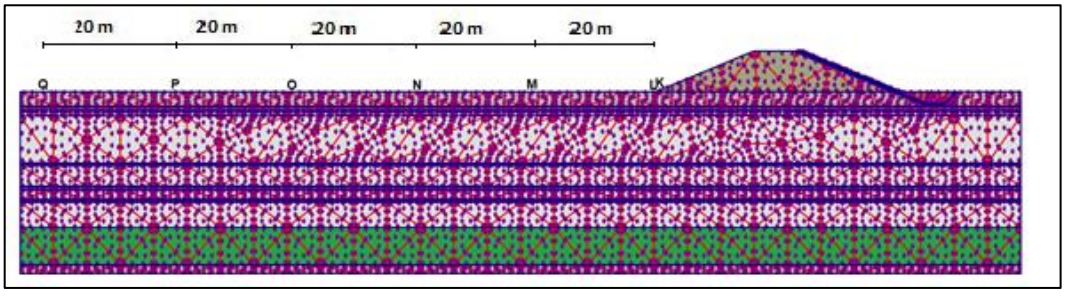

Figure B.81 Location of points near the ground surface for finding extreme velocity

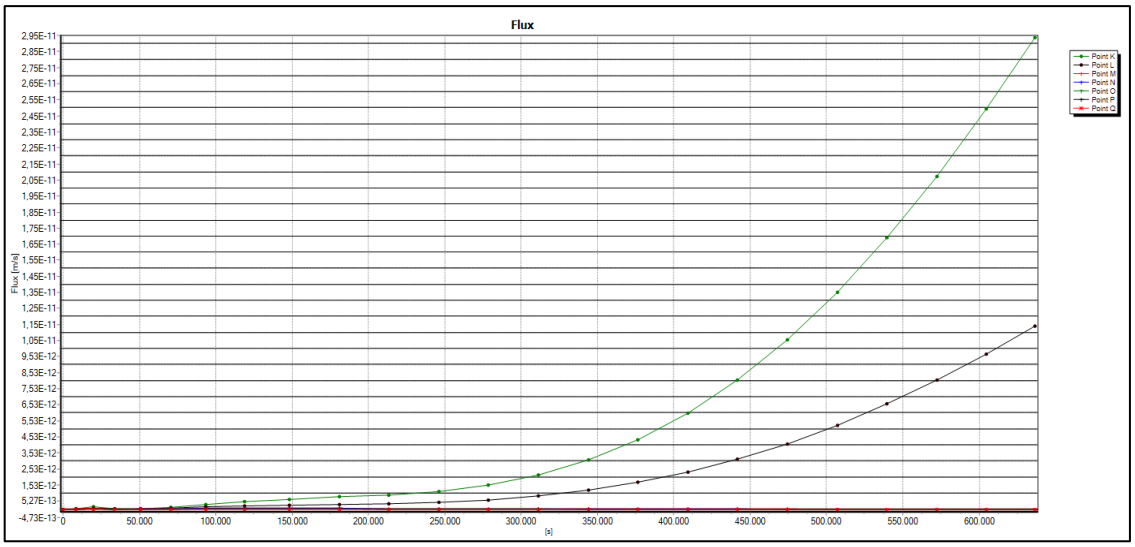

Figure B.82 Extreme velocity graph relation time Filyos Levee

Critical hydraulic gradient is 1.2 for silty sand. Table B.39 shows that piping is not observed at any points due the fact that to exit gradient is zero. See equations B.30, B.32 for calculated critical hydraulic gradients.

Table B.39 Piping Status

Symbol	Max Seepage Velocity (m/s)	Permeability (m/s) (k)	Exit Gradient (*i*)	Piping
K	3×10^{-11}	5×10^{-4}	0	**NaN**
L	1.2×10^{-11}	1×10^{-6}	0	**NaN**
M	5×10^{-13}	1×10^{-6}	0	**NaN**
N	5×10^{-13}	1×10^{-6}	0	**NaN**
O	5×10^{-13}	1×10^{-6}	0	**NaN**
P	5×10^{-13}	1×10^{-6}	0	**NaN**
Q	5×10^{-13}	1×10^{-6}	0	**NaN**

NaN:Not a Number

In order for the sand boiling to occur, the piping must take place. As can be seen in the Table B.40. Critical hydraulic gradient is 1.2 for silty sand so, it did not reach critical gradient for the formation of boiling. See equations B.30, B.32 for calculated critical hydraulic gradients.

- Heaving potential is not observed that levee has cover materials along river since the exit gradients approach zero.

Table B.40 Sand Boil Status

Symbol	Max Seepage Velocity (m/s)	Permeability (m/s) (k)	Exit Gradient (*i*)	Sand Boil
L	1.2×10^{-11}	1×10^{-6}	0	**NaN**
M	5×10^{-13}	1×10^{-6}	0	**NaN**
N	5×10^{-13}	1×10^{-6}	0	**NaN**
O	5×10^{-13}	1×10^{-6}	0	**NaN**
P	5×10^{-13}	1×10^{-6}	0	**NaN**
Q	5×10^{-13}	1×10^{-6}	0	**NaN**

NaN:Not a Number

B.6. Filyos Levee at 758.18 m on Right Shore of Filyos River

Location of Filyos levee at 758.18 m on right shore is seen Figure B.83 the schematic representation of Filyos Levee and soil profile is given in Figure B.84. Filyos levee includes gravelly sand soil type. There is a clayey silt layer under the levee and this layer is 2 m thick.

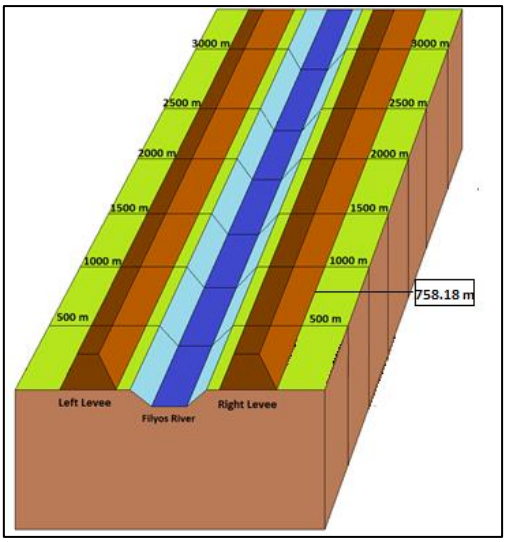

Figure B.83 Filyos Levee at 758.18 m on right shore of Filyos River

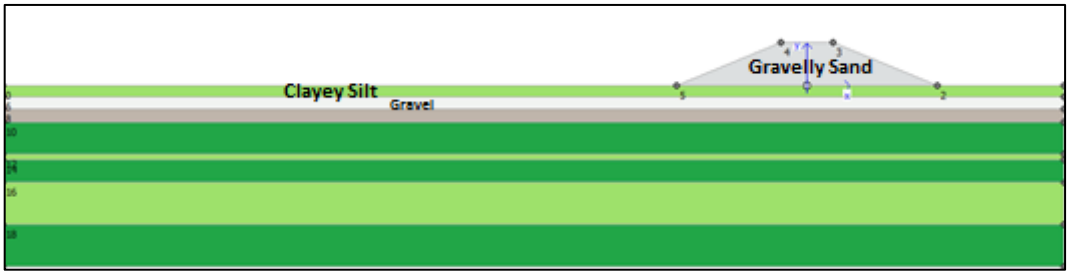

Figure B.84 Filyos Levee at 758.18 m on right shore of Filyos River

Figure B.85 shows that each soil layers have saturated unit weight under the levee for transient analysis and area of under the flow line is saturated during h_{max}.

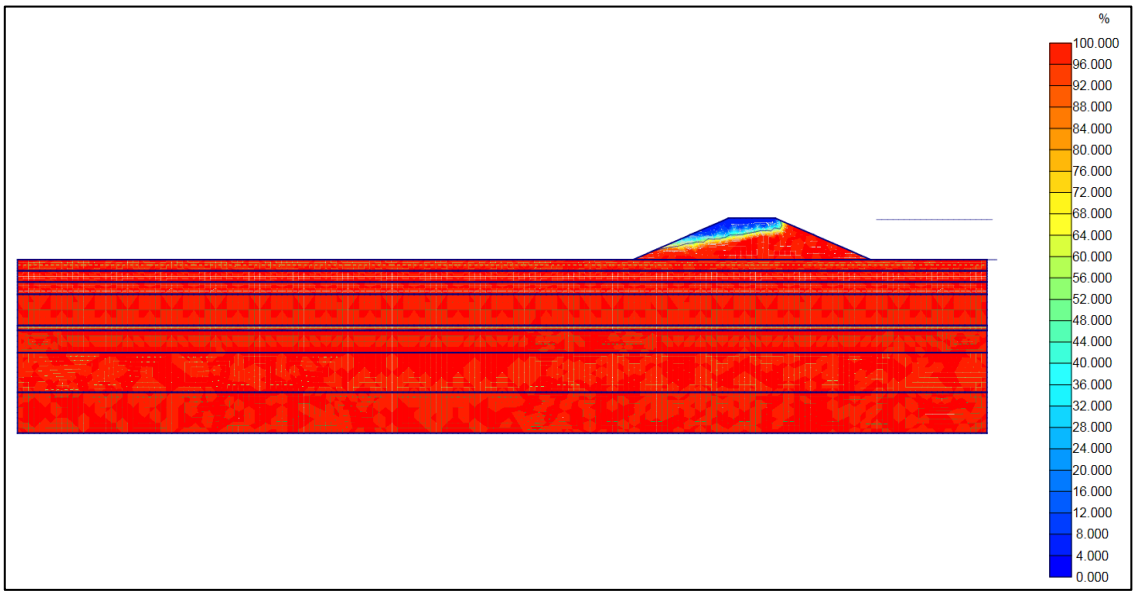

Figure B.85 Degree of Saturation of Filyos Levee at 758.18 m on right shore of Filyos River during h_{max}

It is seen that flow values are high at the red area in case h_{max} under the flow line according to Plaxflow2D (Figure B.86.a). There is a risk that is observed piping at these areas.

Figure B.86. (b) is other notation that is vector stage in case h_{max}. That is called arrows in Plaxflow2D literature. If the vectors values are higher than others, there will be observing piping formations

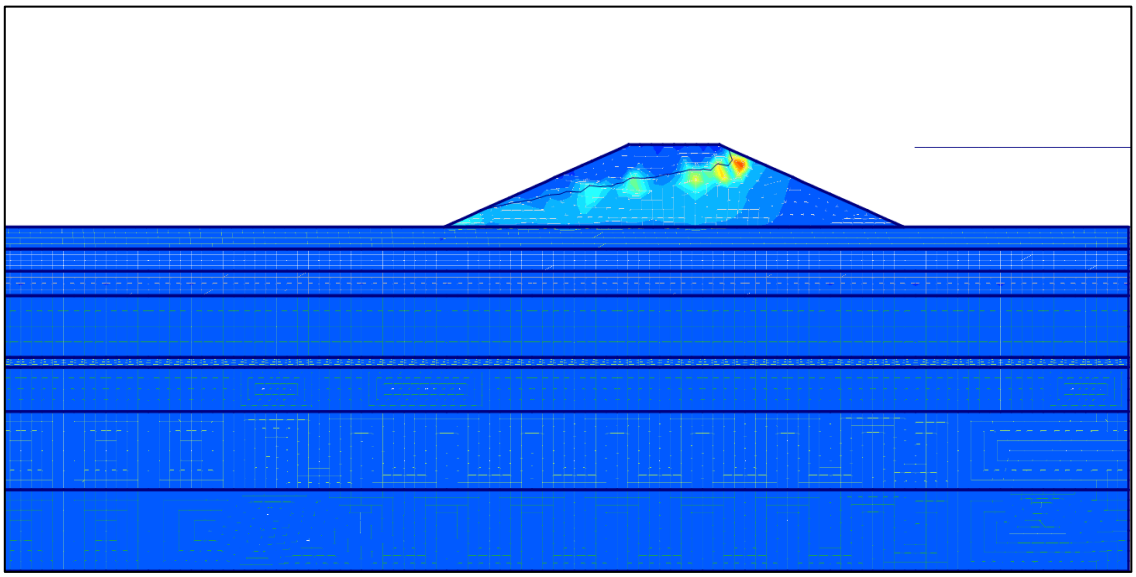

(a)

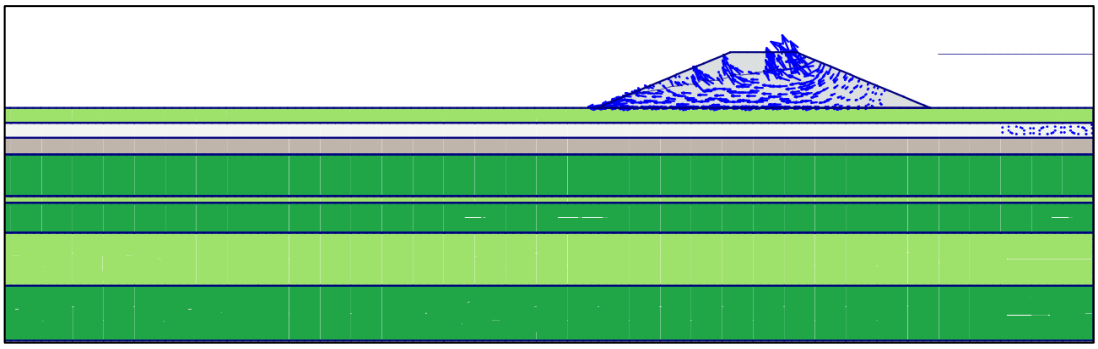

(b)

Figure B.86. Flow field at 758.18 m on right shore of Filyos River during h_{max}
a.) Shadings view b.) Arrows view

Analysis of clayey silt at under the levee;

Figure B.87 shows that location of points near the ground surface for finding extreme velocity and Fig. B.88 presents that results of flow velocity at K, L, M, N, O, P, Q and R. K, L, M etc. points on the ground surface or levee are different from other analyses.

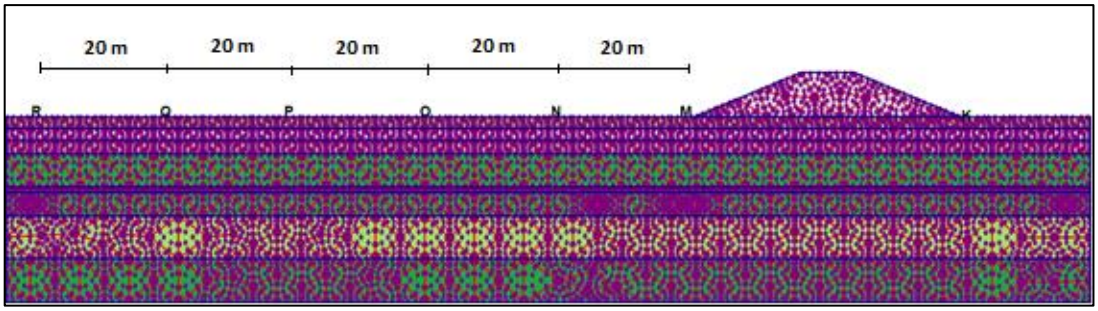

Figure B.87 Location of points near the ground surface for finding extreme velocity

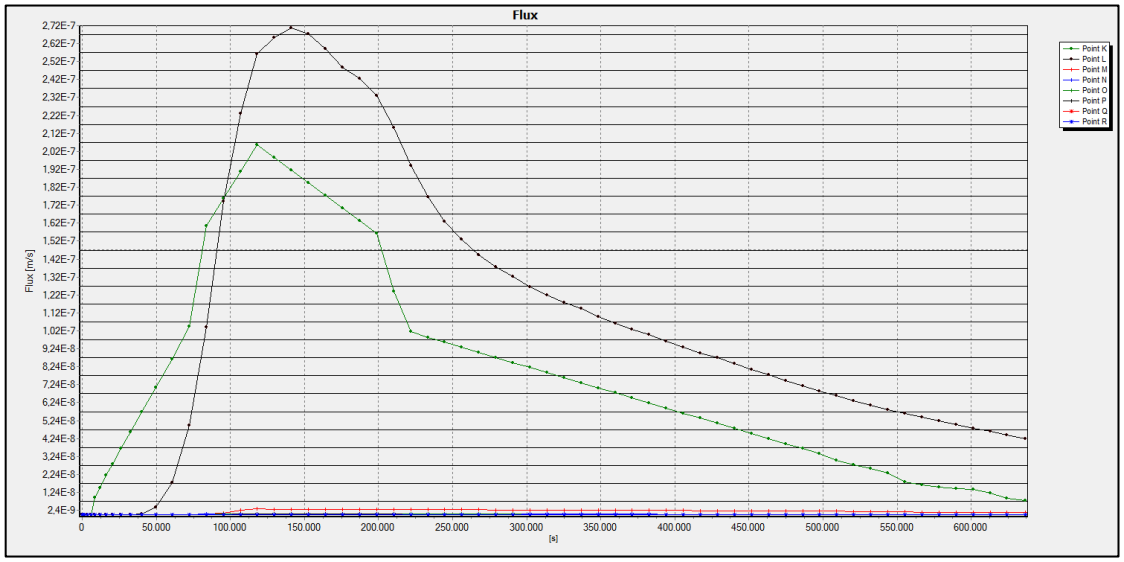

Figure B.88 Extreme velocity graph relation time to seepage velocity

According to Figure B.88, max values of flow are K=2.1x10^{-7}m/s at time=34.7 hours; L=2.7x10^{-7}m/s at time=36 hours; M=2.4 x 10^{-9}m/s at time=62.5 hours; N=2.1x10^{-9}m/s at time=62.5 hours; O=2.0x10^{-9}m/s at time=62.5 hours; P=1.5 x 10^{-9}m/s at time=62.5 hours; Q and R=1.0x 10^{-9}m/s at time=62.5 hours.

Piping formations are simply compate as;

$$v = k.i\,; \tag{B.35}$$

$$i_c = \frac{G_s - 1}{1 + e} = \frac{2.70 - 1}{1 + 0.9} = 0.89 \tag{B.36}$$

Where;

v = flow velocity (m/sec)

k = permeabilty (m/sec)

i = hydraulic gradient

i_c = critical hydraulic gradient

G_s = specific gravity; 2.70 for clayey silt

e = void ratio; 0.9 for clayey silt

Table B.41 shows that piping is observed at some points due to $i_{exit} > i_c$ but it is not insufficient piping formation bucause it does not occur piping at levee toe (Point M).

Table B.41 Piping Status

Symbol	Max Seepage Velocity (m/s)	Permeability (m/s) (k)	Exit Gradient (i)	Piping
K	2.1 x 10^{-7}	1 x 10^{-7}	2.10	$i_{exit} > i_c$
L	2.7 x 10^{-7}	1 x 10^{-7}	2.70	$i_{exit} > i_c$
M	2.4 x 10^{-9}	1 x 10^{-7}	0.02	**NaN**
N	2.1 x 10^{-9}	1 x 10^{-7}	0.02	**NaN**
O	2.0 x 10^{-9}	1 x 10^{-7}	0.02	**NaN**
P	1.5 x 10^{-9}	1 x 10^{-7}	0.02	**NaN**
Q	1.0 x 10^{-9}	1 x 10^{-7}	0.01	**NaN**
R	1.0 x 10^{-9}	1 x 10^{-7}	0.01	**NaN**

NaN:Not a Number

In order for the sand boiling to occur, the piping must take place. As can be seen in the Table B.42. Critical hydraulic gradient is 0.89 for clayey silt so, it did not reach critical slope for the formation of boiling.

Table B.42 Sand Boil Status

Symbol	Max Seepage Velocity (m/s)	Permeability (m/s) (k)	Exit Gradient (*i*)	Sand Boil
M	2.4×10^{-9}	1×10^{-7}	0.02	**NaN**
N	2.1×10^{-9}	1×10^{-7}	0.02	**NaN**
O	2.0×10^{-9}	1×10^{-7}	0.02	**NaN**
P	1.5×10^{-9}	1×10^{-7}	0.02	**NaN**
Q	1.0×10^{-9}	1×10^{-7}	0.01	**NaN**
R	1.0×10^{-9}	1×10^{-7}	0.01	**NaN**

NaN:Not a Number

The analysis above the levee for gravelly sand soil type;

Piping can only observe K, L and M point because these points only are under the phreatic line. K, L, M etc. points on the ground surface or levee are different from other analyses.

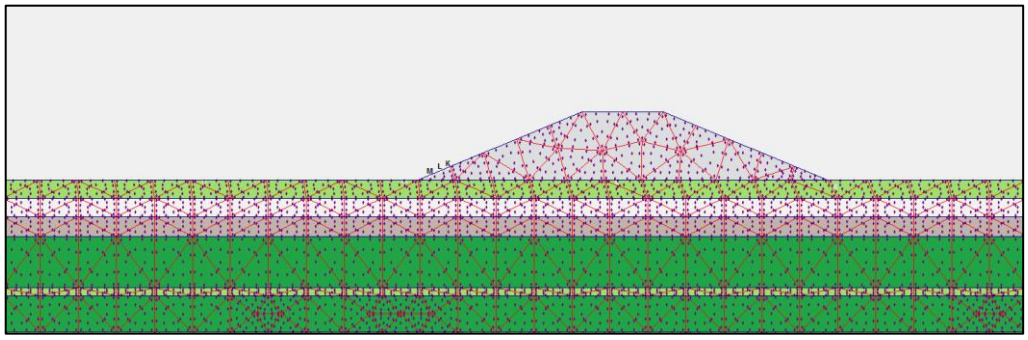

Figure B.89. Location of points above the levee for finding extreme velocity

Extreme velocities of K, L and M point are below and piping formations are investigated for these points.

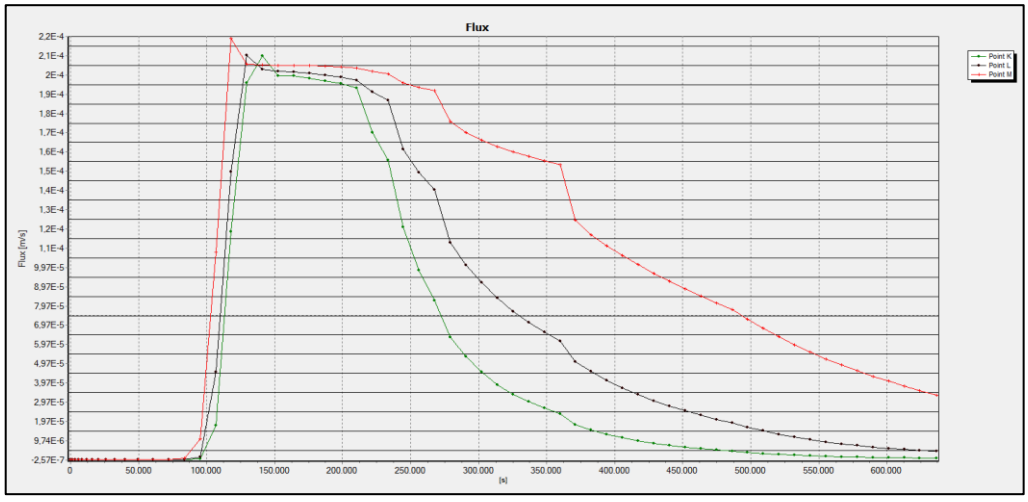

Figure B.89 Extreme velocity graph relation time above the levee

According to Figure B.89, max values of flow are K=2.1x10^{-4}m/s at time=38.9 hours; L=2.1x10^{-4}m/s at time=34.7 hours; M=2.2 x 10^{-4} m/s at time=32 hours.

Piping formations are simply compate as;

$$v = k.i\,; \tag{B.37}$$

$$i_c = \frac{G_s - 1}{1+e} = \frac{2.66-1}{1+0.62} = 1.02\,; \tag{B.38}$$

Where;

v = flow velocity (m/sec)

k = permeabilty (m/sec)

i = hydraulic gradient

i_c = critical hydraulic gradient

G_s = specific gravity; 2.66 for gravelly sand

e = void ratio; 0.62 for gravelly sand

Table 7.9. shows that piping is not observed at any points due to $i_{exit} < i_c$.

Table B.43 Piping Status

Symbol	Max Seepage Velocity (m/s)	Permeability (m/s) (k)	Exit Gradient (*i*)	Piping
K	2.1 x 10^{-4}	5 x 10^{-4}	0.42	**NaN**
L	2.1 x 10^{-4}	5 x 10^{-4}	0.42	**NaN**
M	2.2 x 10^{-4}	5 x 10^{-4}	0.44	**NaN**

NaN:Not a Number

The factor of safety against heave analysis for top layer;

Equation B.39 and B.40 are used to determine the factor of safety against heave analysis for top layer. Heaving potential are only observed ground surface hence a point are investigated at 1 m below the top layer like Figure B.90.

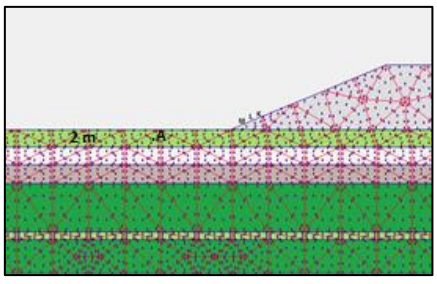

Figure B.90 Analysis against to heave at A point 1 m below the top layer

$$F_{heave} = \frac{H.\gamma_{sat}}{h_m.\gamma_w} > 3.0 \quad \text{(B.39)}$$

$$i_{\max} = \frac{h_m}{H} \quad \text{(B.40)}$$

Where;

H = thickness of overlying top layer(m)

γ_{sat} = saturated unit weight of overlying top layer(kN/m^2)

h_m = average hydraulic head at the point(m)

γ_w = water unit wight(kN/m^2)

$i_{\max}$ = maximum exit gradient

$$0.02 = \frac{h_m}{1.0} \Rightarrow h_m = 0.02 \;;\; F_{heave} = \frac{1.0x18.6}{0.02x10} > 3.0$$

It is not observed heave due to the fact that F_{heave} is higher than 3.0 .

B.6.1. Filyos Levee at 758.18 m on Right Shore of Filyos River according to Current Situation(Upstream face is covered)

The schematic representation of Filyos Levee and soil profile is given in Figure B.91. Filyos levee includes gravelly sand soil type and cover materials against piping and sand boil formations. The cover materials are riprap which is andesite, uniform sand filter layer and geocomposite layer. There is a clayey silt layer under the levee and this layer is 2 m thick.

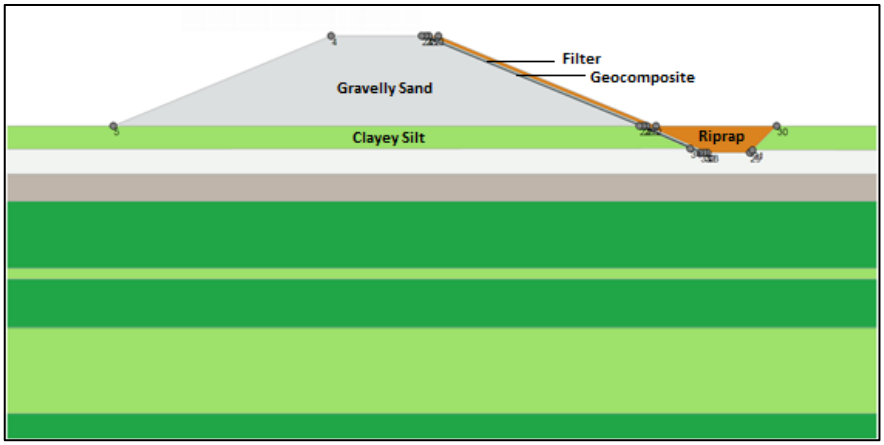

Figure B.91 Filyos Levee with cover materials at 758.18 m on right shore of Filyos River

Filyos levee has covered along rising water level. Table B.44 shows properties of covered materials and levee.

Table B.44 Soil Properties of levee members

	Soil Type / Material	Permeability(k) (m/sec)	Specific Gravity (G_s)	Void Ratio (e)
Levee	Gravelly Sand	$5x10^{-4}$	2.66	0.62
Filter	Uniform Sand	$1x10^{-3}$	2.67	0.70
Riprap	Andesite Rock	0.645	2.65	0.34
Geocomposite Material	Geotextile and Geomembrane	$1x10^{-13}$	-	0.02

Figure B.92 shows that each soil layers have saturated unit weight under the levee with cover materials for transient analysis and area of under the flow line is saturated during h_{max}. Saturation rates of red areas are high and saturation rates of other areas are almost zero without riprap, filter, and areas under levee.

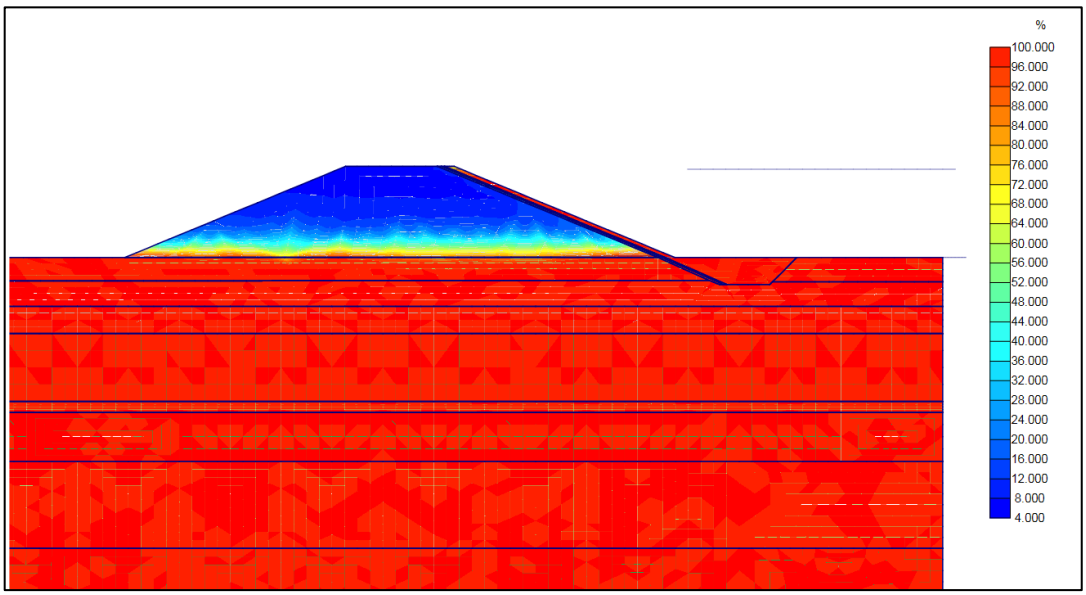

Figure B.92 Degree of Saturation of Filyos Levee with cover materials at 758.18 m on right shore of Filyos River during h_{max}

It is seen that flow values are high at the red area in case h_{max} under the flow line according to Plaxflow2D (Figure B.93.a). There is not a risk that is observed piping into through levee. Figure B.93. (b) is other notation that is vector stage in case h_{max}. That is called arrows in Plaxflow2D literature and there is not risk into through levee.

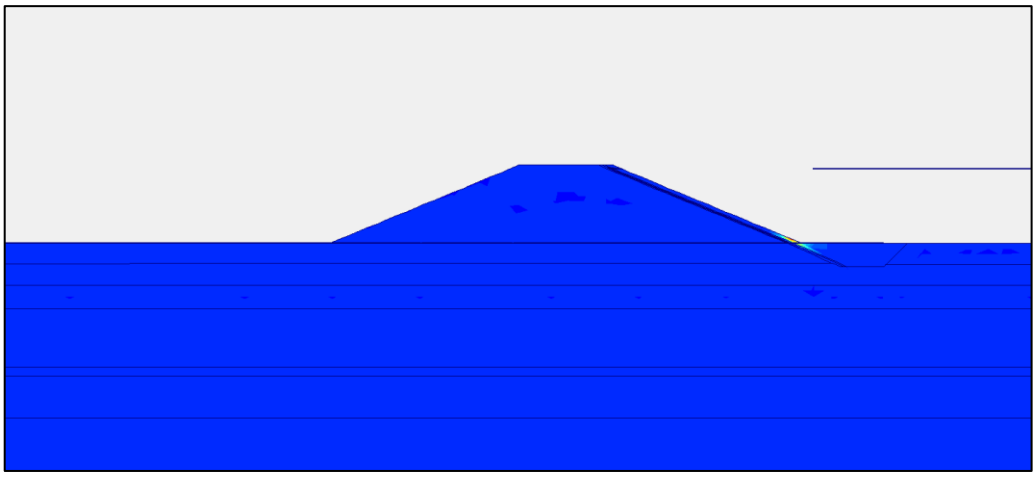

(a)

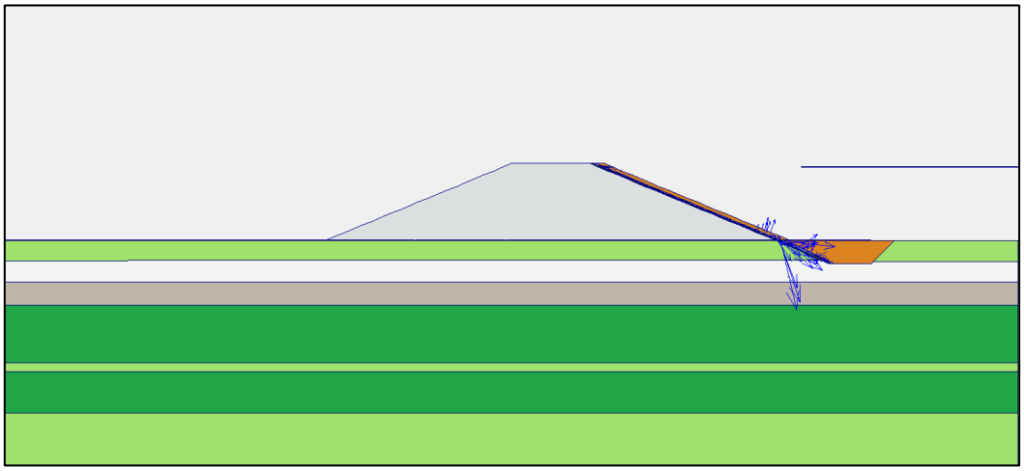

(b)

Figure B.93. Flow field at 758.18 m on right shore of Filyos River during h_{max}
a.) Shadings view b.) Arrows view

Analysis of clayey silt at under the levee;

Figure B.94 shows that location of points near the ground surface for finding extreme velocity and Figure B.95 presents that results of flow velocity at K, L, M, N, O, P and Q . Table B.45 and Table B.46 present that results probility of observing piping and sand boil according to Figure B.95.

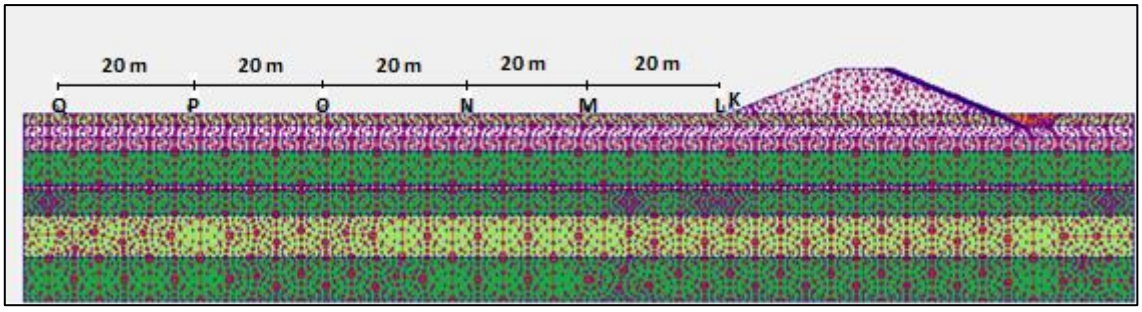

Figure B.94 Location of points near the ground surface for finding extreme velocity

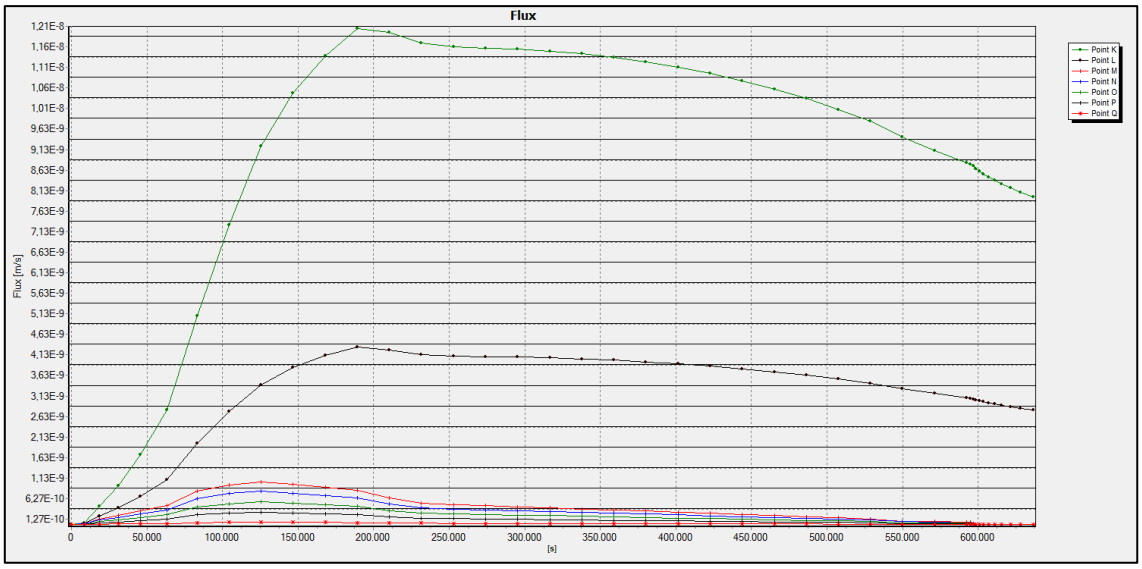

Figure B.95 Extreme velocity graph relation time Filyos Levee

Table B.45 shows that piping is not observed at any points due to $i_{exit} < i_c$. See equations B.36, B.38 for calculated critical hydraulic gradients.

Table B.45 Piping Status

Symbol	Max Seepage Velocity (m/s)	Permeability (m/s) (k)	Exit Gradient (*i*)	Piping
K	1.2×10^{-8}	1×10^{-7}	0.12	**NaN**
L	4.4×10^{-9}	1×10^{-7}	0.04	**NaN**
M	1.1×10^{-9}	1×10^{-7}	0.01	**NaN**
N	6.3×10^{-10}	1×10^{-7}	0	**NaN**
O	4.0×10^{-10}	1×10^{-7}	0	**NaN**
P	2.0×10^{-10}	1×10^{-7}	0	**NaN**
R	1.3×10^{-10}	1×10^{-7}	0	**NaN**

NaN:Not a Number

In order for the sand boiling to occur, the piping must take place. As can be seen in the Table B.46, it did not reach critical gradient for the formation of boiling.

Table B.46 Sand Boil Status

Symbol	Max Seepage Velocity (m/s)	Permeability (m/s) (k)	Exit Gradient (*i*)	Sand Boil
L	4.4×10^{-9}	1×10^{-7}	0.04	**NaN**
M	1.1×10^{-9}	1×10^{-7}	0.01	**NaN**
N	6.3×10^{-10}	1×10^{-7}	0	**NaN**
O	4.0×10^{-10}	1×10^{-7}	0	**NaN**
P	2.0×10^{-10}	1×10^{-7}	0	**NaN**
R	1.3×10^{-10}	1×10^{-7}	0	**NaN**

NaN:Not a Number

- Heaving potential is not observed that levee has cover materials along river since the exit gradients approach zero.

B.7. Filyos Levee at 1+256.4 km on Right Shore of Filyos River

Location of Filyos levee at 1256.4 m on right shore is seen Figure B.96 and the schematic representation of Filyos levee and soil profile is given in Figure B.97. There is a clayey silt layer under the levee and this layer is 4 m thick. Also, silty sand material is used for this layer to need filling under the levee.

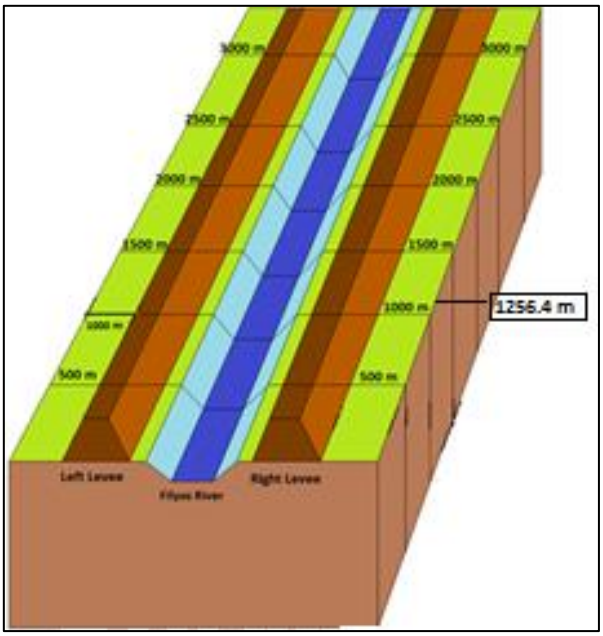

Figure B.96 Filyos Levee at 1256.4 m on right shore of Filyos River

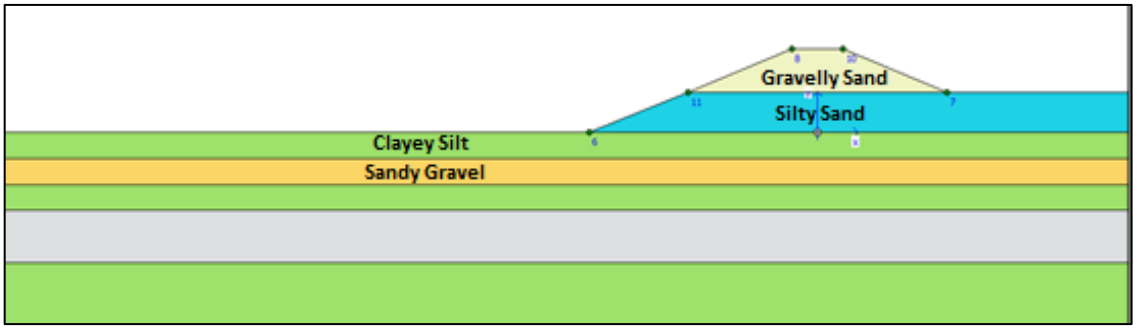

Figure B.97 Filyos Levee at 1+256.4 km on right shore of Filyos River

Figure B.98 shows that each soil layers have saturated unit weight under the levee for transient analysis and area of under the flow line is saturated during h_{max}.

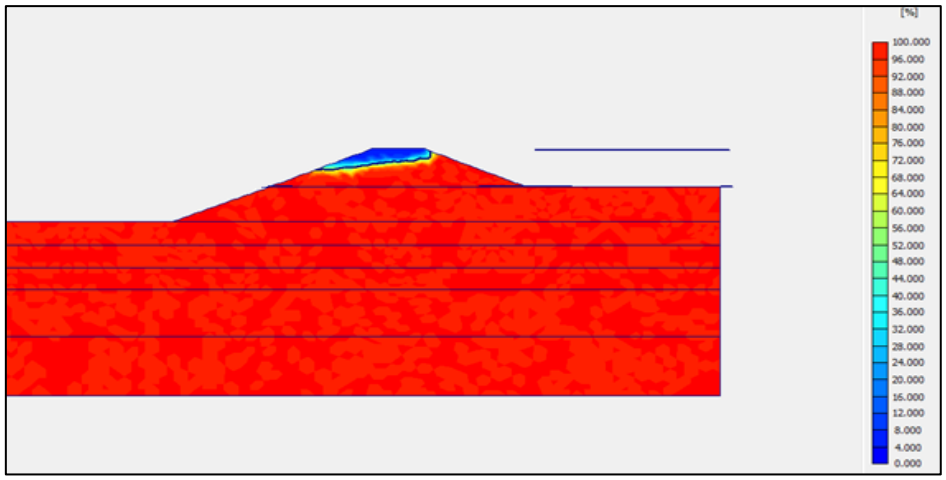

Figure B.98 Degree of Saturation of Filyos Levee at 1+256.4 km on right shore of Filyos River during h_{max}

It is seen that flow values are high at the red area in case h_{max} under the flow line according to Plaxflow2D (Figure B.99.a). There is a risk that is observed piping at these areas.

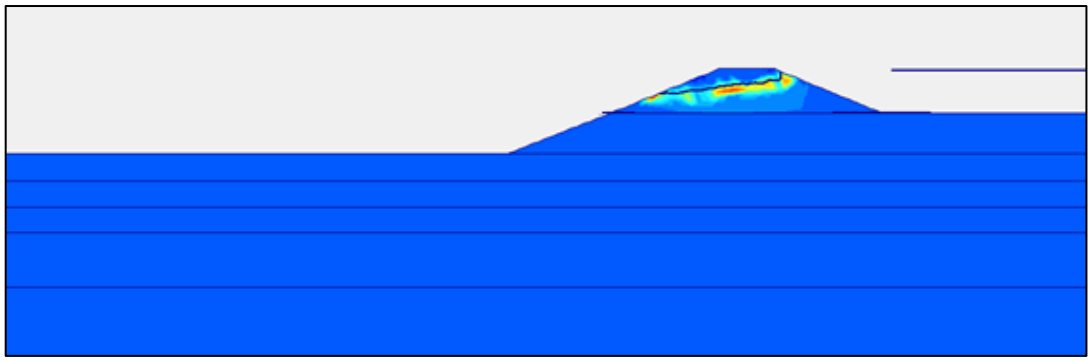

(a)

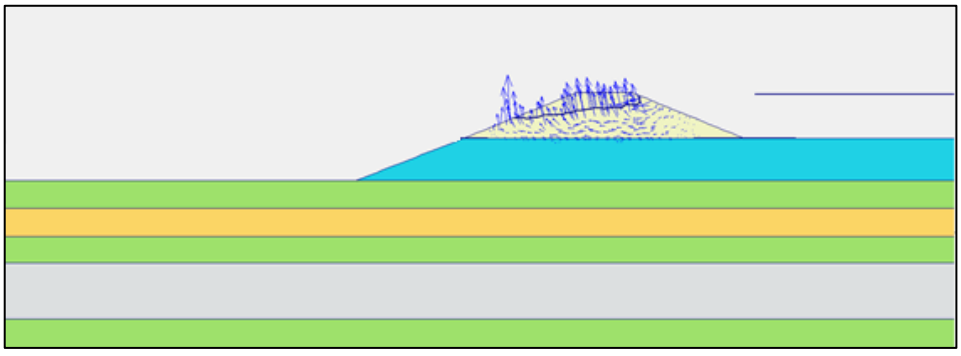

(b)

Figure B.99. Flow field at 1+256.4 km on right shore of Filyos River during h_{max} a.) Shadings view b.) Arrows view

Figure B.99. (b) is other notation that is vector stage in case h_{max}. That is called arrows in Plaxflow2D literature. If the vectors values are higher than others, there will be observing piping formations.

Analysis of clayey silt at under the levee;

Figure B.100 shows that location of points near the ground surface for finding extreme velocity and Figure B.101. presents that results of flow velocity at K, L, M, N, O and P.

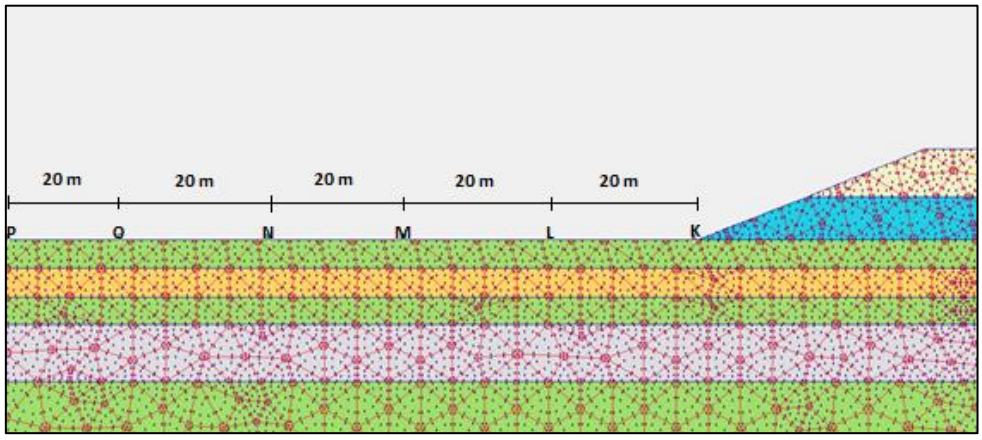

Figure B.100 Location of points near the ground surface for finding extreme velocity

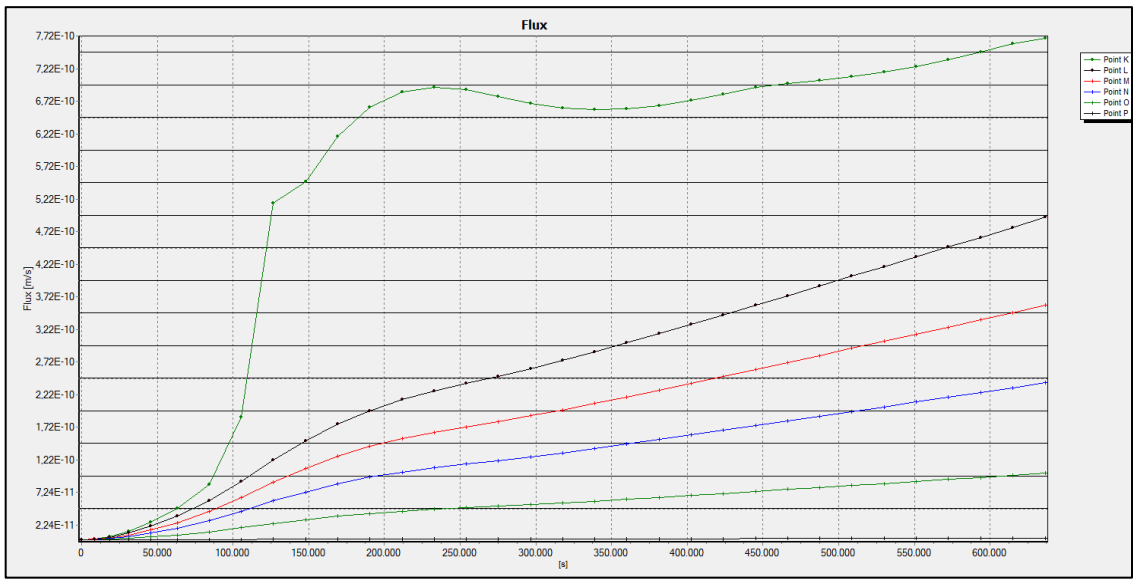

Figure B.101 Extreme velocity graph relation time to seepage velocity

According to Figure B.20, max values of flow are K=7.7x10^{-10} m/s at time=176.5 hours; L=4.4x10^{-10} m/s at time=176.5 hours; M=3.7x10^{-10} m/s at time=176.5 hours; N=2x 10^{-10} m/s at time=176.5 hours, O=9x 10^{-11} m/s at time=176.5 hours, P=2x 10^{-11} m/s at time=176.5 hours.

Piping formations are simply compate as;

$$v = k.i\,; \qquad \text{(B.41)}$$

$$i_c = \frac{G_s - 1}{1 + e} = \frac{2.70 - 1}{1 + 0.9} = 0.89; \quad \text{(B.42)}$$

Where;

v = flow velocity (m/sec)

k = permeabilty (m/sec)

i = hydraulic gradient

i_c = critical hydraulic gradient

G_s = specific gravity; 2.70 for clayey silt

e = void ratio; 0.9 for clayey silt

Table B.47 shows that piping is not observed at any points due to $i_{exit} < i_c$.

Table B.47 Piping Status

Symbol	Max Seepage Velocity (m/s)	Permeability (m/s) (k)	Exit Gradient (*i*)	Piping
K	7.7×10^{-10}	1×10^{-7}	0	**NaN**
L	4.4×10^{-10}	1×10^{-7}	0	**NaN**
M	3.7×10^{-10}	1×10^{-7}	0	**NaN**
N	2×10^{-11}	1×10^{-7}	0	**NaN**
O	9×10^{-11}	1×10^{-7}	0	**NaN**
P	2×10^{-11}	1×10^{-7}	0	**NaN**

NaN:Not a Number

In order for the sand boiling to occur, the piping must take place. As can be seen in the Table B.48, it did not reach critical gradient for the formation of boiling.

Table B.48 Sand Boil Status

Symbol	Max Seepage Velocity (m/s)	Permeability (m/s) (k)	Exit Gradient (*i*)	Sand Boil
K	7.7×10^{-10}	1×10^{-7}	0	**NaN**
L	4.4×10^{-10}	1×10^{-7}	0	**NaN**
M	3.7×10^{-10}	1×10^{-7}	0	**NaN**
N	2×10^{-11}	1×10^{-7}	0	**NaN**
O	9×10^{-11}	1×10^{-7}	0	**NaN**
P	2×10^{-11}	1×10^{-7}	0	**NaN**

NaN:Not a Number

The analysis above the levee for gravelly sand and clayey silt fill soil type;

Piping can only observe K, L and M point because these points only are under the phreatic line. K, L, M etc. points on the ground surface or levee are different from other analyses.

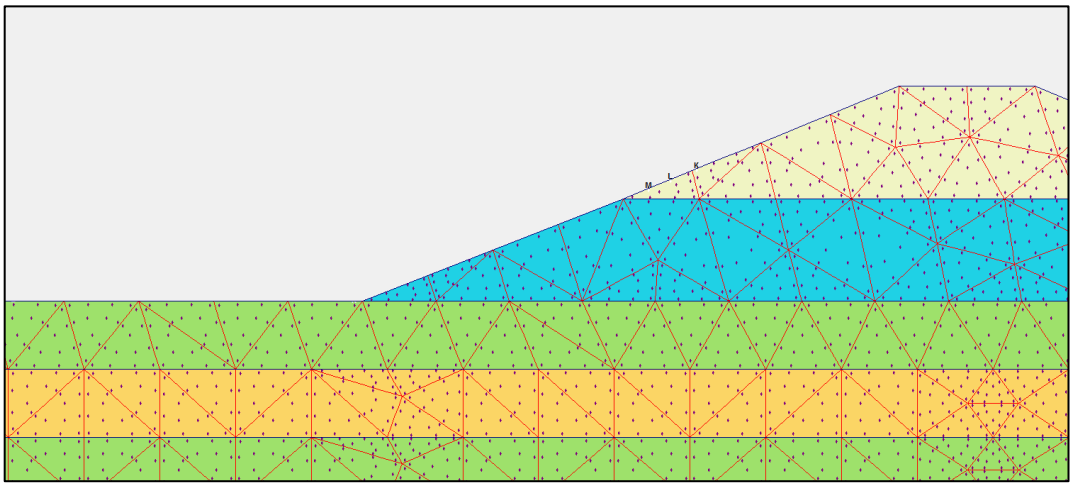

Figure B.102 Location of points above the levee for finding extreme velocity

Extreme velocities of K, L and M point are Fig. B.103 and piping formations are investigated for these points.

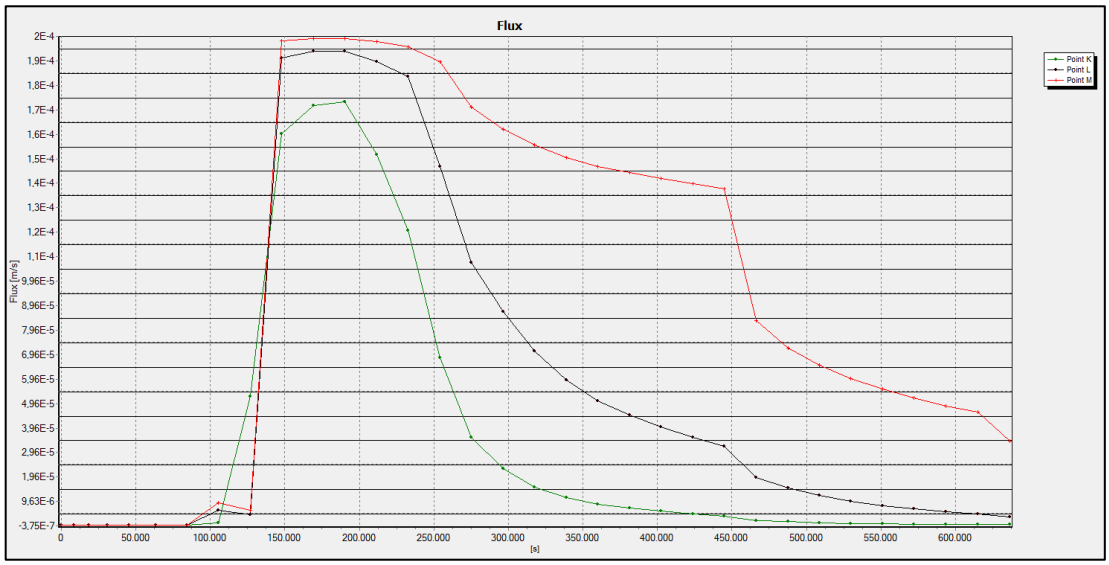

Figure B.103 Extreme velocity graph relation time above the levee

According to Figure B.103, max values of flow are K=1.8x10^{-4}m/s at time=41.7 hours; L=1.95x10^{-4}m/s at time=41.7 hours; M=2 x 10^{-4}m/s at time=41.7 hours.

Piping formations are simply compate as;

$$v = k.i\,; \tag{B.43}$$

$$i_c = \frac{G_s - 1}{1 + e} = \frac{2.66 - 1}{1 + 0.62} = 1.02\,; \tag{B.44}$$

Where;

v = flow velocity (m/sec)

k = permeabilty (m/sec)

i = hydraulic gradient

i_c = critical hydraulic gradient

G_s = specific gravity; 2.66 for gravelly sand

e = void ratio; 0.62 for gravelly sand

Table B.49 shows that piping is not observed at any points due to $i_{exit} < i_c$.

Table B.49 Piping Status

Symbol	Max Seepage Velocity (m/s)	Permeability (m/s) (k)	Exit Gradient (i)	Piping
K	1.75×10^{-4}	5×10^{-4}	0.35	**NaN**
L	1.95×10^{-4}	5×10^{-4}	0.39	**NaN**
M	2×10^{-4}	5×10^{-4}	0.40	**NaN**

NaN:Not a Number

Extreme velocities of K, L and M point are on the silty sand soil layer (Figure B.104).

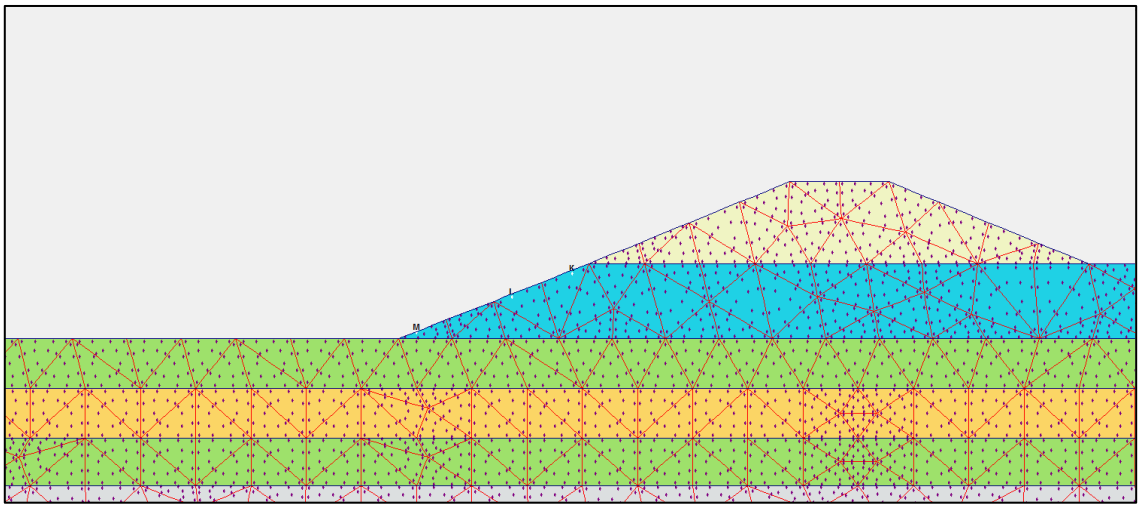

Figure B.104 Location of points above the levee for finding extreme velocity

Figure B.105 shows extreme velocity graph relation time above the levee on the silty sand layer for investigating piping formations.

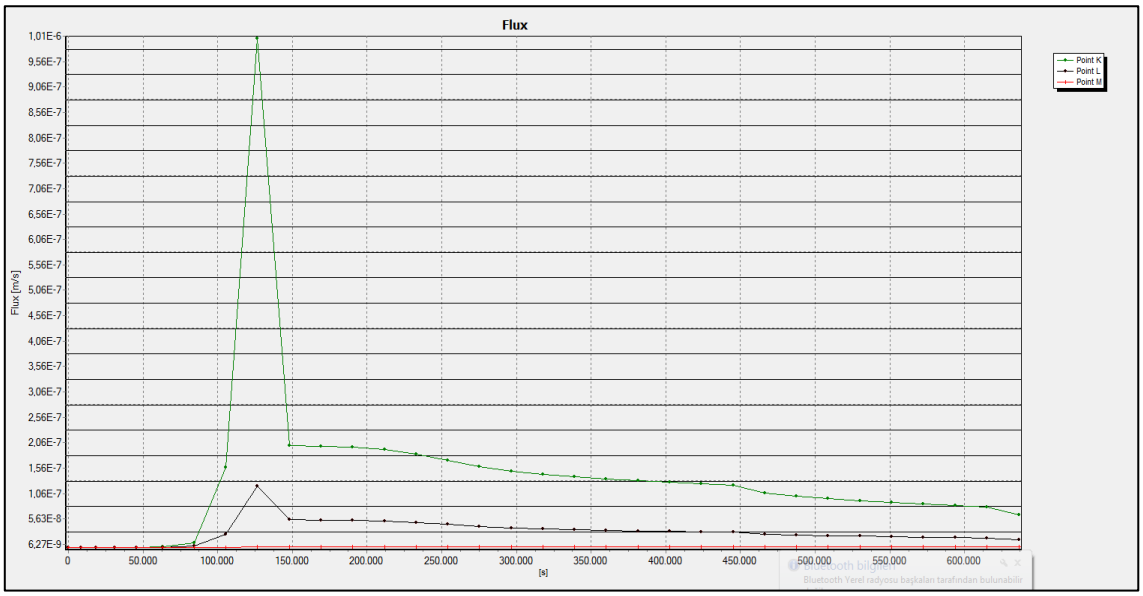

Figure B.105 Extreme velocity graph relation time above the levee

According to Figure B.105, max values of flow are K=1x10^{-6}m/s at time=34.7 hours; L=1.3x10^{-7}m/s at time=34.7 hours; M=6.3x 10^{-9}m/s at time=34.7 hours.

Piping formations are simply compate as;

$$v = k.i\,; \tag{B.45}$$

$$i_c = \frac{G_s - 1}{1+e} = \frac{2.69-1}{1+0.43} = 1.2\,; \tag{B.46}$$

Where;

v = flow velocity (m/sec)

k = permeabilty (m/sec)

i = hydraulic gradient

i_c = critical hydraulic gradient

G_s = specific gravity; 2.69 for silty sand

e = void ratio; 0.43 for silty sand

Critical hydraulic gradients is 1.2 for silty sand. According to max flow velocity, piping is investigated these points. Table B.50 shows that piping is not observed at any points due to $i_{exit} < i_c$.

Table B.50 Piping Status

Symbol	Max Seepage Velocity (m/s)	Permeability (m/s) (k)	Exit Gradient (*i*)	Piping
K	1×10^{-6}	1×10^{-6}	1.0	**NaN**
L	1.3×10^{-7}	1×10^{-6}	0.13	**NaN**
M	6.3×10^{-9}	1×10^{-6}	0	**NaN**

NaN:Not a Number

The factor of safety against heave analysis for top layer;

Equation B.47 and B.48 are used to determine the factor of safety against heave analysis for top layer. Heaving potential are only observed ground surface hence a point are investigated at 1.0 m below the top layer like Figure B.105.

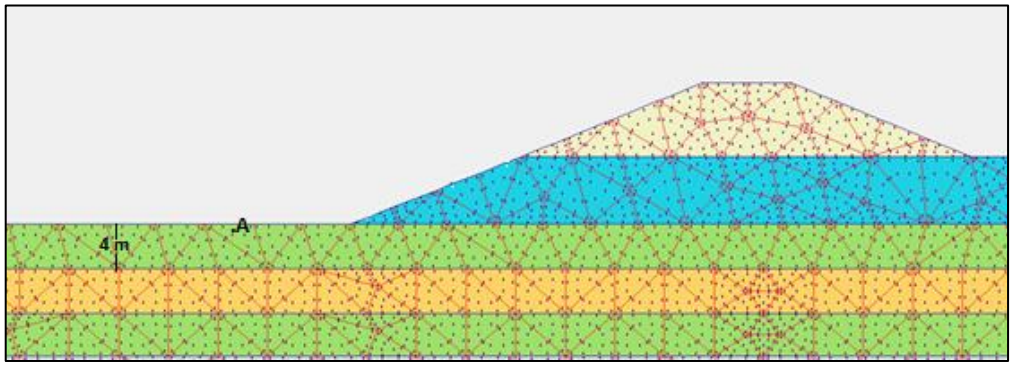

Figure B.105 Analysis against to heave at A point 1.0 m below the top layer

$$F_{heave} = \frac{H.\gamma_{sat}}{h_m.\gamma_w} > 3.0 \qquad \text{(B.47)}$$

$$i_{\max} = \frac{h_m}{H} \qquad \text{(B.48)}$$

Where;

H = thickness of overlying top layer(m)

γ_{sat} = saturated unit weight of overlying top layer(kN/m^2)

h_m = average hydraulic head at the point(m)

γ_w = water unit wight(kN/m^2)

$i_{\max}$ = maximum exit gradient

Since $i_{\max}$ =0, heaving is not likely to ocur.

B.7.1. Filyos Levee at 1+256.4 km on Right Shore of Filyos River according to Current Situation (Upstream face is covered)

The schematic representation of Filyos Levee and soil profile is given in Figure B.106. Filyos levee includes gravelly sand soil type and cover materials against piping and sand boil formations. The cover materials are riprap which is andesite, uniform sand filter layer and geocomposite layer. There is a clayey silt layer under the levee and this layer is 4 m thick.

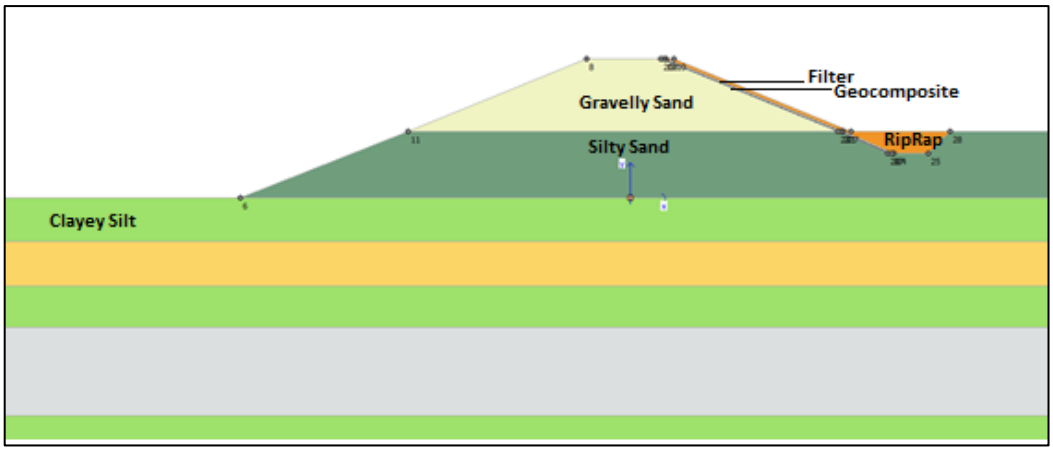

Figure B.106 Filyos Levee with cover materials at 1+256.4 km on right shore of Filyos River

Filyos levee has covered along rising water level. Table B.51 shows properties of covered materials and levee.

Table B.51 Soil Properties of levee members

	Soil Type / Material	**Permeability(k) (m/sec)**	**Specific Gravity (G_s)**	**Void Ratio (e)**	**Thickness (m)**
Filter	Uniform Sand	$1x10^{-3}$	2.67	0.70	0.25
Riprap	Andesite Rock	0.645	2.65	0.34	0.70
Geocomposite Material	Geotextile and Geomembrane	$1x10^{-13}$	-	0.02	0.30

Figure B.107 shows that each soil layers have saturated unit weight under the levee with cover materials for transient analysis and area of under the flow line is saturated during h_{max}. Saturation rates of red areas are high and saturation rates of other areas are almost zero without riprap, filter, and areas under levee.

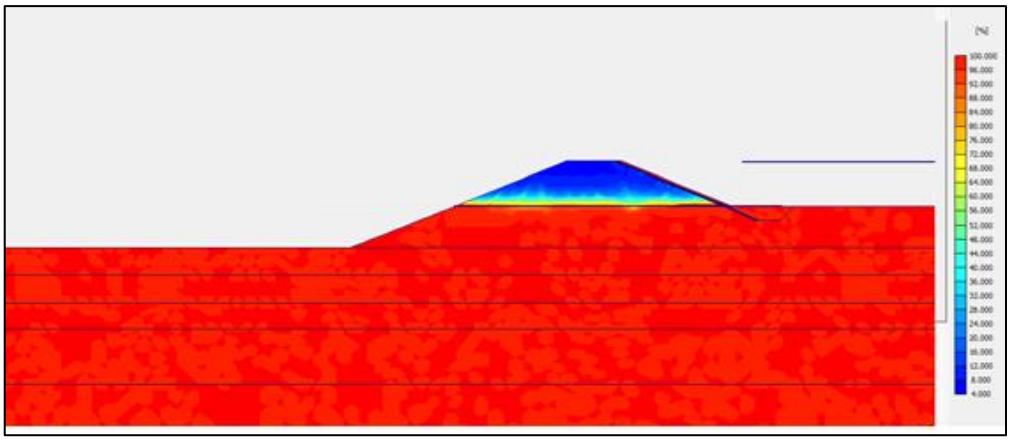

Figure B.107 Degree of Saturation of Filyos Levee with cover materials 1+256.4 km on right shore of Filyos River during h_{max}

It is seen that flow values are high at the red area in case h_{max} under the flow line according to Plaxflow2D (Figure B.108.a). There is not a risk that is observed piping into through levee.

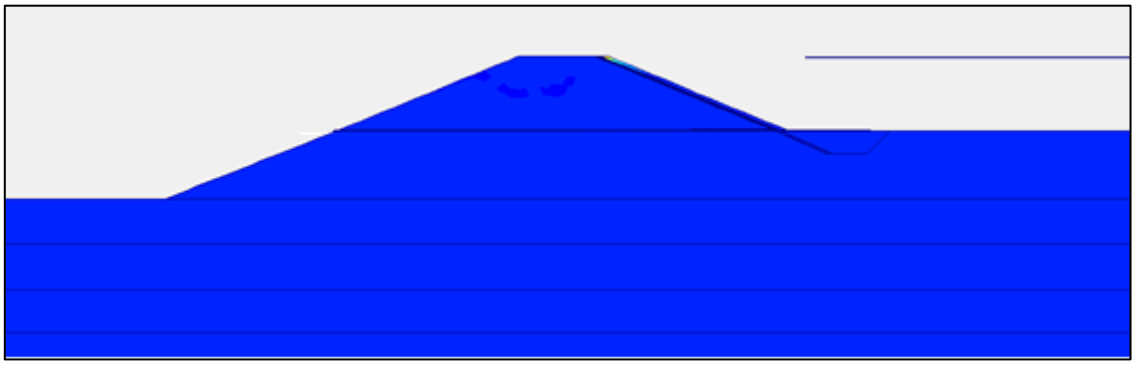

(a)

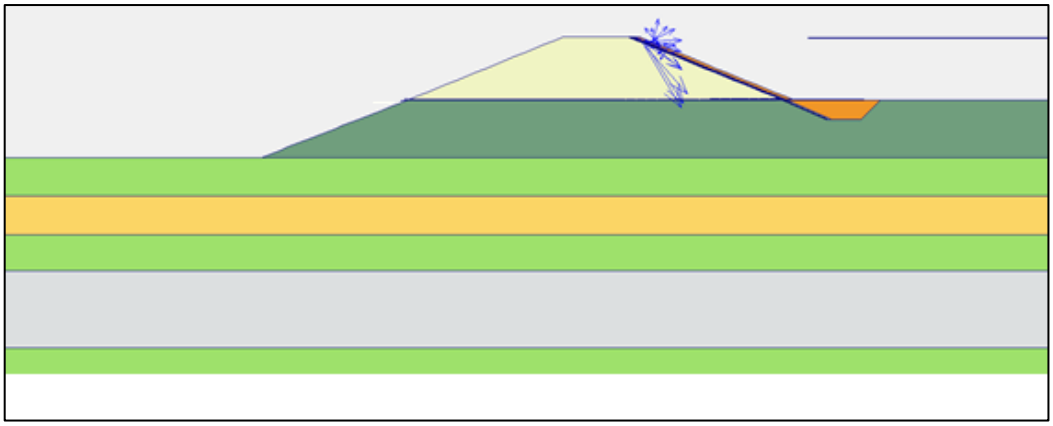

(b)

Figure B.108. Flow field of cover materials at 1+256.4 km on right shore of Filyos River during h_{max} a.) Shadings view b.) Arrows view

Figure B.108. (b) is other notation that is vector stage in case h_{max}. That is called arrows in Plaxflow2D literature and there is not risk into through levee.

Analysis of clayey silt at under the levee;

Figure B.109 shows that location of points near the ground surface for finding extreme velocity and Figure B.110 presents that results of flow velocity at K, L, M, N, O and P.

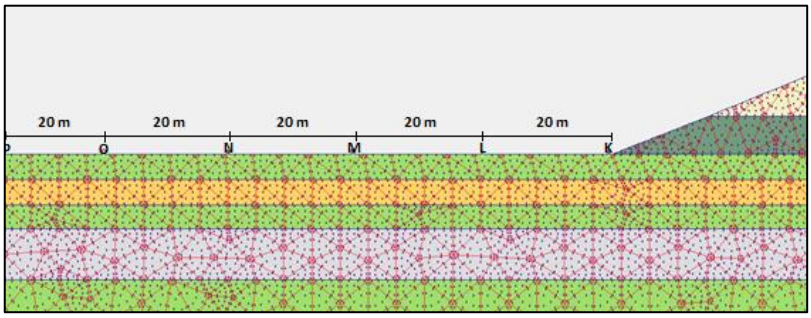

Figure B.109 Location of points near the ground surface for finding extreme velocity

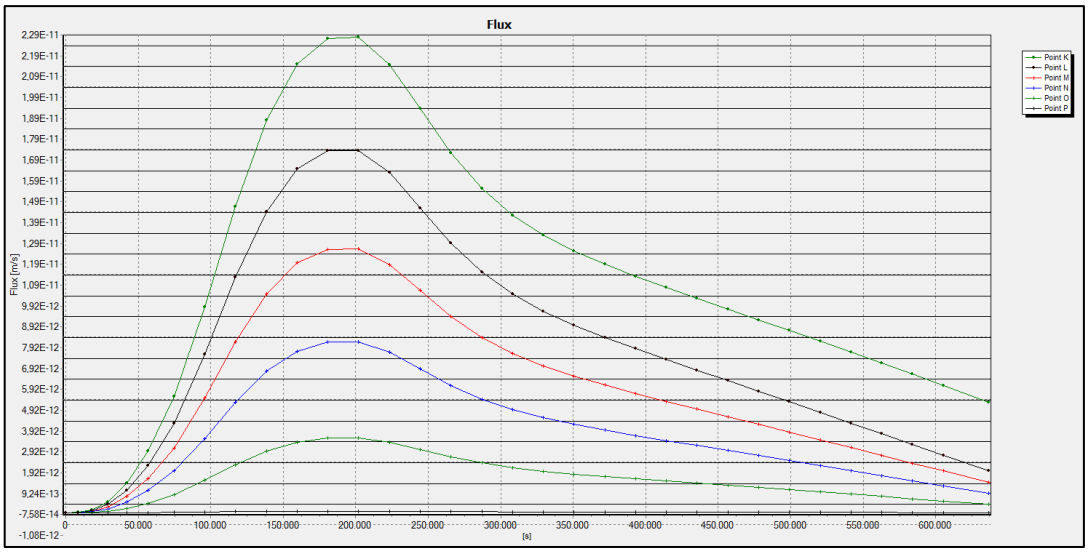

Figure B.110 Extreme velocity graph relation time Filyos Levee

Table B.52 shows that piping is not observed at any points due the fact that to exit gradient is zero. See equation B.46 for calculated critical hydraulic gradients.

Table B.52 Piping Status

Symbol	Max Seepage Velocity (m/s)	Permeability (m/s) (k)	Exit Gradient (*i*)	Piping
K	2.3×10^{-11}	1×10^{-7}	0	**NaN**
L	1.7×10^{-11}	1×10^{-7}	0	**NaN**
M	1.2×10^{-11}	1×10^{-7}	0	**NaN**
N	8.0×10^{-12}	1×10^{-7}	0	**NaN**
O	3.5×10^{-12}	1×10^{-7}	0	**NaN**
P	9.0×10^{-13}	1×10^{-7}	0	**NaN**

NaN:Not a Number

In order for the sand boiling to occur, the piping must take place. As can be seen in the Table B.53, it did not reach critical gradient for the formation of boiling.

Table B.53 Sand boil status

Symbol	Max Seepage Velocity (m/s)	Permeability (m/s) (k)	Exit Gradient (*i*)	Sand Boil
K	2.3×10^{-11}	1×10^{-7}	0	**NaN**
L	1.7×10^{-11}	1×10^{-7}	0	**NaN**
M	1.2×10^{-11}	1×10^{-7}	0	**NaN**
N	8.0×10^{-12}	1×10^{-7}	0	**NaN**
O	3.5×10^{-12}	1×10^{-7}	0	**NaN**
P	9.0×10^{-13}	1×10^{-7}	0	**NaN**

NaN:Not a Number

- Heaving potential is not observed that levee has cover materials along river since the exit gradients approach zero.

The analysis above the levee for gravelly sand and silty sand fill soil type;

Piping can only observe K, L and M point because these points only are under the phreatic line. K, L, M etc. points on the ground surface or levee are different from other analyses. K, L and M points are on the Filyos levee and these points are under the phreatic line and piping formation is observed this point. Piping formations, sand boil formations and heaving potential can be observed these points.

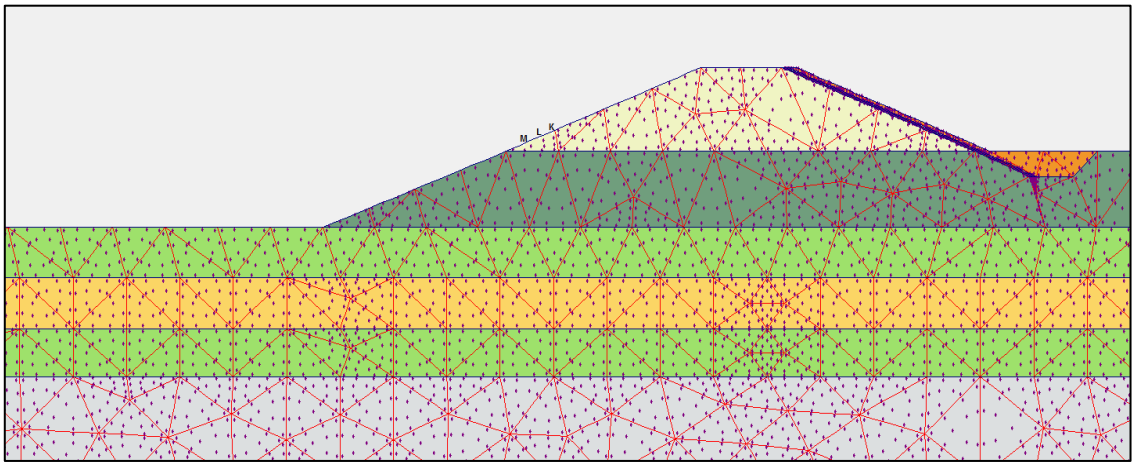

Figure B.111 Location of points above the levee for finding extreme velocity

Extreme velocities of K, L and M point are below and piping formations are investigated for these points (Figure B.112).

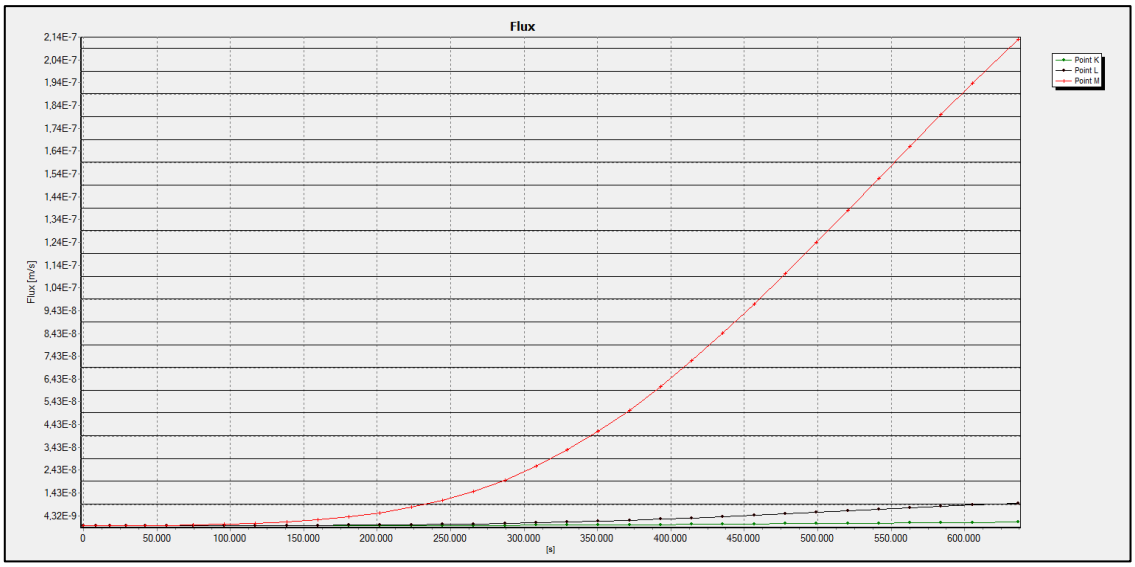

Figure B.112 Extreme velocity graph relation time above the levee

Table B.54 shows that piping is not observed at any points due the fact that to exit gradient is zero. See equation B.44 for calculated critical hydraulic gradients.

Table B.54 Piping Status

Symbol	Max Seepage Velocity (m/s)	Permeability (m/s) (k)	Exit Gradient (*i*)	Piping
K	4×10^{-9}	5×10^{-4}	0	**NaN**
L	4.3×10^{-9}	5×10^{-4}	0	**NaN**
M	2.1×10^{-7}	5×10^{-4}	0	**NaN**

NaN:Not a Number

K, L, M etc. points on the ground surface or levee are different from other analyses. (Figure B.113).

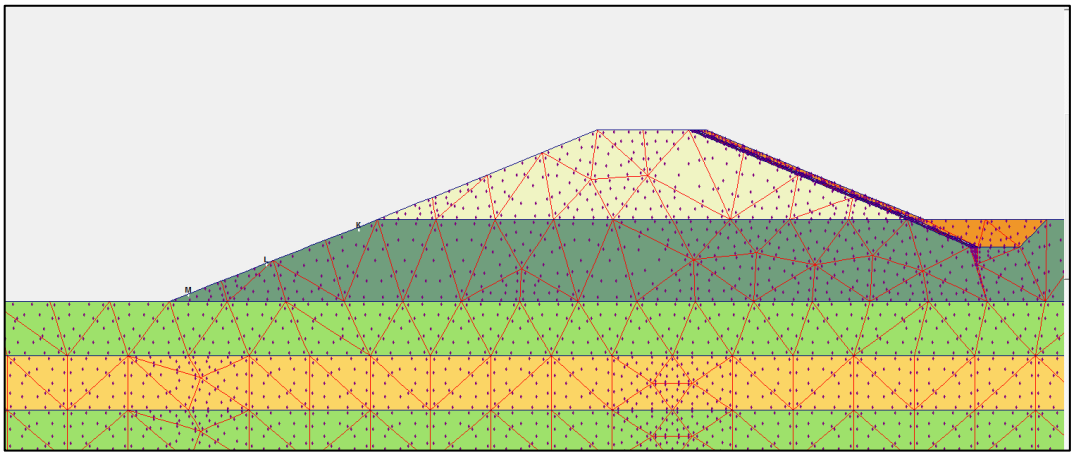

Figure B.113 Location of points above the levee for finding extreme velocity

Extreme velocities of K, L and M point are below and piping formations are investigated for these points.(Figure B.114)

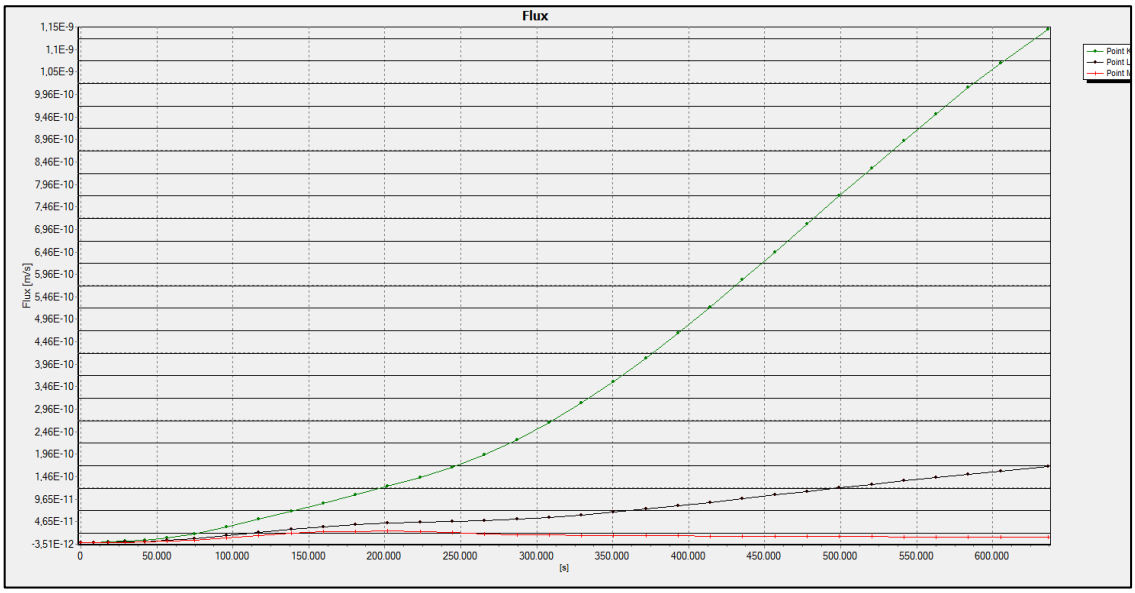

Figure B.114 Extreme velocity graph relation time above the levee

Table B.55 shows that piping is not observed at any points due the fact that to exit gradient is zero. See equation B.46 for calculated critical hydraulic gradients.

Table B.55 Piping Status

Symbol	Max Seepage Velocity (m/s)	Permeability (m/s) (k)	Exit Gradient (*i*)	Piping
K	1.2×10^{-9}	1×10^{-6}	0	**NaN**
L	1.6×10^{-10}	1×10^{-6}	0	**NaN**
M	4.0×10^{-11}	1×10^{-6}	0	**NaN**

NaN:Not a Number

B.8. Filyos Levee at 1+762.17 km on Right Shore of Filyos River

Location of Filyos levee at 1762.17 m on left shore is seen Figure B.115. The schematic representation of Filyos Levee and soil profile is given in Figure B.116. Filyos levee includes gravelly sand soil type. There is a clayey silt layer under the levee and this layer is 4 m thick. Also, silty sand material is used for this layer to need filling under the levee.

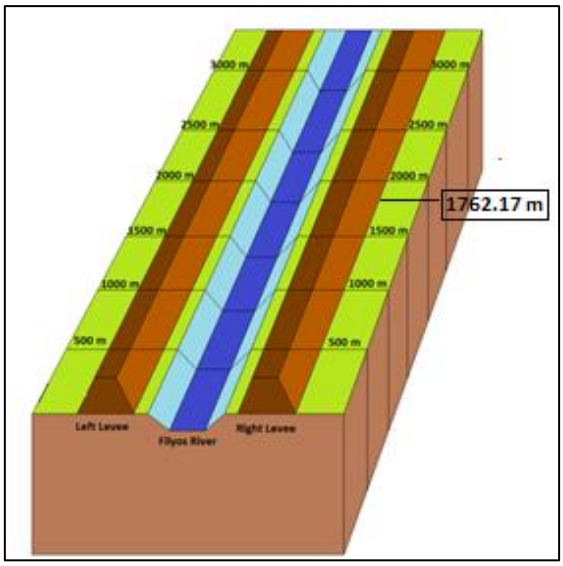

Figure B.115 Locations of Filyos levee at 1762.17 m on right shore of Filyos River

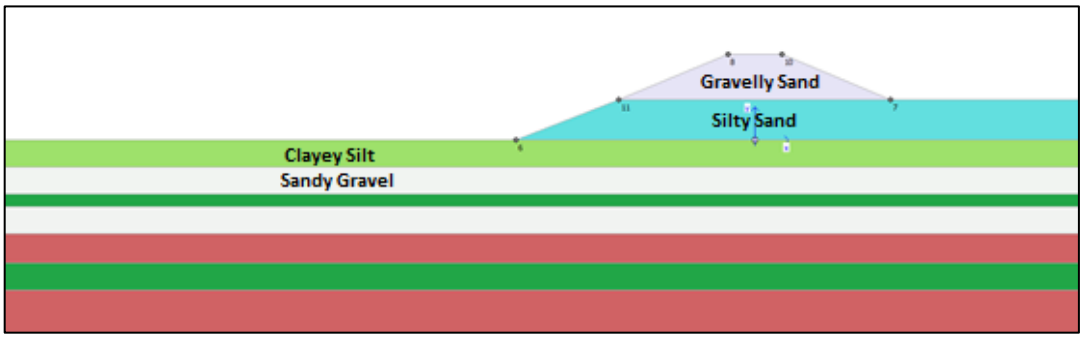

Figure B.116 Filyos Levee with cover materials at 1+762.17 km on right shore shore of Filyos River

Figure B.117 shows that each soil layers have saturated unit weight under the levee for transient analysis and area of under the flow line is saturated during $h_{max.}$

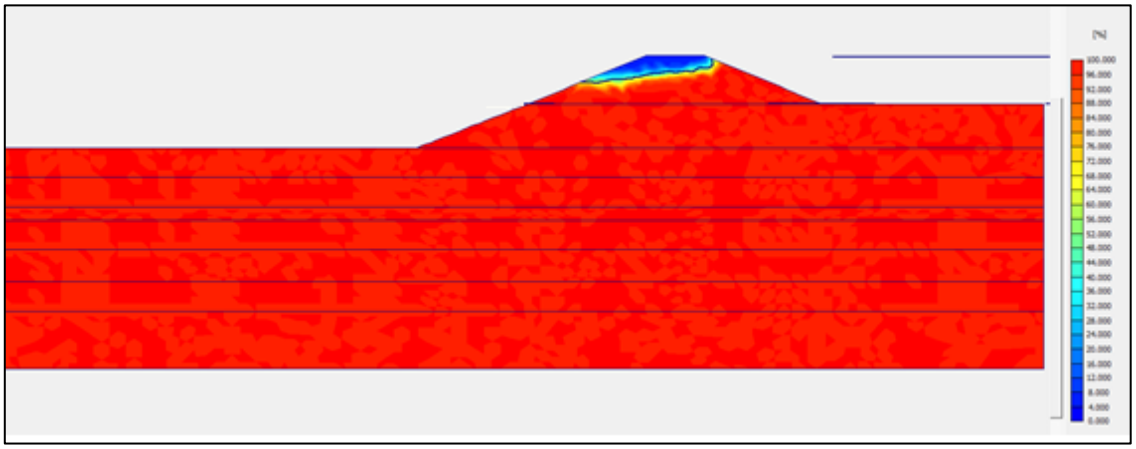

Figure B.117 Degree of Saturation of Filyos Levee at 1+762.17 km on right shore of Filyos River during h_{max}

It is seen that flow values are high at the red area in case h_{max} under the flow line according to Plaxflow2D (Figure B.118.a). There is a risk that is observed piping at these areas.

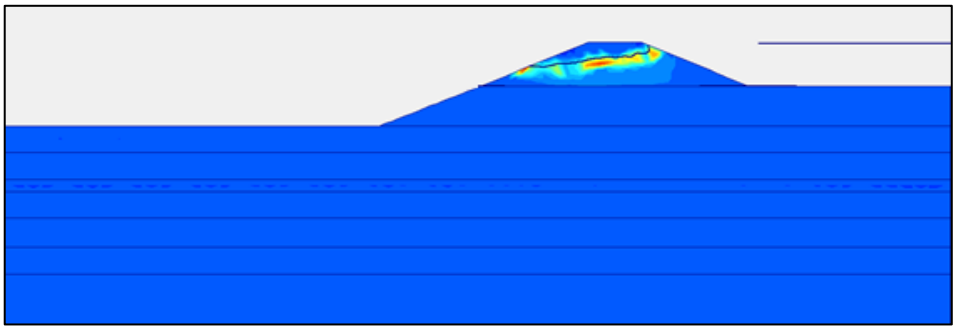

(a)

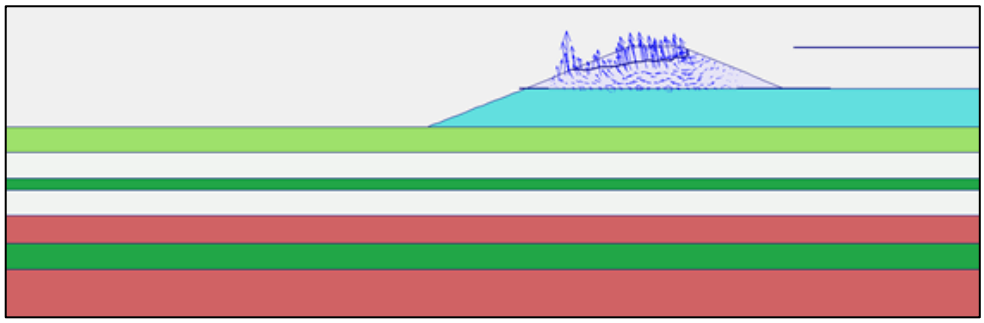

(b)

Figure B.118. Flow field at 1+762.17 km on right shore of Filyos River during h_{max} a.) Shadings view b.) Arrows view

Figure B.118. (b) is other notation that is vector stage in case hmax. That is called arrows in Plaxflow2D literature. If the vectors values are higher than others, there will be observing piping formations.

Analysis of clayey silt at under the levee;

Figure B.119 shows that location of points near the ground surface for finding extreme velocity and Figure B.120 presents that results of flow velocity at K, L, M, N, O and P.

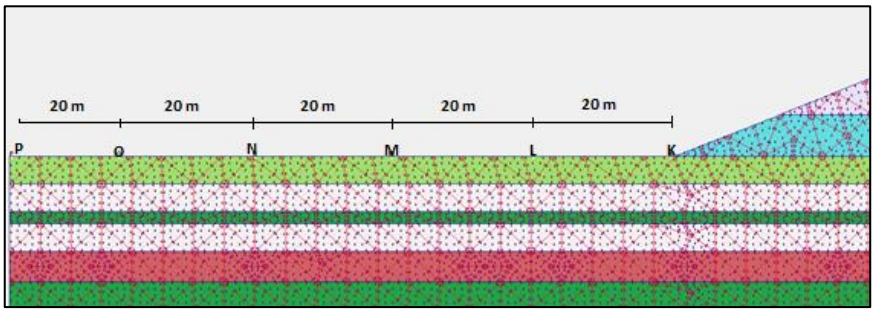

Figure B.119 Location of points near the ground surface for finding extreme velocity

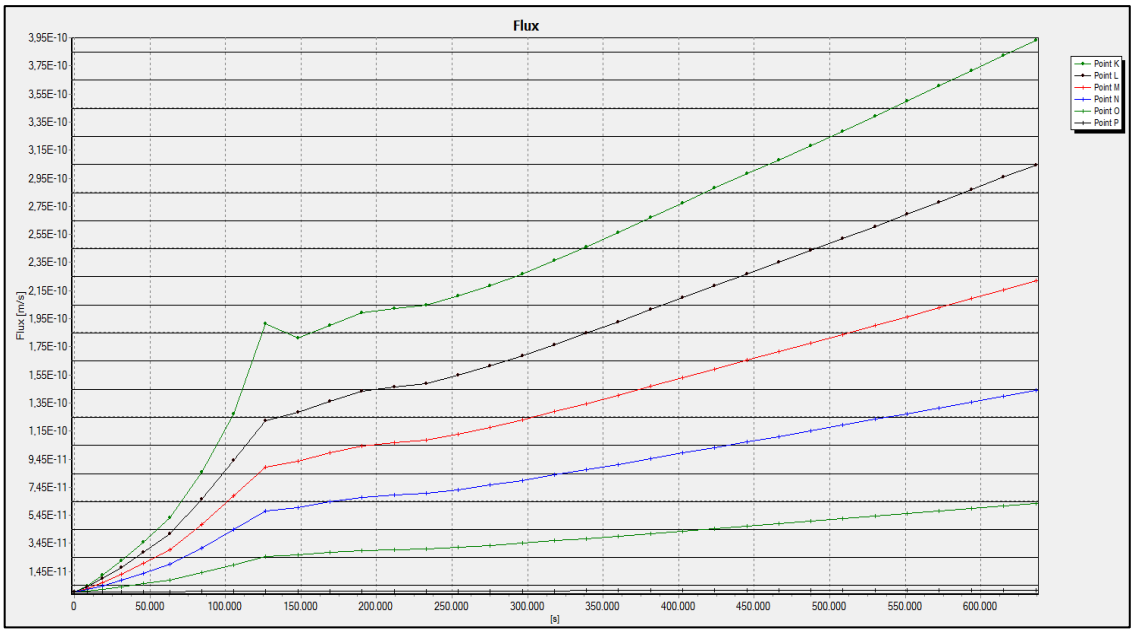

Figure B.120 Extreme velocity graph relation time to seepage velocity

According to Figure B.120, max values of flow are K=4x10^{-10}m/s at time=176.8 hours; L=3x10^{-10}m/s at time=176.8 hours; M=2.2x10^{-10}m/s at time=176.8 hours; N=1.2x10^{-10}m/s at time=176.8 hours; O=6x10^{-11}m/s at time=176.8 hours; P=1x10^{-11}m/s at time=176.8 hours.

Piping formations are simply compate as;

$$v = k.i\,; \tag{B.49}$$

$$i_c = \frac{G_s - 1}{1 + e} = \frac{2.70 - 1}{1 + 0.90} = 0.89\,; \tag{B.50}$$

Where;

v = flow velocity (m/sec)

k = permeabilty (m/sec)

i = hydraulic gradient

i_c = critical hydraulic gradient

G_s = specific gravity; 2.70 for clayey silt

e = void ratio; 0.90 for clayey silt

Critical hydraulic gradient is 0.89 for sand. Table B.56 shows that piping is not observed at any points due the fact that to exit gradient is zero.

Table B.56 Piping Status

Symbol	Max Seepage Velocity (m/s)	Permeability (m/s) (k)	Exit Gradient (*i*)	Piping
K	4×10^{-10}	1×10^{-7}	0	**NaN**
L	3×10^{-10}	1×10^{-7}	0	**NaN**
M	2.2×10^{-10}	1×10^{-7}	0	**NaN**
N	1.2×10^{-10}	1×10^{-7}	0	**NaN**
O	6×10^{-11}	1×10^{-7}	0	**NaN**
P	1×10^{-11}	1×10^{-7}	0	**NaN**

NaN:Not a Number

In order for the sand boiling to occur, the piping must take place. As can be seen in the Table B.57, it did not reach critical gradient for the formation of boiling.

Table B.57 Sand Boil Status

Symbol	Max Seepage Velocity (m/s)	Permeability (m/s) (k)	Exit Gradient (*i*)	Sand Boil
K	4×10^{-10}	1×10^{-7}	0	**NaN**
L	3×10^{-10}	1×10^{-7}	0	**NaN**
M	2.2×10^{-10}	1×10^{-7}	0	**NaN**
N	1.2×10^{-10}	1×10^{-7}	0	**NaN**
O	6×10^{-11}	1×10^{-7}	0	**NaN**
P	1×10^{-11}	1×10^{-7}	0	**NaN**

NaN:Not a Number

The analysis above the levee for gravelly sand and silty sand fill soil type;

Piping can only observe K, L and M point because these points only are under the phreatic line. K, L, M etc. points on the ground surface or levee are different from other analyses.

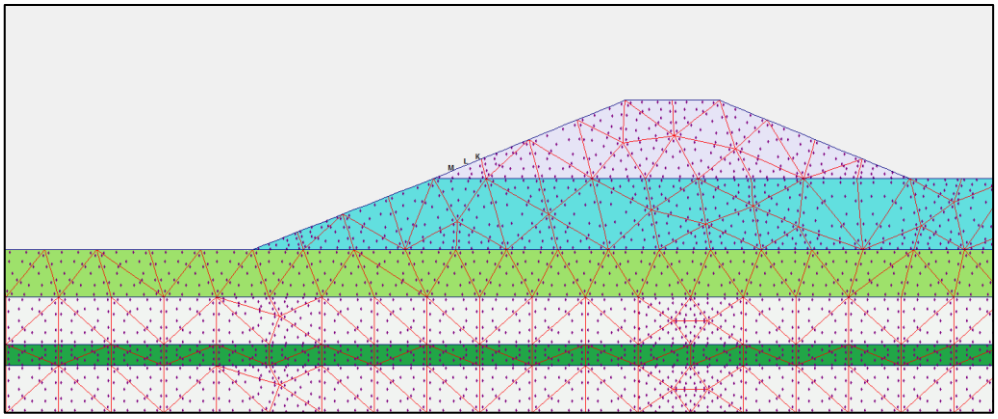

Figure B.121 Location of points above the levee for finding extreme velocity

Extreme velocities of K, L and M point are below and piping formations are investigated for these points.(Figure B.122)

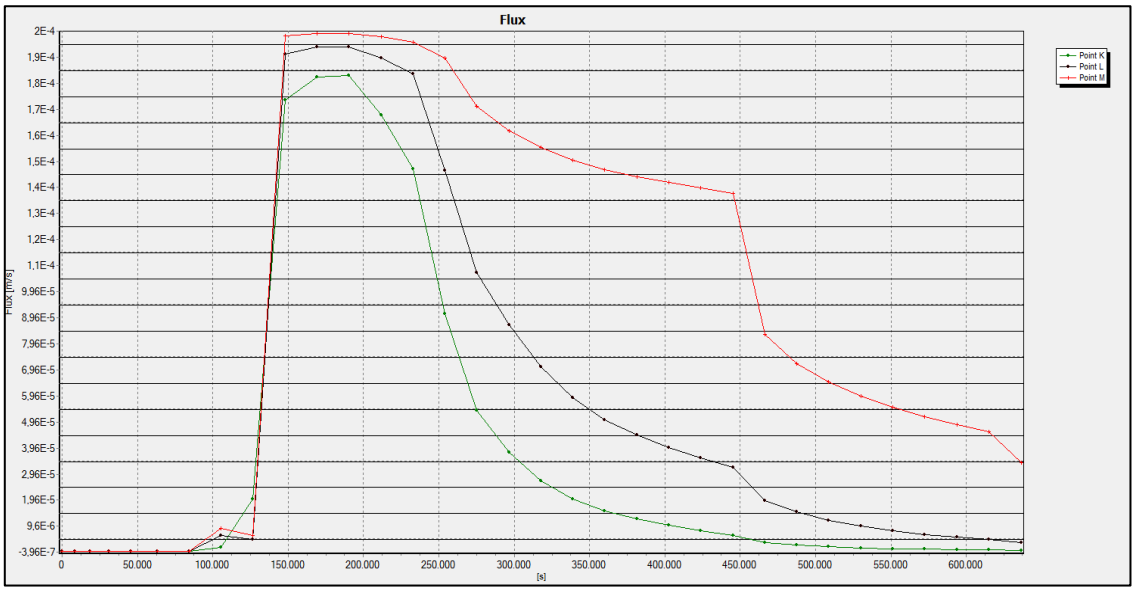

Figure B.122 Extreme velocity graph relation time above the levee

According to Figure B.122, max values of flow are K=1.8x10^{-4}m/s at time=34.7 hours; L=1.95x10^{-4}m/s at time=34.7 hours; M=2x10^{-4}m/s at time=34.7 hours.

Piping formations are simply compate as;

$$v = k.i\,; \tag{B.51}$$

$$i_c = \frac{G_s - 1}{1+e} = \frac{2.66-1}{1+0.62} = 1.02\,; \tag{B.52}$$

Where;

$v =$ flow velocity (m/sec)

$k =$ permeabilty (m/sec)

$i =$ hydraulic gradient

$i_c =$ critical hydraulic gradient

$G_s =$ specific gravity; 2.66 gravelly sand

$e =$ void ratio; 0.62 for gravelly sand

Critical hydraulic gradient is 1.2 for clayey sand Table B.58 shows that piping is not observed at any points due to $i_{exit} < i_c$.

Table B.58 Piping Status

Symbol	Max Seepage Velocity (m/s)	Permeability (m/s) (k)	Exit Gradient (*i*)	Piping
K	1.8×10^{-4}	5×10^{-4}	0.36	**NaN**
L	1.95×10^{-4}	5×10^{-4}	0.39	**NaN**
M	2×10^{-4}	5×10^{-4}	0.40	**NaN**

NaN:Not a Number

Piping can only observe K, L and M point because these points only are under the phreatic line. K, L, M etc. points on the ground surface or levee are different from other analyses.(Figure B.123)

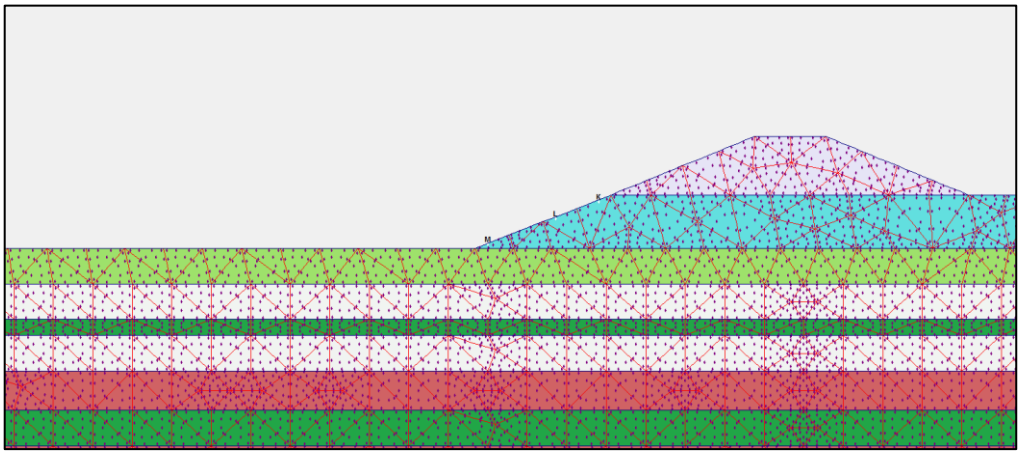

Figure B.123 Location of points above the levee for finding extreme velocity

Extreme velocities of K, L and M point are Figure B.124 and piping formations are investigated for these points.

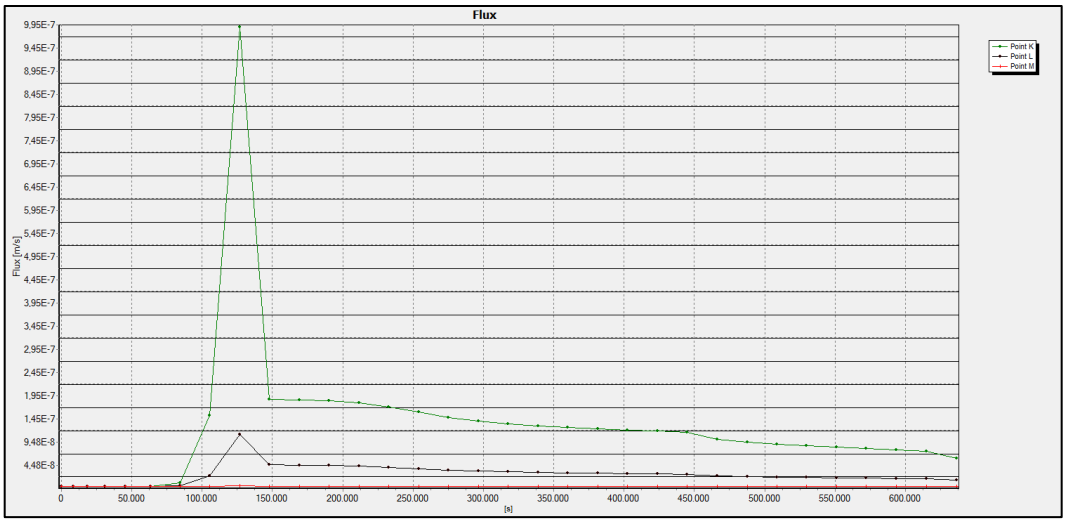

Figure B.124 Extreme velocity graph relation time above the levee

According to Figure B.124, max values of flow are K=1x10^{-6}m/s at time=34.7 hours; L=1x10^{-7}m/s at time=34.7 hours; M=1x10^{-8}m/s at time=34.7 hours.

Piping formations are simply compate as;

$$v = k.i\,; \tag{B.53}$$

$$i_c = \frac{G_s - 1}{1+e} = \frac{2.69-1}{1+0.43} = 1.2\,; \tag{B.54}$$

Where;

v = flow velocity (m/sec)

k = permeabilty (m/sec)

i = hydraulic gradient

i_c = critical hydraulic gradient

G_s = specific gravity; 2.69 for silty sand

e = void ratio; 0.43 for silty sand

Table B.59. shows that piping is not observed at any points due to $i_{exit} < i_c$.

Table B.59 Piping Status

Symbol	Max Seepage Velocity (m/s)	Permeability (m/s) (k)	Exit Gradient (*i*)	Piping
K	1 x 10^{-6}	1 x 10^{-6}	1.0	**NaN**
L	1 x 10^{-7}	1 x 10^{-6}	0.1	**NaN**
M	1 x 10^{-8}	1 x 10^{-6}	0.01	**NaN**

NaN:Not a Number

The factor of safety against heave analysis for top layer;

Equation B.55 and B.56 are used to determine the factor of safety against heave analysis for top layer. Heaving potential are only observed ground surface hence a point are investigated at 1 m below the top layer like Figure B.125.

$$F_{heave} = \frac{H.\gamma_{sat}}{h_m.\gamma_w} > 3.0 \tag{B.55}$$

$$i_{\max} = \frac{h_m}{H} \tag{B.56}$$

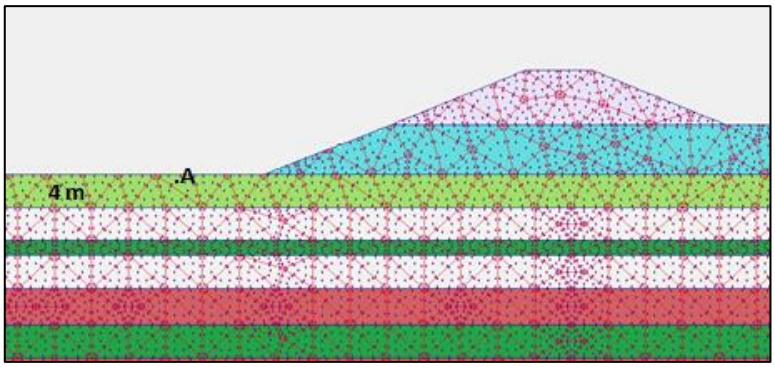

Figure B.125 Analysis against to heave at A point 1 m below the top layer

Where;

H = thickness of overlying top layer(m)

γ_{sat} = saturated unit weight of overlying top layer(kN/m^2)

h_m = average hydraulic head at the point(m)

γ_w = water unit wight(kN/m^2)

$i_{\max}$ = maximum exit gradient

Since $i_{\max}$ =0, heaving is not likely to occur.

B.8.1. Filyos Levee at 1+762.17 km on Right Shore of Filyos River according to current situation(Upstream face is covered)

The schematic representation of Filyos Levee and soil profile is given in Figure B.126. Filyos levee includes gravelly sand soil type and cover materials against piping and sand boil formations. The cover materials are riprap which is andesite, uniform sand filter layer and geocomposite layer. There is a clayey silt layer under the levee and this layer is 4 m thick.

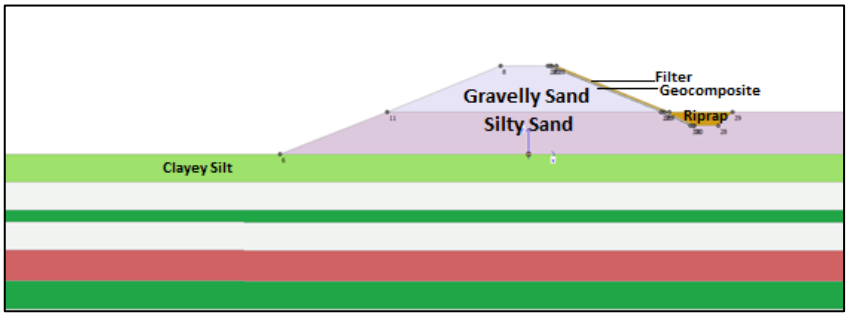

Figure B.126 Filyos Levee with cover materials at 1+762.17 km on right shore of Filyos River

Filyos levee has covered along rising water level. Table B.60 shows properties of covered materials and levee.

Table B.60 Soil Properties of levee members

	Soil Type / Material	Permeability(k) (m/sec)	Specific Gravity (G_s)	Void Ratio (e)	Thickness (m)
Filter	Uniform Sand	$1x10^{-3}$	2.67	0.70	0.25
Riprap	Andesite Rock	0.645	2.65	0.34	0.70
Geocomposite Material	Geotextile and Geomembrane	$1x10^{-13}$	-	0.02	0.30

Figure B.127 shows that each soil layers have saturated unit weight under the levee with cover materials for transient analysis and area of under the flow line is saturated during h_{max}. Saturation rates of red areas are high and saturation rates of other areas are almost zero with riprap, filter and geocomposites.

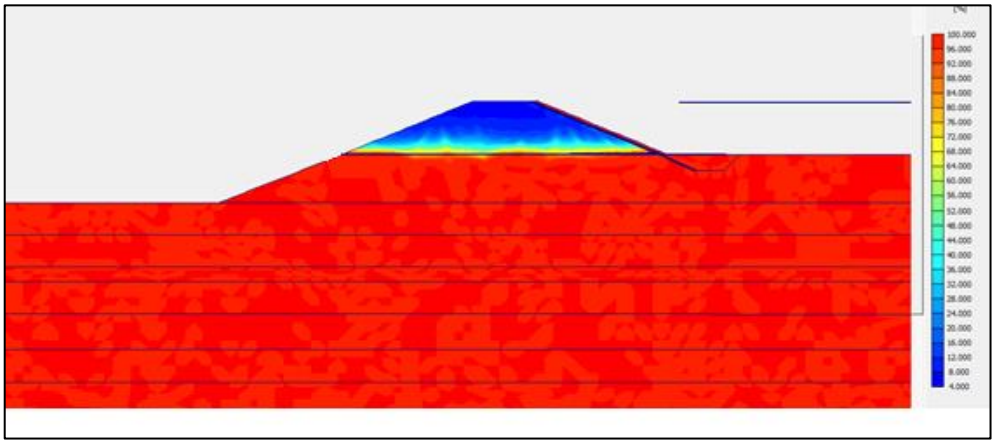

Figure B.127 Degree of Saturation of Filyos Levee with cover materials at 1+762.17 km on right shore of Filyos River during h_{max}

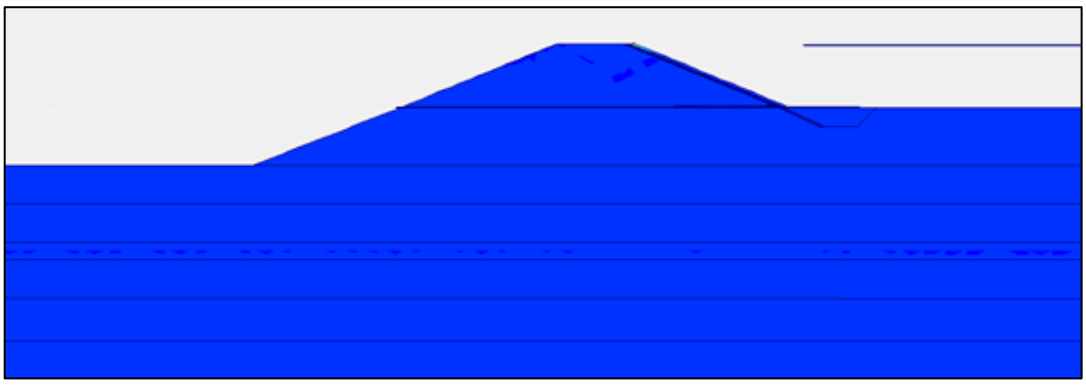

(a)

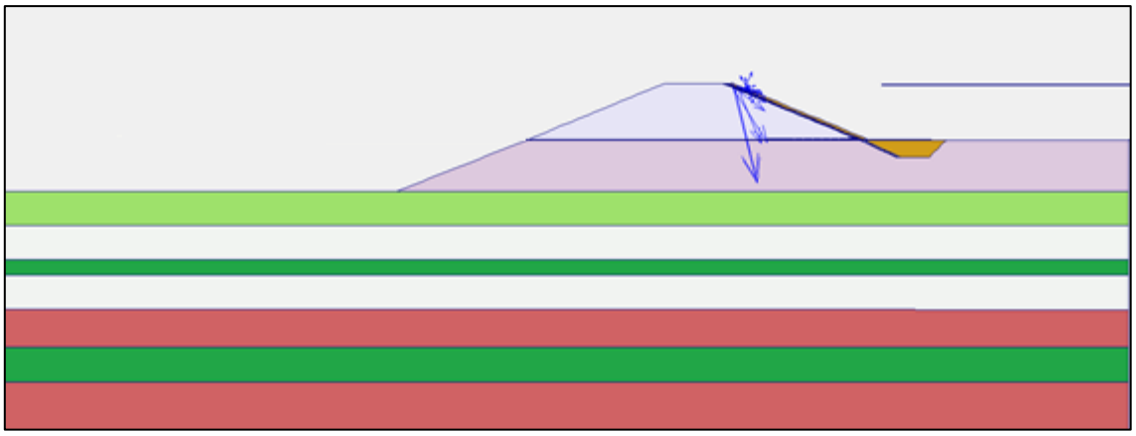

(b)

Figure B.128. Flow field at 1+762.17 km on right shore of Filyos River during h_{max}
a.) Shadings view b.) Arrows view

It is seen that flow values are high at the red area in case h_{max} under the flow line according to Plaxflow2D (Figure B.128.a). There is not a risk that is observed piping into through levee. Figure B.128. (b) is other notation that is vector stage in case h_{max}. That is called arrows in Plaxflow2D literature and there is not risk into through levee.

Analysis of sand at under the levee;

Figure B.129 shows that location of points near the ground surface for finding extreme velocity and Figure B.130 presents that results of flow velocity at K, L, M, N, O and P. One of the most important point is K points. K point is levee toe. Sand boil and heaving potential are investigated for other points.

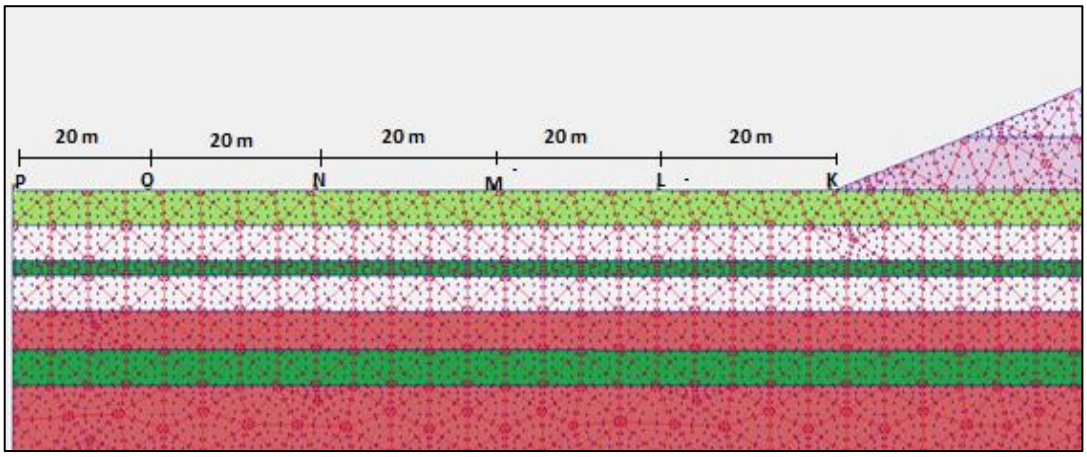

Figure B.129 Location of points near the ground surface for finding extreme velocity

Table B.61 shows that piping is not observed at any points due the fact that to exit gradient is zero. See equation B.50 for calculated critical hydraulic gradients.

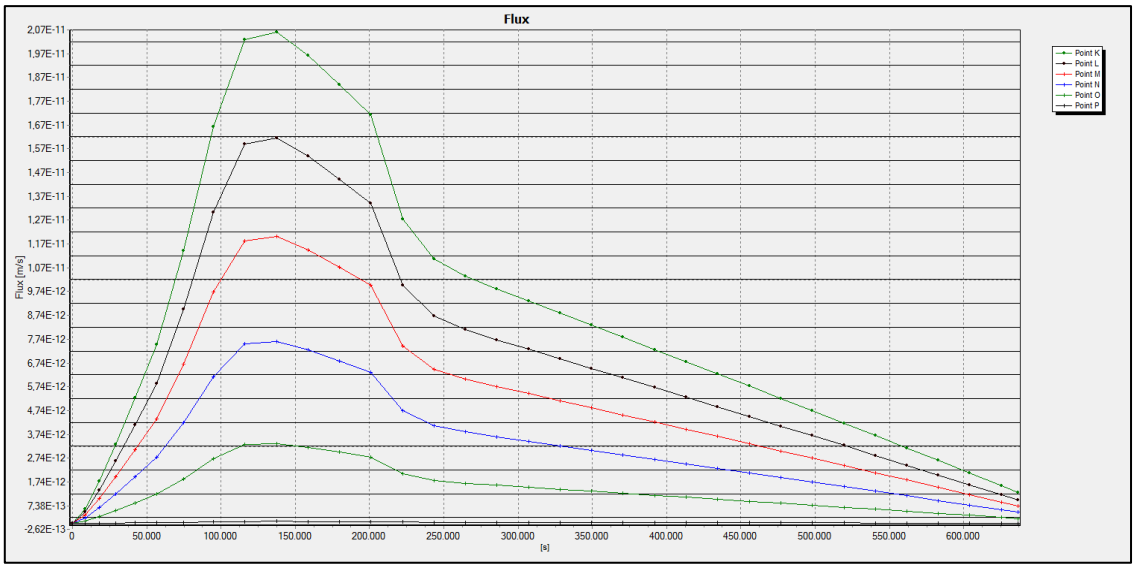

Figure B.130 Extreme velocity graph relation time Filyos Levee

Table B.61 Piping Status

Symbol	Max Seepage Velocity (m/s)	Permeability (m/s) (k)	Exit Gradient (*i*)	Piping
K	2.0×10^{-11}	$1x10^{-7}$	0	**NaN**
L	1.6×10^{-11}	$1x10^{-7}$	0	**NaN**
M	1.2×10^{-11}	$1x10^{-7}$	0	**NaN**
N	7.7×10^{-12}	$1x10^{-7}$	0	**NaN**
O	3.5×10^{-12}	$1x10^{-7}$	0	**NaN**
P	7.0×10^{-13}	$1x10^{-7}$	0	**NaN**

NaN:Not a Number

In order for the sand boiling to occur, the piping must take place. As can be seen in the Table B.62, it did not reach critical gradient for the formation of boiling.

Table B.62. Sand Boil Status

Symbol	Max Seepage Velocity (m/s)	Permeability (m/s) (k)	Exit Gradient (*i*)	Sand Boil
K	2.0×10^{-11}	$1x10^{-7}$	0	**NaN**
L	1.6×10^{-11}	$1x10^{-7}$	0	**NaN**
M	1.2×10^{-11}	$1x10^{-7}$	0	**NaN**
N	7.7×10^{-12}	$1x10^{-7}$	0	**NaN**
O	3.5×10^{-12}	$1x10^{-7}$	0	**NaN**
P	7.0×10^{-13}	$1x10^{-7}$	0	**NaN**

NaN:Not a Number

The analysis above the levee for gravelly sand and silty sand fill soil type;

Piping can only observe K, L and M point because these points only are under the phreatic line. K, L, M etc. points on the ground surface or levee are different from other analyses.

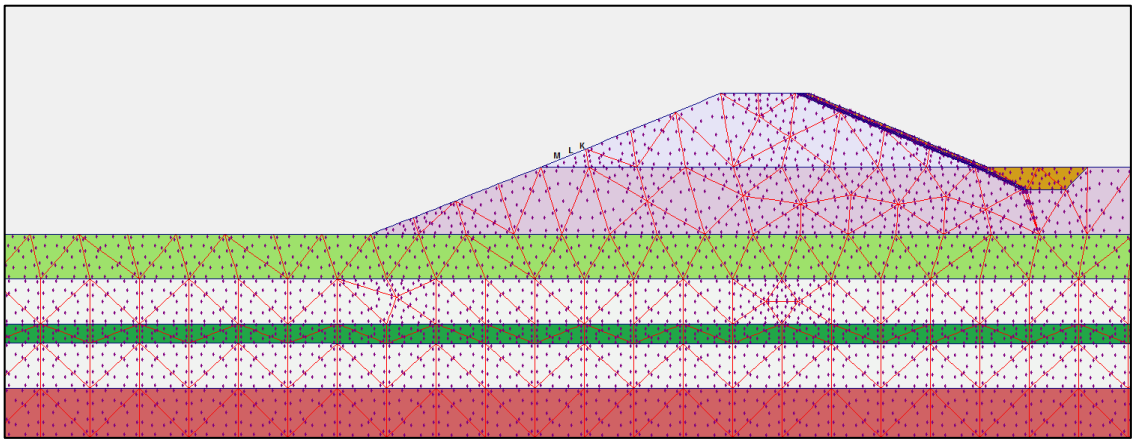

Fig. B.131 Location of points above the levee for finding extreme velocity

Extreme velocities of K, L and M point are Figure B.132 and these extreme velocities are investigated piping formations.

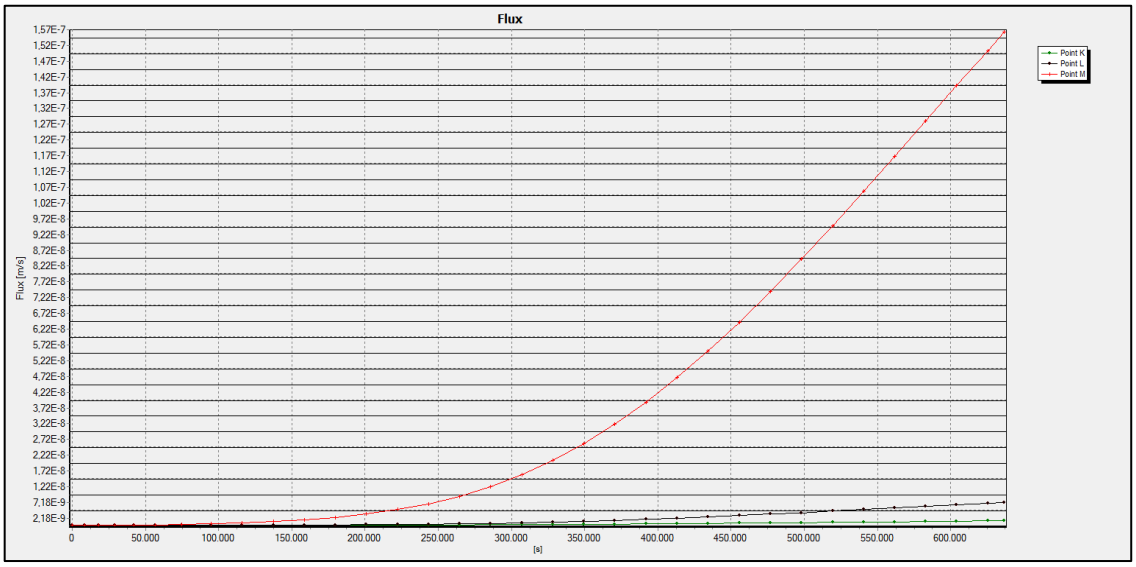

Figure B.132 Extreme velocity graph relation time to seepage velocity

Critical hydraulic gradient is 1.2 for silty sand. Table B.63 shows that piping is not observed at any points due to $i_{exit} < i_c$. See equation B.52 for calculated critical hydraulic gradients.

Table B.63 Piping Status

Symbol	Max Seepage Velocity (m/s)	Permeability (m/s) (k)	Exit Gradient (*i*)	Piping
K	2×10^{-9}	5×10^{-4}	0	**NaN**
L	7.2×10^{-9}	5×10^{-4}	0	**NaN**
M	1.6×10^{-7}	5×10^{-4}	0	**NaN**

NaN:Not a Number

Piping can only observe K, L and M point because these points only are under the phreatic line. K, L, M etc. points on the ground surface or levee are different from other analyses.

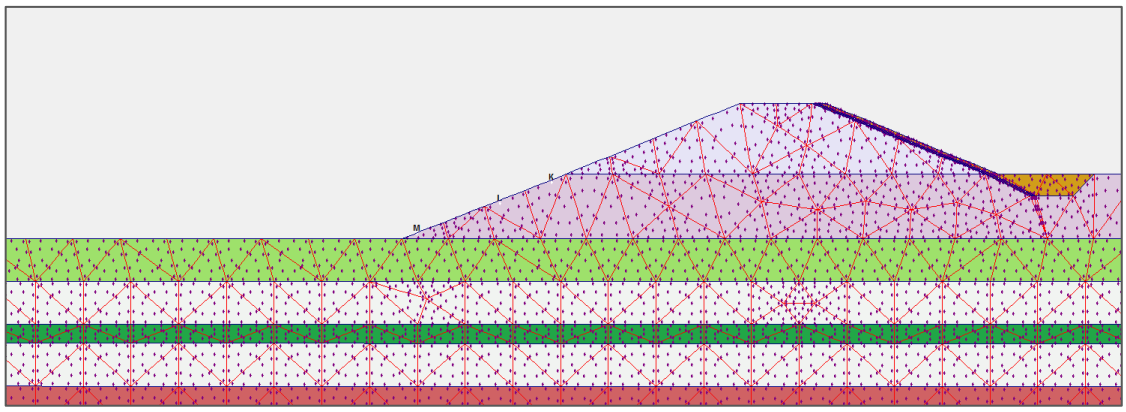

Figure B.133 Location of points above the levee for finding extreme velocity

Extreme velocities of K, L and M point are Figure B.134 and these extreme velocities are investigated piping formations.

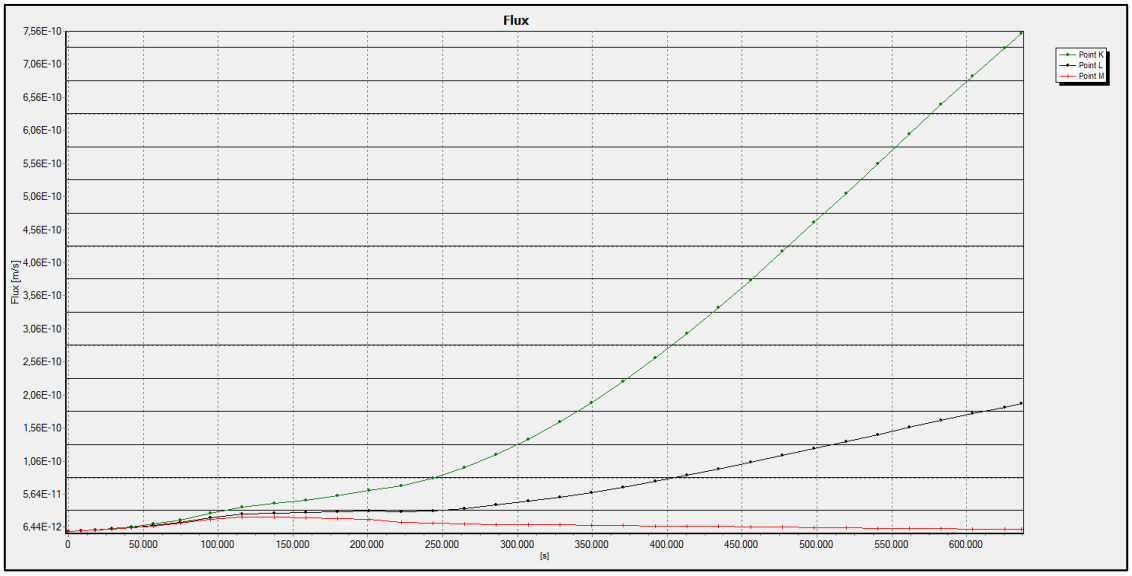

Figure B.134 Extreme velocity graph relation time above the levee

See equations B.54 for calculated critical hydraulic gradients.

Table B.64 Piping Status

Symbol	Max Seepage Velocity (m/s)	Permeability (m/s) (k)	Exit Gradient (*i*)	Piping
K	7.6×10^{-10}	1×10^{-6}	0	**NaN**
L	2.1×10^{-10}	1×10^{-6}	0	**NaN**
M	6.5×10^{-12}	1×10^{-6}	0	**NaN**

NaN:Not a Number

- Heaving potential is not observed that levee has cover materials along river since the exit gradients approach zero.

B.9. Filyos Levee at 2+327.64 km on Right Shore of Filyos River

Location of Filyos levee at 2327.64 m on left shore is seen Figure B.135 and the schematic representation of Filyos Levee and soil profile is given in Figure B.136 Filyos levee includes gravelly sand soil type. There is a clayey silt layer under the levee and this layer is 2 m thick.

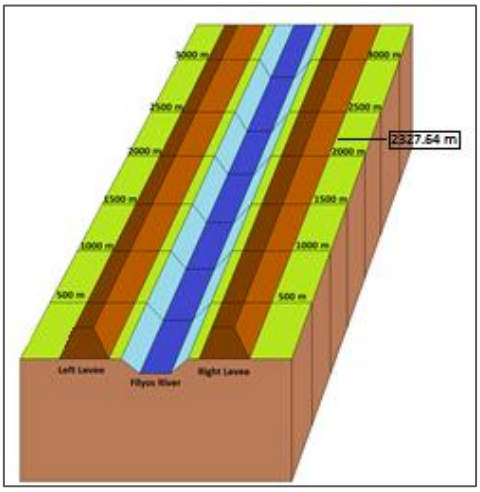

Figure B.135 Locations of Filyos levee at 2+327.64 m on right shore of Filyos River

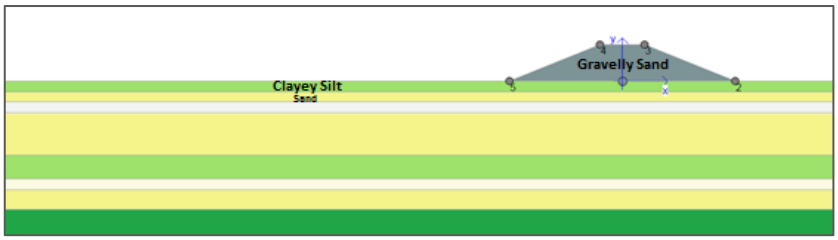

Figure B.136 Filyos Levee at 2+327.64 km on right shore of Filyos River

Figure B.137 shows that each soil layers have saturated unit weight under the levee for transient analysis and area of under the flow line is saturated during h_{max}.

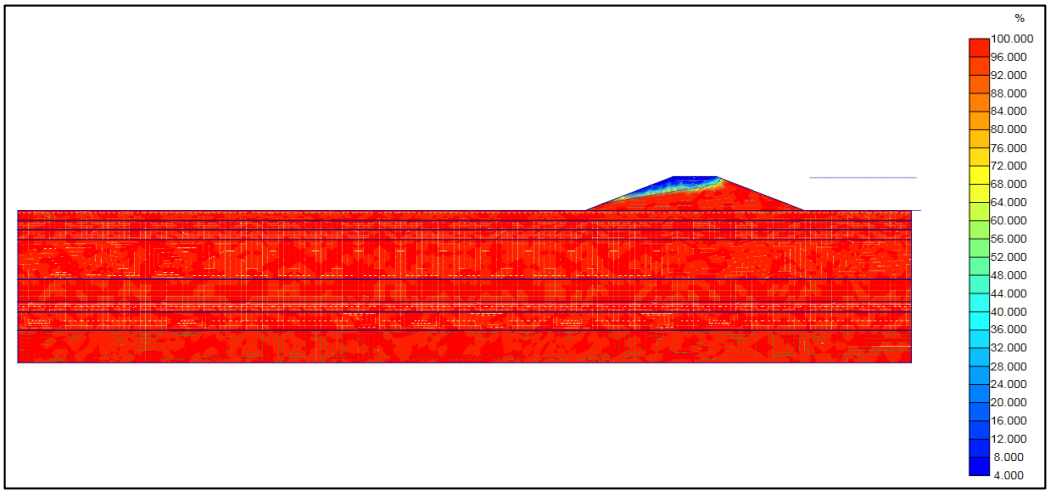

Figure B.137 Degree of Saturation of Filyos Levee at 2+327.64 km on right shore of Filyos River during h_{max}

It is seen that flow values are high at the red area in case h_{max} under the flow line according to Plaxflow2D (Figure B.138.a). There is a risk that is observed piping at these areas.

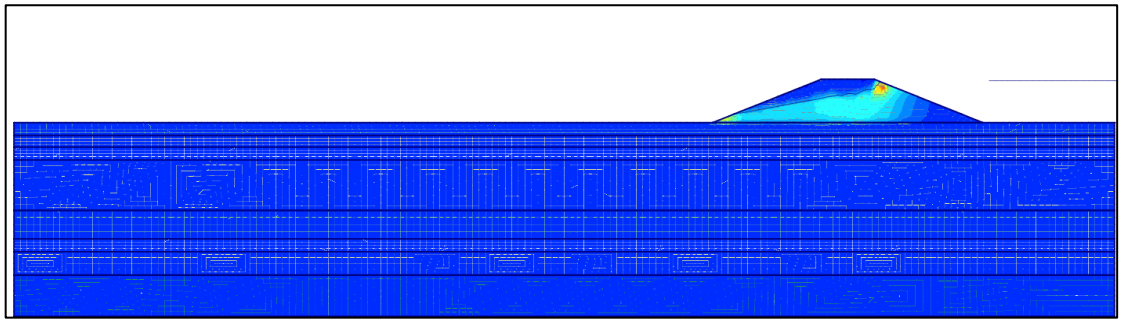

(a)

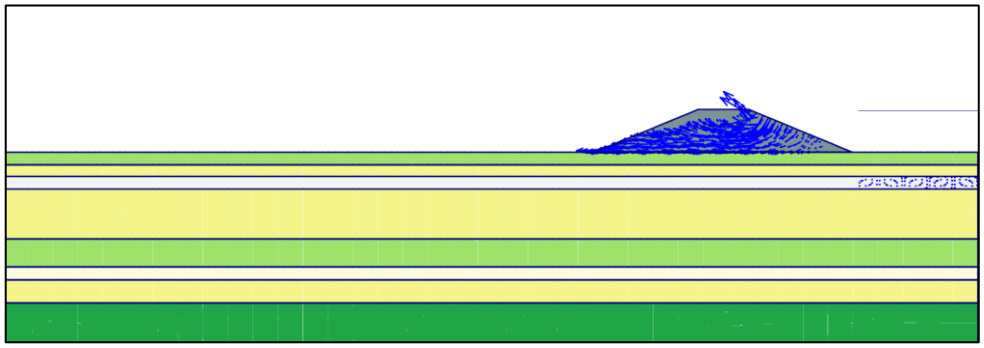

(b)

Figure B.138. Flow field at 2+327.64 km on right shore of Filyos River during h_{max} a.) Shadings view b.) Arrows view

Figure B.138. (b) is other notation that is vector stage in case h_{max}. That is called arrows in Plaxflow2D literature. If the vectors values are higher than others, there will be observing piping formations.

Analysis of clayey silt at under the levee;

Figure B.139 shows that location of points near the ground surface for finding extreme velocity and Figure B.140 presents that results of flow velocity at K, L, M, N, O, P, Q and R.

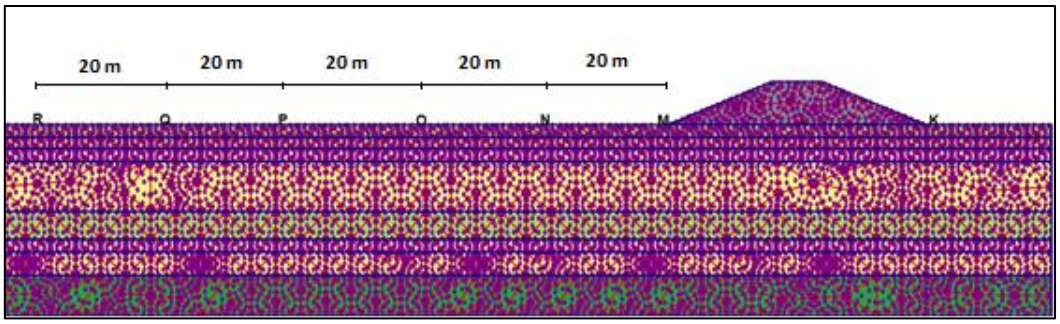

Fig. B.139 Location of points near the ground surface for finding extreme velocity

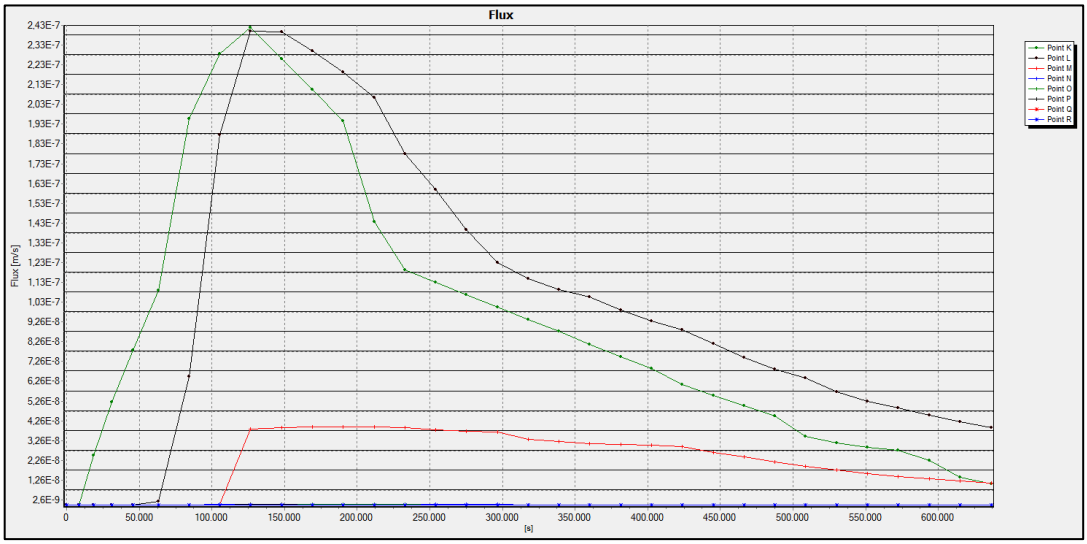

Figure B.140 Extreme velocity graph relation time to seepage velocity

According to Figure B.140, max values of flow are K=2.4x10^{-7} m/s at time=34.7 hours; L=2.4x10^{-7} m/s at time=34.7 hours; M=4.0x10^{-8} m/s at time=34.7 hours; N, O, P, Q and R= 3x10^{-9} m/s at time=34.7 hours.

Piping formations are simply compate as;

$$v = k.i\,; \qquad \text{(B.57)}$$

$$i_c = \frac{G_s - 1}{1 + e} = \frac{2.70 - 1}{1 + 0.9} = 0.89; \quad \text{(B.58)}$$

Where;

v = flow velocity (m/sec)

k = permeabilty (m/sec)

i = hydraulic gradient

i_c = critical hydraulic gradient

G_s = specific gravity; 2.70 for clayey silt

e = void ratio; 0.90 for clayey silt

Table B.65 shows that piping is observed at some points due to $i_{exit} > i_c$.

Table B.65 Piping Status

Symbol	Max Seepage Velocity (m/s)	Permeability (m/s) (k)	Exit Gradient (i)	Piping
K	2.4×10^{-7}	1×10^{-7}	2.40	$i_{exit} > i_c$
L	2.4×10^{-7}	1×10^{-7}	2.40	$i_{exit} > i_c$
M	4.0×10^{-8}	1×10^{-7}	0.40	**NaN**
N	3.0×10^{-9}	1×10^{-7}	0.03	**NaN**
O	3.0×10^{-9}	1×10^{-7}	0.03	**NaN**
P	3.0×10^{-9}	1×10^{-7}	0.03	**NaN**
Q	3.0×10^{-9}	1×10^{-7}	0.03	**NaN**
R	3.0×10^{-9}	1×10^{-7}	0.03	**NaN**

NaN:Not a Number

Table B.66 shows that sand boil is not observed at levee toe becouse maximum exit gradient does not approach critical hydraulic gradient.

Table B.66 Sand Boil Status

Symbol	Max Seepage Velocity (m/s)	Permeability (m/s) (k)	Exit Gradient (i)	Sand Boil
M	4.0×10^{-8}	1×10^{-7}	0.40	**NaN**
N	3.0×10^{-9}	1×10^{-7}	0.03	**NaN**
O	3.0×10^{-9}	1×10^{-7}	0.03	**NaN**
P	3.0×10^{-9}	1×10^{-7}	0.03	**NaN**
Q	3.0×10^{-9}	1×10^{-7}	0.03	**NaN**
R	3.0×10^{-9}	1×10^{-7}	0.03	**NaN**

The analysis above the levee for gravelly sand soil type;

Piping can only observe K, L and M point because these points only are under the phreatic line. K, L, M etc. points on the ground surface or levee are different from other analyses.

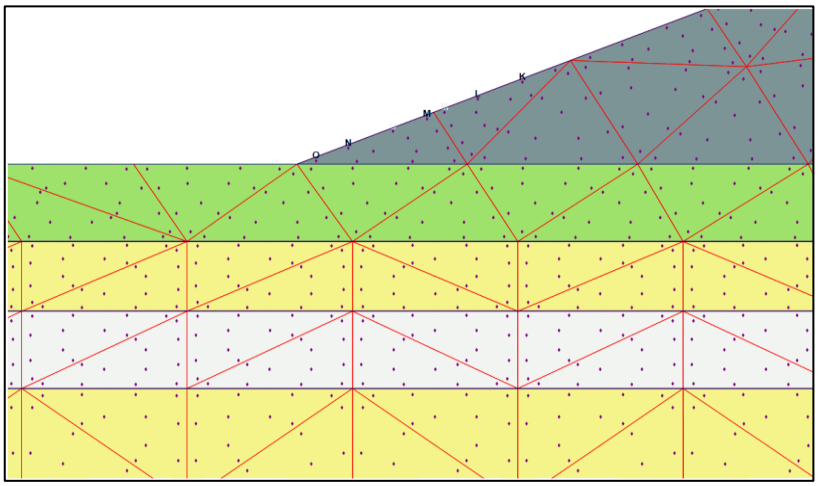

Figure B.141 Location of points above the levee for finding extreme velocity

Extreme velocities of K, L and M point are B.142 and these extreme velocities are investigated piping formations these points.

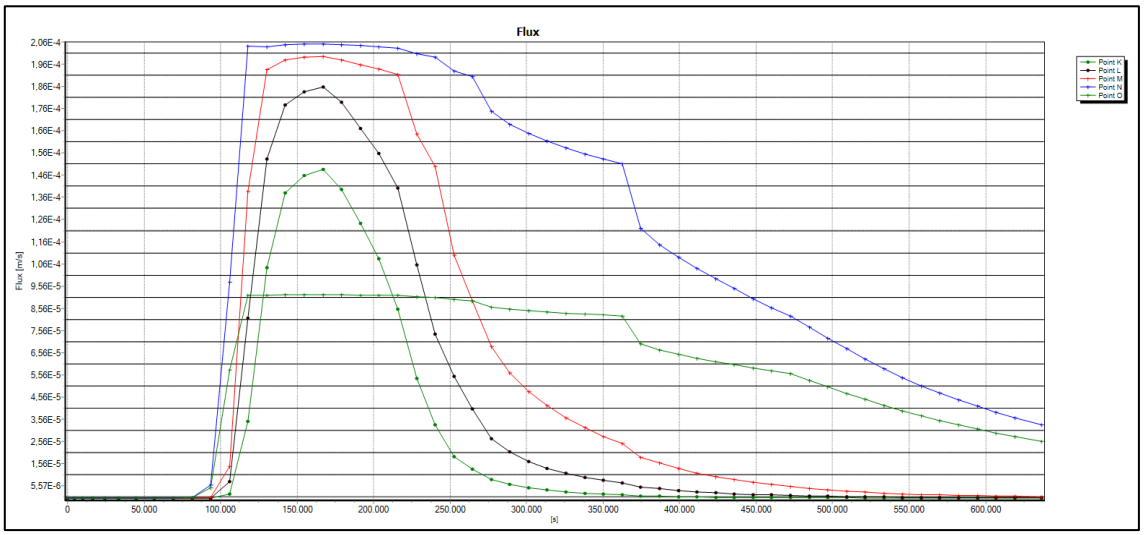

Figure B.142 Extreme velocity graph relation time above the levee

According to Figure B.142, max values of flow are K=1.5x10^{-4}m/s at time=44.4 hours; L=1.9x10^{-4}m/s at time=44.4 hours; M=2.0 x 10^{-4}m/s at time=44.4 hours; M=2.1 x 10^{-4}m/s at time=44.4 hours; M=9.0 x 10^{-5}m/s at time=44.4 hours.

Piping formations are simply compate as;

$$v = k.i\,; \tag{B.59}$$

$$i_c = \frac{G_s - 1}{1 + e} = \frac{2.66 - 1}{1 + 0.62} = 1.02\,; \tag{B.60}$$

Where;

v = flow velocity (m/sec)

k = permeabilty (m/sec)

i = hydraulic gradient

i_c = critical hydraulic gradient

G_s = specific gravity; 2.66 for gravelly sand

e = void ratio; 0.62 for gravelly sand

Table B.67 shows that piping is not observed at any points due to $i_{exit} < i_c$.

Table B.67 Piping Status

Symbol	Max Seepage Velocity (m/s)	Permeability (m/s) (k)	Exit Gradient (*i*)	Piping
K	1.5×10^{-4}	5×10^{-4}	0.30	**NaN**
L	1.9×10^{-4}	5×10^{-4}	0.38	**NaN**
M	2.0×10^{-4}	5×10^{-4}	0.40	**NaN**
N	2.1×10^{-4}	5×10^{-4}	0.42	**NaN**
O	9.0×10^{-5}	5×10^{-4}	0.18	**NaN**

NaN:Not a Number

The factor of safety against heave analysis for top layer;

Equation B.61 and B.62 are used to determine the factor of safety against heave analysis for top layer. Heaving potential are only observed ground surface hence a point are investigated at 1 m below the top layer like Figure B.143.

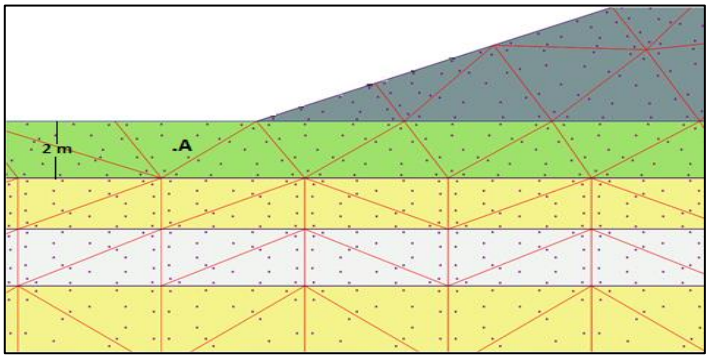

Figure B.143 Analysis against to heave at A point 1 m below the top layer

$$F_{heave} = \frac{H.\gamma_{sat}}{h_m.\gamma_w} > 3.0 \quad \text{(B.61)}$$

$$i_{\max} = \frac{h_m}{H} \quad \text{(B.62)}$$

Where;

H = thickness of overlying top layer(m)

γ_{sat} = saturated unit weight of overlying top layer(kN/m^2)

h_m = average hydraulic head at the point(m)

γ_w = water unit wight(kN/m^2)

$i_{\max}$ = maximum exit gradient

$$0.06 = \frac{h_m}{1};\ h_m = 0.1 \Rightarrow F_{heave} = \frac{1x18.6}{0.1x10} = 18.6 > 3.0$$

It is not observed heave due to the fact that F_{heave} is higher than 3.0 .

B.9.1. Filyos Levee at 2+327.64 km on Right Shore of Filyos River according to Current Situation(Upstream face is covered)

The schematic representation of Filyos Levee and soil profile is given in Figure B.144. Filyos levee includes gravelly sand soil type and cover materials against piping and sand boil formations. The cover materials are riprap which is andesite, uniform sand filter layer and geocomposite layer. There is a clayey silt layer under the levee and this layer is 2 m thick.

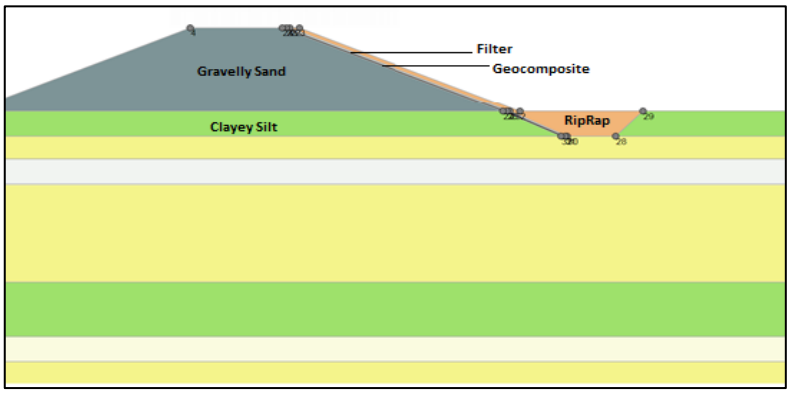

Figure B.144 Filyos Levee with cover materials at 2+327.64 km on right shore of Filyos River

Filyos levee has covered along rising water level. The covered members are filter, riprap and geocomposite materials. Table B.68 shows properties of covered materials and levee.

Table B.68 Soil Properties of levee members

	Soil Type / Material	**Permeability(k) (m/sec)**	**Specific Gravity (G_s)**	**Void Ratio (e)**	**Thickness (m)**
Filter	Uniform Sand	$1x10^{-3}$	2.67	0.70	0.25
Riprap	Andesite Rock	0.645	2.65	0.34	0.70
Geocomposite Material	Geotextile and Geomembrane	$1x10^{-13}$	-	0.02	0.30

Figure B.145 shows that each soil layers have saturated unit weight under the levee with cover materials for transient analysis and area of under the flow line is saturated during h_{max}. Saturation rates of red areas are high and saturation rates of other areas are almost zero with riprap, filter and geocomposites.

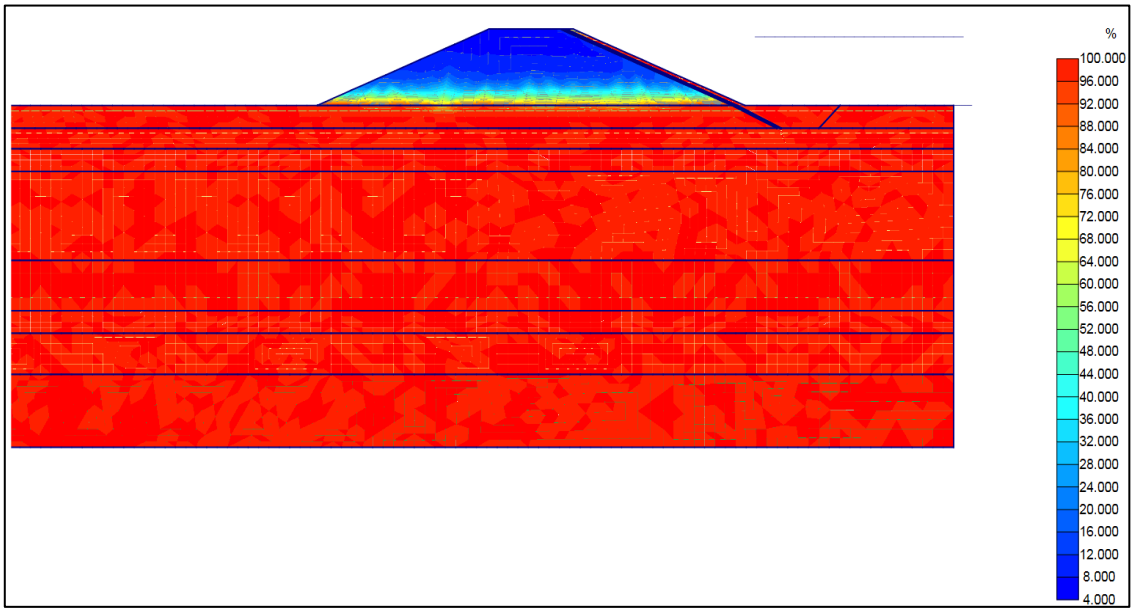

Figure B.145 Degree of Saturation of Filyos Levee with cover materials at 2+327.64 km on right shore of Filyos River during h_{max}

It is seen that flow values are high at the red area in case h_{max} under the flow line according to Plaxflow2D (Figure B.146.a). There is not a risk that is observed piping into through levee.

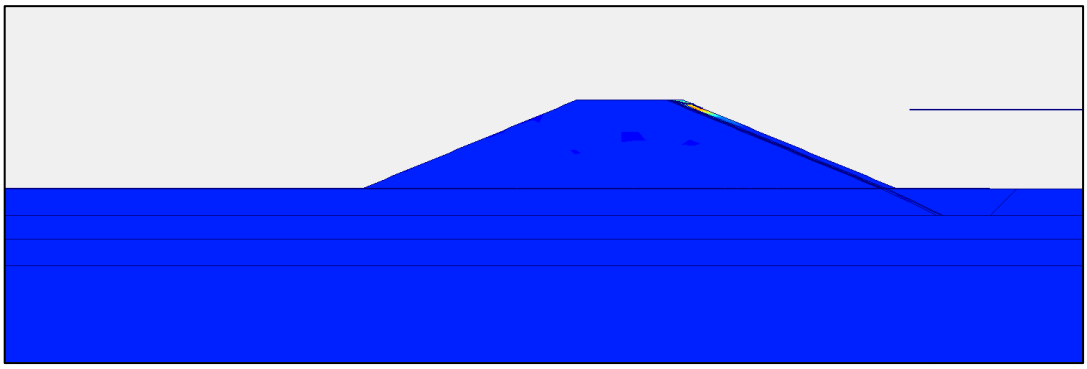

(a)

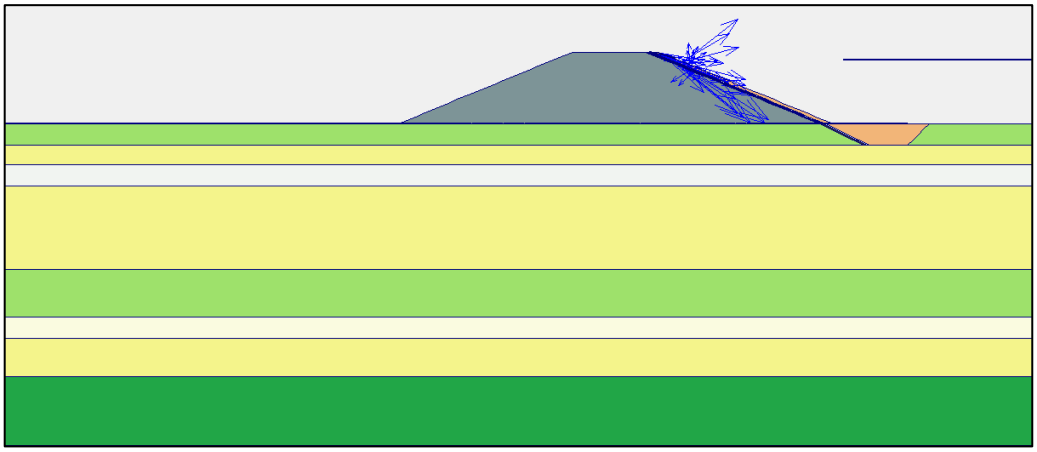

(b)

Figure B.146. Flow field at 2+327.64 km on right shore of Filyos River during h_{max}
a.) Shadings view b.) Arrows view

Figure B.146. (b) is other notation that is vector stage in case h_{max}. That is called arrows in Plaxflow2D literature and there is not risk into through levee.

Analysis of clayey silt at under the levee;

Figure B.147 shows that location of points near the ground surface for finding extreme velocity and Figure B.148 presents that results of flow velocity at K, L, M, N, O, P and Q .

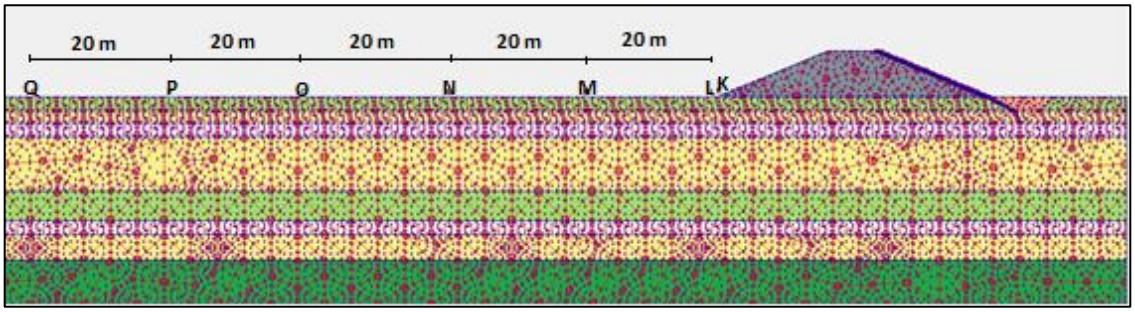

Figure B.147 Location of points near the ground surface for finding extreme velocity

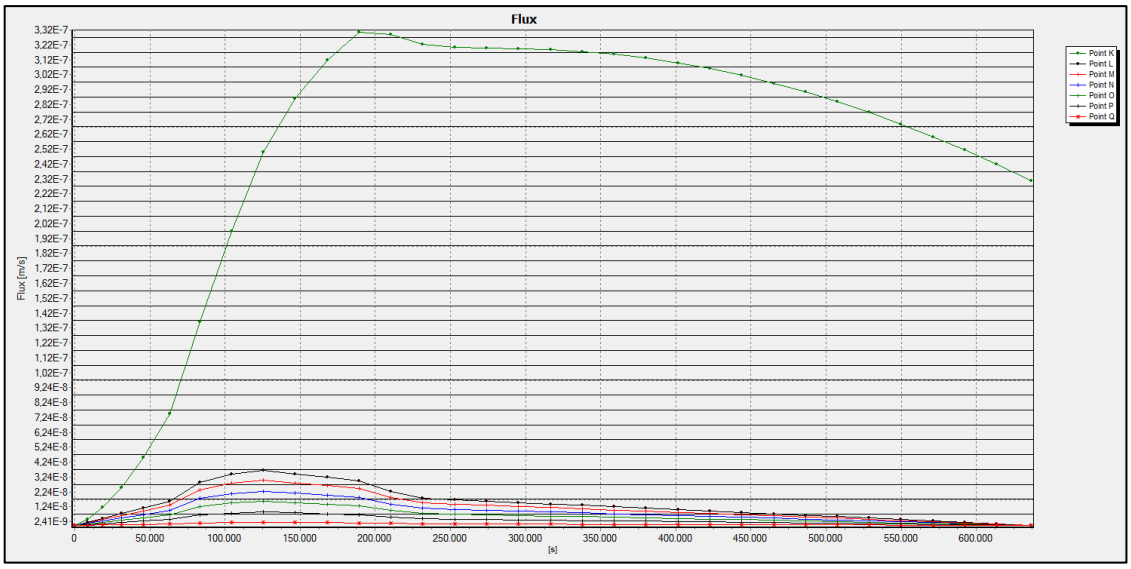

Figure B.148 Extreme velocity graph relation time Filyos Levee

Table B.69 shows that piping is not observed at any points due to $i_{exit} < i_c$. See equations B.58 and B.60 for calculated critical hydraulic gradients.

Table B.69 Piping Status

Symbol	Max Seepage Velocity (m/s)	Permeability (m/s) (k)	Exit Gradient (*i*)	Piping
K	3.3×10^{-7}	5×10^{-4}	0	**NaN**
L	3.7×10^{-8}	1×10^{-7}	0.37	**NaN**
M	3.2×10^{-8}	1×10^{-7}	0.32	**NaN**
N	2.2×10^{-8}	1×10^{-7}	0.22	**NaN**
O	1.7×10^{-8}	1×10^{-7}	0.17	**NaN**
P	2.9×10^{-9}	1×10^{-7}	0.03	**NaN**
Q	2.4×10^{-9}	1×10^{-7}	0.02	**NaN**

NaN:Not a Number

Table B.70. shows that sand boil is not observed at any points.

Table B.70 Sand Boil Status

Symbol	Max Seepage Velocity (m/s)	Permeability (m/s) (k)	Exit Gradient (*i*)	Sand Boil
L	3.7×10^{-8}	1×10^{-7}	0.37	**NaN**
M	3.2×10^{-8}	1×10^{-7}	0.32	**NaN**
N	2.2×10^{-8}	1×10^{-7}	0.22	**NaN**
O	1.7×10^{-8}	1×10^{-7}	0.17	**NaN**
P	2.9×10^{-9}	1×10^{-7}	0.03	**NaN**
Q	2.4×10^{-9}	1×10^{-7}	0.02	**NaN**

NaN:Not a Number

- Heaving potential is not observed that levee has cover materials along river since the exit gradients approach zero.